

2007

Fabrication of DNA microarrays on Poly (methacrylate) substrates for biomolecular reporting

Catherine N. Situma

Louisiana State University and Agricultural and Mechanical College, csitum1@lsu.edu

Follow this and additional works at: https://digitalcommons.lsu.edu/gradschool_dissertations



Part of the [Chemistry Commons](#)

Recommended Citation

Situma, Catherine N., "Fabrication of DNA microarrays on Poly (methacrylate) substrates for biomolecular reporting" (2007). *LSU Doctoral Dissertations*. 946.

https://digitalcommons.lsu.edu/gradschool_dissertations/946

This Dissertation is brought to you for free and open access by the Graduate School at LSU Digital Commons. It has been accepted for inclusion in LSU Doctoral Dissertations by an authorized graduate school editor of LSU Digital Commons. For more information, please contact gradetd@lsu.edu.

FABRICATION OF DNA MICROARRAYS ONTO POLY (METHYLMETHACRYLATE) SUBSTRATES FOR BIOMOLECULAR REPORTING

A Dissertation

Submitted to the Graduate Faculty of the
Louisiana State University and
Agricultural and Mechanical College
in partial fulfillment of the
requirements for the degree of
Doctor of Philosophy

in

The Department of Chemistry

by

Catherine N. Situma

B.S., Jomo Kenyatta University of Agriculture and Technology, 2000

May 2007

DEDICATION

To my late Dad:

Richard Situma Zadock

I know right now you have a broad smile on your face as you watch from heaven. Thank you for always telling me to aim higher when you were around.

To my mum:

Juliet Mutonyi Situma

Thank you for your endless love, support, encouragement, motivation and most of all the prayers. Mum you are the most beautiful and strong person I have ever known. You shall forever be my inspiration.

To my son:

Richard

Your smiles always bring joy to mama - you are my superman!

ACKNOWLEDGEMENTS

First I give God all the glory because without Him none of this would have been possible.

To my advisor Dr. Steven A. Soper, thank you for your guidance from the beginning to the end of this journey. Your patience, understanding, encouragement and support of both my research and professional development are highly appreciated.

To my dissertation committee members: Dr. Isiah Warner, Dr. Steven Watkins, Dr. Robert Cook, and Dr. Stephania Cormier. I sincerely appreciate your patience and time reading my dissertation and for all your valuable comments.

To Dr. Robin McCarley, Dr. Robert Hammer and Dr. Wieslaw Stryjewski thank you all for the advice and contributions you made towards my research.

To the past and present Soper group members; Musundi Wabuye, Yun Wang, Michelle Galloway, Zhu Li, Shawn Llopis, Harrison Musyimi, Hamed Shadpour, Masahiko Hashimoto, Peter Tate, Michael Allen, Jifeng Chen, Matteusz Hupert, Margazota Witek, Guofang Chen, Jason Guy, Frank, Vera Verdree, André Adams, Rodendrick Sinville, Annie Obubuafo, Jason Emory, Zhiyong Peng, Wonbae Lee, Paul Ogkbare, John Osiri, Samuel Njoroge, Hui-Wen Chen and Udara Dharmasiri-thank you all for your support and encouragement whenever it was required.

To my siblings and friends, Benard Wamukota, Harriet Nabachenja, Monica Namalwa, Jacqueline Maua, Michael Kiara , Jentrix Nanjala, Lavender Nambo, George Okeyo, Mokandu Mogeni, Joyce Mamle, Celinah, Janet and all the others that I can not mention here, thank you all for your love, understanding, support, encouragement and sacrifices that you have made for me to have a smooth way during my studies. Lastly, to ken, thank you for your support and unconditional love.

TABLE OF CONTENTS

| | |
|------------------------------------------------------------------------------------------------------------------------------------------------------------------|------|
| DEDICATION..... | ii |
| ACKNOWLEDGMENTS..... | iii |
| LIST OF TABLES..... | vii |
| LIST OF FIGURES..... | viii |
| COMMON ABBREVIATIONS AND ACRONYMS | xiv |
| ABSTRACT..... | xvi |
| CHAPTER 1. INTRODUCTION TO MICROARRAY TECHNOLOGY..... | 1 |
| 1.1 DNA Microarray Technology | 1 |
| 1.2 Applications of Microarray Technology..... | 5 |
| 1.3 Probe Array Preparation Techniques..... | 6 |
| 1.3.1. In-Situ Light Directed Synthesis of DNA Probes onto Solid Support..... | 7 |
| 1.3.2. Fabrication of Pre-Synthesized Probes onto Solid Supports..... | 9 |
| 1.4 Detection of Hybridization Events on Microarrays..... | 13 |
| 1.4.1 Radioactive Detection..... | 13 |
| 1.4.2 Electrochemical Detection of Microarrays..... | 15 |
| 1.4.3 Detection of Microarrays by Surface Plasmon Resonance Techniques..... | 16 |
| 1.4.4 Fluorescence Detection of Microarrays..... | 18 |
| 1.5 References..... | 24 |
| CHAPTER 2. MERGING MICROFLUIDICS WITH MICROARRAY TECHNOLOGY..... | 27 |
| 2.1 Introduction..... | 27 |
| 2.2 Microfluidics: Basic Fabrication and Operation..... | 28 |
| 2.3 Why Merge Microfluidics with Microarrays..... | 32 |
| 2.4 Hybridization Speed Enhancement in Microfluidic Devices..... | 35 |
| 2.5 Applications of Microfluidic-Based Microarrays..... | 40 |
| 2.5.1 DNA Microarray Systems..... | 45 |
| 2.5.2 Protein Microarray Systems..... | 46 |
| 2.5.3 Cell-Based Microarray Systems..... | 46 |
| 2.6 Conclusions..... | 47 |
| 2.7 References..... | 49 |
| CHAPTER 3. FABRICATION OF DNA MICROARRAYS ONTO POLY (METHYLMETHACRYLATE)(PMMA) BY UV PATTERNING FOR THE DETECTION OF LOW ABUNDANT DNA POINT MUTATIONS..... | 54 |
| 3.1 Introduction..... | 54 |
| 3.1.1 Covalent Immobilization of DNA Probes onto Polymeric Substrates..... | 54 |
| 3.1.2 UV-Photomodification of Polymeric Substrates..... | 56 |
| 3.1.3 Ligase Detection Reaction (LDR) for Detection of Low Abundant Mutations..... | 57 |
| 3.2 Experimental Section..... | 62 |
| 3.2.1 Materials..... | 62 |
| 3.2.2 Fabrication of PDMS Microfluidic Devices..... | 64 |

| | |
|------------------------------------------------------------------------------------------------------------------------------------------------------------------------------------------------|-----|
| 3. 2.3 Surface Modification of <i>PMMA, PC and PDMS</i> Substrates..... | 65 |
| 3.2.4 Radioisotope Labeling Assays..... | 66 |
| 3. 2.5 DNA Microarray Construction..... | 66 |
| 3.2.6 Extraction of DNA from Cell Lines..... | 68 |
| 3. 2.7 PCR Amplification of Genomic DNA. | 69 |
| 3.2.8 Detection of <i>KRAS2</i> Mutations by LDR/Hybridization..... | 69 |
| 3.3 Results and Discussions..... | 70 |
| 3.3.1 Adsorption Behavior of Oligonucleotide Probes onto Pristine PMMA and PC..... | 70 |
| 3.3.2 Attachment of Oligonucleotide Probes onto Carboxyl-terminated, UV- Activated PMMA and PC..... | 72 |
| 3.3.3 Coupling Microarrays to Microfluidics..... | 76 |
| 3. 4 Conclusions..... | 80 |
| 3.5 References..... | 81 |
| | |
| CHAPTER 4. IMMOBILIZATION OF MOLECULAR BEACONS: A NEW STRATEGY USING UV-ACTIVATED PMMA SURFACES TO PROVIDE LARGE FLUORESCENCE SENSITIVITIES FOR REPORTING ON MOLECULAR ASSOCIATION EVENTS..... | 84 |
| 4.1 Introduction..... | 84 |
| 4.1.1 Molecular Beacon Technology..... | 84 |
| 4.1.2 Hairpin versus Linear Oligonucleotide Probes..... | 88 |
| 4.1.3 Molecular Beacons Used on Arrays..... | 89 |
| 4.2 Experimental Section..... | 92 |
| 4. 2.1 Design of the Molecular Beacon Probes..... | 92 |
| 4. 2.2 Preparation of cDNA Targets..... | 94 |
| 4. 2.3 Immobilization of Molecular Beacons onto Solid Substrates..... | 95 |
| 4.2.4 Hybridization of MB Probes to Their Target..... | 96 |
| 4.3 Results and Discussion | 97 |
| 4.3.1 MB Design | 97 |
| 4.3.2 Fluorescence of Hybridized MBs in Solution..... | 99 |
| 4.3.3 Immobilization of MBs onto PMMA and Glass Surfaces..... | 99 |
| 4.3.4 Sensitivity and Selectivity of MBs Immobilized onto PMMA Substrates..... | 104 |
| 4.4 Conclusions..... | 107 |
| 4.5 References..... | 108 |
| | |
| CHAPTER 5. QUENCHING STUDIES OF PHTHALOCYANINES FOR USE IN FLUORESCENCE RESONANCE ENERGY TRANSFER APPLICATIONS..... | 112 |
| 5.1 Introduction..... | 112 |
| 5.1.1. Phthalocyanines: Spectroscopic Properties and Applications..... | 112 |
| 5.1.2. Fluorescence Quenching Mechanisms..... | 116 |
| 5.1.3 Research Focus..... | 119 |
| 5.2 ExperimentalSection..... | 121 |
| 5.2.1. Materials and Methods..... | 121 |
| 5.2.2. Calculations: Stern-Volmer Quenching Constants, Overlap Integrals and Förster Distances..... | 122 |
| 5.3 Results and Discussions..... | 125 |
| 5.4 Conclusions..... | 134 |
| 5.5 References..... | 134 |

| | |
|------------------------------------------------------------------------------------------------------------------------------------------------------------|-----|
| CHAPTER 6 LABELING OF OLIGONUCLEOTIDE PROBES FOR FRET APPLICATIONS..... | 137 |
| 6.1 Introduction..... | 137 |
| 6.1.1 Non-Covalent Labeling of Oligonucleotide Probes..... | 137 |
| 6.1.2 Covalent Labeling of Oligonucleotide Probes..... | 137 |
| 6.1.3 Research Summary..... | 141 |
| 6.2 Synthesis of Molecular Beacon Probes with Carboxylated Zinc Phthalocyanine Reporter Groups and Carboxylated Nickel Phthalocyanine Acceptor Groups..... | 143 |
| 6.2.1 Probe Design..... | 143 |
| 6.2.2 Labeling of Free3' Amino Group with Carboxylated Zinc Phthalocyanine..... | 143 |
| 6.2.3 Deprotection of 5' MMT- Amino Group..... | 146 |
| 6.2.4 Labeling of Free 5' Amino Group with Carboxylated Nickel Phthalocyanine..... | 148 |
| 6.3 References..... | 149 |
| CHAPTER 7 CONCLUSIONS AND FUTURE WORK..... | 151 |
| 7.1 Conclusions..... | 151 |
| 7.2 Current and Future Work | 153 |
| 7.2.1 Molecular Beacons for Real-Time Analysis of EpCAM mRNAs Expressed in MCF-7 Cells..... | 153 |
| 7.2.2 Reverse-Molecular Beacons for Detection of Low Abundant DNA Point Mutation and Pathogenic Analysis via Single Molecule Detection..... | 155 |
| 7.3 References..... | 156 |
| APPENDIX:LETTERS OF PERMISSION..... | 157 |
| VITA..... | 163 |

LIST OF TABLES

| | |
|-------------------------------------------------------------------------------------------------------------------------------------------------------------------------------------------------------------------------------------------------------------------------------------------------------------------------------------------------------------------------------------------------------------------------------------------------------------------------------------------------------------------------------------------------------------------------------------------------------------------------------------------------------------------------------------------------------------------------------------|-----|
| Table 1.1. Characteristics of radioisotopes commonly used for labeling DNA and RNA probes..... | 13 |
| Table 1.2. Advantages and disadvantages of commonly used microarray detection techniques..... | 23 |
| Table 2.1. Abbreviated list of literature reports highlighting the coupling of DNA microarrays to microfluidics..... | 40 |
| Table 2.2. Abbreviated list publications outlining the coupling of Protein / cell microarrays to microfluidics..... | 43 |
| Table 3.1. Universal zip code probe sequences and their melting temperatures..... | 63 |
| Table 3.2. Primers used for <i>KRAS</i> mutation analysis by LDR with microarray detection Sequences in italic (discriminating primers) are complementary to zip code sequences. ; P-phosphorylated; DY 675- fluorescent label used, Spacer NH ₂ -PO ₄ (CH ₂ CH ₂ O) ₆ PO ₃ (CH ₂) ₃ NH ₂ | 68 |
| Table 4.1. Molecular beacon probes and target sequences. MB1 and MB2 are molecular beacon sequences. Lower case denotes the stem sequences of the beacons while the upper case is the recognition loop sequence. T1 and T2 are target sequences complementary to MB1 and MB2 respectively. The underlined sequence is the section complementary to the MBs. T3 is non-complementary to both MB1 and MB2. All targets (T1, T2, and T3) are cDNAs extracted from <i>Drosophila melanogaster</i> for <i>fruitless (fru)</i> , <i>Ods-site homeobox (OdsH)</i> and <i>Actin 5C (Act5C)</i> genes, respectively. Actin 5 c is non-complementary both to MB 1 and MB 2 and it was used as a negative control in these studies..... | 93 |
| Table 5.1 Molecular structures of the organic dyes used in the quenching studies..... | 123 |
| Table 5.2 Molar extinction coefficients of the quenchers used in this study..... | 125 |
| Table 5.3. Stern-Volmer constants (KSV), overlap integrals ($J \lambda$) and the Förster distance (R_0) of different fluorophore/quencher pairs used in quenching studies..... | 133 |

LIST OF FIGURES

- Figure 1.1:** Chemical structures of DNA / RNA nucleotides (Guanine, Cytosine, Thymine and Adenosine for DNA); Uracil instead of Thymine for RNA.....2
- Figure 1.2:** Complementary base pairing during a hybridization event. In DNA, Adenine pairs with Thymine and Guanine pairs with Cytosine. The pairing is the same in RNA except Uridine replaces Thymine.....4
- Figure 1.3:** Microarrays preparation. Probes are covalently attached onto solid surfaces; target molecules are prepared and labeled with fluorescent dyes then hybridized to the surface immobilized probes. The array is then read out by fluorescence scanning microscopy.....5
- Figure 1.4:** Light-directed synthesis of oligonucleotides. A surface bearing photoprotected hydroxyls (X-O) is illuminated through a photolithographic mask (M1), generating free hydroxyl groups in the photodeprotected regions. The hydroxyl groups are then coupled to a deoxynucleoside phosphoramidite (5'-photoprotected). A new mask pattern (M2) is applied, and a second photoprotected phosphoramidite is coupled. Rounds of illumination and coupling are repeated until the desired set of products is obtained.....8
- Figure 1.5:** Reaction Scheme for immobilization of DNA on amine-modified silicon wafer. A layer of t-boc protected 10-aminodec-1-ene is bound onto silicon surface by applying a thin layer of the protected amine to the wafer and exposing it to UV light from a low pressure mercury vapor lamp. Deprotection is achieved by treating the surface with 25% TFA in methylene chloride for 1 h followed by a 5 min rinse in 10 % NH₄OH. The heterobifunctional crosslinker, succinimidyl-4-(N-maleimidomethyl)cyclohexane-1-carboxylate (SSMCC) is added to the surface which binds to the free amines through an N-hydroxysuccinimidyl ester. Thiol terminated DNA is then bound to the maleimide groups of the SSMCC.....11
- Figure 1.6:** The surmodics probe attachment chemistry. A polymer surface is coated with the Surmodics' photoreactive coating reagent and exposed to UV light yielding to functional groups that allow amine-terminated oligonucleotide probes to be covalently attached on the surface via a Schiff-base reaction.....12
- Figure 1.7:** Kinase end-labeling of oligonucleotides. The 5'-terminal phosphate of the oligonucleotide is replaced in an exchange reaction by the ³²P-labeled γ-phosphate of [γ-³²P]ATP. The same procedure can be used to label the two 5' termini of double-stranded DNA.....14
- Figure 1.8:** Electrochemical coding of all eight possible one-base mismatches using inorganic nanocrystal tracers. Mismatch-containing hybrids were captured on magnetic beads followed by sequential additions of ZnS-linked adenosine-5-monophosphate, CdS-linked cytidine monophosphate, PbS-linked guanosine-5-monophosphate, and CuS-linked thymidine-5 monophosphate.....16
- Figure 1.9:** Principle of SPR Spectroscopy. One binding partner is immobilized on the surface of a sensor chip in a flow cell. The other binding partner is flowing over the surface of the sensor chip and allowed to interact with the immobilized molecules. A binding event on the surface of

the sensor chip is monitored by a change in refractive index close to the surface of the sensor chip.....17

Figure 1.10: Jablonski diagram. Block energy diagram illustrating the various radiative and non-radiative processes that occur when a molecule absorbs a photon of light.....20

Figure 1.11: A diagram of the confocal principle. The principle of confocal microscopy is the elimination of out of focus light, thus producing a high z-resolution image. First, incident light is focused to a particular point within the specimen by passing it through a very small aperture, such as a pinhole or slit. The focusing helps to limit the excitation of fluorophores above and below the plane of focus. Second, any emission that is above or below the plane of focus is blocked from reaching the detector by passing it through a second pinhole. The specimen is placed in the light-path at a conjugate focal plane such that movement in the vertical (z) direction keeps the focus at a fixed distance from the objective, and effectively scans in layers through the specimen.....21

Figure 1.12: A diagrammatic representation of the fluorescence scanner built in house for imaging microarrays. The sample is excited by an excitation beam which is passed through the neutral density and line filters. Fluorescence is collected and transmitted through the dichroic and a stack of long-pass and band-pass filters and passed on to the SPAD detector.....22

Figure 2.1. Processing steps required to prepare a mold master using X-ray LiGA and molding finished parts. The process starts with a lithography step using a mask that transfers the desired pattern into a photoresist. Following development of the resist, the underlying metal layer is exposed, which serves as a plating base for another metal that fills the voids left by the resist that was removed due to exposure to the patterning radiation. The deposited metal forms the desired microstructures. The unexposed resist is then removed, forming the finished mold master. This mold master is then available for micro-replicating parts in polymers or other materials using hot-embossing or injection molding. Shown on the right in this figure is a picture of the mold master and some parts that have been prepared from the mold master.....30

Figure 2.2. (A) Schematic of an array of electrodes fabricated on Si. The 25 electrodes, made from Pt, are 80 μm in diameter and cover an area of 1 cm^2 . The insulating layer consists of silicon nitride layer and over the Pt electrodes was a gel permeation layer consisting of agarose gel loaded with streptavidin. The bottom panel shows a cross section of one element of the array with the immobilized DNA probes. The probes are attached to the permeation layer via a biotin-streptavidin association. **(B)** Electric field enhanced transport of a poly d(T)₁₂ target to the Pt electrode surface with different bias voltages applied to the Pt electrode: C1 – positive potential; C2 – negative potential; C3 – no potential. R3 and R5 correspond to biotinylated and non-biotinylated probes, respectively.....38

Figure 3.1 Schematic representation of the ligase reaction: Step1; formation of an enzyme – adenylate complex, Step 2; Activation of 5'-phosphotase at the site of a nick in the DNA substrate, Step 3; Nick closure in which a covalent bond is formed between an adjacent 3'-hydroxyl group and activated 5' phosphotase in duplex DNA structures with the release of AMP from the adenylated DNA intermediate.....59

Figure 3.2 (A) Picture of the brass mold insert used for casting PDMS microfluidic devices. It consisted of sixteen channels; each channel had a width of 300 μm , a depth of 30 μm and a channel length of 34,000 μm . The interchannel spacing was 2,000 μm . Also shown (B) is a picture of the PDMS stencil obtained after mixing the pre-polymer and curing agent by pouring this solution onto the brass mold and letting it to polymerize.....64

Figure 3.3: A schematic diagram of the microfluidic array construction. PMMA was UV irradiated for 20 min and sealed with a PDMS chip containing 16 channels passivated with MES. Sixteen different oligonucleotide probes (shown in Table 1) were passed through the channels and allowed to incubate followed by removal of the PDMS. After washing, the PMMA substrate, containing immobilized probes, was sealed with another PDMS chip placed perpendicular to the existing channels containing the probes. Fluorescently dye-labeled, complementary targets were passed through the channels, hybridized and imaged using a near-IR fluorescence scanner.....67

Figure 3.4: Fluorescence images of oligonucleotide probes deposited on pristine PMMA and PC slides. The near-IR fluorescence images of PMMA and PC are shown in panels A and B, respectively. The intensity profiles from a cross section of the top three spots on PMMA and PC are shown in panels C and D, respectively. Both slides were prepared by spotting 100 μM oligonucleotide probe C₆-amino 34-mer in 200 mM phosphate solution to native slide surfaces in a 3 x 3 pattern (0.2 $\mu\text{L}/\text{spot}$), incubated at 37°C overnight, and followed by hybridization in 10 nM dye-labeled complements (M₁₃ Fwd (-29)-IRD 800) in 5x SSPE, 0.1% SDS, at 60°C for 1 h.71

Figure 3.5: Effect of UV exposure times on probe attachment to surfaces. (A) PMMA slides were UV irradiated at varied times (5 -30 min), 1 μM of ³²P radiolabeled M13 Fwd(-29)-(0.5 μl) were spotted on the slides and allowed to incubate for 1h. Quantitative measurements were performed by liquid scintillation counting. (B) Relative fluorescence intensities shown with respect to UV exposure time. PMMA slides were UV irradiated at varied times (5 -30 min), 1 μM (0.2 μl) of M₁₃Fwd(-29)- probe was attached on PMMA slides for 1 h followed by hybridization with 10 nM IRD 700 dye-labeled complementary target for 1 h.....74

Figure 3.6: Parallel arrays: Sixteen universal zip code array probe sequences shown in table 1 (100 μM in 0.1 M MES buffer pH 5.5) were addressed to UV modified PMMA via microfluidic channels in PDMS, each channel containing a different zip code probe. Immobilization was done at room temperature for 1 h followed by hybridization with 50 nM IRD 700 dye labeled complementary fragments in 5X SSPE,0.1% SDS hybridization solution for 20 min. Fluorescence images were scanned at a step resolution of 50.8 $\mu\text{m}/\text{step}$ and integration time of 0.1s per pixel. The images of each channel (1-16) represent hybridization interactions of the each zip code probe (zipcode 1 – zipcode 25) with their respective complements.....77

Figure 3.7: Mutation analysis: Four different zip code arrays were addressed in quadruplicates through the microfluidic device and allowed to incubate at room temperature for 1 h. From left; channels 1, 2, 3 and 4 are specific for K-ras 12.2 D mutation; channels 5, 6, 7 & 8 specific for K-ras 12.2A mutation; channels 9, 10, 11 &12 specific for K- ras 12.2V mutation while channels 13, 14, 15 & 16 were specific for K -ras 13.4 D mutations. The LDR products were directed through the channels followed by hybridization at 55 °C for 20 min and they were all captured at their correct zip codes. Fluorescence imaging was done using the near-IR scanner at a step resolution of 12.5 $\mu\text{m}/\text{step}$ and integration time of 0.1 per pixel.....78

Figure 4.1: Molecular beacons. In the absence of a complimentary target sequence, the molecular beacon remains closed and there is no appreciable fluorescence. When the molecular beacon unfolds in the presence of the complementary target sequence, the fluorophore is no longer quenched, and the molecular beacon fluoresces.....85

Figure 4.2: Catalytic molecular beacon. In the absence of targets, the MB hybridizes with the deoxyribozyme module. When the target is present, the MB changes its conformation and allows the substrate (a stemless fluorogenic oligonucleotide) to hybridize with the deoxyribozyme module. The deoxyribozyme cleaves the substrate, which results in increasing fluorescence, substrate dissociation and beacon hybridization with the deoxyribozyme.....86

Figure 4.3: The scorpion-probe approach. A stem-loop shaped probe is incorporated into PCR primer, allowing unimolecular target detection, which ensures faster kinetics and higher stability of the complex than the bimolecular reaction.....87

Figure 4.4: Molecular beacon probes for detection of fru gene MB1 (a) and ods-H gene MB 2 (b). Their stem structure has a C6 amino linker attached to aid in surface immobilization via a discrete polyethylene glycol (dPEG) cross linker (c)98

Figure 4.5: Solution based hybridization results for molecular beacons MB1 (A) and MB2 (B) respectively. Three solutions were used; 100nM MB without target molecules, 100 nM MB with 10 fold excess of non-complementary targets and 100 nM MB with 10 fold complementary target molecules. The solutions were incubated for 30 min in a hybridization buffer (20 mM Tris-HCl, 10 mM MgCl₂, and 10 mM KCl at pH 7.5) then their fluorescence spectra was obtained using a fluorimeter ($\lambda_{exc} = 675$ and $\lambda_{em} = 694$)-.....99

Figure 4.6: Comparison of fluorescence hybridization results for molecular beacons immobilized on glass (A) and poly(methyl methacrylate) (PMMA) (B) surfaces. Functionalized PMMA and glass substrates were used for coupling a bifunctional polyethylene glycol linker through carbodiimide coupling chemistry. These linker molecules were thereafter used for attachment of 100 nM MB probes. The probes were then used for capturing a 10 fold excess of perfectly complementary targets. Fluorescence images were obtained before hybridization (left) and after hybridization of the immobilized MB probes with their fully complementary targets (right) for both MB1 and MB2.....101

Figure 4.7: Fluorescence increment ratios for solution-based hybridization events and surface-immobilized beacons on glass and PMMA; The fluorescence increment was obtained by getting the ratios of; observed intensities of MB probe after hybridization with targets subtracted from the background with observed intensities of MB hairpin probes before hybridization with targets minus the background).....103

Figure 4.8: PMMA substrates were activated by being exposed to UV radiation for 20 min followed by immobilization of 100 nM MB probe solutions. These probes were used for hybridization with 10 fold excess of perfectly complementary targets and 10 fold excess of non-complementary targets for 2 h at room temperature. Fluorescence images were obtained after hybridization of surface immobilized molecular beacons; (A) without targets, (B) with fully complementary targets (C) with non-complementary targets. The complementary targets T1 / T2

and non-complementary targets T3 (refer to table 1) are cDNAs extracted from drosophila melanogaster fruit flies.....105

Figure 4.9: The calibration curves for the observed fluorescence intensities versus target concentrations for MB1 (A) and MB2 (B) respectively. A solution containing 100 nM of the MBs was immobilized onto PMMA slides and they were used for binding with their complementary target solutions varying from a range of 100nM to 2.5 μ M. The error bars represent \pm the standard deviation of three measurements taken.....106

Figure: 5.1: Molecular structure of a normal phthalocyanine (A) and a typical main group metal phthalocyanine complex (B).....112

Figure 5.2: Actual and potential industrial applications of phthalocyanines.....114

Figure 5.3: Molecular orbital (left) and state level (right) diagrams of metal phthalocyanine complexes showing the one-electron transitions that are predicted to give rise to absorption bands in the 280 nm to 1000 nm range. The orbital ordering on the left is based on Gouterman's model of the inner ring of phthalocyanines while the orbitals on the right are the four aza-nitrogen lone pair orbitals. The associated bands are referred to in the sequence Q, second $\pi - \pi^*$, B1, B2, N and L in ascending energy.....115

Figure 5.4: Modified Jablonski diagram for the processes of absorption ($h\nu_A$), Fluorescence emission ($h\nu_F$), non-radiative pathways (Σk_i), dynamic quenching $k_q[Q]$ and FRET.....119

Figure 5.5: (a) Fluorescence spectra ($\lambda_{exc} = 675$) of 1 μ M carboxylated zinc phthalocyanine and variable concentrations of carboxylated nickel phthalocyanine (500 nM, 1000 nM, 1500 nM and 2000 nM) in DMSO. (b) F_o / F versus carboxylated nickel phthalocyanine concentration relationship (Stern-Volmer plot) at 690 nm fluorescence emission maximum. (C) τ_o / τ versus carboxylated nickel phthalocyanine concentration.127

Figure 5.6: Absorption spectra of carboxylated nickel phthalocyanine, carboxylated zinc phthalocyanine and a mixture of both. The spectrum of carboxylated nickel phthalocyanine and carboxylated zinc phthalocyanine complex has a much broader band which could be attributed to aggregation.....128

Figure 5.7: Stern–Volmer plots showing τ_o / τ versus carboxylated nickel phthalocyanine with quencher concentrations of 50 nm, 100 nm, 150 nm and 200 nm.129

Figure 5.8: Left: Fluorescence spectra ($\lambda_{exc} = 675$) of quenching of carboxylated zinc phthalocyanine by (a) carboxylated copper phthalocyanine (b) BHQ-3 (c) carboxylated palladium phthalocyanine in DMSO. **Right:** Stern-Volmer plot for quenching of carboxylated zinc phthalocyanine by (a) carboxylated copper phthalocyanine (b) BHQ-3 (c) carboxylated palladium phthalocyanine in DMSO.....130

Figure 6.1: Oligonucleotide synthesis reaction cycle. DMTr = 4, 4'- dimethoxytriphenylmethyl; CPG = controlled pore glass, B = base, n is the number of nucleosides, R = DNA. Addition of one phosphoramidite to the growing cycle involves four chemical steps: Detritylation that leads to cleavage of the DMTr protecting group providing a free 5' hydroxyl group (1), activation and

coupling (2, 3) steps involves condensation of two nucleotide units, the phosphite group is of the phosphoramidite is not reactive towards hydroxyl groups but can easily be activated by weak 1 H tetrazole acid which converts the amidite into a tetrazolide. Capping (4) of any unreacted 5' hydroxyl groups then follows by using a mixture of acetic anhydride, 4-dimethylaminopyridine, and 2, 4, 6-collidine in acetonitrile. The phosphite triester is then oxidized (5) to the more stable phosphate triester by using a mixture of iodine, collidine, and water in acetonitrile before starting the next cycle.....139

Figure 6.2: Schematic representation of an oligonucleotide strand with arrows indicating the possible 5' end, 3' end, base and sugar labeling sites. Bⁿ is number of bases.....140

Figure 6.3: (A) Amino modified controlled pore glass (CPG) as a solid support which provides a reactive group for 3' post labeling. (B) Chemical structure of a 5' amino-modifier phosphoramidite, R = amino protecting group (4-monomethoxytriphenyl; trifluoroacetyl). Both are commercially available from Glen Research.....141

Figure 6.4: (A) Conversion of carboxylated dyes to their N-hydroxysuccinimidyl ester derivatives (B) Initial labeling of oligonucleotide using carboxylated nickel phthalocyanine...144

Figure 6.5: HPLC analysis of deprotected oligonucleotides. The oligonucleotides were chromatographed using a Zorbax SB-C18 column (Hewlett Packard, Wilmington, DE, USA) consisting of particle size 5 μm, 150 mm length and 4.6 mm diameter as the stationary phase. The mobile phase consisted of methanol and triethylammonium acetate (TEAA) buffer. The elution was done using the following gradient conditions: 5 min 95% methanol, 15min 50 % TEAA followed by 5 min 50 % TEAA. The HPLC system was operated at 1 ml / min with the diode array detector set at 260 nm and an injection volume of 10 μl.....147

Figure 6.6.: Second labeling of oligonucleotide using carboxylated nickel phthalocyanine.....148

Figure 7.1: Illustration of the use of reverse molecular beacon technology for analysis.....155

COMMON ABBREVIATIONS AND ACRONYMS

| | |
|-------|-----------------------------------------------|
| A | Adenine |
| Act5C | Actin 5c control gene |
| AMP | Adenosine monophosphate |
| APC | Adenomatous Polyposis coli |
| ATP | Adenosine triphosphate |
| C | Cytosine |
| cDNA | Complementary deoxyribonucleic acids |
| DCC | deleted in colorectal cancer |
| DNA | Deoxyribonucleic acids |
| dNTP | Deoxynucleoside triphosphate |
| dPEG | discrete polyethylene glycol |
| dsDNA | double stranded deoxyribonucleic acids |
| EDC | 1-ethyl-3[3-dimethylaminopropyl] carbodiimide |
| FRET | Fluorescence resonance energy transfer |
| Fru | Fruitless gene |
| G | Guanine |
| IPA | Isopropyl alcohol |
| KRAS | Kirsten rat sarcoma |
| LDR | Ligase detection reaction |
| MB | Molecular beacon |
| MES | 2-(N-morpholine) ethanesulfonic acid |
| mRNA | Messenger Ribonucleic acids |
| NAD | Nicotinamide Adenine dinucleotide |
| NHS | N-hydroxysuccinimide |
| NMN | Nicotinimide monophosphate |
| OdsH | Ods-site-homeobox gene |
| PC | Polycarbonate |
| PCR | Polymerase chain reaction |
| PDMS | Poly (dimethylsiloxane) |
| PMMA | Poly (methylmethacrylate) |
| PNK | Polynucleotide kinase |

| | |
|-------|-------------------------------------------------------------------------------|
| RET | Resonance energy transfer |
| RNA | Ribonucleic acids |
| RT | Reverse transcription |
| SDS | Sodium dodecyl sulfate |
| SPAD | Single photon avalanche detector |
| SSPE | Sodium chloride, Sodium hydrogen phosphate, ethylene diamine tetraacetic acid |
| ssDNA | Single stranded deoxyribonucleic acids |
| T | Thymine |
| U | Uridine |

ABSTRACT

DNA microarrays require the use of substrates with well-established surface modification/probe attachment chemistries. Glass/quartz have been widely adopted as typical support materials since their surface modification chemistries which involve the use of siloxane –based chemistries have been widely studied however; these chemistry is susceptible to hydrolytic cleavage especially at high or low pH values. Recently, polymers have been sought as alternative microarray support materials but their surface modification strategies are not well characterized compared to glass. In this work, we report on surface photo-modification of PMMA polymer substrates by UV irradiation which produced functional scaffolds of carboxylic groups that allowed covalent attachment of amine-terminated oligonucleotide probes onto these surfaces via carbodiimide coupling chemistries. The photo-modification process for microarray fabrication involved only three steps; (1) broadband UV exposure of the polymer surface; (2) carbodiimide coupling of amine-terminated oligonucleotide probes to the surface (via an amide bond) and; (3) washing of the surface. Since microfluidics offer several advantages such as reduction in reagent cost, reduction in hybridization assay times and parallel processing of samples; we incorporated them in the microarray construction by using poly (dimethylsiloxane) microchannels that were reversibly sealed to the photoactivated PMMA substrates. Parallel sample processing minimizes contamination effects that can give rise to false positives which can be a significant issue especially for diagnostic applications. We demonstrated use of these protocols with linear oligonucleotide probes for screening multiple *KRAS 2* mutations possessing high diagnostic value for colorectal cancers whereby a Ligase Detection Reaction/universal zipcode array assays were carried out using parallel detection of two different low abundant DNA point mutations in *KRAS 2* oncogenes with allelic composition evaluated at one locus. The same covalent attachment protocols were utilized for immobilizing hairpin probes (molecular beacons) in a microarray

format that were used to report on the analysis of complementary DNA (cDNA) specific for *fruitless (fru)* and *ods-site homeobox (OdsH)* genes extracted from *Drosophila Melanogaster* fruit flies. To further improve the analytical sensitivities exhibited by these hairpin probes; we used Phthalocyanine dyes as fluorescence reporting molecules which are known to be stable and possess high quantum yields for dual labeling of oligonucleotide probes that will be used for reporting on biomolecular association events.

CHAPTER 1

INTRODUCTION TO MICROARRAY TECHNOLOGY

1.1 DNA Microarray Technology

Biological/biomedical research is driven by the massive increases in the amount of Deoxyribonucleic acids (DNA) sequence information that has been compiled upon completion of sequencing of the genome. This large and rapidly increasing information pool, however, does not provide complete understanding of the genome, such as the function of the genes, how the cells work, what goes wrong in disease states or how to develop a drug based on sequence anomalies. As such, there has been the need for the development of new technologies that take advantage of the known sequence information for understanding the genes, their specific functions and how they work together to comprise functioning cells and organisms. One such technique is microarray technology; a powerful tool that can be configured to monitor the presence of molecular signatures in a highly parallel fashion by searching either for unique nucleic acid structures (DNA microarrays) or proteins (antibody-based microarrays) as well as different types of cells (whole-cell microarrays).

DNA microarrays consist of oligonucleotides that are attached onto solid supports (probes) and are used to interrogate the presence or the amount of analyte (i.e., targets, DNA/RNA) in sample solutions. DNA is the common name for Deoxyribonucleic acid, which is made of long chains of nucleotide bases. A nucleotide consists of: (i) A nitrogenous base, purine for Adenine (A) or Guanine (G); pyrimidine for Cytosine (C) or Thymine (T); (ii) a deoxyribose sugar and; (iii) a phosphate group. RNA (ribonucleic acid) differs from DNA by having a Uridine (U) nucleotide instead of a Thymine (T) and a Ribose sugar instead of the deoxyribose sugar (see Figure 1.1 below for the structures of these nucleotides). The terms DNA microarrays or DNA chips are used interchangeably in the literature. DNA microarrays were first developed

at Stanford University, where single-stranded DNAs (ssDNAs; 500-5000 bases long) were immobilized to a solid surface and exposed to their complementary targets either separately or in

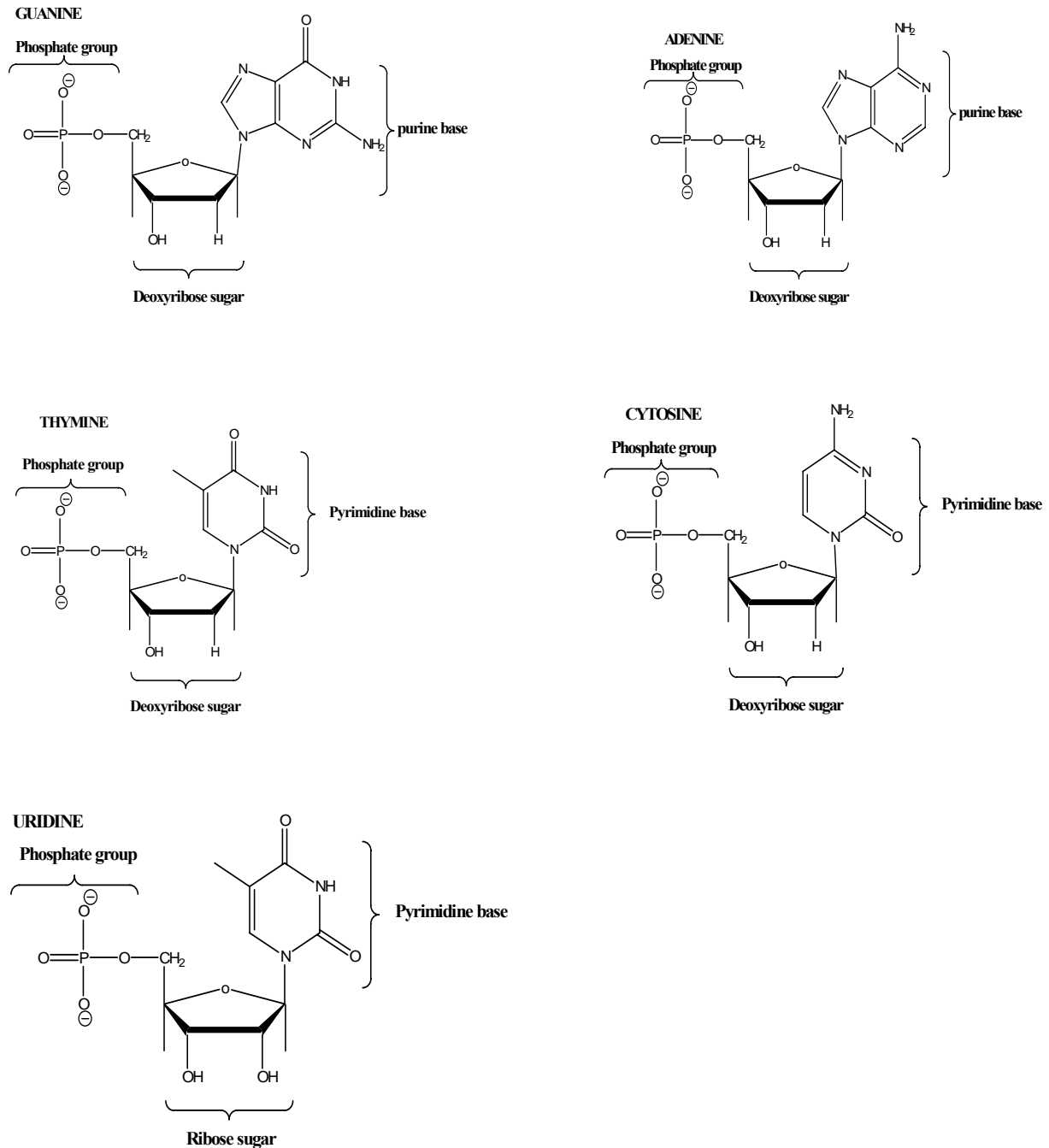


Figure 1.1: Chemical structures of DNA/RNA nucleotides (Guanine, Cytosine, Thymine and Adenosine for DNA); Uracil instead of Thymine for RNA.

a mixture.¹The DNA chip developed at Affymetrix Inc is known by *Gene Chip*® trademark and consists of oligonucleotides that are 20-80 bases long that are synthesized directly on the chip or synthesized by conventional means and immobilized on the solid support.²

DNA microarrays function through a hybridization event (non-covalent chemical bonding) between probes that are chemically attached at specific locations on a solid substrate and their complementary targets in solution. DNA hybridization assays first began in the mid 1970's with methods such as the Southern blot created by E. M. Southern in 1975.³ This is one of the first methods that utilized various ssDNA sequences known as “probes” and a radioisotope-tagged complement to one of the probes called “targets”. The disadvantages associated with this technique are; (i) the whole process is complex, cumbersome and time consuming, (ii) the procedure requires gel electrophoretic separation hence slow diffusion of the probes and targets into the gel membrane, (iii) when using this technique, only one gene or RNA can be analysed at a time and it gives information about the presence of DNA, RNA or proteins but does not give information about gene regulation. In an attempt to make this process more rapid and easier to use, efforts have been focused on the immobilization of the probe DNA on a solid support in a 2D-array, where the location of each probe is known. The target, which can be labeled by means other than radioisotopes, is then identified according to the location in which it hybridizes.

The binding between the probes and targets is based on the principle of specific molecular recognition events that occur for nucleic acids through pairing of the nucleotides via formation of hydrogen bonds as described by Watson and Crick.⁴ The nucleotide pairing occurs such that A always pairs with T while C always pairs with G as shown in Figure 1.2 below. The above figure illustrates how G specifically binds to C by formation of three hydrogen bonds, while A binds with T by forming two hydrogen bonds.

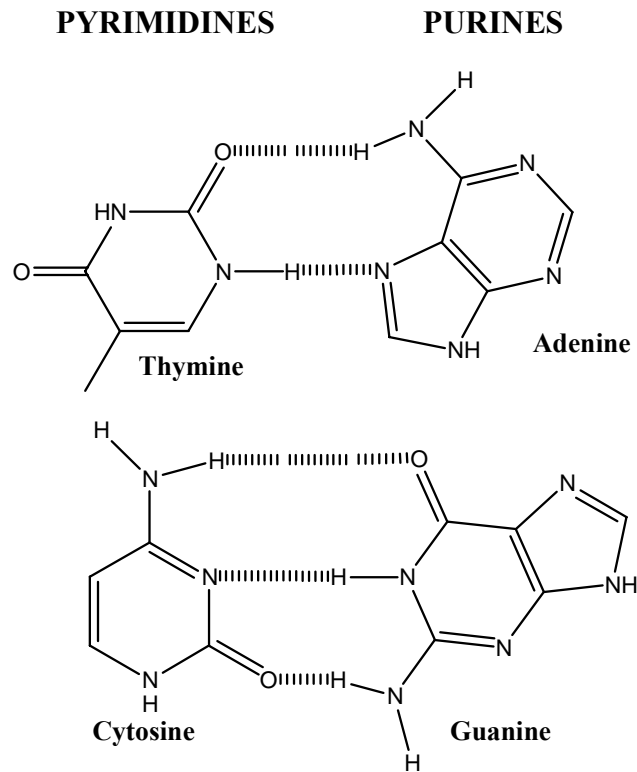


Figure 1.2: Complementary base pairing during a hybridization event. In DNA, A pairs with T and G pairs with C, the pairing is the same in RNA except U replaces T.

These binding events are referred to as the Watson crick base pairing⁴ and the paired bases are said to be complementary. During a hybridization assay, the base pairing between probes and targets lead to formation of a duplex. The two sequences involved in duplex formation must have some degree of sequence complementarity and the stability of this duplex depends on the extent of complementarity. This enables the hybridization assay to be selective and any binding of targets and probes that are non-complementary do not form thermodynamically strong hybrids, which can be selectively tuned out through stringent washing with buffers or temperature regulation. A standard microarray experiment typically involves several steps; (1) extraction/purification of the targets from the cells following lysis; (2) in the case of messenger RNA (mRNAs), reverse transcription is carried out to copy mRNA into its complementary DNA (cDNAs); (3) labeling of the solution targets with reporter molecules, such as fluorescent dyes, which can be added during the Polymerase Chain Reaction (PCR)

amplification in the case of DNAs and; (4) incubation (hybridization) of the targets with the arrayed probes. The targets are bound to complementary probes affixed onto the solid surface and they are then scanned producing a fluorescent image.

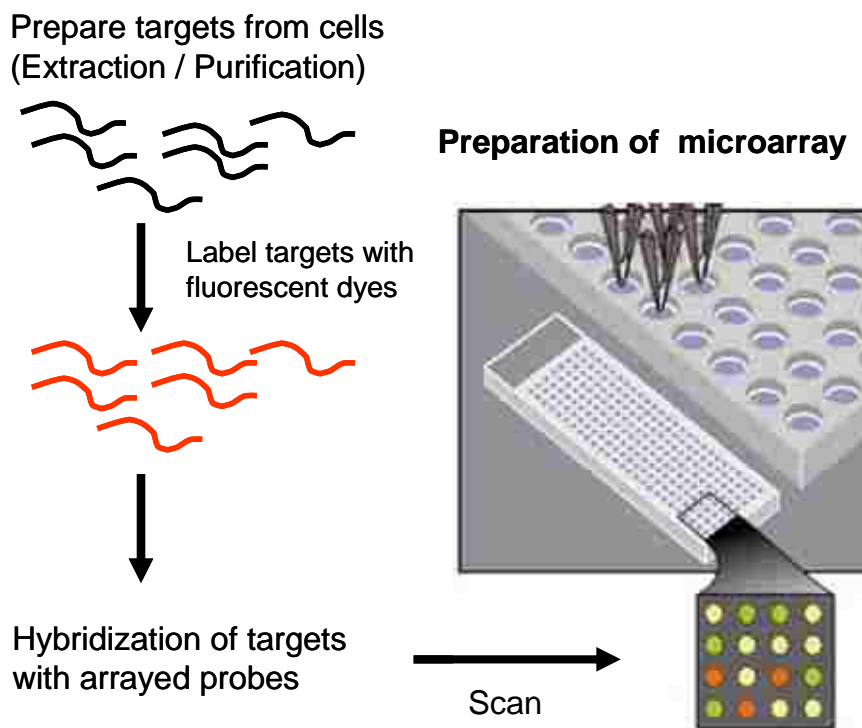


Figure 1.3: Microarrays preparation. Probes are covalently attached onto solid surfaces; target molecules are prepared and labeled with fluorescent dyes then hybridized to the surface immobilized probes. The array is then read out by fluorescence scanning microscopy.

The fluorescence intensity at any particular probe location indicates the relative concentration of the complementary DNA sequence in the sample. A general overview of a microarray experiment is depicted in Figure 1.3 above.

1.2 Applications of the Microarray Technology

Because microarrays allow one to investigate large numbers of analytes or targets rapidly and efficiently, researchers have applied this technology not only in gene expression analysis⁵, but also in drug screening/therapeutic studies,⁶ proteomics,^{7,8} cell analysis,⁹ and DNA sequencing/fragment analysis.¹⁰ Microarray technology was initially fostered in genomic applications however, its basic operational concepts have also been applied in proteomics for the

analysis and quantification of a large number of proteins comprising a proteome. Microarray applications in protein analyses includes screening binding specificities of a protein expression library,¹¹ high-throughput antibody screening,¹² or the detection of protein-protein interactions, enzymatic targets and protein-small molecule interactions.⁸ Not only can DNAs and proteins be successfully printed onto substrates in microarray formats, but cells have also been patterned onto substrates in a microarray format, which has advanced the study of cellular functions and metabolism, identification of the phenotype of a cell in a population of heterogeneously transfected cells,¹³ the detection of toxic agents and high-throughput screening of combinatorial libraries/gene products.¹⁴

Many complex diseases and traits are caused by rare alleles, which can only be detected by sequencing complete genomic regions in multiple individuals first for the identification of the variants and then for disease diagnostics. Progress in microarray systems, which enable highly multiplexed genotyping, is therefore very useful for genome-wide Single Nucleotide Polymorphism (SNP) genotyping. There exists a database of hundreds of SNPs/single base differences in the human genome, which can be used as genetic markers. As such, microarrays can be used in genotyping assays and also in comparative genomic hybridization (CGH), a technique that reveals how many copies of given genes are actually in a sample being interrogated. Microarrays have been demonstrated widely in SNP genotyping applications.¹⁵⁻²¹

1.3 Probe Array Preparation Techniques

DNA microarrays, which utilize short (< 25 bp) oligonucleotide probes, can either be synthesized directly on the substrate or pre-synthesized separately and then micro-printed or spotted onto the support in an orderly or fixed manner, typically in a two-dimensional format. Identification of the presence of a particular DNA sequence is transduced by a recognition signal produced through an association event between the surface-tethered probe and its solution complement and locating the address of the signal in the two-dimensional array, which allows

for highly parallel processing of multiple structures within a target. High quality probe arrays are usually desired to improve the sensitivity of the microarray assay. The probe array quality depends intimately on the probe attachment chemistry and deposition (spotting) technique used. Any non-uniform surface morphology that might arise during surface activation or spotting can lead to variances in the array element shape and probe surface concentration uniformity across the particular element, which eventually affects the data quality. The availability of these surface attached probes to interact with their complementary targets during hybridization is also highly desirable. The surface probe density as well as its spacing from the surface will determine the extent to which the immobilized probes are able to capture their targets from solution because, other than thermodynamic conditions, the immobilized probes can also be kinetically or sterically inaccessible.²²

1.3.1 In-Situ Light Directed Synthesis of DNA Probes onto Solid Supports

Direct on-chip probe synthesis is achieved by combining solid-phase chemistry, photolabile protecting groups and photolithography.^{10, 23, 24} This synthesis technology developed at Affymetrix Inc. combines photolithography technology from the semiconductor industry with DNA-synthetic chemistry to enable high-density oligonucleotide-microarray manufacture²³ (Figure 1.4 below). In this process, a glass wafer modified with photo-labile protecting groups is selectively activated for DNA synthesis by shining light onto the wafer through a photomask. The wafer is then flooded with a photo-protected DNA base, resulting in spatially defined coupling on the chip surface. A second photomask is used to de-protect defined regions of the wafer. Repeated de-protection and coupling cycles enable the preparation of high-density oligonucleotide microarrays. A key advantage of this approach is that photo-protected versions of the four DNA building blocks allow chips to be manufactured directly from sequence databases, thereby removing the uncertain and burdensome aspects of sample handling and tracking.

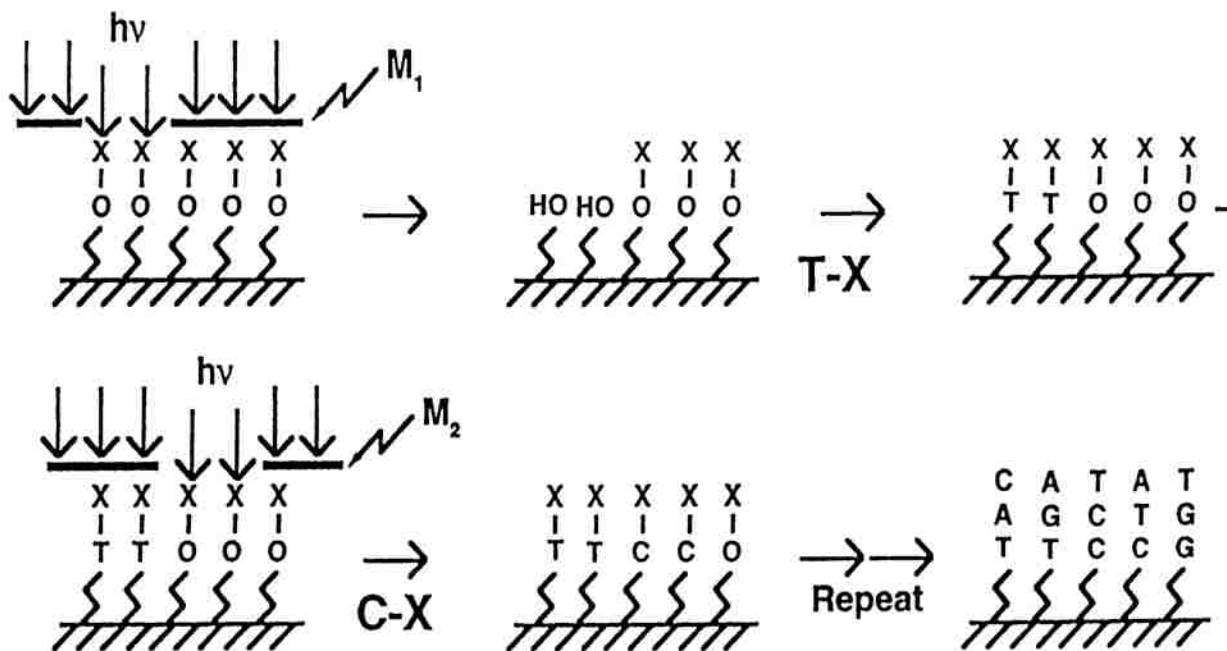


Figure 1.4: Light-directed synthesis of oligonucleotides. A surface bearing photoprotected hydroxyls (X-O) is illuminated through a photolithographic mask (M_1), generating free hydroxyl groups in the photodeprotected regions. The hydroxyl groups are then coupled to a deoxynucleoside phosphoramidite (5'-photoprotected). A new mask pattern (M_2) is applied, and a second photoprotected phosphoramidite is coupled. Rounds of illumination and coupling are repeated until the desired set of products is obtained.²³

The basic strategy for light-directed oligonucleotide synthesis²³ is outlined in Figure 1.4. The surface of a solid support modified with photolabile protecting groups (X) is illuminated through a photolithographic mask, yielding reactive hydroxyl groups in the illuminated regions. A 3'-O-phosphoramidite activated deoxynucleoside (protected at the 5'-hydroxyl with a photolabile group) is then presented to the surface and coupling occurs at sites that were exposed to light. Following capping, and oxidation, the substrate is rinsed and the surface is illuminated through a second mask, to expose additional hydroxyl groups for coupling. A second 5'-protected, 3'-O-phosphoramidite-activated deoxynucleoside is presented to the surface. The selective photodeprotection and coupling cycles are repeated until the desired set of products is obtained.²³ Since photolithography is used, the process can be miniaturized to generate high-

density arrays of oligonucleotide probes. Furthermore, the sequence of the oligonucleotides at each site is known. Another advantage of this technology is that the use of synthetic reagents minimizes chip-to-chip variation by ensuring a high degree of precision in each coupling cycle. One disadvantage of this approach is, however the need for photomasks, which are expensive and time-consuming to design and build because the actual process by which this is done involves the use of photolithography and the sequential use of unique masks. Lastly, the making of such chips depends on the exact chemistry, a correct set of masks and, of course, the exact oligonucleotide sequences one wants to place in each location.

1.3.2 Fabrication of Pre-Synthesized Probes onto Solid Supports

Pre-synthesized oligonucleotide probes can be covalently or physically arrayed onto a variety of chip surfaces using several different chemistries.^{25, 26} This usually requires the use of chemically modified oligonucleotide probes, which are generally modified by the introduction of both a suitable moiety, such as an amino or thiol group for the end attachment onto solid supports. The performance of a surface in terms of signal intensity and signal-to-noise ratio is directly influenced by the amount of DNA probes attached onto the surface and the accessibility of the probes to the labeled target. An ideal support should have a surface chemistry that allows stable covalent binding of DNA at high capacity. Two key parameters of a microarray are the number of different probe sites (spots) per unit area, which reflects its information density, and the number of probe molecules per unit area within an individual probe site. All these are dependent on the attachment chemistries of the probes onto the supports. A comprehensive review of the different available attachment protocols has been detailed by Pirrung.²⁷ This review summarizes many chemical reactions that have been developed for the attachment of DNA probes onto solid surfaces.

An example of an immobilization strategy for the covalent attachment of pre-synthesized thiol modified oligonucleotides onto activated silicon surfaces containing amine groups have

been described by Strother and coworkers.²⁸ Silicon substrates were derivatized by being exposed to UV light which mediated the reaction of t-butyloxycarbonyl (t-Boc) protected ω -unsaturated aminoalkane (10-aminodec-1-ene) with the hydrogen terminated silicon as illustrated in Figure 1.5 below. After removal of the t-Boc protecting groups, the silicon substrates contained amino groups which were eventually used for coupling thiol modified oligonucleotides.

Another example of probe attachment is by immobilization of pre-synthesized probes onto nitrocellulose membranes, such as Nylon, by simply air-drying or baking the membrane. Air-drying typically involves exposure for 2–8 h. The alternative is oven-drying at 80°C for 2 h.²⁹ Drying and baking are believed to result in the nucleic acids becoming attached to the membrane through hydrophobic interactions, although the exact nature of the binding is not well understood. Nylon can also be surface-modified during manufacture.⁴¹ In this case, positively charged groups introduced during production are able to enhance separation from the liquid phase by means of electrostatic interaction with the phosphate backbone of the nucleic acid.

When the nucleic acid is dried, a portion of the thymine residues may cross-link to amine groups on the surface of the membrane. This cross-linking can be furthered by exposure to UV radiation,³⁰ which is used for covalent binding of a nylon membrane to a nucleic acid probe through thymine residues (and through other nucleotides to a lesser extent) that react with amine groups present on the nylon membrane when they are activated.³¹ Since some of these bases become covalently linked to the membrane surface, they are unavailable for hybridization. Therefore, the UV linkage can destroy subsequent hybridization especially if the membrane is overexposed.

Immobilizations of acrylamide modified oligonucleotides by co-polymerization have also been described.³² This solid phase attachment of oligonucleotides involves use of oligonucleotides

bearing 5'-terminal acrylamide modifications that efficiently co-polymerize with acrylamide monomers to form thermally stable DNA-containing polyacrylamide co-polymers. Co-polymerization attachment is specific for the terminal acrylamide group. Stable probe-containing layers are easily fabricated on supports bearing exposed acrylic groups, including plastic microtiter plates and silanized glass. Attachment can be accomplished using standard polyacrylamide gel recipes and polymerization techniques with supports having a surface density of hybridizable oligonucleotide of $\sim 200 \text{ fmol/mm}^2$.⁴³

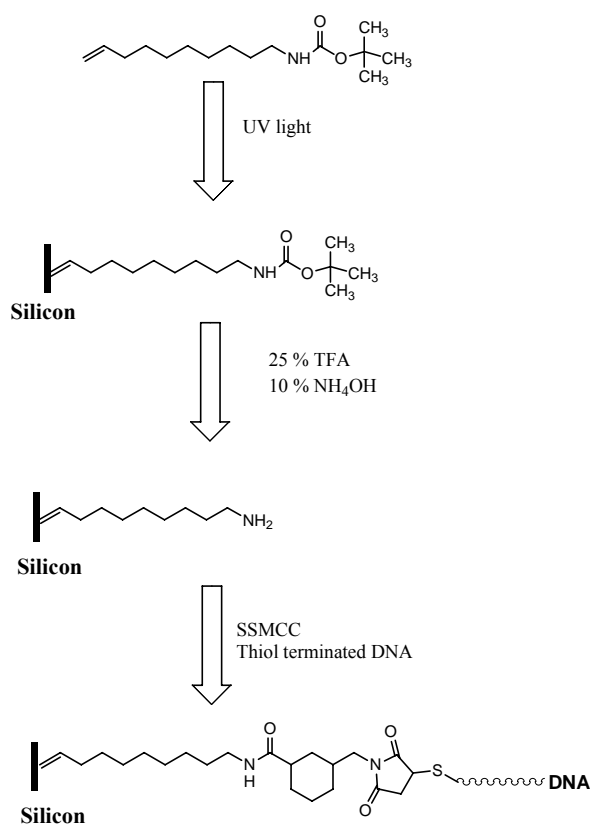


Figure 1.5: Reaction Scheme for immobilization of DNA on amine-modified silicon wafer. A layer of t-boc protected 10-aminodec-1-ene is bound onto silicon surface by applying a thin layer of the protected amine to the wafer and exposing it to UV light from a low pressure mercury vapor lamp. Deprotection is achieved by treating the surface with 25% TFA in methylene chloride for 1 h followed by a 5 min rinse in 10 % NH_4OH . The heterobifunctional crosslinker, succinimidyl-4-(N-maleimidomethyl)cyclohexane-1-carboxylate (SSMCC) is added to the surface which binds to the free amines through an N-hydroxysuccinimidyl ester. Thiol terminated DNA is then bound to the maleimide groups of the SSMCC.²⁸

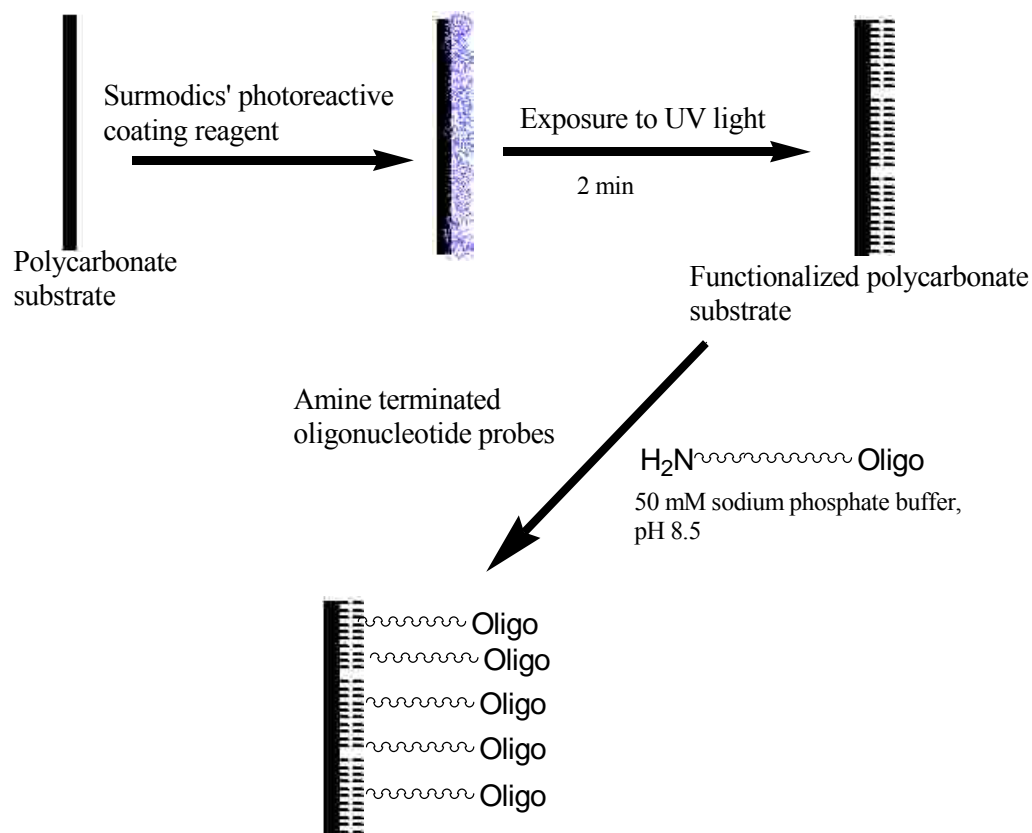


Figure 1.6: The surmodics probe attachment chemistry. A polymer surface is coated with the Surmodics' photoreactive coating reagent and exposed to UV light yielding functional groups that allow amine-terminated oligonucleotide probes to be covalently attached on the surface via a Schiff-base reaction.

Ralf Lenigk and coworkers³³ have also demonstrated printing of pre-synthesized probes onto polycarbonate (PC) substrates coated with bi-functional linker molecules for the immobilization of pre-synthesized amine-terminated oligonucleotide probes (see Figure 1.6). In this work, surmodics photoreactive coating reagents were used for coating the polymeric surfaces. The Surmodics' PhotoLink reagents contain diradical aromatic ketone groups which, when illuminated with blue or ultraviolet light, generate a relatively longer-lived di-radical triplet state. This highly reactive intermediate is then capable of insertion into carbon-hydrogen bonds by abstraction of a hydrogen atom from the polymer surface, followed by collapse of the resulting radical pair to form a new carbon-carbon bond. The high energy of the triplet state makes the photochemical coupling process relatively independent of the chemical composition of the

surface, with the efficiency of the process being determined by the relative stability of the free radicals formed on the surface of the polymer.

1.4 Detection of Hybridization Events on Microarrays

1.4.1 Radioactive Detection

Radioactive detection usually involves the use of targets labeled with ^3H , ^{32}P , ^{33}P , or ^{35}S . Traditionally, labeling of nucleic acids has been conducted by incorporating nucleotides containing radioisotopes. Such radiolabeled probes contain nucleotides with a radioisotope (often ^{32}P , ^{33}P , ^{35}S or ^3H), which can be detected specifically in solution or, much more commonly, within a solid specimen. The intensity of an autoradiographic signal is dependent on the intensity of the radiation emitted by the radioisotope, and the time of exposure, which may often be long (one or more days, or even weeks in some applications). ^{32}P has been used widely in Southern blot hybridization, dot-blot hybridization, colony and plaque hybridization (see Table 1.1 below) because it emits high energy β -particles which afford a high degree of sensitivity of detection. It has the disadvantage, however, that it is relatively unstable.

Table 1.1. Characteristics of radioisotopes commonly used for labeling DNA and RNA probes

| Radioisotope | Half-life | Decay type | Energy of emission (MeV) |
|-----------------|-----------|------------|--------------------------|
| ^3H | 12.4 yrs | β^- | 0.019 |
| ^{32}P | 14.3 days | β^- | 1.710 |
| ^{33}P | 25.5 days | β^- | 0.248 |

Additionally, its high energy β -particle emission can be a disadvantage under circumstances when fine physical resolution is required to interpret the resulting image unambiguously. ^{35}S and ^{33}P have moderate half-lives while ^3H has a very long half-life.

However, the latter isotope is disadvantaged by its comparatively low energy β -particle emission which necessitates very long exposure times. ^{32}P -labeled and ^{33}P -labeled nucleotides used in DNA strand synthesis labeling reactions have the radioisotope at the α -phosphate position, because the β - and γ -phosphates from dNTP precursors are not incorporated into the growing DNA chain. Kinase-mediated end-labeling, however, uses $[\gamma\text{-}^{32}\text{P}]\text{ATP}$ (see Figure 1.7) In the case of ^{35}S -labeled nucleotides which are incorporated during the synthesis of DNA or RNA strands, the NTP or dNTP carries a ^{35}S isotope in place of the O of the α -phosphate group. ^3H -labeled nucleotides carry the radioisotope at several positions. After hybridization with a radioactive labeled target, the distribution of hybridized targets is detected by either exposing the array slide to an X-ray film or dipping the slides in photographic emulsion to obtain radioactive images.

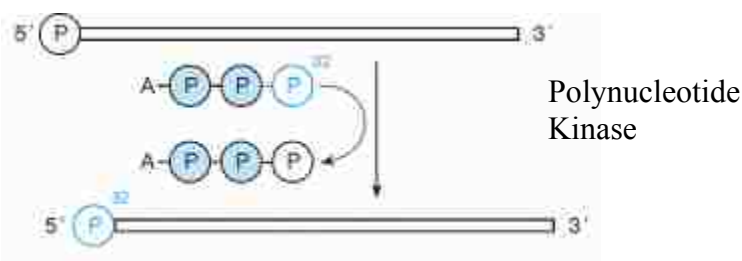


Figure 1.7: Kinase end-labeling of oligonucleotides. The 5'-terminal phosphate of the oligonucleotide is replaced in an exchange reaction by the ^{32}P -labeled γ -phosphate of $[\gamma\text{-}^{32}\text{P}]\text{ATP}$. The same procedure can be used to label the two 5' termini of double-stranded DNA.³⁴

Radioactive detection offers several advantages; for example it has a wide dynamic range and quantitative analysis is very precise. It is also easy to label targets to a high specific activity by using well-established labeling methods. In general, the drawbacks of using radio-labeled targets are that long exposure times are needed, radioactive decay leads to a limited visualization window and the safety and disposal problems associated with radioactive material.

1.4.2 Electrochemical Detection of Microarrays

Microarrays can also be detected by electrochemical techniques. Electrochemical detection systems require small currents or voltages, they are portable, simple, and less expensive and the fewer component requirements result in smaller foot prints. These methods have a spatial array of electrodes that are hardwired to individually addressable locations and scanning is performed by measuring an electrical property independently at each electrode in either a serial or parallel manner. For example, capacitance at a surface can be determined by the existence of charge and the ability of the region near the surface to charge or discharge. As such, capacitance at the surface with ssDNA will be different from hybridization events creating dsDNA, therefore, by measuring the capacity, the existence of a hybrid can be determined. Another example of electrochemical detection of DNA arrays have been described by Guodong Lieu et al.³⁵ They used inorganic nanocrystal tracers for coding SNPs. In their work, they demonstrate that the electrodiverse population of inorganic nanocrystal tags 20 yields distinct four potential voltammetric signatures for all eight unknown SNPs. They linked, ZnS, CdS, PbS, and CuS to A, C, G and T mononucleotides by using phosphoramidite chemistry through a cysteamine linker. Sequential introduction of the monobase-conjugated nanocrystals to the hybrid-coated magnetic-bead solution leads to their specific binding, via base-pairing, to different complementary mismatched sites, as well as to previously linked conjugates (Figure 1.8). Each mutation thus captured different nanocrystal-monomucleotide conjugates. Taking, for example, the T-G mutation (bottom of Figure 1.8), where the T and G capture A-ZnS and C-CdS, respectively, followed by base pairing of T-CuS and G-PbS to the captured A-ZnS and C-CdS, respectively. This resulted in a characteristic four-potential voltammogram, whose peak potentials reflect the identity of the mismatch. Other examples of electrochemical detection methods for microarray applications have been described in the literature.³⁶⁻³⁸

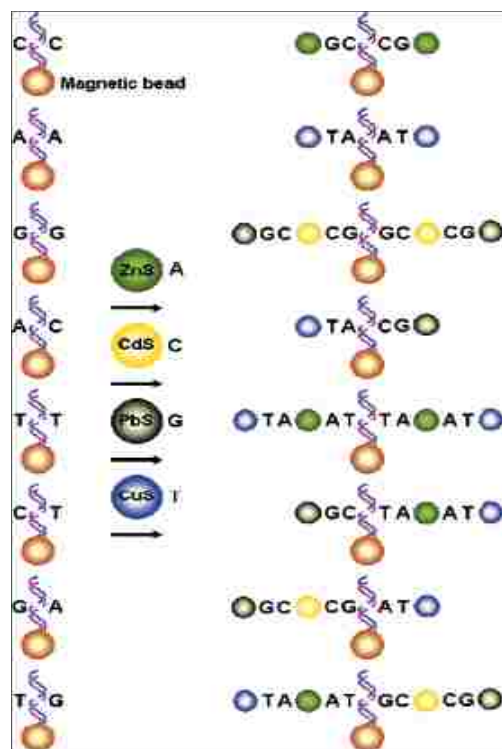


Figure 1.8: Electrochemical coding of all eight possible one-base mismatches using inorganic nanocrystal tracers. Mismatch-containing hybrids were captured on magnetic beads followed by sequential additions of ZnS-linked adenosine-5' monophosphate, CdS-linked cytosine-5' monophosphate, PbS-linked guanosine-5' monophosphate, and CuS-linked thymidine-5' monophosphate.³⁵

1.4.3 Detection of Microarrays by Surface Plasmon Resonance Techniques

Surface Plasmon Resonance (SPR) is an optical detection technique based on reflection and refraction. In SPR, a solution containing the target molecules flows across a chip with probes immobilized on the surface. On the other side of the chip is a thin film of metal (usually gold). When plane-polarized light hits the gold film at a certain angle under total internal reflection conditions, light will be absorbed by the gold film and changed into surface plasmon on the gold surface.³⁹ The technique can be used to measure interactions of various biomolecules including peptides, proteins, nucleic acids, carbohydrates and phospholipid vesicles.^{40, 41} One binding partner is immobilized on the surface of a sensor chip, whereas the other binding partner is carried in a flow of buffer solution through a miniature flow cell (Figure 1.9). Any binding event on the surface of the sensor chip leads to a change in refractive index at the surface layer and is

monitored by a detector (e.g. diode array). The mass of the molecules bound on the gold film varies proportionally to the SPR angle. Therefore, as the solution flows by, target molecules bind to the probes leading to change to the SPR angle. Since the detection of target molecule only requires the solution to flow pass the chip, SPR has a significantly easier procedure than fluorescent techniques. The stability of the sample is increased because the light beam does not pass through the sample but only reflects from the sample. Without the bleaching problem of the fluorescence dyes, high intensity of light can be applied to shorten the detection time. Furthermore, the adsorption characteristics can be evaluated continuously with time. This allows kinetic, affinity, and mass transport measurements. Automation of the system enables accuracy and precision in all steps of the analysis, and increases both ease of use and reproducibility.⁴⁴⁻⁴⁶

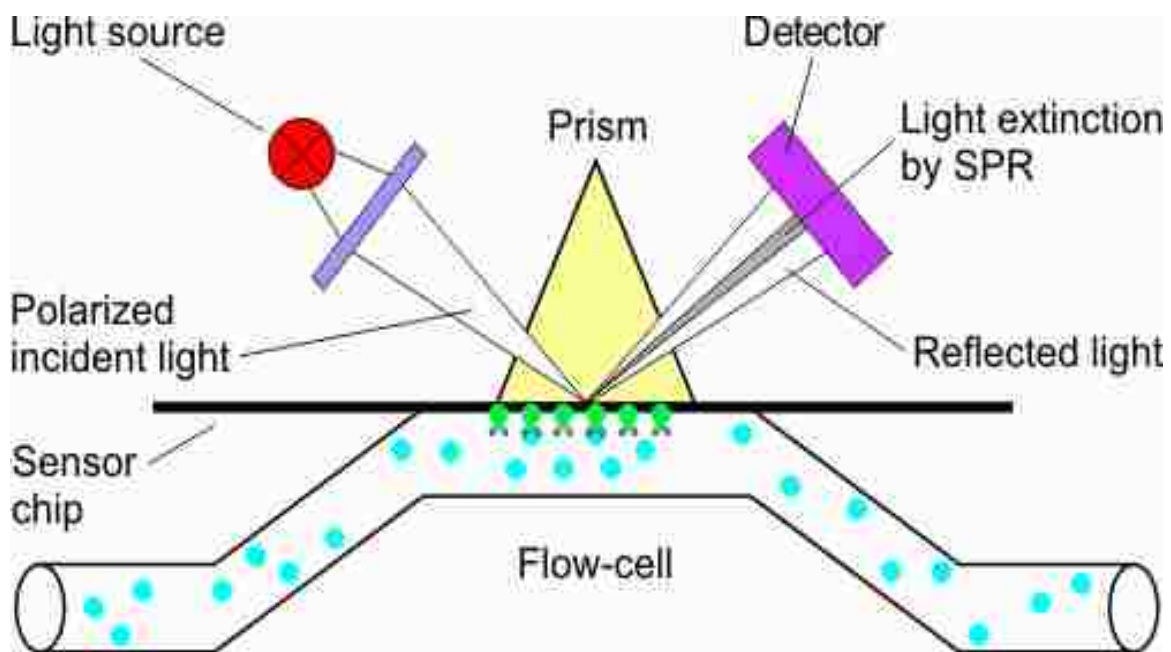


Figure 1.9: Principle of SPR Spectroscopy. One binding partner is immobilized on the surface of a sensor chip in a flow cell. The other binding partner is flowing over the surface of the sensor chip and allowed to interact with the immobilized molecules. A binding event on the surface of the sensor chip is monitored by a change in refractive index close to the surface of the sensor chip.^{42,43}

1.4.4 Fluorescence Detection of Hybridization Events on Arrays

Fluorescence detection technique was adopted after the first demonstrations of the use of fluorescence tags to label DNA oligonucleotides, making it the predominant detection protocol in DNA microarrays. Fluorescence is a form of luminescence; which involves the emission of light from any substance and it occurs from electronically excited states. Fluorescence typically occurs from aromatic molecules. Light is absorbed by these molecules in about 10^{-15} seconds which causes electrons to become excited to a higher electronic state. The electrons remain in the excited state for about 10^{-8} seconds then, assuming all of the excess energy is not lost by collisions with other molecules, the electron returns to the ground state. Energy is emitted during the electrons' return to their ground state. Emitted light is always a longer wavelength than the absorbed light due to limited energy loss by the molecule prior to emission.⁴⁷ Besides fluorescence emission, it is possible for the spin states of the excited molecules to be unpaired (excited triplet state) and their return to the ground state is accompanied by emission of a photon; a process called phosphorescence.⁴⁷ An energy-level schematic, known as the Jablonski diagram, is typically used to illustrate the light absorption and emission process of these two processes (Figure 1.10). This diagram shows a series of increasing energy levels; ground electronic state, excited singlet state and the triplet excited state. At each of these electronic energy states, there also exist a number of vibrational energy levels indicated by the solid horizontal lines. When a fluorophore in the ground state is excited (absorbs photons of the appropriate wavelength), some of the electrons in the ground state jump to higher vibrational energy levels of the excited singlet state. These excited state electrons relax rapidly to the lowest vibrational level of the excited singlet state in 10^{-12} s, a process called internal conversion, from there they return to the ground state energy level with the accompanying emission of photons in 10^{-8} s; this process is called fluorescence emission.⁴⁷ Other than fluorescence emission, electrons in the excited state can also

undergo a spin conversion (intersystem crossing) after which they move to the excited triplet state followed by a return to the ground state level with the emission of photons, a process called phosphorescence. Phosphorescence emission has longer time scales that could last fractions of seconds to several minutes as compared to fluorescence emission because the electronic transitions involved (triplet to singlet) are spin-forbidden. Other factors that could compete with the fluorescence emission, which are not illustrated in the Jablonski diagram, are solvent effects, solvent relaxation, quenching and a variety of excited state reactions.⁴⁷

Use of fluorescence chromophores has different advantages. In particular, they allow double labeling and high resolution imaging which is very attractive especially when read out of multiple expression patterns in cells or biological components is desired. Use of confocal imaging microscopy for instance reduces noise by removing out of focus background. In a confocal imaging system a single point of excitation light (or sometimes a group of points or a slit) is scanned across the specimen. The point is a diffraction limited spot on the specimen and is produced either by imaging an illuminated aperture situated in a conjugate focal plane to the specimen or, more usually, by focusing a parallel laser beam. With only a single point illuminated, the illumination intensity rapidly falls off above and below the plane of focus as the beam converges and diverges, thus reducing excitation of fluorescence for interfering objects situated out of the focal plane being examined. Fluorescence emission light (i.e. signal) passes back through the dichroic reflector and then passes through a pinhole aperture situated in a conjugate focal plane to the specimen. Any light emanating from regions away from the vicinity of the illuminated point will be blocked by the aperture, thus providing yet further attenuation of out-of focus interference. Light passing through the image pinhole is detected by a photo detector as illustrated in Figure 1.11 below. In summary, a confocal imaging system achieves out-of-focus rejection by two strategies; (a) illuminating a single point of the specimen at any

one time with a highly focused beam so that illumination intensity drops off rapidly above and below the plane of focus and; (b) by the use of blocking a pinhole aperture in a conjugate focal plane to the specimen so that light emitted away from the point in the specimen being illuminated is blocked from reaching the detector. In the experiments reported herein, we adopted a confocal principle to develop a fluorescence scanner that could produce complete images of relatively large regions for use in the detection of hybridization events on microarrays.

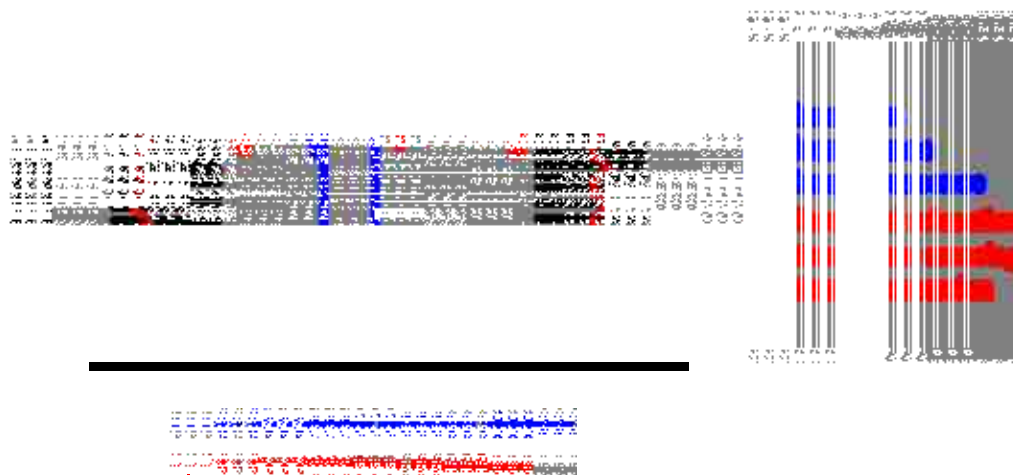


Figure 1.10: Jablonski diagram. Block energy diagram illustrating the various radiative and non-radiative processes that occur when a molecule absorbs a photon of light.

All microarray experiments performed were read out by using a near-IR fluorescence scanner set up built in-house (see Figure 1.12 below) that is based on the confocal microscopy principle. It consisted of a laser diode excitation source lasing at 670 nm with an optical output power of 10 mW (Thorlabs, Newton, NJ). The excitation beam was passed through a neutral density filter (ND 0.6, Thorlabs) and a line filter (670DF20, Omega Optical, Brattleboro, VT). A beam splitter (690DRLP, Omega Optical) was positioned at a 45° angle and focused onto the array surface using a 40X high-numerical aperture (numerical aperture = 0.85) microscope objective (Nikon, Natick, MA). The fluorescence was then collected by the same microscope

objective and transmitted through the dichroic and finally, through stacked filters consisting of a 700 ALP long-pass filter and a 720 DF20 band-pass filter (Omega Optical). After passing through the filters, the fluorescence was sent through a pin hole and focused onto a Single Photon Avalanche Diode (SPAD) detector. The entire detector was mounted on an X/Y microtranslational stage interfaced to a PC computer. This was controlled by two bipolar stepper motors also interfaced to the PC computer by using STP-100 stepper motor controller boards that were obtained from Pontech, Inc. (Upland, CA). The motors drove the x and y directions of the micro-translational stages.

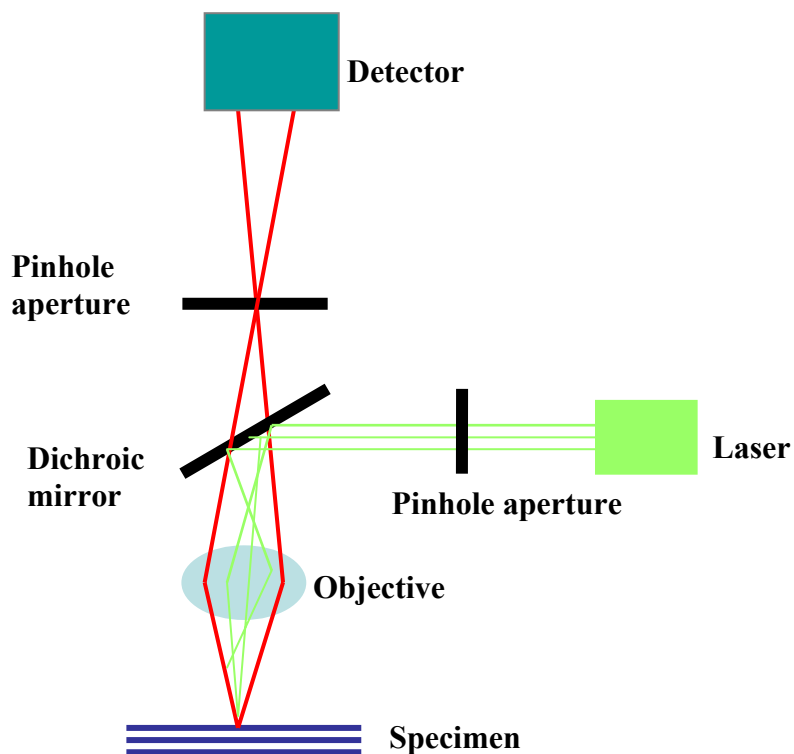


Figure 1.11: A diagram of the confocal principle. The principle of confocal microscopy is the elimination of out of focus light, thus producing a high z-resolution image. First, incident light is focused to a particular point within the specimen by passing it through a very small aperture, such as a pinhole or slit. The focusing helps to limit the excitation of fluorophores above and below the plane of focus. Second, any emission that is above or below the plane of focus is blocked from reaching the detector by passing it through a second pinhole. The specimen is placed in the light-path at a conjugate focal plane such that movement in the vertical (z) direction keeps the focus at a fixed distance from the objective, and effectively scans in layers through the specimen.

Each STP-100 was equipped with the RS-485 interface allowing full duplex, multi-drop communication with the host computer. A PP232-485 interface (Pontech, InC.) was used to convert RS485 into the PC's RS232 protocol. Hall sensors were used to monitor the travel limits of the X/Y stages. The smallest step resolution of these stages was 12.7 μm with a scan range of 4 cm by 7cm in the X and Y coordinates, respectively.

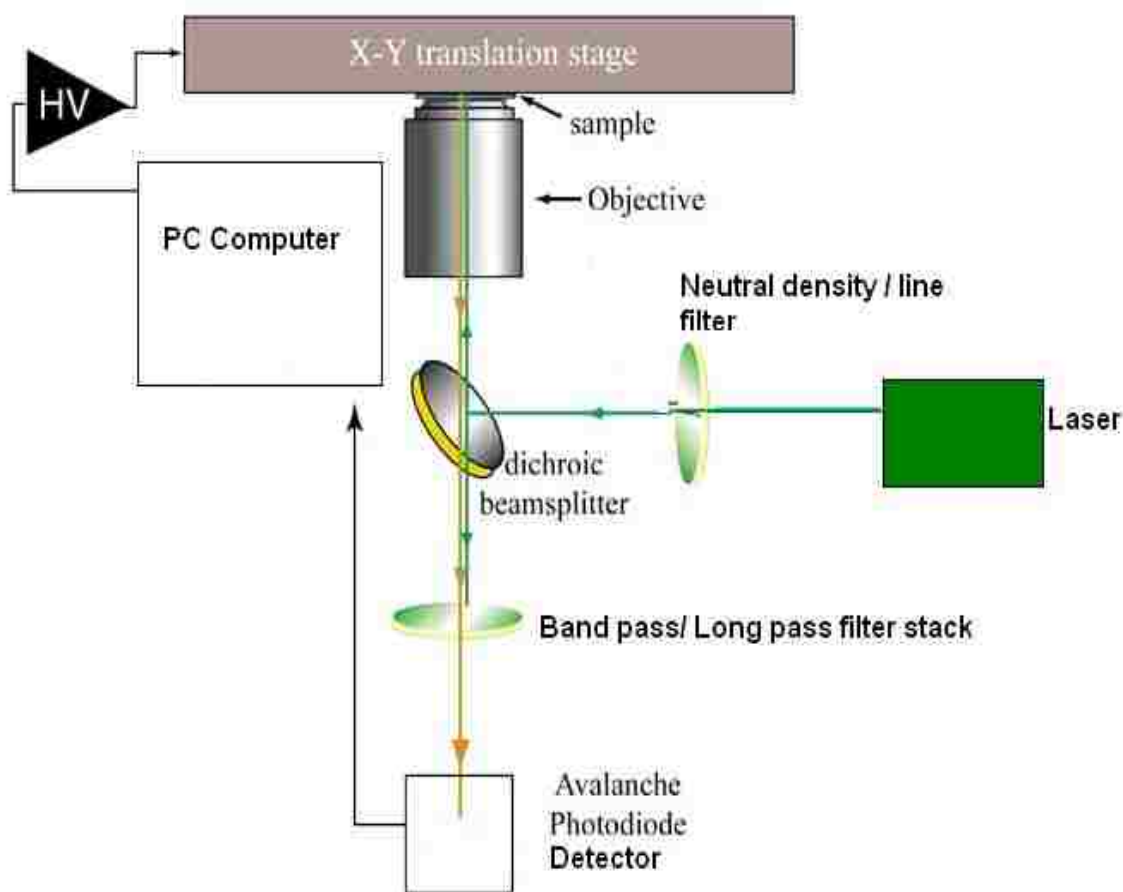


Figure 1.12: A diagrammatic representation of the fluorescence scanner built in house for imaging microarrays. The sample is excited by an excitation beam which is passed through the neutral density and line filters. Fluorescence is collected and transmitted through the dichroic and a stack of long-pass and band-pass filters and passed on to the SPAD detector.

The scanner was operated by taking a single step and then, acquiring the fluorescence data for a software-selectable integration period (10 ms - 10 s). The data acquisition software was written in Visual Basic and consisted of several control and data acquisition functions such as, recording

the position of the scanning head, streaming data to the hard drive and providing real-time visualization of the acquired images. During a typical experiment, 4 – 12 MB of data was generated and stored in chunks of 2 GB. After imaging the array, the data was compressed one scan line at a time and subsequently assembled into one contiguous file.

The most common method for analyzing hybridization events of DNA microarrays is fluorescence. However, many different methods have been demonstrated as discussed above. Table 1.2 below summarizes the commonly used microarray detection techniques giving some advantages and shortcomings of each detection method.

Table 1.2. Advantages and disadvantages of commonly used microarray detection techniques

| Detection Technique | Advantages | Disadvantages |
|---------------------|-------------------------------------------------------------------------------------------------------------------------------------------------------------------------------------------------------------------------------------------------------------------------------------------------------------------------------------------------------------------------------------------------------------------------|---------------------------------------------------------------------------------------------------------------------------------------------------------------------------------------------------------------------------------------------------------------------------------|
| Fluorescence | <ul style="list-style-type: none"> (i) Very sensitive (ii) Highly specific and it is less susceptible to interferences because fewer materials absorb and also fluoresce (iii) Fluorescence output is linear to sample concentration over a very broad range (iv) It is a relatively simple analytical technical (v) Multilabeling allows multiplexing capabilities. | <ul style="list-style-type: none"> (i) Requires costly optical systems with good scanning systems (ii) Scanning resolution depends on the width of the laser beam therefore becomes crucial for high density microarrays whose array spot is very small |
| Radiochemical | <ul style="list-style-type: none"> (i) Quantitative analysis is very precise (ii) Very sensitive but the sensitivity of the detection correlates to the rate of decay of the radioisotope label being used (iii) Can easily be incorporated into analytes without altering their structure or reactivity | <ul style="list-style-type: none"> (i) Radioactive decay of radio labels leads to a limited visualization window (short shelf-life of labels) (ii) Waste handling of radioactive material is crucial |

(table cont'd.)

| | | |
|---------------------------|--------------------------------------------------------------------------------------------------------------------------------------------------------------------------------------------------------|--------------------------------------------------------------------------------------------------------------------------------------------------------------------------------------------------------------------------|
| Electrochemical | (i) Requires small voltages and current (ii) Easily portable (iii) It is simple and less expensive (iv) Requires no labeling | (i) Not very sensitive (ii) Non-specific |
| Surface Plasmon Resonance | (i) Label free detection (ii) Distinguishes surface bound material from bulk material (iii) Monitors molecular interactions in real-time kinetics (iv) Highly sensitive (ng of adsorbed mass) | (i) SPR biosensors lack the sensitivity to detect the interactions of proteins with very small ligands (ii) Unsuitable for high throughput applications because they are unable to handle many samples simultaneously |

1.5 References

- (1) Schena, M.; Shalon, D.; Davis, R. W.; Brown, P. O. *Science (Washington, D. C.)* **1995**, *270*, 467-470.
- (2) Dolan, P. L.; Wu, Y.; Ista, L. K.; Metzberg, R. L.; Nelson, M. A.; Lopez, G. P. *Nucleic Acids Research* **2001**, *29*, e107/101-e107/108.
- (3) Southern, E. M. *Journal of Molecular Biology* **1975**, *98*, 503-517.
- (4) Watson, J. D.; Crick, F. H. C. *Nature (London, United Kingdom)* **1953**, *171*, 737-738.
- (5) Zhang, Y.; Coyne, M. Y.; Will, S. G.; Levenson, C. H.; Kawasaki, E. S. *Nucleic Acids Research* **1991**, *19*, 3929-3933.
- (6) Lebrun, S. J. *Pharmaceutical Discovery* **2005**, *Suppl.*, 53-56.
- (7) MacBeath, G. *Nature genetics* **2002**, *32 Suppl*, 526-532.
- (8) MacBeath, G.; Schreiber, S. L. *Science (Washington, D. C.)* **2000**, *289*, 1760-1763.
- (9) McClain, M. A.; Culbertson, C. T.; Jacobson, S. C.; Allbritton, N. L.; Sims, C. E.; Ramsey, J. M. *Analytical Chemistry* **2003**, *75*, 5646-5655.
- (10) Pease, A. C.; Solas, D.; Sullivan, E. J.; Cronin, M. T.; Holmes, C. P.; Fodor, S. P. *Proceedings of the National Academy of Sciences of the United States of America* **1994**, *91*, 5022-5026.

- (11) Postier, B. L.; Wang, H.-L.; Singh, A.; Impson, L. A.; Andrews, H. L.; Klahn, J.; Li, H.; Risinger, G.; Pesta, D.; Deyholos, M.; Galbraith, D. W.; Sherman, L. A.; Burnap, R. L. *BMC Genomics* **2003**, *4*, No pp given.
- (12) Bussow, K.; Nordhoff, E.; Lubbert, C.; Lehrach, H.; Walter, G. *Genomics* **2000**, *65*, 1-8.
- (13) Wu, R. Z.; Bailey, S. N.; Sabatini, D. M. *Trends in Cell Biology* **2002**, *12*, 485-488.
- (14) Kapur, R. *Microarray Technology and Its Applications* **2005**, 335-343.
- (15) Baner, J.; Isaksson, A.; Waldenstroem, E.; Jarvius, J.; Landegren, U.; Nilsson, M. *Nucleic Acids Research* **2003**, *31*, e103/101-e103/107.
- (16) Erali, M.; Schmidt, B.; Lyon, E.; Wittwer, C. *Clinical Chemistry (Washington, DC, United States)* **2003**, *49*, 732-739.
- (17) Grimm, V.; Ezaki, S.; Susa, M.; Knabbe, C.; Schmid, R. D.; Bachmann, T. T. *Journal of Clinical Microbiology* **2004**, *42*, 4918.
- (18) Ishikawa, S.; Komura, D.; Tsuji, S.; Nishimura, K.; Yamamoto, S.; Panda, B.; Huang, J.; Fukayama, M.; Jones, K. W.; Aburatani, H. *Biochemical and Biophysical Research Communications* **2005**, *333*, 1309-1314.
- (19) Lin, M.; Wei, L.-J.; Sellers, W. R.; Lieberfarb, M.; Wong, W. H.; Li, C. *Bioinformatics* **2004**, *20*, 1233-1240.
- (20) Lovmar, L.; Fock, C.; Espinoza, F.; Bucardo, F.; Syvanen, A.-C.; Bondeson, K. *Journal of Clinical Microbiology* **2003**, *41*, 5153-5158.
- (21) Meaburn, E.; Butcher, L. M.; Schalkwyk, L. C.; Plomin, R. *Nucleic Acids Research* **2006**, *34*, e27.
- (22) Peterson, A. W.; Heaton, R. J.; Georgiadis, R. M. *Nucleic Acids Research* **2001**, *29*, 5163-5168.
- (23) Fodor, S. P. A.; Read, J. L.; Pirrung, M. C.; Stryer, L.; Lu, A. T.; Solas, D. *Science (Washington, DC, United States)* **1991**, *251*, 767-773.
- (24) Southern, E. M.; Case-Green, S. C.; Elder, J. K.; Johnson, M.; Mir, K. U.; Wang, L.; Williams, J. C. *Nucleic Acids Research* **1994**, *22*, 1368-1373.
- (25) Gingeras, T. R.; Kwoh, D. Y.; Davis, G. R. *Nucleic Acids Research* **1987**, *15*, 5373-5390.
- (26) Okamoto, T.; Suzuki, T.; Yamamoto, N. *Nature biotechnology* **2000**, *18*, 438-441.
- (27) Pirrung, M. C. *Angewandte Chemie, International Edition* **2002**, *41*, 1276-1289.
- (28) Strother, T.; Hamers, R. J.; Smith, L. M. *Nucleic Acids Research* **2000**, *28*, 3535-3541.

- (29) Nierzwicki-Bauer, S. A.; Gebhardt, J. S.; Linkkila, L.; Walsh, K. *BioTechniques* **1990**, *9*, 472-474, 476, 478.
- (30) Li, J. K.; Parker, B.; Kowalik, T. *Analytical biochemistry* **1987**, *163*, 210-218.
- (31) Saito, I.; Sugiyama, H.; Furukawa, N.; Matsuura, T. *Tetrahedron Letters* **1981**, *22*, 3265-3268.
- (32) Rehman, F. N.; Audeh, M.; Abrams, E. S.; Hammond, P. W.; Kenney, M.; Boles, T. C. *Nucleic Acids Research* **1999**, *27*, 649-655.
- (33) Lenigk, R.; Liu, R. H.; Athavale, M.; Chen, Z.; Ganser, D.; Yang, J.; Rauch, C.; Liu, Y.; Chan, B.; Yu, H.; Ray, M.; Marrero, R.; Grodzinski, P. *Analytical Biochemistry* **2002**, *311*, 40-49.
- (34) Strachan, T.; Read, A. P. *Human Molecular Genetics, 2nd Edition*, 1999.
- (35) Liu, G.; Lee, T. M. H.; Wang, J. *Journal of the American Chemical Society* **2005**, *127*, 38-39.
- (36) Hashimoto, K.; Ishimori, Y. *Lab on a chip* **2001**, *1*, 61-63.
- (37) Yu, C. J.; Wan, Y.; Yowanto, H.; Li, J.; Tao, C.; James, M. D.; Tan, C. L.; Blackburn, G. F.; Meade, T. J. *Journal of the American Chemical Society* **2001**, *123*, 11155-11161.
- (38) Dill, K.; Montgomery, D. D.; Ghindilis, A. L.; Schwarzkopf, K. R.; Ragsdale, S. R.; Oleinikov, A. V. *Biosensors & Bioelectronics* **2004**, *20*, 736-742.
- (39) Bohren, C. F.; Huffman, D. R. *Absorption and Scattering of Light by Small Particles*, 1983.
- (40) Malmqvist, M. *Current Opinion in Immunology* **1993**, *5*, 282-286.
- (41) Malmqvist, M. *Nature* **1993**, *361*, 186-187.
- (42) Fischer, T.; Beyermann, M.; Koch, K. W. *Biochemical and biophysical research communications* **2001**, *285*, 463-469.
- (43) Lange, C.; Koch, K. W. *Biochemistry* **1997**, *36*, 12019-12026.
- (44) Nelson, R. W.; Krone, J. R.; Jansson, O. *Analytical chemistry* **1997**, *69*, 4363-4368.
- (45) Rich, R. L.; Myszka, D. G. *Journal of Molecular Recognition* **2001**, *14*, 273-294.
- (46) Rich, R. L.; Myszka, D. G. *Journal of Molecular Recognition* **2001**, *14*, 223-228.
- (47) Lakowicz, J. R. *Principles of Fluorescence Spectroscopy*, 1983.

CHAPTER 2

MERGING MICROFLUIDICS WITH MICROARRAY TECHNOLOGY*

2.1 Introduction

Microarray technologies provide powerful tools for biomedical researchers and medicine, since arrays can be configured to monitor the presence of molecular signatures in a highly parallel fashion and can be configured to search either for nucleic acids (DNA microarrays) or proteins (antibody-based microarrays) as well as different types of cells. Microfluidics on the other hand, provides the ability to analyze small volumes (micro, nano or even pico-liters) of sample and minimize costly reagent consumption as well as automate sample preparation and reduce sample processing time. The marriage of microarray technologies with the emerging field of microfluidics provides a number of advantages such as, reduction in reagent cost, reductions in hybridization assay times, high-throughput sample processing, and integration and automation capabilities of the front-end sample processing steps. However, this potential marriage is also fraught with some challenges as well, such as developing low-cost manufacturing methods of the fluidic chips, providing good interfaces to the macro-world, minimizing non-specific analyte/wall interactions due to the high surface-to-volume ratio associated with microfluidics, the development of materials that accommodate the optical readout phases of the assay and complete integration of peripheral components (optical and electrical) to the microfluidic to produce autonomous systems appropriate for point-of-care testing. In this Chapter, we provide an overview and recent advances on the coupling of DNA, protein and cell microarrays to microfluidics and discuss potential improvements required for the implementation of these technologies into biomedical and clinical applications.

* Reprinted with permission from *Biomolecular Engineering* 2006, 23(5), 213-231

2.2 Microfluidics: Basic Fabrication and Operation

Microfluidics is an emerging and relatively new technology platform that typically requires a multi-disciplinary approach for building effective systems through the interface of physics, chemistry, engineering and biochemistry. These devices usually consist of structures that are fabricated in the micrometer-scale and can be designed to produce diagnostically useful systems for potential point-of-care measurements. Systems based upon microfluidic operation possess a unique set of potential advantages, such as reduction in reagent cost, enhancement of assay speed, potential for mass production of devices at low cost and the ability to integrate several processing steps into a single system (i.e., high levels of system automation). Decreased reagent consumption eventually results in the reduction of assay cost, which could translate into large-scale molecular screening of certain diseases for early detection. The accelerated analysis time is directly gained from the reduced footprint of these devices. Other benefits of microfluidic-based systems include high-throughput biological screening by parallel processing of multiple samples achieved with multiple fluidic paths and the minimization of cross contamination, since different samples flow through separate fluidic processors in closed architectures.

Microfluidic devices can be fabricated from a variety of materials using different techniques. Based primarily on the fabrication techniques developed in the microelectronics sector, silicon and glass have traditionally been used to create microfluidic devices.^{1, 2} Microfabrication in glass/silicon substrates has been accomplished through the use of lithography, plasma etching or reactive ion etching techniques.³ The particularly attractive advantages of glass and quartz include their well defined surfaces and excellent optical properties, which are highly desired for signal readout of microarrays by fluorescence. However,

the fabrication processes involved are fairly time consuming, labor intensive and relatively expensive.

Polymers are rapidly evolving as alternative substrate materials for many microfluidic applications due to their diverse properties that can be selected to suite the particular application need and the ability to microfabricate structures in a high production mode and at low cost. The fabrication of the prerequisite fluidic networks on polymer substrates can be achieved by lithography, UV laser ablation, hot embossing, injection molding, or direct micromilling techniques.⁴⁻¹² Hot embossing and/or injection molding involve the use of mold masters containing the desired microstructures to stamp (reverse-duplicate) patterns into the required substrate. The patterns poised on the mold masters can be made either by micromachining or by a lithography-based approach, such as LiGA; German acronym for Lithography (Lithographie), Electroplating (Electroformung) and Molding (Abformung). A schematic of the LiGA processing steps using X-ray lithography to build the microstructures on the mold master is shown in Figure 2.1. The important aspect of this technology is that the difficult fabrication steps, lithography and electroplating, are performed but once and then, parts are micro-replicated from this mold master using either injection molding or hot embossing. For hot embossing, three steps are required: (1) First, the polymer substrates are placed between two metal plates, one containing the microstructure topology, and are heated above their glass transition temperature. (2) A force is applied on the softened polymer by pressing with the heated mold master under vacuum. (3) The metal plates and polymer substrate are cooled below the polymer's glass transition temperature and the metal plates are withdrawn from the polymer part. Due to the simplicity of the process and the fact that the mold master only requires one lithography step to fabricate it, the procedure is very cost effective in that it can mass produce thousands of parts and the whole production process can be completed in < 5 min. Examples of polymer parts

embossed from a mold master are depicted in Figure 2. 1. In addition, the process is conducive to replicating parts in a variety of materials from the same mold master as long as the glass

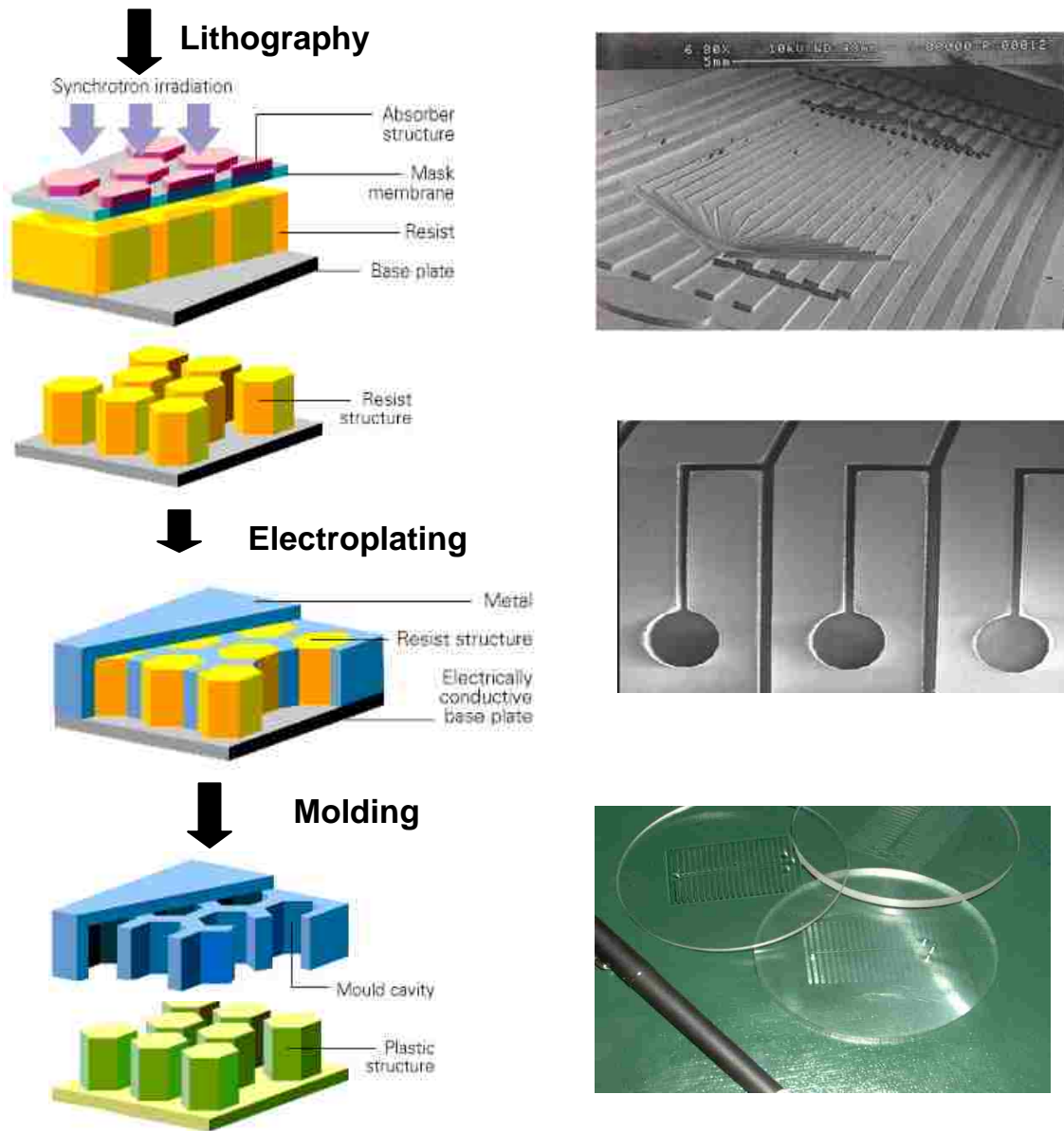


Figure 2.1. Processing steps required to prepare a mold master using X-ray LiGA and molding finished parts. The process starts with a lithography step using a mask that transfers the desired pattern into a photoresist. Following development of the resist, the underlying metal layer is exposed, which serves as a plating base for another metal that fills the voids left by the resist that was removed due to exposure to the patterning radiation. The deposited metal forms the desired microstructures. The unexposed resist is then removed, forming the finished mold master. This mold master is then available for micro-replicating parts in polymers or other materials using hot-embossing or injection molding. Shown on the right in this figure is a picture of a mold master and some parts that have been prepared from the mold master.¹²

transition temperature of the substrate is below the melting point of the master. Once the fluidic network is formed, a cover plate of the same material can be sealed to the substrate to enclose the fluidic channels using a low-temperature sealing process. Using UV laser ablation or micromilling, a polymer substrate can be exposed to laser radiation or a milling bit resulting in the direct writing of the microstructures into the polymer part. In the case of laser ablation, the laser photons, typically from a pulsed excimer laser, are focused directly on the polymer. Fluidic channels are produced either by moving the polymer substrate or by moving a focused laser beam across the surface. This method offers the ability to form complex features with various geometries, even in the third dimension, because the patterning beam can be moved both horizontally and vertically on the substrates. In either case, fluidic prototypes can be rapidly produced using direct write techniques to optimize the device performance prior to mass production using micro-replication techniques.

Poly(dimethylsiloxane) (PDMS) fabrication technology, sometimes called soft lithography, was developed by Whitesides and co-workers and has been widely adopted for the fabrication of different microfluidic networks.¹³⁻¹⁷ Fabrication of microfluidic structures using PDMS technology involves pouring a solution containing the PDMS prepolymer and a curing agent over a relief (mold) containing the prerequisite microstructures followed by curing to cross-link the polymer. This technology first requires creation of positive reliefs using a variety of techniques,^{15,18,19} such as wet etching of silicon or glass following photolithography, micromachining metals or reactive ion etching of silicon. A solution containing the pre-polymer and curing agent is then cast against the relief and the cross-linked polymer conforms to the shape of the relief. After casting, the polymer is simply removed from the relief resulting in a replica that contains the network of microfluidic channels. Finally, the PDMS replicate can be plasma oxidized and sealed to other surfaces by conformal contact to enclose the fluidic network.

Plasma oxidation also renders the PDMS channels hydrophilic so that they can easily be filled with aqueous solutions. Besides plasma oxidation, Quake et al. has also described a method for sealing fluidic networks created in PDMS, which involves the use of two slabs²⁰ one slab consists of an excess of base while the other contains the curing agent. These two are then brought into conformal contact followed by curing.

2.3 Why Merge Microarray Technology With Microfluidics?

For conventional microarrays, several shortcomings exist including: (1) The hybridization (analyte binding) process on supports requires long incubation times to produce the optimal signal because of slow diffusional kinetics as the target molecules must travel to the arrayed probes situated on a surface. This process is typically diffusion-controlled and the fact that reactions on the surface are slow due to local target depletion near the probe environment. (2) The consumption of large amounts of precious sample material for interrogating the array due to the large area occupied by high density arrays ($\sim 1 \text{ cm}^2$). In order to completely cover the array, the volume of sample analyzed must be such that the fluid covers every element of the array. In addition, the large lateral distances that must be traveled by low concentration species for high density arrays in order to find their appropriate binding partners can add to the incubation time, slowing down assay processing rate. (3) The linkage chemistry of the probe to the support can undergo solution-dependent cleavage over the extended incubation times, lowering the reproducibility and sensitivity of the assay. For example, siloxane-based chemistry is typically used to tether molecules to glass, and this is susceptible to hydrolytic cleavage, especially at high or low pH values. Therefore, any process that can enhance the rate of producing the maximum signal for surface-confined association events can provide a number of important benefits, such as reducing the development time and its associated consequences. The use of microfluidic platforms can directly address many of the issues cited above for microarrays

and thus, the merging of microfluidics with microarrays can provide some unique opportunities that are not obtainable when arrays are configured into conventional planar 2-D formats. For example, microfluidic addressing of the array can accelerate hybridization speeds due to the enhanced mass transport of target molecules and reduced diffusional distances required of targets when delivered in a micro-scale flow-through hybridization chamber. In addition, microfluidics can offer the potential for parallel processing of multiple samples. Other advantages offered by the incorporation of microfluidics into the microarray includes reduced reagent and sample volumes and the integration capabilities of sample pre-processing prior to incubation with the array, which can provide high levels of system automation and also, provide closed architectures for sample processing minimizing contamination effects that can give rise to false positives, which can be a significant issue for diagnostic applications.

Since microfluidics is a relatively new field of research, there are likely to be challenges when attempting to merge it to a relatively mature technology platform, such as microarrays. For instance, there is a need for the development or discovery of new materials that are easily fabricated on the size-scale demanded by the microfluidic application and at the same time, offer modification chemistries that allow for the stable attachment of probes. In addition, the fabrication technologies as well as the material used for the device must be low cost if intended for diagnostic screening using microarray-based assays.

Even though miniaturized devices offer the advantages associated with the small scale reactors and fluidic vias used in their implementation, the high surface area to volume ratio associated with these small scales produce surface effects that dominate volume effects. As such, there is the potential for increased surface adsorption of solution molecules that can lead to high-levels of non-specific adsorption, providing poor microarray spot definition or even false positive results. Methods to ameliorate these non-specific adsorption artifacts must be

employed, which can consist of selecting the appropriate substrate for the microfluidic that demonstrates minimal non-specific adsorption for the intended application or to use dynamic or covalent coating procedures of the fluidic substrate.²¹⁻²⁸

While microfluidics can potentially provide the use of reduced sample and reagent volumes due to the small size of these elements, the detection of molecules in dilute solutions will require highly sensitive detection devices, maybe even at the single molecule level. This is so because the number of molecules sampled scales as the cube of the volume analyzed and hence, with low concentration samples the number of molecules interrogated is low for microfluidic based devices, which typically have interrogation volumes that are <1 nL. In addition, the substrate selected for the microfluidic must accommodate the sensitivity requirements for readout. For example, while polymers are attractive due to their low cost and high production capabilities using micro-replication methods, many polymers display poor optical properties that are not conducive to the readout modality required for the array. Judicious selection of the polymer must be undertaken, since several materials do display excellent properties for optical readout, especially when using visible or near-IR fluorescence.²⁹ In order to realize cost-savings in terms of reagent consumption using microchips, precious reagents can be distributed to multi-channel chips by using low-volume fluidic distribution networks.³⁰

Another issue that should be considered is that while the footprint of microfluidic chips have been substantially reduced, these devices must be interfaced to the macro-world. In most cases, microfluidic chip loading, both with reagents and samples, is accomplished using conventional pipettes with fluid movement actuated either electrokinetically or hydrodynamically. In addition, readout of molecular association events must be accomplished using techniques such as laser-induced fluorescence. In most cases, these operational processes are carried out using off-chip apparatus, such as mechanical pumps, high voltage power supplies

and optical readers, similar to those used for reading conventional 2-D microarrays. While efforts have been initiated to package these components into a complete and autonomous system with a footprint similar to that of the fluidic elements, these efforts are still in their infancy. In this Chapter, we will focus primarily on miniaturization efforts focused on the fluidic elements. For information on packaging and integration of ancillary components to the fluidic elements, the reader is referred to the following references.³¹⁻³⁴ This Chapter gives a review of the current research that involves coupling microarrays to microfluidics with emphasis on DNA arrays, protein arrays and cell-based arrays with concluding remarks on potential improvements required for future developments that will allow the benefits of microfluidics/microarray devices to be fully utilized for applications in diagnostics and the understanding of biological function for discovery-based projects.

2.4 Hybridization Speed Enhancement in Microfluidic Devices

In all microarray applications, whether they are DNA or protein-based arrays, the target is typically found in solution and must diffuse to the surface to interact with its probe, since the probe is chemically tethered to the surface and thus, immobile. In addition, it must move laterally to find the location of its appropriate binding partner in 2-D gridded arrays. As such, in many cases, several hours of incubation time are required to allow probe saturation to be obtained due to the slow mass transfer of target to its appropriate probe. For example, with a 1 cm² array area and a low target concentration in the solution, depletion of target near the probe recognition element of the two-dimensional array will require new target to diffuse laterally to “find” its appropriate probe. As a reference, the translational diffusion coefficient for a single-stranded DNA molecule of 30 bases is approximately $2.4 \times 10^{-7} \text{ cm}^2 \text{ s}^{-1}$ at room temperature and in free solution. Therefore, for a molecule to travel laterally 1 cm across the array would require approximately 289 h!

Several techniques have been employed to enhance mass transport of analytes and reduce diffusional distances or by using shallow microchannels (< 100 μm) to reduce the hybridization incubation time. One such technique is the use of continuous flow of targets within microchannels by hydrodynamic pumping.^{35,36-38} Forced flow of the target solution over the probe array surface provides enhanced mass transport of targets to the surface-immobilized probes since the transport does not depend solely on diffusion, but also on convection leading to reduced hybridization times. In addition, the use of shallow fluidic channels reduces the diffusional distances that must be traveled to reach the probe. Hydrodynamic flow has been shown to reduce the hybridization time to less than one minute.³⁶

Introduction of high sample velocities can induce extensional strain to solution targets reducing hybridization time and efficiency as well.³⁹⁻⁴¹ Chung et al. demonstrated that long DNA targets tend to change into a super coil form in solution that reduces hybridization efficiencies due to the inaccessibility of the recognition sequence in the target. Therefore, extensional strain can help to uncoil the long DNA molecules improving hybridization efficiency. The authors were able to show a nearly 9-fold increase in hybridization signal due to strain-induced extension of a 1.4 kbp single-stranded DNA target by introducing a taper within the fluidic channel. Vanderhoeven and coworkers also developed a shear-driven flow system that induced enhanced lateral transport rates in hybridization chambers increasing hybridization efficiencies as well.⁴¹

Another approach for reducing hybridization time is by using active mixing of samples. While the use of devices with small dimensions reduces the target diffusional lengths, the fluidic flow within these devices are uniaxial and laminar due to their low Reynolds numbers. Mixing in such flows is due primarily to molecular diffusion.⁴² The hybridization rate can be improved by active mixing because it can replenish the target concentration in the vicinity of each probe

due to depletion created through binding. Active mixing also relieves the dependence of only lateral diffusion to replenish target near its probe.

Mixing-enhanced hybridization can be described as a three-step process; (1) transport (diffusion and convective flow) of targets in the solution to the diffusion (stagnant) boundary layer, (2) transport (primarily diffusion) of target within the diffusion boundary layer to the probes on the chip surface and, (3) reaction of target with probes on the surface.⁴³ Conventional microstreaming has the ability to provide rapid lateral mass transport and enhanced vertical mass transport of the target DNA in solution. This combination results in rapid transport of targets in solution to the diffusion boundary layer, which allows a continuous replenishment of DNA targets around probes depleted of complementary targets. This phenomenon was later used to perform DNA hybridizations with electrochemical detection on a fully integrated biochip, which consisted of fluidic components that were used to enhance target cell capture and accelerate hybridization reactions.³³

Yaralioglu et al. demonstrated the use of ultrasonic transducers for mixing by an acoustic streaming mechanism. They showed that when reagents were localized within discrete droplets in a microchannel with a low Reynolds number, they could be mixed quickly by re-circulating flows caused by the shearing interaction of the fluid in the plug with the walls of the microchannel.⁴²

Lenigk et al. demonstrated the use of an integrated cartridge, which was comprised of fluidic channel networks and a micropump for the oscillation of the hybridization mixture. Accelerated hybridization times were realized in these channels due to the ability to pass a large number of target molecules per unit time over a probe spot during filling of the channel. This model was then used for the simultaneous detection of four pathogenic bacteria surrogate strains in a parallel format.⁴⁴

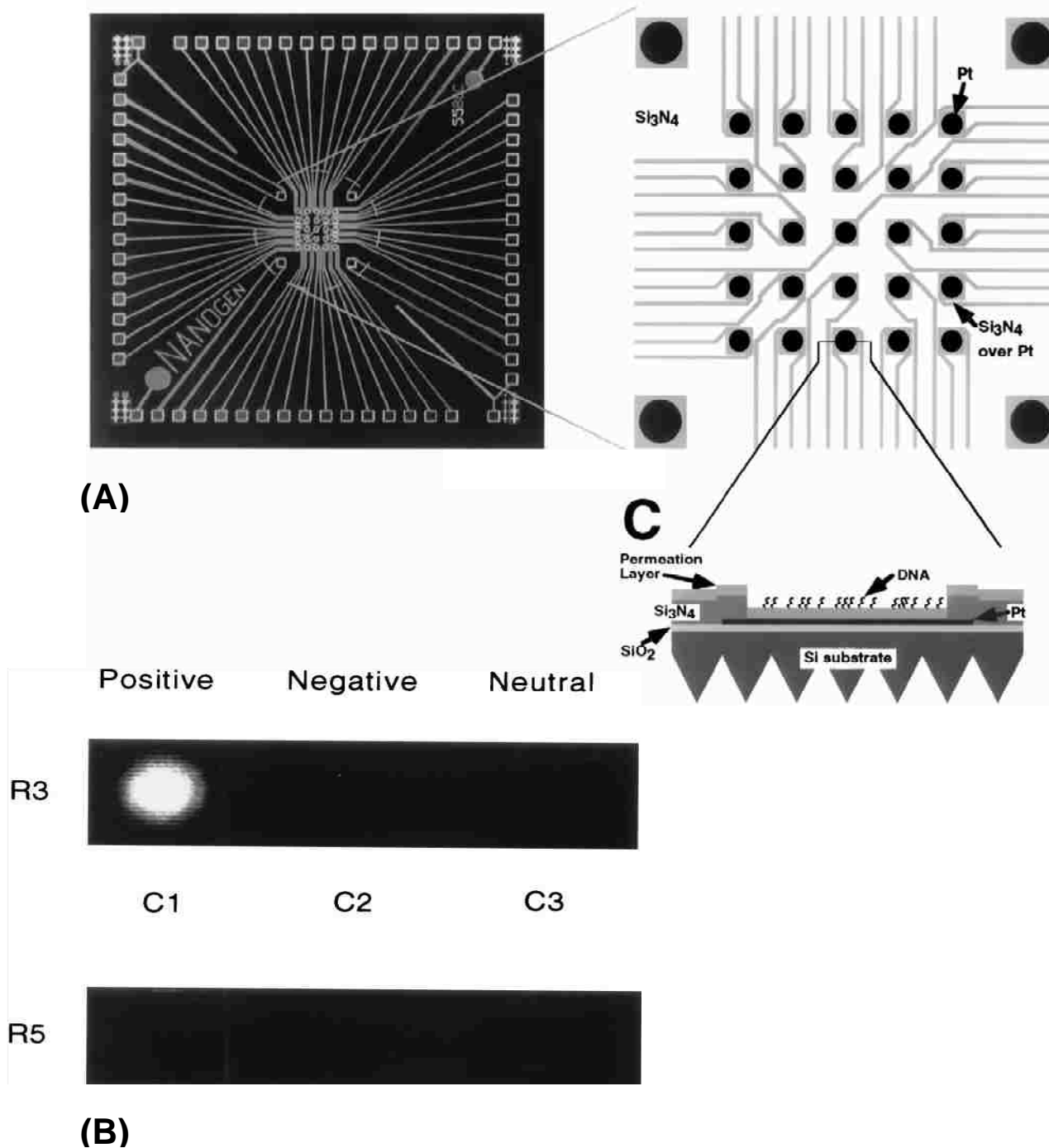


Figure 2.2. (A) Schematic of an array of electrodes fabricated on Si. The 25 electrodes, made from Pt, are 80 μm in diameter and cover an area of 1 cm^2 . The insulating layer consists of silicon nitride layer and over the Pt electrodes was a gel permeation layer consisting of agarose gel loaded with streptavidin. The bottom panel shows a cross section of one element of the array with the immobilized DNA probes. The probes are attached to the permeation layer via a biotin-streptavidin association. (B) Electric field enhanced transport of a poly d(T)₁₂ target to the Pt electrode surface with different bias voltages applied to the Pt electrode: C1 – positive potential; C2 – negative potential; C3 – no potential. R3 and R5 correspond to biotinylated and non-biotinylated probes, respectively.⁴⁹

Bynum et al. used a microfluidic platform consisting of a two-axis centrifuge, whose fluidic chambers rotated in a planetary relationship to produce a radial gravitational field to produce effective mixing based on the promise that this process would overcome surface and viscous forces in microchambers.⁴⁵

Yuen et al. have also developed a microchip device for closed loop fluidic circulation and mixing. The device consisted of two interconnected reaction chambers molded in PDMS with a standard microscope glass slide. Mixing and circulation of fluid samples was accomplished by rotation of a magnetic stirring bar driven by a standard magnetic stirrer.⁴⁶ Other examples of convective mixing involve cavitation microstreaming, which has been reported to accelerate hybridization kinetics by nearly 5-fold.⁴³ In this process, tiny air-filled chambers were added to a backing slide; the air bubbles resting on a surface were set into vibration by a sound field generating steady circulatory flows that resulted in convective flows producing rapid mixing and therefore, enhancing hybridization kinetics.

Accelerated hybridization achieved by mixing has also been described by Wei et al. who used fluidic channels that were scrambled into discrete plugs to induce droplet mixing. The plugs were thoroughly mixed by the natural re-circulating flows shuttled back and forth along the channels sweeping over the array probes, which reduced the hybridization times to 500 s with reduced sample volumes of 1 μ l.⁴⁷

DNA hybridizations can also be accelerated by electrokinetic delivery of samples.⁴⁸⁻⁵⁰ Electrokinetic transport of targets offers the advantages of controlled fluidic flow and the capability of miniaturization without having to use pumps or active valves. The electrokinetic control allows rapid and efficient mass transfer of samples and therefore, hybridization equilibrium is rapidly attained leading to reduced reaction times. Figure 2.2 shows an example of electrokinetic addressing of a DNA microarray.

2.5 Applications of Microfluidic-Based

A comprehensive description of applications involving the use of microfluidics coupled to DNA microarrays^{33, 35-38, 40, 44, 46, 47, 50-58} is summarized in Table 2.1 while those of protein and cell microarrays^{55, 59, 60 61-65} are summarized in Table 2.2. The information provided illustrates a full range of microarrays performed in microfluidic devices detailing the important achievements obtained in terms of volume reduction, analysis speed, applications, integration, automation and limit of detection.

The advantages exhibited by microfluidics, including their ability to integrate several processing steps into a fully functional system, has attracted several examples where the biological sample is fully processed in the microfluidic prior to hybridization interrogation. Systems have been reported that utilize microfluidics to process the biological sample and prepare it for structure analysis using either DNA, protein or cell-based microarrays. In the following sections, examples will be given from the literature in which sample-preprocessing using microfluidics was invoked prior to interrogation of the targets using a microarray.

Table 2.1 Abbreviated list of literature reports highlighting the coupling of DNA microarrays to microfluidics.

| Ref | Sample volume | Support material | Analysis speed (minutes) | Detection limits | Functions integrated | Applications/ achievements |
|-------------------------|----------------------|-------------------------|---------------------------------|-------------------------|--------------------------------------------|---------------------------------------------------------------------------------------------------------------------------------------------|
| Lillierholm et al.,2005 | 1 μ l | glass | n/a | n/a | Ultrasonic microtransducers | A model bioassay of a multiplexed bead-trapping microarray consisting of piezoelectric microtransducers integrated in microfluidic channels |
| Lenigk et al.,2002 | 25 μ l | PC | 30 | n/a | Integrated air pump for sample oscillation | (i)Accelerated hybridization process by |

| | | | | | | |
|------------------------|------------|---------|------|----------------------|---------------------------------------------------|----------------------------------------------------------------------------------------------------------------------------------------------|
| | | | | | | sample oscillation (ii) Application in single nucleotide polymorphism detection, detection of pathogen bacteria surrogate. |
| Wei et al., 2005 | 1 μ l | PMMA | ~8 | 19 amol | n/a | Enhanced microarray processing speed in microfluidics by “shuttle hybridization” |
| Anderson et al., 2000 | 15 μ l | PC | 20 | n/a | Multiple enzymatic reactions and reagent handling | Parallel multi-step molecular operations and hybridization assays integrated on a miniaturized device. |
| Dimalanta et al., 2004 | ~ μ l | PDMS | n/a | ~25 pg / μ l | DNA elongation, deposition and digestion | Restriction enzyme mapping and identification of human genomic DNA molecules |
| Ali et al., 2003 | 1.5 ml | silicon | < 10 | ~10 ⁻¹³ M | Fluid transport | (i)Chip-based sensor array incorporated DNA capture probes into microporous microbeads (ii) Multiplexed oligonucleotide microarray assays |

| | | | | | | |
|------------------------|-------------|--------------|-----|-------------------------------------|-------------------------------------------------------------------------------------------------------------------------------|------------------------------------------------------------------------------------------------------------------------|
| Wang et al., 2003 | 0.2 μ l | PMMA | 5 | 1 Mutant in 10,000 Wild type copies | n/a | Detection of point mutations in certain gene fragments using universal zipcode arrays |
| Hashimoto et al., 2006 | 0.1 μ l | PMMA /PC | <20 | 1 mutant in 100 wild type copies | Ligase reaction / hybridization assay | Flow throughput biochip for mutational analysis |
| Liu et al., 2004 | 1 ml | PC | 60 | n/a | Fully integrated for cell capture / cell preconcentration /purification /cell lysis and PCR amplification / DNA hybridization | Pathogenic bacterial DNA detection / single nucleotide polymorphism genetic analysis. |
| Erickson et al.,2004 | ~nano liter | Glass / PDMS | 5 | 50 pM | Synchronized online DNA hybridization, washing and detection | (i) Reduced sample volumes (ii) Rapid removal of nonspecifically adsorbed materials (iii) Enhanced hybridization |
| Benoit et al.,2001 | 0.5 μ l | Glass | 180 | 40 pM | n/a | Multiplexed DNA detection |
| Lee et al., 2001 | 1 μ l | Gold /PDMS | 60 | 20 fmol | n/a | Parallel detection of specific adsorptions of DNA /RNA. |
| Cheek et al.,2001 | 50 μ l | Glass | 180 | 250 amol | n/a | Flow-through chemiluminescence detection of multiple enzymes in a microarray format. |

(Table cont'd)

| | | | | | | |
|-----------------------|------------|-------------------------|-----|------------------|-----------------------------------------|-------------------------------------------------------------------------------------------------------------------------------------|
| Keramas et al., 2004 | 10 μ l | PMMA/ glass/PD MS | 120 | n/a | n/a | (i) Hybrid multiplexed detection of <i>campylobacter</i> DNA (ii) Effective mechanical protection and reduced sample evaporation |
| Noerholm et al., 2004 | 10 μ l | PC | 300 | 10 nM | Temperature control and liquid handling | Online monitoring of DNA hybridization assays |
| Yuen et al., 2003 | 50 μ l | PDMS /Glass | 120 | 1.25pg / μ l | n/a | Enhanced hybridizations by 2-5 fold through Sample fluid circulation and mixing. |
| Chung et al., 2004 | n/a | PMMA /Glass | 30 | n/a | n/a | Enhanced hybridization efficiencies via strain rate |

n/a, not available

Table 2.2 Abbreviated list publications outlining the coupling of Protein / cell microarrays to microfluidics.

| Ref | Sample volume | Support material | Analysis speed (minutes) | Detection limits | Functions integrated | Applications/ achievements |
|-----------------------------|---------------|------------------|--------------------------|--------------------------------|----------------------|--------------------------------------------------------------------------------------------------------------|
| Khademhosseini et al., 2004 | n/a | PDMS | 360 | $\sim 2 \times 10^7$ Cells /ml | n/a | Polyethylene glycol-based microstructures used to immobilize cells with potential applications in cell-based |

| | | | | | | |
|-----------------------|--------|---------------|-----|-----------------------------|---------------------------|-----------------------------------------------------------------------------------------------------------------------------------|
| | | | | | | biosensors. |
| Ostuni et al., 2001 | 5 ml | PDMS | n/a | 10 ⁵ Cells | n/a | (i)Fabrication of arrays of microwells for patterning proteins (i)Selective adhering of cells onto the wells |
| Yang et al., 2001 | 2 μl | PDMS | n/a | 230 pmol | n/a | Immunoassays based on solid supported lipid bilayers for multivalent binding between surface-bound ligands and aqueous receptors. |
| Nagamine et al., 2005 | 0.2 μl | Silicon /PDMS | n/a | 10-30 ng / μl | n/a | On-chip transformation of <i>Escherichia coli</i> cells |
| Tani et al., 2004 | 3 μl | Silicon /PDMS | 60 | 1 ng /ml | n/a | On chip bioassays for carrying out genotoxicity tests in agarose hydrogel wells. |
| Kanda et al., 2004 | n/a | Gold / PDMS | 10 | n/a | n/a | Low density protein arrays patterned on gold by using fluidic networks containing SAMs. |
| Thompson et al., 2004 | n/a | PDMS | n/a | 1-10 ⁶ Cells /ml | High-throughput molecular | Profiling expression dynamics |

| | | | | | | |
|--------------------|------------|---------------------|-----|-----|-----|-----------------------------------------------------------------------------|
| | | | | | | stimulation and non destructive cell monitoring of expression events |
| Koh et al., 2003 | 10 μ l | Glass /silicon/PDMS | n/a | n/a | n/a | (i)Multiplexed fabrication of cell phenotypes (ii)reduced sample volumes |
| n/a, not available | | | | | | |

2.5.1 DNA Microarray Systems

An attractive feature of microfluidic systems is their ability to process the sample in a close architecture and with high levels of automation. This provides the ability to not only reduce processing time, but also minimize sample contamination and simplify assay implementation and cost. Recently, a flow through microchip assembly containing two biochips was fabricated to carry out a sequential ligase detection reaction (LDR) followed by an hybridization assay.³⁵ The system was used to detect rare point mutations in genomic DNA that possess high diagnostic value for colorectal cancers.

The LDR generates products that bear a fluorescence label and also, a short sequence appended to the DNA primers involved in the ligation reaction that directs a successfully formed ligation product to a location on the array. The tethered probes are complements to the short sequence found on one of the LDR primers. This “universal array format” consisting of zip code probes and zip code complements allows for the hybridization detection of a variety of biologically derived products. PC and PMMA chips were integrated into a single unit by using PDMS-assisted interconnect technology. The PC chip was used for performing the LDR on chip

while the PMMA chip was used for detection of these LDR products in a microarray format. Hydrodynamic pumping of fluids on this 3-D microfluidic network enabled an LDR/hybridization assay to be carried out with applications in the detection of low-abundant point mutations in *K-ras* genes in less than 20 min (total processing time). This processing time was significantly reduced compared to previous work performed, which involved carrying out a PCR / LDR with array readout using conventional bench-top equipment, which required approximately 270 min.

2.5.2 Protein Microarray Systems

Protein arrays are based on biospecific binding, e.g. antibody/antigen interactions. Yang et al. designed a multivalent immunoassay for monitoring the binding of bivalent anti-dinitrophenyl (anti-DNP) antibodies to phospholipid bilayer surfaces containing dinitrophenyl haptens.⁶⁵ These assays were conducted inside linear arrays of bilayer-coated microchannels formed by placing patterned PDMS molds into conformal contact with borosilicate cover slips. Twelve microchannels were arrayed onto a single chip to allow heterogeneous assays to be performed rapidly with reduced protein sample volumes.

2.5.3 Cell-Based Microarray Systems

The ability of microfluidics to enhance controlled cellular interactions and increase response times has also resulted in their incorporation into cell studies. Cell studies provide information on the dynamics of gene expression or their morphological characteristics. Arrays of different phenotypes of cells can be useful in clinical diagnostics as well. Thompson et al. reported a living cell array platform for the simultaneous stimulation and monitoring of gene expression in living cells.⁶⁴ They used a PDMS/glass chamber coated with fibronectin to promote cell attachment. This platform was used to control dynamic inputs and measure the outputs from adherent mammalian cells. One advantage offered by this device over conventional

cell microarrays was its ability to simultaneously screen many conditions and efficiently explore the large parameter space relating to stimulation of certain cell responses.

Protein and cell microarrays have allowed the reduction in sample and reagent volumes and analysis speed to be achieved, however, they are still in their infancy in terms of development and as such, are faced with several operational challenges. For example, it is difficult to observe low abundant targets by direct molecular association assays because the trace amount of target has to compete with the mixed population of higher abundant interferents for binding onto the recognition element situated on the support.⁶⁶ Also, high content analysis of cell microarrays in living cells require the imaging time of an entire slide at sufficient time-resolution so as not to obscure transitory phenotypes of interest.⁶⁷

2.6 Conclusions

Microfluidics has advanced the rapid growth in biochip applications due in part to their ability to pre-process the sample in an automated fashion prior to incubation with the array and the fact that the operational characteristics of the array can be improved when scaled to the micrometer domain. One particularly compelling advantage associated with the marriage of microfluidics with microarrays is the reduction in reaction times exhibited in all applications ranging from DNA arrays, protein arrays and cell bioassays. The reduced reaction times are attributed to improved kinetics compared to conventional non-microfluidic techniques and often times is a consequence of enhanced mass transport to the surface tethered recognition elements by the target and small diffusional distances. Successful integration of sample pre-treatment processes, such as cell culture/lysis, sample purification, pre-concentration and amplification, with the hybridization reaction on a single microfluidic platform has shown significant reduction in analysis time, improved sensitivities, fully automated sample processing, and the reduction in hardware demands for the intended assay, which are very useful for transitioning high end molecular analysis to a point-of-care format. Parallelization capability of microfluidics on a

single chip is also important, since different samples can be simultaneously processed with highly controlled reaction conditions allowing high-throughput analysis as well as reducing inter-sample variability. Also, the closed architecture of the microfluidic provides reduction in possible sample contamination, which will have important clinical ramifications in the area of DNA forensics. The use of inexpensive polymers as the substrate for microfluidic devices allows one to employ these systems as single-use devices, which will be particularly attractive to eliminate cross-contaminations during operation, eliminating false positive results due to sample carryover. Coupling microfluidics to DNA arrays, protein arrays or cell arrays therefore will have a major impact on understanding many fundamental biological activities, since these technology platforms make high end technologies for studying these processes available to a large research community due to the simplicity of their operation and the low cost of their production.

Another challenge associated with coupling microfluidics and microarrays is the ability to manipulate microfluidics in a complicated fully integrated fluidic network. With this, many multi-step microarray hybridization processes that require manual handling can be eliminated when all the processes are integrated into a single system. These automated platforms may eventually lead to improved reproducibility of microarray results with acceptable array-to-array coefficients of variation. Microfluidics has also improved microarray sensitivities enabling detection of even low expressed genes however, array analyses still lacks an efficient data analysis tool (bioinformatics) for the generated microarray information. Improved bioinformatics tools and fully integrated microfluidic devices will therefore enable microarrays to be fully exploited in gene expression analysis and clinical diagnostics with reduced analysis time. While microfluidics can offer some attractive advantages for microarray-based assays, these systems still depend on conventional peripheral equipment for their operation, such as

sample / reagent loading, fluid actuation and readout. It is clear that complete packaging of these peripherals into a system that is on the same size as the fluidic element will allow the creation of instruments that can be envisioned for potential point-of-care testing. This realization will provide increased accessibility of microarray technologies to a potentially larger user base and expand on their capabilities.

2.7 References

- (1) Li, J.; Thibault, P.; Bings, N. H.; Skinner, C. D.; Wang, C.; Colyer, C.; Harrison, J. *Analytical Chemistry* **1999**, *71*, 3036-3045.
- (2) McClain, M. A.; Culbertson, C. T.; Jacobson, S. C.; Allbritton, N. L.; Sims, C. E.; Ramsey, J. M. *Analytical Chemistry* **2003**, *75*, 5646-5655.
- (3) Boerner, M. W.; Kohl, M.; Pantenburg, F. J.; Bacher, W.; Hein, H.; Schomburg, W. K. *Microelectronic Engineering* **1996**, *30*, 505-508.
- (4) Grass, B.; Neyer, A.; Johnck, M.; Siepe, D.; Eisenbeiss, F.; Weber, G.; Hergenroder, R. *Sensors and Actuators, B: Chemical* **2001**, *B72*, 249-258.
- (5) Ihlemann, J.; Rubahn, K. *Applied Surface Science* **2000**, *154-155*, 587-592.
- (6) Martynova, L.; Locascio, L. E.; Gaitan, M.; Kramer, G. W.; Christensen, R. G.; MacCrehan, W. A. *Analytical chemistry* **1997**, *69*, 4783-4789.
- (7) Qi, S.; Liu, X.; Ford, S.; Barrows, J.; Thomas, G.; Kelly, K.; McCandless, A.; Lian, K.; Goettert, J.; Soper, S. A. *Lab on a Chip* **2002**, *2*, 88-95.
- (8) Rossier, J. S.; Schwarz, A.; Reymond, F.; Ferrigno, R.; Bianchi, F.; Girault, H. H. *Electrophoresis* **1999**, *20*, 727-731.
- (9) Roberts, M. A.; Rossier, J. S.; Bercier, P.; Girault, H. *Analytical Chemistry* **1997**, *69*, 2035-2042.
- (10) Friedrich, C. R.; Coane, P. J.; Vasile, M. J. *Microelectronic Engineering* **1997**, *35*, 367-372.
- (11) Soper, S. A.; Ford, S. M.; Qi, S.; McCarley, R. L.; Kelly, K.; Murphy, M. C. *Analytical Chemistry* **2000**, *72*, 643A-651A.
- (12) Ford, S. M.; Davies, J.; Kar, B.; Qi, S. D.; McWhorter, S.; Soper, S. A.; Malek, C. K. *J Biomech Eng*: **1999**, *121*, 13-21.

- (13) Sia Samuel, K.; Whitesides George, M. *Electrophoresis* **2003**, *24*, 3563-3576.
- (14) Anderson, J. R.; Chiu, D. T.; Jackman, R. J.; Cherniavskaya, O.; McDonald, J. C.; Wu, H.; Whitesides, S. H.; Whitesides, G. M. *Analytical Chemistry* **2000**, *72*, 3158-3164.
- (15) Duffy, D. C.; McDonald, J. C.; Schueller, O. J. A.; Whitesides, G. M. *Analytical Chemistry* **1998**, *70*, 4974-4984.
- (16) Duffy, D. C.; Schueller, O. J. A.; Brittain, S. T.; Whitesides, G. M. *Journal of Micromechanics and Microengineering* **1999**, *9*, 211-217.
- (17) McDonald, J. C.; Whitesides, G. M. *Accounts of Chemical Research* **2002**, *35*, 491-499.
- (18) Becker, H.; Gartner, C. *Electrophoresis* **2000**, *21*, 12-26.
- (19) Love, J. C.; Wolfe, D. B.; Jacobs, H. O.; Whitesides, G. M. *Langmuir* **2001**, *17*, 6005-6012.
- (20) Unger, M. A.; Chou, H.-P.; Thorsen, T.; Scherer, A.; Quake, S. R. *Science (Washington, D. C.)* **2000**, *288*, 113-116.
- (21) Gong, Y.-K.; Luo, L.; Petit, A.; Zukor, D. J.; Huk, O. L.; Antoniou, J.; Winnik, F. M.; Mwaile, F. *Journal of Biomedical Materials Research, Part A* **2005**, *72A*, 1-9.
- (22) Henry, A. C.; Tutt, T. J.; Galloway, M.; Davidson, Y. Y.; McWhorter, C. S.; Soper, S. A.; McCarley, R. L. *Analytical chemistry* **2000**, *72*, 5331-5337.
- (23) Hu, S.; Ren, X.; Bachman, M.; Sims, C. E.; Li, G. P.; Allbritton, N. L. *Analytical Chemistry* **2004**, *76*, 1865-1870.
- (24) Lee, K.-B.; Yoon, K. R.; Woo, S. I.; Choi, I. S. *Journal of Pharmaceutical Sciences* **2003**, *92*, 933-937.
- (25) Lu, H. H.; Cooper, J. A.; Manuel, S.; Freeman, J. W.; Attawia, M. A.; Ko, F. K.; Laurencin, C. T. *Biomaterials* **2005**, *26*, 4805-4816.
- (26) McCarley, R. L.; Vaidya, B.; Wei, S.; Smith, A. F.; Patel, A. B.; Feng, J.; Murphy, M. C.; Soper, S. A. *Journal of the American Chemical Society* **2005**, *127*, 842-843.
- (27) Nuzzo Ralph, G. *Nature materials* **2003**, *2*, 207-208.
- (28) Sebra, R. P.; Masters, K. S.; Bowman, C. N.; Anseth, K. S. *Langmuir* **2005**, *21*, 10907-10911.
- (29) Shadpour, H.; Musyimi, H.; Chen, J.; Soper, S. A. *Journal of Chromatography, A* **2006**, *1111*, 238-251.
- (30) Liu, J.; Hansen, C.; Quake, S. R. *Analytical Chemistry* **2003**, *75*, 4718-4723.

- (31) Burns, M. A.; Mastrangelo, C. H.; Sammarco, T. S.; Man, F. P.; Webster, J. R.; Johnson, B. N.; Foerster, B.; Jones, D.; Fields, Y.; et al. *Proceedings of the National Academy of Sciences of the United States of America* **1996**, *93*, 5556-5561.
- (32) Burns, M. A.; Johnson, B. N.; Brahmasandra, S. N.; Handique, K.; Webster, J. R.; Krishnan, M.; Sammarco, T.; Man, P. M.; Jones, D.; Heldsinger, D.; Mastrangelo, C. H.; Burke, D. T. *Science (Washington, D. C.)* **1998**, *282*, 484-487.
- (33) Liu, R. H.; Yang, J.; Lenigk, R.; Bonanno, J.; Grodzinski, P. *Analytical Chemistry* **2004**, *76*, 1824-1831.
- (34) Auroux, P.-A.; Iossifidis, D.; Reyes, D. R.; Manz, A. *Analytical Chemistry* **2002**, *74*, 2637-2652.
- (35) Hashimoto, M.; Barany, F.; Soper, S. A. *Biosensors & Bioelectronics* **2006**, *21*, 1915-1923.
- (36) Wang, Y.; Vaidya, B.; Farquar, H. D.; Stryjewski, W.; Hammer, R. P.; McCarley, R. L.; Soper, S. A.; Cheng, Y.-W.; Barany, F. *Analytical Chemistry* **2003**, *75*, 1130-1140.
- (37) Cheek, B. J.; Steel, A. B.; Torres, M. P.; Yu, Y.-Y.; Yang, H. *Analytical Chemistry* **2001**, *73*, 5777-5783.
- (38) Noerholm, M.; Bruus, H.; Jakobsen Mogens, H.; Telleman, P.; Ramsing Niels, B. *Lab on a chip* **2004**, *4*, 28-37.
- (39) Chung, Y.-C.; Lin, Y.-C.; Hsu, Y.-L.; Chang, W.-N. T.; Shiu, M.-Z. *Journal of Micromechanics and Microengineering* **2004**, *14*, 1376-1383.
- (40) Chung, Y.-c.; Lin, Y.-c.; Shiu, M.-z.; Chang, W.-n. T. *Lab on a Chip* **2003**, *3*, 228-233.
- (41) Vanderhoeven, J.; Pappaert, K.; Dutta, B.; Vanhummelen, P.; Baron, G. V.; Desmet, G. *Electrophoresis* **2004**, *25*, 3677-3686.
- (42) Yaralioglu, G. G.; Wygant, I. O.; Marentis, T. C.; Khuri-Yakub, B. T. *Analytical Chemistry* **2004**, *76*, 3694-3698.
- (43) Liu, R. H.; Lenigk, R.; Druyor-Sanchez, R. L.; Yang, J.; Grodzinski, P. *Analytical Chemistry* **2003**, *75*, 1911-1917.
- (44) Lenigk, R.; Liu, R. H.; Athavale, M.; Chen, Z.; Ganser, D.; Yang, J.; Rauch, C.; Liu, Y.; Chan, B.; Yu, H.; Ray, M.; Marrero, R.; Grodzinski, P. *Analytical Biochemistry* **2002**, *311*, 40-49.
- (45) Bynum, M. A.; Gordon, G. B. *Analytical Chemistry* **2004**, *76*, 7039-7044.
- (46) Yuen, P. K.; Li, G.; Bao, Y.; Mueller, U. R. *Lab on a Chip* **2003**, *3*, 46-50.

- (47) Wei, C.-W.; Cheng, J.-Y.; Huang, C.-T.; Yen, M.-H.; Young, T.-H. *Nucleic Acids Research* **2005**, *33*, e78/71-e78/11.
- (48) Edman, C. F.; Raymond, D. E.; Wu, D. J.; Tu, E.; Sosnowski, R. G.; Butler, W. F.; Nerenberg, M.; Heller, M. *Nucleic Acids Research* **1997**, *25*, 4907-4914.
- (49) Sosnowski, R. G.; Tu, E.; Butler, W. F.; O'Connell, J. P.; Heller, M. J. *Proceedings of the National Academy of Sciences of the United States of America* **1997**, *94*, 1119-1123.
- (50) Erickson, D.; Liu, X.; Krull, U.; Li, D. *Analytical Chemistry* **2004**, *76*, 7269-7277.
- (51) Anderson, R. C.; Su, X.; Bogdan, G. J.; Fenton, J. *Nucleic acids research* **2000**, *28*, E60.
- (52) Lee, H. J.; Goodrich, T. T.; Corn, R. M. *Analytical Chemistry* **2001**, *73*, 5525-5531.
- (53) Lilliehorn, T.; Nilsson, M.; Simu, U.; Johansson, S.; Almqvist, M.; Nilsson, J.; Laurell, T. *Sensors and Actuators, B: Chemical* **2005**, *B106*, 851-858.
- (54) Benoit, V.; Steel, A.; Torres, M.; Yu, Y. Y.; Yang, H.; Cooper, J. *Analytical chemistry* **2001**, *73*, 2412-2420.
- (55) Koh, W.-G.; Itle Laura, J.; Pishko Michael, V. *Analytical chemistry* **2003**, *75*, 5783-5789.
- (56) Ali, M. F.; Kirby, R.; Goodey, A. P.; Rodriguez, M. D.; Ellington, A. D.; Neikirk, D. P.; McDevitt, J. T. *Analytical Chemistry* **2003**, *75*, 4732-4739.
- (57) Dimalanta, E. T.; Lim, A.; Runnheim, R.; Lamers, C.; Churas, C.; Forrest, D. K.; de Pablo, J. J.; Graham, M. D.; Coppersmith, S. N.; Goldstein, S.; Schwartz, D. C. *Analytical Chemistry* **2004**, *76*, 5293-5301.
- (58) Keramas, G.; Perozziello, G.; Geschke, O.; Christensen, C. B. V. *Lab on a Chip* **2004**, *4*, 152-158.
- (59) Kanda, V.; Kariuki, J. K.; Harrison, D. J.; McDermott, M. T. *Analytical Chemistry* **2004**, *76*, 7257-7262.
- (60) Khademhosseini, A.; Yeh, J.; Jon, S.; Eng, G.; Suh, K. Y.; Burdick, J. A.; Langer, R. *Lab on a Chip* **2004**, *4*, 425-430.
- (61) Tani, H.; Maehana, K.; Kamidate, T. *Analytical Chemistry* **2004**, *76*, 6693-6697.
- (62) Nagamine, K.; Onodera, S.; Torisawa, Y.; Yasukawa, T.; Shiku, H.; Matsue, T. *Analytical Chemistry* **2005**, *77*, 4278-4281.
- (63) Ostuni, E.; Chen, C. S.; Ingber, D. E.; Whitesides, G. M. *Langmuir* **2001**, *17*, 2828-2834.
- (64) Thompson, D. M.; King, K. R.; Wieder, K. J.; Toner, M.; Yarmush, M. L.; Jayaraman, A. *Analytical Chemistry* **2004**, *76*, 4098-4103.

- (65) Yang, T.; Jung, S.-y.; Mao, H.; Cremer, P. S. *Analytical Chemistry* **2001**, *73*, 165-169.
- (66) MacBeath, G. *Nature Genetics* **2002**, *32*, 526-532.
- (67) Wheeler, D. B.; Carpenter, A. E.; Sabatini, D. M. *Nature Genetics* **2005**, *37*, S25-S30.

CHAPTER 3

FABRICATION OF DNA MICROARRAYS ONTO POLY (METHYLMETHACRYLATE) PMMA, BY UV PATTERNING FOR THE DETECTION OF LOW ABUNDANT DNA POINT MUTATIONS*

3.1 Introduction

3.1.1 Covalent Immobilization of DNA Probes onto Polymeric Substrates

To construct a microarray, attention to the probes (length and sequence content), selection of the solid substrate, and the linkage chemistry used to attach the probes to the substrate surface are essential. Glass has been widely used due to its well characterized coupling chemistries but in recent years, polymers have become an attractive alternative to glass supports due to a greater choice in physical and chemical properties and fabrication advantages for micro-analytical devices.^{1,2} The selection of appropriate linkage chemistries for polymers however, are less developed compared to glass.

Several polymer substrates have been investigated for the covalent or non-covalent attachment of oligonucleotide probes. Among them, polystyrene plates are the most widely reported polymer substrate for the immobilization of DNA probes.³ Immobilization on polystyrene can be realized by using passive adsorption,⁴ covalent cross-linking of DNA upon UV irradiation leading to immobilization of target DNA,⁵ or biotin-labeled DNA probes attached to streptavidin-coated polystyrene plates.⁶ In the case of passive immobilization, DNA probes in high buffer concentrations are incubated with the plate for probe attachment.^{3,4,7} Chemically modified polystyrene plates are also commercially available for the immobilization of oligonucleotide probes; for example, the “NucleoLink” plate is available from Nalge Nunc International. Nucleic acids are covalently attached to the Nucleolink surface via 5’ amino or phosphate groups using carbodiimide chemistry (www.nalgene.com).

Other polymer substrates, such as polypropylene, poly(methyl methacrylate), PMMA, and polycarbonate, PC, have also been used as supports for the covalent immobilization of DNA probes.⁸⁻¹⁰ PMMA has been shown to be a viable support for DNA microarray applications.^{9,10} The general procedure for the chemical functionalization of PMMA involves; (1) amination in N-lithioethylenediamine solution; (2) addition of a homo-bi-functional cross-linker molecule, such as glutardialdehyde; (3) reaction of amine-terminated oligonucleotide probes to the cross-linker; (4) capping of the unreacted functional groups (aldehydes) with a reducing agent, such as sodium borohydride and; (5) extensive washing of the surface and the multiple chemical steps in the procedure required extensive amount of processing time to create the array.¹¹ Unfortunately, due to the inefficiency of each step in this multi-step process, the surface density of DNA probes was comparatively low (~ 33.1 fmol/cm²).⁹

Fixe and coworkers¹⁰ also described a chemical procedure to functionalize PMMA substrates by reaction of the PMMA polymer with hexamethylene diamine, which yielded an aminated surface for immobilizing DNA during microarray generation. The density of functional primary amine (NH₂) groups was found to be 0.29 nmol/cm² that resulted in immobilized and hybridized densities of 10 and 0.75 pmol/cm², respectively, for microarrays constructed onto these chemically aminated PMMA. These authors also explored whether a non-modified PMMA surface could be used for direct immobilization of 5' end-labeled amine or thiol terminated oligonucleotides.¹⁰ The direct immobilization protocols were based on the aminolysis reaction of esters in the presence of electron donors at basic pH conditions. By using the methyl esters present on non-modified PMMA, they demonstrated that it was possible to establish a covalent bond between the electron donor of a DNA probe and the C terminal ester of the PMMA substrate.

This new approach for DNA immobilization was compared to DNA microarrays made using activated PMMA substrates and silanized glass and the hybridization density obtained, as well as the hybridization efficiency, was equal to the commercially available silylated glass and plastic Euray slides.

3.1.2 UV-Photomodification of Polymeric Substrates

Direct UV-photochemical modification of certain polymer substrate surfaces could be envisioned as a simple and universally general approach to provide a functional scaffold from which appropriately prepared DNA probes could be tethered covalently without the need for multi-step, low efficiency reactions or additional coating materials. Many polymers absorb UV radiation within specific wavelength regions, where surface photo-chemical modification is likely to occur. Two different absorption maxima for PC photo-oxidation have been reported, 295 nm¹² and 264 nm.¹³ The wavelength maximum for photo-induced oxidation of PMMA lies between 290 nm and 315 nm. Photo-oxidation produces a variety of physical and chemical changes to the polymer surface. Chain scission and cross-linking are the general reactions that take place, often accompanied by formation of oxygen-containing groups. These moieties are typically peroxides, hydroxyl, carboxylic, or carbonylic groups for PC.¹³ Additionally, photo-modification occurs primarily at the surface, suggesting that the effect of UV radiation may not extend into the bulk polymer significantly. Several papers have been published in which UV radiation was employed to modify a polymer surface, but none have discussed the selective immobilization of oligonucleotide probes onto direct UV-activated polymer substrates. UV (220 nm) radiation has been used, however, to increase surface hydrophilicity of PC¹⁴ and to increase the surface charge density of PMMA substrates.¹⁵ In addition, UV-radiation has been reported to produce carboxylate groups onto PC surfaces and the resulting surfaces in PC microchannels have been used as an immobilization bed in the Solid-Phase Reversible Immobilization (SPRI)

process for DNA purification prior to gel electrophoretic sorting.¹⁶In this work, we detail the use of a simple approach to produce functional scaffolds on polymers for the covalent immobilization of oligonucleotide probes for DNA microarray applications. Exploiting the rich photochemistry associated with most polymeric materials, UV radiation (254 nm) was used for the surface modification of two test materials, PMMA and PC. Both substrates are in widespread use for fabricating microfluidic devices^{1,9,14,17-22} and thus potentially allow the coupling of microfluidics to microarrays. In addition, the technique is flexible enough to allow selective patterning of spots by creating “activated” sites using a contact photomask, followed by appropriate oligonucleotide probe attachment. Also, wide-field illumination of the entire substrate surface can be performed followed by patterning the probes using conventional spotting or microfluidics. To investigate the influence of pre-existing surface groups that may result from photo-chemical reactions triggered by ambient UV exposure,²³ oligonucleotide probes were directly deposited onto pristine polymer surfaces and their interaction with the polymer surface monitored through the hybridization of these probes to their dye-labeled complements. In separate experiments, oligonucleotide probe solutions were deposited onto polymer surfaces, which were UV (254 nm) irradiated. These surfaces were subsequently examined to determine the optimal conditions in terms of probe density. Also, the appropriate substrate for immobilization (PMMA or PC) was examined based on minimal non-specific adsorption effects and active group density.

3.1.3 Ligase Detection Reaction (LDR) for Detection of Low Abundant DNA Mutations

We have demonstrated the use of colorectal cancer as a model system for the detection of low abundant mutations. Colorectal cancer can involve genetic alterations in *APC*, *hMSH2*, *hMLK1*, *KRAS*, *DCC* and *P53* genes. Approximately 35-50% of the colorectal cancers and adenomas have point mutations in the *KRAS* gene, which are localized in codons 12, 13 and

61.²⁴⁻²⁶ During the early development of most cancers, there are a high population of wild type (normal) cells as compared to mutated cells. In early diagnosis of these cancers, there is a great challenge of detecting the low abundant mutated cells from the highly abundant normal ones. Techniques such as direct sequencing,²⁷ phage cloning or allele specific PCR²⁸ and electrophoresis²⁹ have been used to detect *KRAS* mutations, however, they do not allow detection of the full spectrum of *KRAS* mutations. We therefore sought to couple a Ligase Detection Reaction (LDR) that was initially developed by Barany and co-workers^{27,30} with microarrays to detect multiple *KRAS* mutations.

An LDR reaction involves the use of a DNA ligase enzyme, which catalyzes the formation of a phosphodiester bond between the 3'-hydroxyl group at the end of one DNA chain (primer) and the 5'- phosphate group at the end of another primer.^{31,32} NAD⁺ or ATP is the energy source required to drive this thermodynamic reaction. NAD⁺ dependent ligases are found exclusively in bacteria, while ATP dependent ligases have been found in bacteriophages, eubacteria, archaea and viruses.³² They both, however, use the same catalytic mechanism during a ligase reaction. The mechanism of this reaction involves three discrete and reversible steps in forming a phosphodiester link between two DNA primer strands resulting in the loss of adenosine monophosphate (AMP) and nicotinimide monophosphate (NMN), as shown in Figure 3.1 below.

In the first step, hydrolysis of the NAD⁺ yields an adenylated-enzyme intermediate in which AMP is attached covalently to the α -amino group of a lysine residue within the active site with the loss of NMN; next, the AMP moiety is transferred from the active site lysine to the free 5'-phosphoryl group at the position of the nick in the DNA strand on primer 1. Finally, a nucleophilic attack by the 3'-OH terminus of the second primer 2, results in the formation of a phosphodiester bond on the activated 5'- phosphorylated end of primer 1 and subsequent release

of AMP from the adenylated DNA intermediate.^{30, 32, 33} When using LDR for mutational analysis, a thermostable DNA ligase discriminates between normal and mutant DNA. Two primers are used; a 5' phosphorylated common primer and a discriminating primer. Any mismatch at the 3' end of the discriminating primer prevents the DNA ligase from joining the two primers together (no ligation). The high fidelity of LDR to distinguish matched targets in a large population of mismatches depends on the ability of the thermostable ligase to rapidly dissociate from the target containing mismatches. This high specificity eventually enables mutational screening of low abundant mutations during the early stages of cancer development.

Step1:

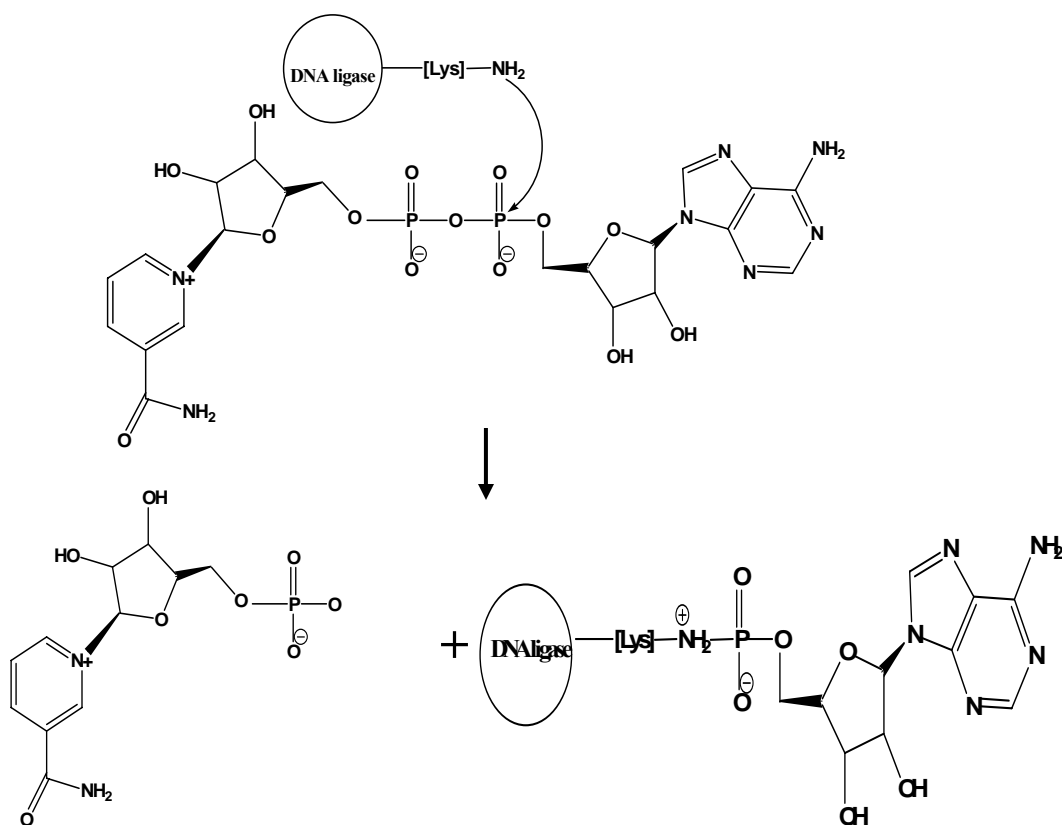


Figure 3.1 Schematic representation of the ligase reaction: Step1; formation of an enzyme – adenylate complex, Step 2; Activation of 5'-phosphatase at the site of a nick in the DNA substrate, Step 3; Nick closure in which a covalent bond is formed between an adjacent 3'hydroxyl group and activated 5' phosphatase in duplex DNA structures with the release of AMP from the adenylated DNA intermediate.³²

Step 2:

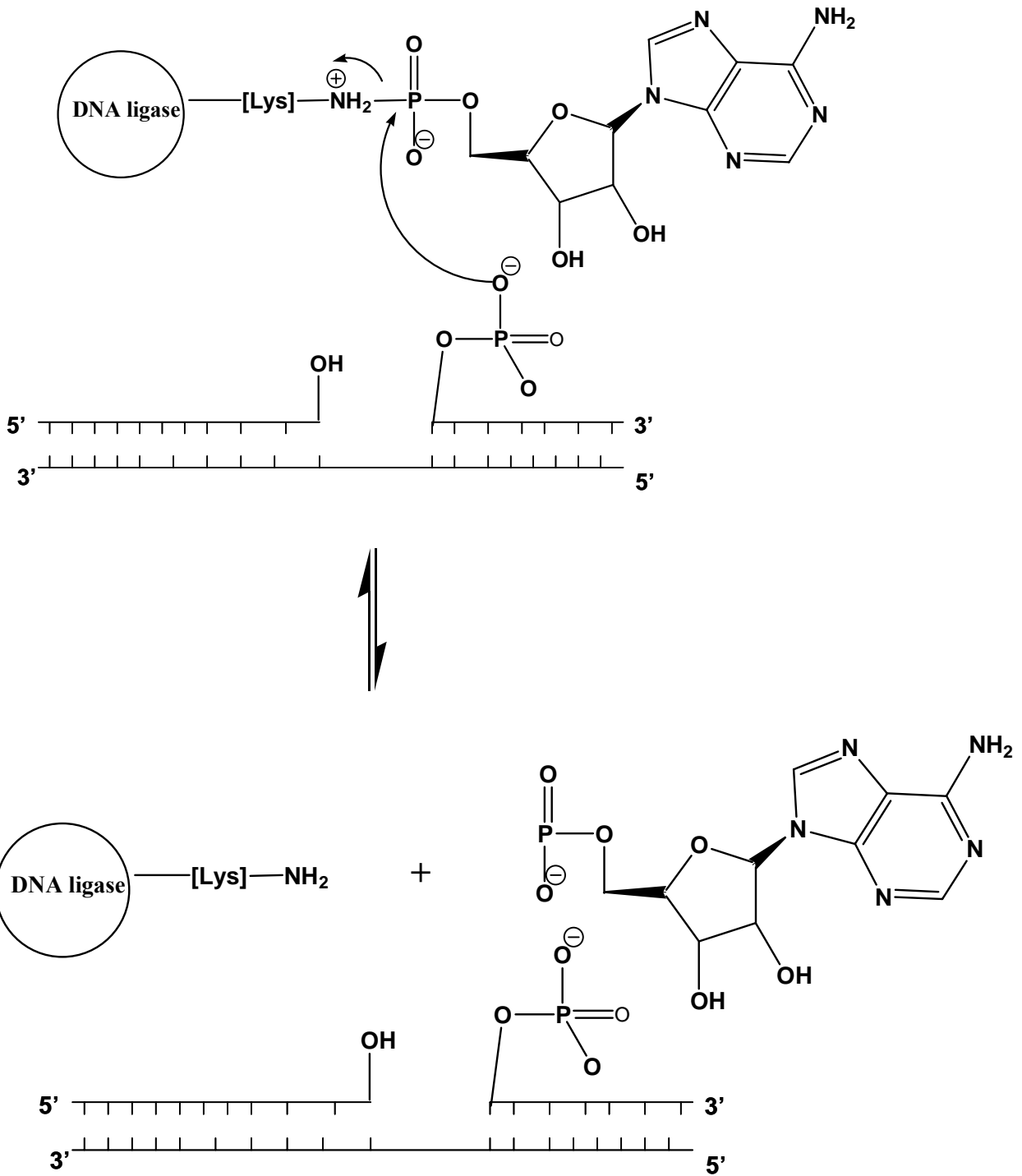


Figure 3.1 continued.

Step3:

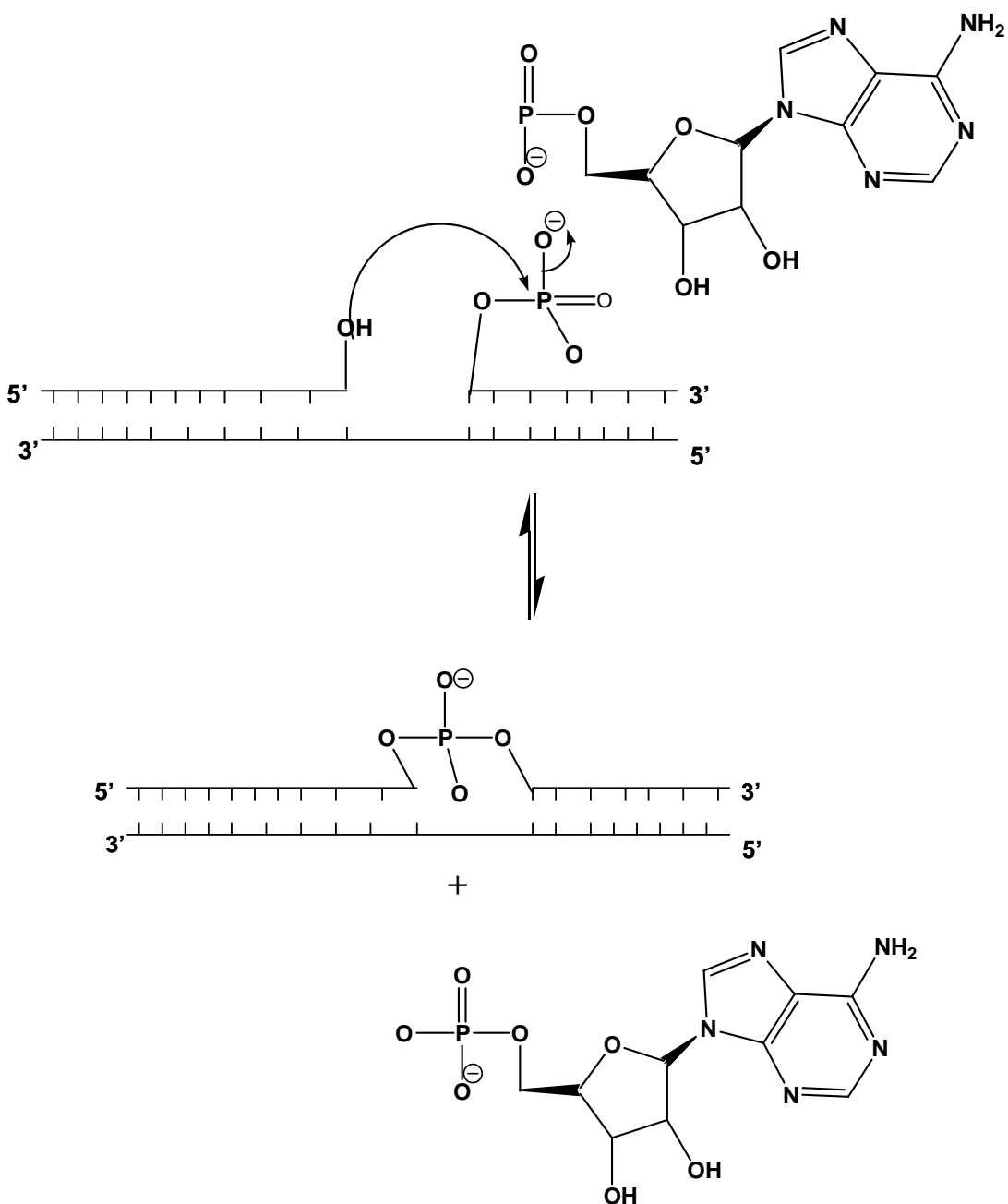


Figure 3.1 continued.

In this Chapter, photo-modification chemistry was used to build universal arrays for the detection of point mutations in *KRAS2* genes following an allele-specific Ligation Detection Reaction (LDR) assay. A simple UV-photo-modification protocol of poly(methyl methacrylate) and polycarbonate was used to produce functional scaffolds consisting of carboxylic groups that

allow covalent attachment of amine-terminated oligonucleotide probe arrays to these surface groups through carbodiimide coupling. This photo-modification procedure coupled to microfluidics allowed for the rapid generation of medium density DNA microarrays. The method reported herein involves the use of poly (dimethylsiloxane) microchannels reversibly sealed to photo-modified poly(methyl methacrylate) surfaces to serve as stencils for patterning the oligonucleotide probes. After array construction, the poly(dimethylsiloxane) stencil is rotated 90° to allow interrogation of the array using microfluidics.^{34,35} We demonstrate the use of this procedure for screening multiple *KRAS2* mutations possessing high diagnostic value for colorectal cancers. A Ligase Detection Reaction / universal array assay was carried out using parallel detection of two different low abundant DNA point mutations in *KRAS2* oncogenes with the allelic composition evaluated at one locus. Four zip code probes immobilized onto the poly(methyl methacrylate) surface directed allele-specific ligation products containing mutations in the *KRAS2* gene (12.2 D, 12.2A, 12.2V K and 13.4 D) to the appropriate address of a universal array with minimal amounts of cross-hybridization or misligation.

3.2 Experimental Section

3.2.1 Materials

The prepolymer of PDMS and the curing agent (Sylgard 184) were purchased from Dow Corning (Midland, MI). PMMA and PC polymer substrates (5 mm thickness) were obtained from Goodfellow (Berwyn, PA). 2-[N-morpholino]ethanesulfonic acid (MES), 1-ethyl-3-(3-dimethylaminopropyl) carbodiimide hydrochloride (EDC) and 20X Saline-Sodium Phosphate-EDTA buffer (SSPE) stock solutions were obtained from Sigma (Milwaukee, WI). The 5' end radio-labeling kit was purchased from Promega (Madison, WI) and [γ -³²P] ATP (3000 Ci/mmol, 10 mCi/ ml) from Amersham Biosciences, NJ.

Table 3.1: Universal zip code probe sequences and their melting temperature.

| Oligonucleotides | Sequences (5'-3') | T _m (°C) |
|------------------|------------------------------------------------------------------------------|---------------------|
| M13 Fwd (-29)- | *C ₆ Amino-TTT TTT TTT TTT TTT GTC GTT TTA CAA CGT CGT G | 59.4 |
| Zip code 1 | *C ₆ Amino-TTT TTT TTT TTT TTT TGC GAC CTC AGC ATC GAC CTC AGC | 66.7 |
| Zip code 2 | *C ₆ Amino-TTT TTT TTT TTT TTT ATC GGA CCG GTA TGC GGA CCG GTA | 66.7 |
| Zip code 3 | *C ₆ Amino-TTT TTT TTT TTT TTT CAG CAC CTG ACC ATC GAT CGC AGC | 66.7 |
| Zip code 4 | *C ₆ Amino-TTT TTT TTT TTT TTT GGT AGA CCA CCT TGC GTG CGG GTA | 67.4 |
| Zip code 5 | *C ₆ Amino-TTT TTT TTT TTT TTT GAC CAC CTT GCG ATC GGG TAC AGC | 66.6 |
| Zip code 6 | *C ₆ Amino-TTT TTT TTT TTT TTT ACC TGA CCA TCG TGC GCA GCG GTA | 67.4 |
| Zip code 11 | *C ₆ Amino-TTT TTT TTT TTT TTT TGC GGG TAC AGC ACC TAC CTT GCG | 66.9 |
| Zip code 12 | *C ₆ Amino-TTT TTT TTT TTT TTT ATC GCA GCG GTA GAC CGA CCA TCG | 66.1 |
| Zip code 13 | *C ₆ Amino-TTT TTT TTT TTT TTT CAG CGG TAG ACC ACC TAT CGT GCG | 66.1 |
| Zip code 14 | *C ₆ Amino-TTT TTT TTT TTT TTT GGT ACA GCA CCT GAC CTG CGA TCG | 66.4 |
| Zip code 15 | *C ₆ Amino-TTT TTT TTT TTT TTT GAC CGG TAT GCG ACC TGG TAT GCG | 66.5 |
| Zip code 16 | *C ₆ Amino-TTT TTT TTT TTT TTT ACC TCA GCA TCG GAC CCA GCA TCG | 66.3 |
| Zip code 21 | *C ₆ Amino-TTT TTT TTT TTT TTT TGC GAT CGC AGC GGT AAC CTG ACC | 66.9 |
| Zip code 22 | *C ₆ Amino-TTT TTT TTT TTT TTT ATC GTG CGG GTA CAG CGA CCA CCT | 67.2 |
| Zip code 23 | *C ₆ Amino-TTT TTT TTT TTT TTT CAG CAT CGG ACC GGT AAT CGG ACC | 66.2 |
| Zip code 25 | *C ₆ Amino-TTT TTT TTT TTT TTT GAC CAT CGT GCG GGT AGG TAG ACC | 66.0 |

Oligonucleotides were purchased from Integrated DNA Technologies, Inc. (IDT) (Coralville, IA), LI-COR Biosciences (IRD700 dye-labeled primers, Lincoln, NE), and Synthegen LLC (Houston, TX). The sequences of the oligonucleotides used in these studies are listed in

Tables 3.1 and 3.2. All dilutions were performed using deionized water (17.9 M Ω) from an E-pure water purification system (Barnstead, Dubuque, IA).

3.2.2 Fabrication of PDMS Microfluidic Devices

A mold master for casting PDMS was fabricated in brass (353 engravers' brass, McMaster-Carr, Atlanta, GA) using a high-precision micromilling machine (KERN MMP 2522, KERN Micro- und Feinwerktechnik GmbH & Co., Germany). Micromilling was carried out at 40,000 rpm using 500 μm and 200 μm diameter milling bits (McMaster-Carr, Atlanta, GA). A typical milling cycle consisted of a pre-cut of the entire surface with a 500 μm milling bit to ensure parallelism between both faces of the brass plate to guarantee uniform height of the milled microstructures over the entire pattern; rough milling of the microstructures using the 500 μm diameter milling bit; and finishing with a 200 μm bit.

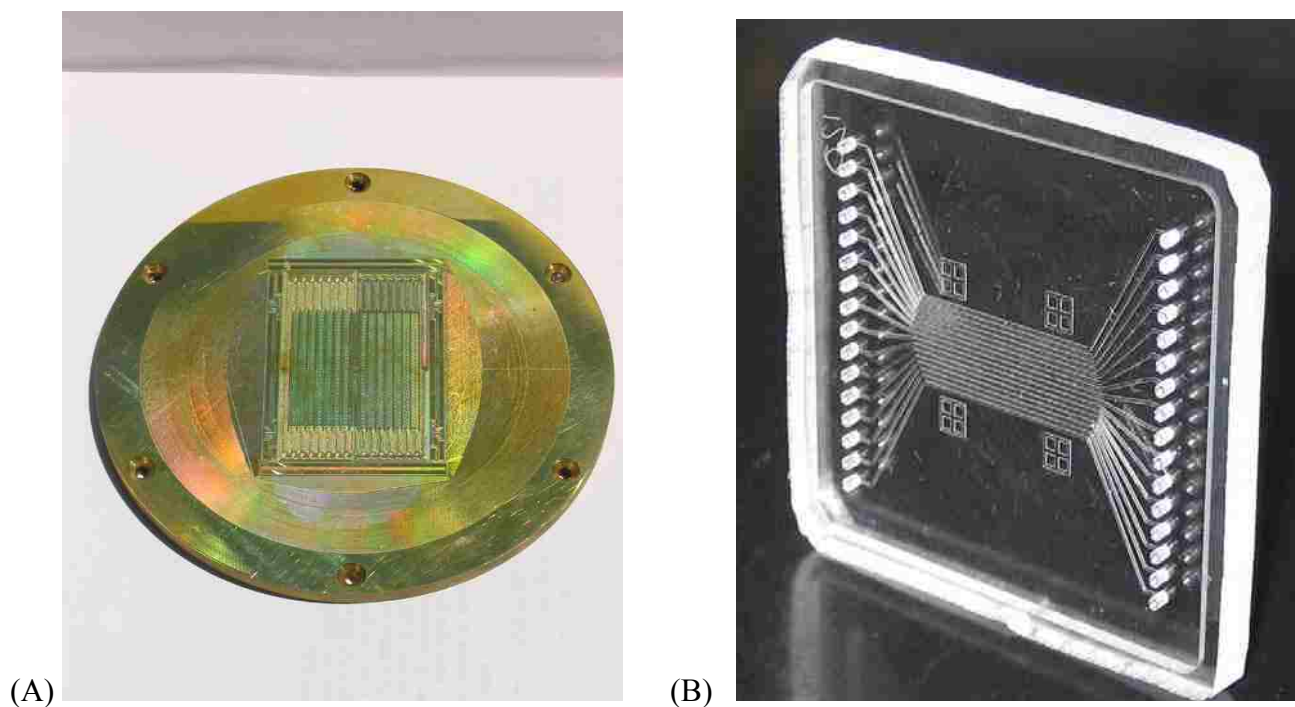


Figure 3.2: (A) Picture of the brass mold insert used for casting PDMS micro-stencils. It consisted of sixteen channels; each channel had a width of 300 μm , a depth of 30 μm and a channel length of 34,000 μm . The interchannel spacing was 2,000 μm . Also shown (B) is a picture of the PDMS stencil obtained after mixing the pre-polymer and curing agent by pouring this solution onto the brass mold and letting it to polymerize.

In order to remove burrs produced by the milling process, the microstructures were lapped with a lapping machine using a 1 μm particle-size diamond slurry (Hyprez Diamond Lapping System, Engis and Wheeling, IL). A mixture containing 10:1 (v/v) PDMS prepolymer and curing agent were thoroughly stirred and degassed under vacuum for 30 min. This mixture was subsequently poured onto the mold master and cured for 2 h at 70°C. After curing, the PDMS was cooled to room temperature and the replica was removed from the master. Patterns of the negative relief channels were produced in the PDMS and holes with a diameter of 500 μm were punched at the end of each microchannel to create solution reservoirs. The PDMS was ultrasonically cleaned in acetone and ddH₂O (17.9 M Ω) for 5 min followed by drying with pressurized air. Figure 3.2 shows the brass mold master with its dimensions and the finished PDMS stencil.

3.2.3 Surface Modification of PMMA, PC and PDMS Substrates

PMMA and PC substrates were thoroughly rinsed with isopropyl alcohol (IPA), then with ddH₂O followed by drying under nitrogen gas. UV modification was performed using a UV station equipped with a UV light (500 W DUV, model UXM-501 MA, Ushio America, Cypress, CA). The substrates were placed at a distance of 1 cm from the source for a time ranging from 5-30 min with radiation intensities applied from the source equal to 15 mW cm⁻². The cast PDMS fluidic stencil was placed in a plasma cleaner (PDC-3XG, Harrick, Ossining, NY) and oxidized for 1 min prior to use. Immediately after removal from the plasma cleaner, PDMS and UV-modified PC and PMMA substrates were brought into conformal contact forming a reversible seal. The PDMS microfluidic channels were further passivated with 100 mM of MES for 15 min followed by introduction of the amine-terminated oligonucleotide probes. The immobilized probes were hybridized to their dye-labeled complementary targets (20 nM) in a hybridization solution containing 5X SSPE, 0.1% SDS for 1 h followed by washing in 2X SSPE, 0.1% SDS

buffer for 15 min. Fluorescence images of the arrays were collected with a near-IR fluorescence scanner built in-house as described in Chapter 1.

3.2.4 Radioisotope Labeling Assays

An M₁₃ Fwd(-29) oligonucleotide (sequence in Table 3.1) was labeled at its 5' end with [³²P] ATP (3000 Ci/mmol, 10 mCi/ml) according to the manufacture's instructions (Promega, Madison, WI). A reaction cocktail containing 10 µl of 10 pmol oligonucleotide, 2 µl of 10X T4 Polynucleotide kinase (PNK) buffer, 2 µl of [³²P] ATP, 1 µl of kinase enzyme and 5 µl of water were incubated at 37°C. After 45 min, the reaction was stopped by raising the temperature to 65°C and heating for 10 min. Purification of the radio-labeled probe was accomplished by ethanol precipitation. From measured specific activities, the surface probe density was determined via liquid scintillation counting using an LS 6000 liquid scintillation system (Beckmann instruments, Fullerton, CA).

3. 2.5 DNA Microarray Construction

Sixteen different universal zip code probes were used in this study.³⁰ Each zip code probe consisted of a 5' amino modification to facilitate amide bond formation to the carboxylic acid-terminated polymer substrate and a poly-dT tail (15-mer) Each sequence differed from all others by at least six bases to minimize cross-hybridization (sequences shown in Table 3.1). Upon UV modification of PMMA and sealing to plasma oxidized PDMS, 100 µM of each oligonucleotide probe solution prepared in 0.1 M MES at pH 5.5 containing 10 mM EDC was directed through a different channel of the PDMS stencil and allowed to incubate at room temperature. After incubation, the PDMS microchannels were washed in MES buffer to remove any excess oligonucleotide probes and the stencil removed from the PMMA surface. Next, another PDMS device of the same geometry was sealed perpendicular to the probe stencil and complementary dye-labeled targets were delivered through the channels and hybridization performed at 60°C. A

diagrammatic representation of this procedure is shown in Figure 3.3. The PDMS channels were flushed with a washing buffer (2X SSPE, 0.1% SDS) prior to removing the stencil from the PMMA microarray to remove excess, unbound DNA target.

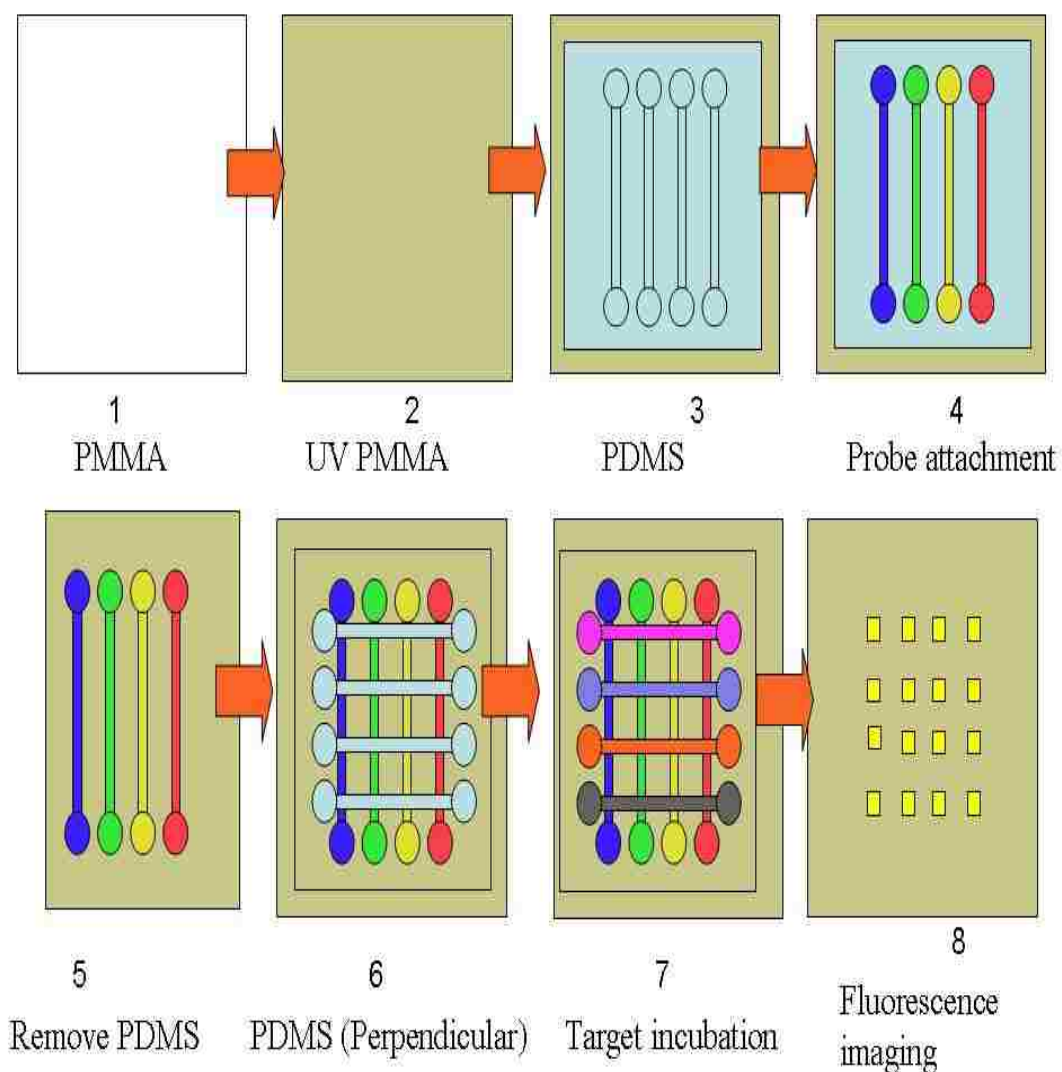


Figure 3.3: A schematic diagram of the microfluidic array construction. PMMA was UV irradiated for 20 min and sealed with a PDMS chip containing 16 channels passivated with MES. Sixteen different oligonucleotide probes (shown in Table 3.1) were passed through the channels and allowed to incubate followed by removal of the PDMS. After washing, the PMMA substrate, containing immobilized probes, was sealed with another PDMS chip placed perpendicular to the existing channels containing the probes. Fluorescently dye-labeled, complementary targets were passed through the channels, hybridized and imaged using a near-IR fluorescence scanner.

3.2.6 Extraction of DNA from Cell Lines

Genomic DNA was extracted from cell lines of known *KRAS2* genotype.⁹ Cell lines were grown in RPMI culture media with 10% bovine serum. Harvested cells ($\sim 1 \times 10^7$ cells cm^{-3}) were resuspended in DNA extraction buffer (10 mM Tris-HCl, pH 7.5, 150 mM NaCl, 2 mM EDTA, pH 8.0) containing 0.5% SDS and 200 $\mu\text{g}/\text{mL}$ proteinase K and incubated at 37°C for 4 h. Thirty-percent (v/v) of 6 M NaCl was added to the mixture and the samples centrifuged. DNA was precipitated from the supernatant with 3 volumes of EtOH, washed with 70% EtOH and resuspended in TE buffer (10 mM Tris-HCl, pH 7.2, 2 mM EDTA, pH 8.0).

Table 3.2: Primers used for K-ras mutation analysis by LDR with microarray detection Sequences in italic (discriminating primers) are complementary to zip code sequences; P-phosphorylated; DY 675- fluorescent label used, Spacer NH_2 - PO_4 $(\text{CH}_2\text{CH}_2\text{O})_6$ $\text{PO}_3(\text{CH}_2)_3\text{NH}_2$.

| Primer | Sequence (5'→3') |
|--------------------|---------------------------------------------------------------------------|
| Zip 1 | TGC GAC CTC AGC ATC GAC CTC AGC -spacer -NH ₂ |
| Zip 2 | ATC GGA CCG GTA TGC GGA CCG GTA- spacer -NH ₂ |
| Zip 3 | CAG CAC CTG ACC ATC GAT CGC AGC- spacer -NH ₂ |
| Zip 4 | GGT AGA CCA CCT TGC GTG CGG GTA- spacer -NH ₂ |
| cZip1-K-rasc12.2D | <i>GCT GAG GTC GAT GCT GAG GTC GCA</i> AAA ACT TGT GGT AGT TGG AGC TGA |
| cZip2-K-ras 12.2 A | <i>TAC CGG TCC GCA TAC CGG TCC GAT</i> AAA ACT TGT GGT AGT TGG AGC TGC |
| cZip3-K-ras 12.2 V | <i>GCT GCG ATC GAT GGT CAG GTG CTG</i> AAA ACT TGT GGT AGT TGG AGC TGT |
| czip4-K-ras 13.4 D | <i>TAC CCG CAC GCA AGG TGG TCT ACC</i> TGT GGT AGT TGG AGC TGG TGA |
| czip5-K-ras 13.4 A | <i>GCT GTA CCC GAT CGC AAG GTG GTC</i> TGT GGT AGT TGG AGC TGG TGC |
| K-ras c12 com-2 | <i>p</i> TGG CGT AGG CAA GAG TGC CT-DY 675 |
| K-ras c13 com-4 | <i>P</i> CGT AGG CAA GAG T GC CTT GAC A-DY 675 |

3. 2.7 PCR Amplification of Genomic DNA

PCR amplifications were carried out in 50 μL of 10 mM Tris-HCl buffer (pH 8.3) containing 10 mM KCl, 4.0 mM MgCl_2 , 250 μM dNTPs, 1 μM forward and reverse primers (50 pmol of each primer), and between 1 and 50 ng of genomic DNA extracted from the cell lines.^{9,27,30} After a 2 min denaturation step, 1.5 units of Amplitaq DNA polymerase (Perkin Elmer, Norwalk, CT) was added under hot start conditions and amplification achieved by thermal cycling for 35 - 40 cycles at 95°C for 30 s, 60°C for 30 s, 72°C for 1 min and a final extension at 72°C for 3 min. PCR products were stored at -20°C until required for the LDR assays.

3. 2.8 Detection of *KRAS2* Mutations by LDR/Hybridization.

LDRs were carried out using a mixture containing four mutation-specific primers and two common primers for codons 12 and 13 as listed in Table 3.2. The reaction cocktail, consisting of 1 μM discriminating primers (cZip1-*KRAS2* 12.2D, cZip2-*KRAS2* 12.2A, cZip3-*KRAS2* 12.2V, czip4-*KRAS2* 13.4D, and czip5-*KRAS2* 13.4 A), 1 μM of fluorescently-labeled common primers (*KRAS2* c12 com-2, *KRAS2* c13 com-4), mutant:wild-type PCR products in a concentration ratio of 1:10 and 1X Taq DNA Ligase Reaction Buffer (New England Biolabs, Beverly, MA), was pre-heated for 2 min at 94°C. Taq DNA Ligase enzyme, (40 units/ μl) (New England Biolabs), was then added followed by thermal cycling for 20 cycles using the following conditions: 94°C for 30 s and 65°C for 4 min. One hundred μmol s of zip code probes 1, 2, 3 and 4 (see Table 3.2) were dissolved in 0.1 M MES buffer containing 10 mM EDC at pH 5.5 with each being directed through the microfluidic network in quadruplicates and allowed to incubate at room temperature for 1 h as described above. The PMMA polymer substrate was pre-heated to 55°C and the LDR product passed through the microchannels for hybridization to their surface-bound complements. The PDMS channels were washed in MES buffer to remove any non-bound DNA target before disassembly of the PDMS/PMMA microfluidic device.

3.3 Results and Discussions

3.3.1 Adsorption Behavior of Oligonucleotide Probes onto Pristine PMMA and PC

To examine the effects of possible attachment of amine-modified oligonucleotide probes to unmodified (pristine) polymers, hybridization assays were performed both on pristine PMMA and PC slides using short oligonucleotide probes bearing an amine group on their 5' ends and solution dye-labeled complements. The oligonucleotide probe solution was made in buffer containing the EDC coupling reagent, spotted (0.2 $\mu\text{L}/\text{spot}$) and allowed to incubate with the pristine surface for 2 h. The solution complement labeled with a fluorescent dye was then allowed to hybridize to any surface-bound probes following extensive washing of the surface using the SSPE buffer. Figure 3.4 shows fluorescence images resulting from these assays.

In the case of pristine PMMA, the array generated only weak fluorescence signals against a uniform background. The image also showed a high degree of non-uniformity in the signal and poor spot definition. To make valid comparisons between microarray slides fabricated on different substrates, we used the signal-to-noise ratio (SNR) as a comparison indicator due to fluorescence background differences observed from slide to slide. The SNR was defined simply as; $(\text{Signal} - \text{Background})/(\text{Background})^{1/2}$, where Background is the intensity of the polymer substrate outside the defined spot region and Signal is the fluorescence intensity arising from defined probe-spot regions on the slide. Typical SNR values for pristine PMMA slides were <10 using these experimental conditions. In contrast, pristine PC demonstrated much higher SNR (~ 340) and well-defined, more uniform spots. However, the PC Background was five-times higher than that observed for PMMA. The choice of PMMA or PC for the intended application is predicated on several factors, such as displaying low levels of autofluorescence if fluorescence is used for array readout and minimal non-specific adsorption effects to the substrate material by the solution complements. While pristine PC allowed the facile coupling of oligonucleotide

probes to its surface forming well-defined hybridization spots, it produced higher levels of non-specific adsorption of fluorescently-labeled complements to its surface compared to pristine PMMA.³⁶ High temperatures (close to the T_m of the duplexed DNA) are generally believed to ensure stringency for hybridization and reduce non-specific adsorption of dye-labeled targets to the support surface.³⁷

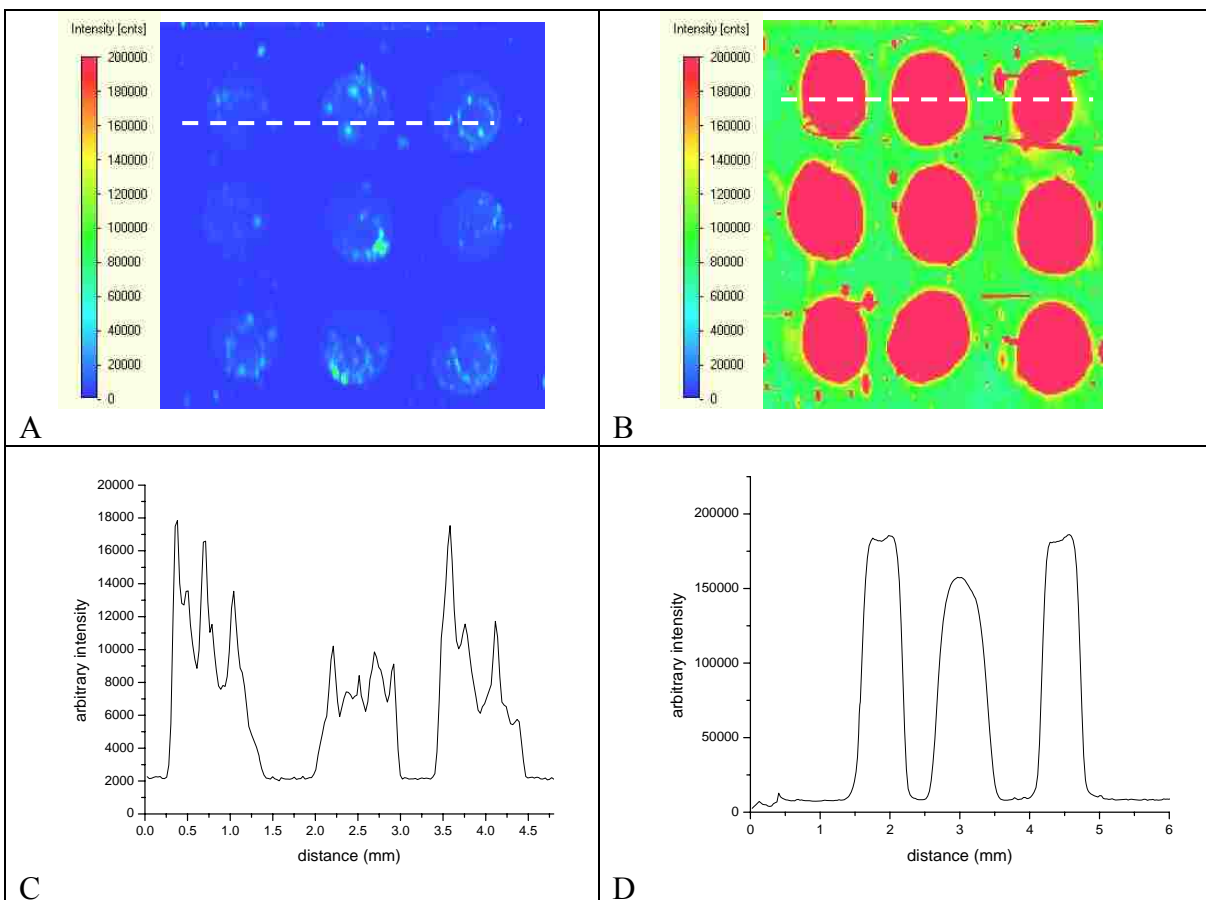


Figure 3.4: Fluorescence images of oligonucleotide probes deposited on pristine PMMA and PC slides. The near-IR fluorescence images of PMMA and PC are shown in panels A and B, respectively. The intensity profiles from a cross section of the top three spots on PMMA and PC are shown in panels C and D, respectively. Both slides were prepared by spotting 100 μ M oligonucleotide probe C₆-amino 34-mer in 200 mM phosphate solution to native slide surfaces in a 3 x 3 pattern (0.2 μ L/spot), incubated at 37°C overnight, and followed by hybridization in 10 nM dye-labeled complements (M₁₃ Fwd (-29)-IRD 800) in 5x SSPE, 0.1% SDS, at 60°C for 1 h.

After incubating the oligonucleotide solution to pristine PC surfaces overnight at 60°C in the hybridization solution, neither a significant loss of fluorescent signal at the hybridization spot

or non-specifically adsorbed DNA was observed. These results show that the interaction between the oligonucleotide probes and the pristine PC surfaces are very strong, indicating a high propensity to non-specifically adsorb oligonucleotides to its surface. In the case of PMMA, this affinity was significantly lower. Thermally stable attachment of amine-modified oligonucleotide probes to pristine PC does take place producing well defined and fairly homogenous spots as indicated by the hybridization-based assays (see Figure 3.4). This observation indicates that under non-critical conditions, where the copy number of solution targets is relatively high, this surface can be used in its native state for monitoring hybridization events. The attractive nature of this format is that the material does not require any type of activation (chemical or photochemical), special coating cocktails or capping, simplifying the production of DNA microarrays. In addition, the autofluorescence level of pristine PC has also been noted to be higher than that seen for pristine or photo-activated PMMA.³⁶ When laser scanning the array to produce a fluorescence image, the background level will be higher for PC as compared to PMMA, which will lower the signal-to-noise ratio in the readout phases of the assay.

3.3.2 Attachment of Oligonucleotide Probes onto Carboxyl-terminated, UV-Activated PMMA and PC

Previous work in our group and others have generated attractive modification chemistries developed for covalently linking oligonucleotide probes to various polymer surfaces.^{7, 9, 10, 18, 37-39} However, these methods require a significant number of processing steps, produce low probe densities on the solid support, demand large amounts of processing time and require spotting to build the array. As such, we sought to use the known photochemical behavior of PMMA and PC to build functional scaffolds for high-surface density DNA probe attachment for microarray applications.

PC and PMMA surfaces were next exposed to UV light (254 nm) and then, an amine-modified oligonucleotide probe solution (M₁₃Fwd (-29)) containing EDC was spotted onto these

UV-activated substrates. EDC was utilized here because it is a widely accepted water-soluble cross-linking agent used to form amide bonds between primary amines and carboxylate groups.⁴¹ The carbodiimide first reacts with carboxylate-containing substrates to form a highly reactive, O-acylisourea intermediate. This activated species then reacts with a primary amine-bearing oligonucleotide probe forming an amide bond between the probe and the carboxylate groups produced from UV-irradiation of the polymer substrate.

After immobilization of the probe and hybridization to complementary target molecules, the slides were rinsed with SSPE buffer and subsequently imaged using our fluorescence scanner. The fluorescence intensity difference between the UV-exposed and non-exposed regions indicated that more oligonucleotide probes were immobilized onto the UV-exposed regions for both polymers. However, the UV-exposed PC slide demonstrated a significant amount of non-specific adsorption of the dye-labeled solution complement to its surface. Although the fluorescence intensity of UV-exposed PC was comparable to that of pristine PC hybridization spots, the SNR on the exposed region was only ~26 due to the high level of non-specific adsorption and/or autofluorescence generated from this substrate. In the case of PMMA, the SNR for hybridization assays onto photoactivated PMMA was found to be 550 with minimal amounts of non-specific adsorption of dye-labeled oligonucleotides to the UV-activated PMMA surface. In fact, no difference in fluorescence was noticed between the pristine and UV-activated PMMA surface after incubation with a solution dye-labeled oligonucleotide. Due to the low degree of non-specific adsorption to PMMA by the dye-labeled complement and its low autofluorescence level, the remainder of our experiments utilized PMMA as the substrate of choice, which was photochemically modified with carboxylate-groups for covalent DNA probe attachment bearing a primary amine group. The relationship between the density of photo-generated functional groups and the UV dose was further studied using PMMA substrates. UV

exposure was performed for various times (5, 10, 15, 20, 25, and 30 min) and probe surface densities were determined via ^{32}P radio-isotopic labeling. Fluorescence hybridization assays were also performed as a comparison. Figure 3.5 depicts the surface probe density as a function of radiation time monitored by scintillation counting of the ^{32}P probe. As can be seen, the probe density reached a maximum value after 15 min of UV exposure with a probe surface concentration calculated to be 2.5×10^{13} molecules/cm 2 (~ 41.5 pmol cm $^{-2}$). When the fluorescence was monitored by performing a hybridization-based assay using a dye-labeled solution complement, the fluorescence intensity was found to increase with dose until about 15 min after which it remained fairly constant (see Figure 3.5 B), similar to what was seen for the ^{32}P experiment.

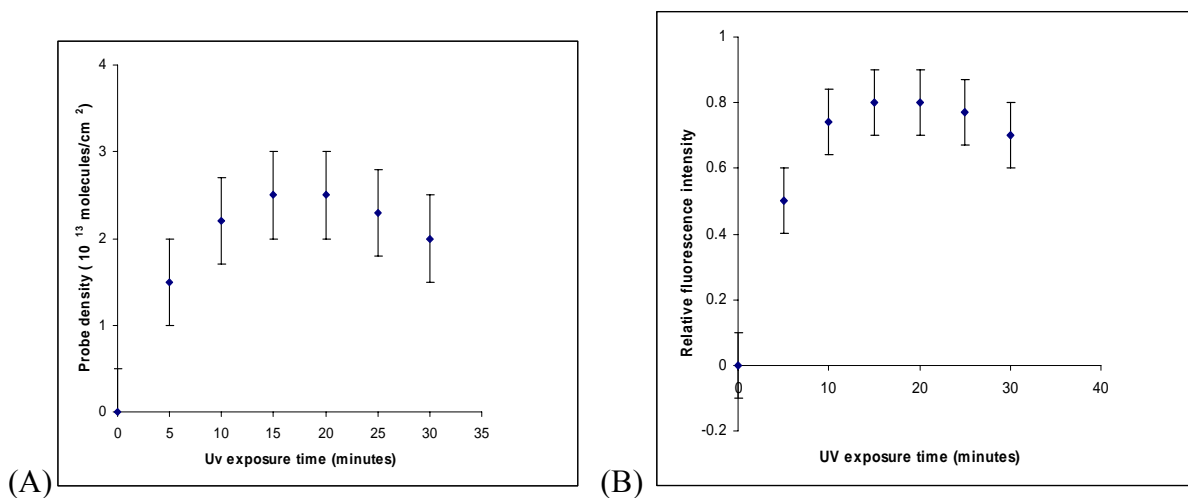


Figure 3.5: Effect of UV exposure times on probe attachment to surfaces. (A) PMMA slides were UV irradiated at various times (5 -30 min), 1 μM of ^{32}P radiolabeled M13 Fwd(-29)-(0.5 μl) oligonucleotide probe was spotted on the slides and allowed to incubate for 1 h. Quantitative measurements were performed by liquid scintillation counting. (B) Relative fluorescence intensities shown with respect to UV exposure time. PMMA slides were UV irradiated at various times (5 -30 min), 1 μM (0.2 μl) of M $_{13}$ Fwd(-29) probe was attached on PMMA slides for 1 h followed by hybridization with 10 nM IRD 700 dye-labeled complementary target for 1 h.

Activation of PMMA and PC by UV irradiation producing surface-confined carboxylic acids was demonstrated, which reached saturation within 15 min (see Figure 3.5) in terms of

surface-probe density. The production of this activated surface allowed the facile covalent immobilization of amine-terminated probes to their surfaces using EDC coupling to form amide bonds between the activated polymer surface and the oligonucleotide probe. For PMMA, probe densities of $\sim 41 \text{ pmol cm}^{-2}$ were achieved. The UV-based probe immobilization protocol reported herein resulted in a higher surface concentration of probe compared to an earlier chemical modification procedure of PMMA, which yielded an immobilization surface concentration of only $33.1 \text{ fmol cm}^{-2}$.¹¹ Recently, Fix et al. reported a chemically-based immobilization procedure for probe attachment to PMMA for constructing DNA microarrays that showed probe densities $\sim 10 \text{ pmol cm}^{-2}$,¹⁰ which is similar to surface densities obtained on silanized glass. The surface coverage we report here is close to the maximum surface coverage determined by steric considerations for DNAs loaded onto a surface, which has been determined to be 50 pmol cm^{-2} .⁴² The surface probe density observed here was found to be reduced after 20 min of UV-photo-oxidation, which could be attributed to surface degradation of the polymer substrate at long exposure times. For example, main-chain scissions of methyl ester groups have been noted for high UV doses.^{12,13} Because the number of methyl ester groups accessible in the PMMA polymer backbone after photochemical modification determines the number of carboxylic groups that are available for interaction with the amine-modified oligonucleotides, scission reactions and cross-linking of olefin sites from scission reactions may explain why the probe densities are reduced with UV exposure times >20 min. The same trend was observed when monitoring dose-dependent responses via fluorescence elicited from hybridization-based measurements (see Figure 3.5). Using this UV-photomodification protocol, minimal processing steps are required to create robust microarrays (high surface density, stable linkage chemistry). For example, in the current method, only three steps were required to create the array (UV-activation; EDC coupling and; washing) while in reported chemical modification methods of

PMMA^{9,10}, 5 steps were necessary (amination; cross-linking with glutardialdehyde; probe coupling; washing and; surface capping of residual surface active groups). The photo-activation method makes array fabrication simple, less time consuming and does not require extensive amounts of specialized reagents to produce robust linkages with high surface densities.

3.3.3 Coupling Microarrays to Microfluidics

Our modification protocol was used to build medium-density arrays using microchannels fabricated in PDMS to direct fluids to a location on the functionalized PMMA substrate.^{34, 35} The PDMS “stencil” was first used to pattern the oligonucleotide probes onto the PMMA surface, and then, to address the array using microfluidics. PDMS can easily be fabricated by soft lithography techniques from a master that can be used many times for making microchannels through replica molding.⁴³ However, PDMS is extremely hydrophobic, making it difficult to fill microchannels with aqueous solutions. This can be circumvented by oxygen plasma treatment and/or dynamic coating of the channels with surfactants.^{39,44,45} We found that we could reversibly seal an “activated” PMMA substrate to plasma-oxidized PDMS to form a hybrid microfluidic device. This reversible seal allowed the PDMS stencil to be used for patterning the probes onto the functionalized PMMA surface followed by interrogation of the array via microfluidics. The stencil could then be simply removed to permit fluorescence imaging of the array.

To demonstrate the use of this microfluidic concept to pattern medium-density arrays onto our carboxy-terminated PMMA solid support, 16 different oligonucleotide probes containing a unique universal zip code sequences³⁰ (sequences shown in Table 3. 1) were used with each probe being directed through a different channel of the PDMS device. Complementary dye-labeled oligonucleotides were then directed through each of the 16 channels after rotation of the PDMS stencil by 90° followed by hybridization and imaging.

Figure 3.6 provides an image of a 16 x 16 array interrogated on the carboxylated-PMMA solid support using a microfluidic PDMS stencil. The 16 zip code sequences (24-mers) were designed such that each differed from all others by at least six bases to minimize cross-hybridization.³⁰ Clear fluorescence spots were observed in each channel and along the 16 spots of each channel with fairly uniform intensity across the array.

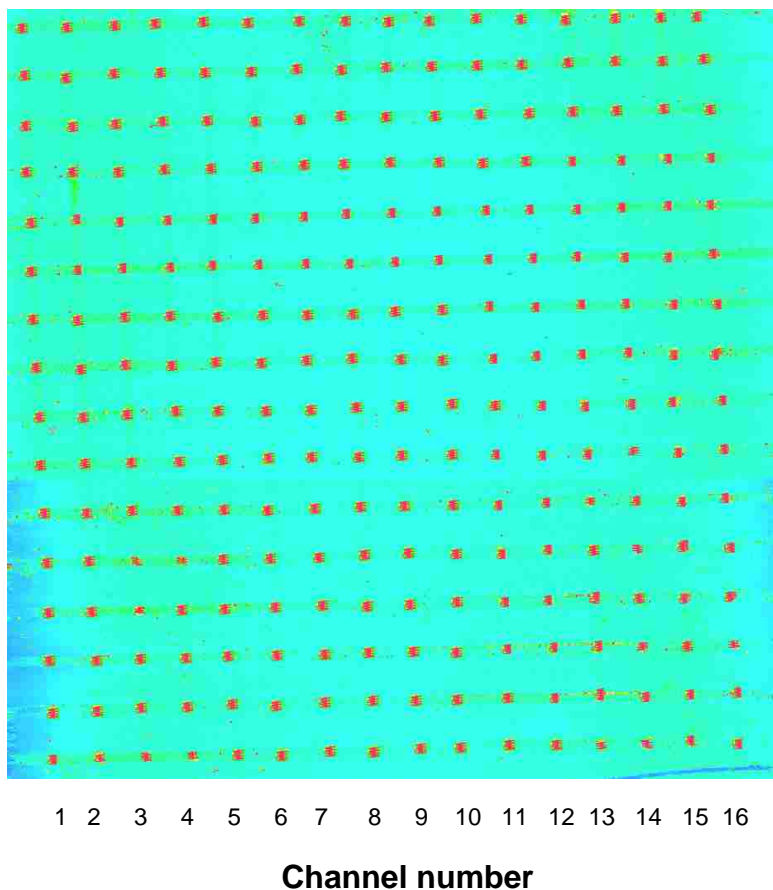


Figure 3.6: Parallel arrays: Sixteen universal zip code array probe sequences shown in Table 3.1 (100 μ M in 0.1 M MES buffer pH 5.5) were addressed to UV modified PMMA via microfluidic channels in PDMS, each channel containing a different zip code probe. Immobilization was done at room temperature for 1 h followed by hybridization with 50 nM IRD 700 dye labeled complementary fragments in 5X SSPE, 0.1% SDS hybridization solution for 20 min. Fluorescence images were scanned at a step resolution of 50.8 μ m/step and integration time of 0.1 s per pixel. The images of each channel (1-16) represent hybridization interactions of the each zip code probe (zipcode 1 – zipcode 25) with their respective complements.

Demonstration of this process for creating medium density arrays for screening multiple mutations in certain genes was next examined. The proof-of-concept involved coupling an allele-

specific ligation assay (LDR) to a universal array configured on a carboxy-generated PMMA surface to detect point mutations in *KRAS2* genes. The LDR cocktail consisted of discriminating primers that possessed 24-mer zip code complement sequences at their 5' ends (*italics*, see Table 3.2) with discriminating bases on their 3' ends and common primers phosphorylated at their 5' ends with a fluorescent label at their 3' ends (sequences shown in Table 3. 2).

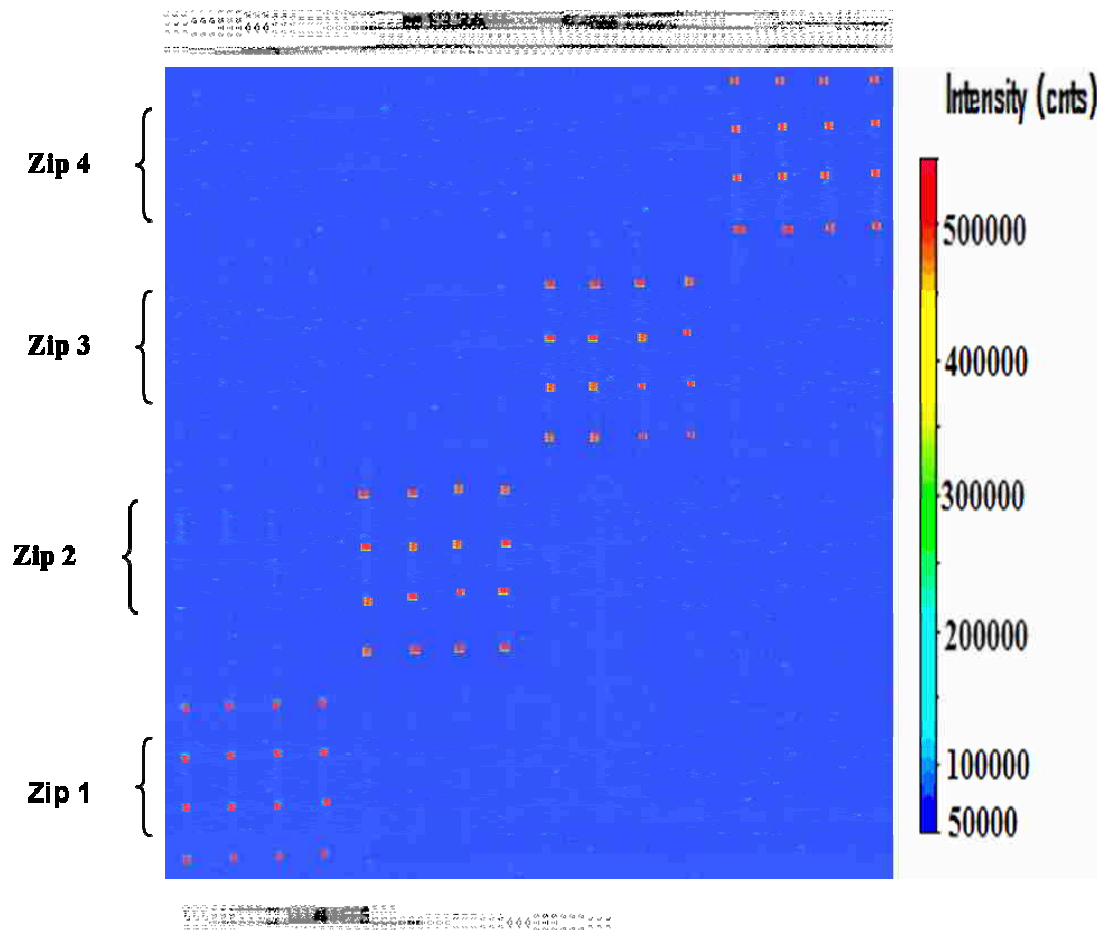


Figure 3.7: Mutation analysis: Four different zip code arrays were addressed in quadruplicates through the microfluidic device and allowed to incubate at room temperature for 1 h. From left; channels 1, 2, 3 and 4 are specific for K-ras 12.2 D mutation; channels 5, 6, 7 & 8 specific for K-ras 12.2A mutation; channels 9, 10, 11 & 12 specific for K-ras 12.2V mutation while channels 13, 14, 15 & 16 were specific for K-ras 13.4 D mutations. The LDR products were directed through the channels followed by hybridization at 55°C for 20 min and they were all captured at their correct zip codes. Fluorescence imaging was done using the near-IR scanner at a step resolution of 12.5 $\mu\text{m}/\text{step}$ and integration time of 0.1 per pixel.

During an LDR, the discriminating primer corresponding to a specific point mutation and the dye-labeled common primer are ligated only if a match is present between the discriminating base and the particular locus being interrogated. Detection of fluorescence at each particular zip code position indicates the presence of a specific mutation. When the mutation is absent, the two primers are not ligated^{9,30} and as such, do not generate a fluorescence signature at a specific location on the array. The oligonucleotide probes used for our medium density arrays act as zip codes,^{9,30} which direct an allele-specific ligation product formed as a result of a successful LDR to the appropriate address of a universal array. The primers required for the LDR (common and discriminating primers) carry either a fluorescent tag (common primer) or a zip code complement (discriminating primer) that directs the LDR product to the appropriate location on the array for multiplexed readout. We desired the ability to produce universal arrays on polymer substrates that could be accessed using microfluidics, due to the ability to rapidly address the array⁹ and also to pattern the array using simple procedures that did not require spotting, thereby minimizing front-end preparation of the array.

Four universal zip code probes; zip 1, zip 2, zip 3 and zip 4 (sequences in Table 3.2) were directed in quadruplicates onto activated PMMA and hybridization assays with the appropriate LDR products performed. Fluorescence images observed for several *KRAS2* mutations are shown in Figure 3.7. The signals observed at zip code 1 resulted from a positive *KRAS2* 12.2D mutation. These are due to hybridization events occurring between this zip code probe and its complementary sequence on the discriminating primer upon successful ligation of the fluorescence-bearing (common) primer to the zip code (discriminating) primer. The ligated product for this mutation contains a discriminating primer, which is only complementary to zip code 1. No signal was observed at other zip code probes (zip codes 2, 3 and 4) in these channels (1-4) because of a lack of a successful ligation reaction between the common and the appropriate

discriminating primers during LDR. In line with the *KRAS2* 12.2D results, the *KRAS2* 12.2A mutation was detected at zip code 2 (see channels 5-8, Figure 2.7); *KRAS2* 12.2V at zip code 3 (see channels 9-12, Figure 3.7) and *KRAS2* 13.4D captured at zip code 4 (see channels 13-16, Figure 3.7). As can be seen from the results depicted in Figure 3.7, no noticeable cross-hybridization or mis-ligation events were observed in the fluorescence image.

3. 4 Conclusions

The photo-activation protocol developed herein was merged with microfluidics to allow parallel processing of different DNA targets for diagnostic applications using a coupled LDR/universal array assay. To eliminate the need for spotting to the activated surface, a PDMS stencil was used.^{34,35} This was accomplished by patterning the probes to the surface with a 16-channel PDMS stencil brought into conformal contact with the activated PMMA surface, followed by probe tethering. Addressing of the array was accomplished by rotating the PDMS stencil by 90° and flowing through it solution complements containing fluorescent labels. Because of the small dimensions of the fluidic channels, the efficient movement of sample or probe solution through the microchannels ensured that there were homogeneous and sufficient amounts of target DNA or probe molecules distributed across the entire array enabling uniform hybridization signals (see Figure 3.6). In addition, the fluidic arrangement used herein allowed saturation of the available binding sites between the tethered probes and solution complements in <2 min, as reported earlier by our group when coupling microfluidics to microarrays.⁹ As can also be seen in the image presented in Figure 3.6, no observable non-specific adsorption of the solution, dye-labeled complement to the surface was noticed, which would have created “streaking” in the image if present. This lack of non-specific interaction between poly-anionic DNA and the PMMA surface would be expected based on electrostatic considerations because the photo-activation of PMMA creates a negatively charged surface through generation of surface-carboxylates. In addition, the lack of non-specific adsorption of solution complements to

this activated PMMA surface indicates that capping of residual functional groups following probe attachment is not necessary, simplifying array construction.

A 16 x 16 element, universal array was prepared to screen for the allelic composition at one mutation site and the presence of a second mutation in a *KRAS2* oncogene that possesses high diagnostic value for colorectal cancers. The array was fabricated using zip-code probes, which direct products formed from a successful ligation reaction (LDR) to a particular pixel of a 256-element array. The results indicated (see Figure 3.7) minimal amounts of cross-hybridization and no observable mis-ligation at the levels in which the experiment was conducted (wild-type to mutant ratio = 10 to 1). In addition, the image obtained indicated the presence of a successful LDR at the appropriate address of the universal array.

3.5 References

- (1) Soper, S. A.; Ford, S. M.; Qi, S.; McCarley, R. L.; Kelly, K.; Murphy, M. C. *Analytical Chemistry* **2000**, *72*, 643A-651A.
- (2) Martynova, L.; Locascio, L. E.; Gaitan, M.; Kramer, G. W.; Christensen, R. G.; MacCrehan, W. A. *Analytical chemistry* **1997**, *69*, 4783-4789.
- (3) Nagata, Y.; Yokota, H.; Kosuda, O.; Yokoo, K.; Takemura, K.; Kikuchi, T. *Febs Letters* **1985**, *183*, 379-382.
- (4) Nikiforov, T. T.; Rogers, Y. H. *Analytical Biochemistry* **1995**, *227*, 201-209.
- (5) Schena, M.; Editor *DNA Microarrays: A Practical Approach*; Oxford university Press: Oxford, 1999.
- (6) Lueneberg, E.; Jensen, J. S.; Frosch, M. *Journal of Clinical Microbiology* **1993**, *31*, 1088-1094.
- (7) Hirayama, H.; Tamaoka, J.; Horikoshi, K. *Nucleic Acids Research* **1996**, *24*, 4098-4099.
- (8) Matson, R. S.; Rampal, J. B.; Coassin, P. J. *Analytical biochemistry* **1994**, *217*, 306-310.
- (9) Wang, Y.; Vaidya, B.; Farquar Hannah, D.; Stryjewski, W.; Hammer Robert, P.; McCarley Robin, L.; Soper Steven, A.; Cheng, Y.-W.; Barany, F. *Analytical chemistry* **2003**, *75*, 1130-1140.

- (10) Fixe, F.; Dufva, M.; Telleman, P.; Christensen, C. B. V. *Nucleic Acids Research* **2004**, *32*, e9/1-e9/8.
- (11) Waddell, E.; Wang, Y.; Stryjewski, W.; McWhorter, S.; Henry, A. C.; Evans, D.; McCarley, R. L.; Soper, S. A. *Analytical Chemistry* **2000**, *72*, 5907-5917.
- (12) Hirt, R. C.; Searle, N. Z.; Schmitt, R. G. *SPE Transactions* **1961**, *1*, 21-24.
- (13) Rabek, J. F. *Polymer Photodegradation: Mechanisms and Experimental Methods*; Chapman & Hall: London, 1994.
- (14) Liu, Y.; Ganser, D.; Schneider, A.; Liu, R.; Grodzinski, P.; Kroutchinina, N. *Analytical Chemistry* **2001**, *73*, 4196-4201.
- (15) Johnson, T. J.; Waddell, E. A.; Kramer, G. W.; Locascio, L. E. *Applied Surface Science* **2001**, *181*, 149-159.
- (16) Xu, Y. C.; Vaidya, B.; Patel, A. B.; Ford, S. M.; McCarley, R. L.; Soper, S. A. *Analytical Chemistry* **2003**, *75*, 2975-2984.
- (17) Ford, S. M.; Davies, J.; Kar, B.; Qi, S. D.; McWhorter, S.; Soper, S. A.; Malek, C. K. *Journal of biomechanical engineering* **1999**, *121*, 13-21.
- (18) Soper, S. A.; Henry, A. C.; Vaidya, B.; Galloway, M.; Wabuye, M.; McCarley, R. L. *Analytica Chimica Acta* **2002**, *470*, 87-99.
- (19) Liu, Y.; Rauch, C. B.; Stevens, R. L.; Lenigk, R.; Yang, J.; Rhine, D. B.; Grodzinski, P. *Analytical Chemistry* **2002**, *74*, 3063-3070.
- (20) Anderson, R. C.; Su, X.; Bogdan, G. J.; Fenton, J. *Nucleic acids research* **2000**, *28*, e60.
- (21) Xu, J.; Locascio, L.; Gaitan, M.; Lee, C. S. *Analytical Chemistry* **2000**, *72*, 1930-1933.
- (22) Fan, Z. H.; Mangru, S.; Granzow, R.; Heaney, P.; Ho, W.; Dong, Q.; Kumar, R. *Analytical Chemistry* **1999**, *71*, 4851-4859.
- (23) Guillet, J. *Polymer Photophysics and Photochemistry: An Introduction to the Study of Photoprocesses in Macromolecules*, 1985.
- (24) Smith, A. J.; Stern, H. S.; Penner, M.; Hay, K.; Mitri, A.; Bapat, B. V.; Gallinger, S. *Cancer research* **1994**, *54*, 5527-5530.
- (25) Bos, J. L. *Mutation research* **1988**, *195*, 255-271.
- (26) Breivik, J.; Meling, G. I.; Spurkland, A.; Rognum, T. O.; Gaudernack, G. *British journal of cancer* **1994**, *69*, 367-371.

- (27) Khanna, M.; Park, P.; Zirvi, M.; Cao, W.; Picon, A.; Day, J.; Paty, P.; Barany, F. *Oncogene* **1999**, *18*, 27-38.
- (28) Sidransky, D.; Tokino, T.; Hamilton, S. R.; Kinzler, K. W.; Levin, B.; Frost, P.; Vogelstein, B. *Science* **1992**, *256*, 102-105.
- (29) Thomas, G.; Sinville, R.; Sutton, S.; Farquar, H.; Hammer, R. P.; Soper, S. A.; Cheng, Y.-W.; Barany, F. *Electrophoresis* **2004**, *25*, 1668-1677.
- (30) Gerry, N. P.; Witowski, N. E.; Day, J.; Hammer, R. P.; Barany, G.; Barany, F. *Journal of Molecular Biology* **1999**, *292*, 251-262.
- (31) Luo, J.; Barany, F. *Nucleic acids research* **1996**, *24*, 3079-3085.
- (32) Gul, S.; Brown, R.; May, E.; Mazzulla, M.; Smyth, M. G.; Berry, C.; Morby, A.; Powell, D. J. *Biochemical Journal* **2004**, *383*, 551-559.
- (33) Luo, J.; Barany, F. *Nucleic Acids Research* **1996**, *24*, 3079-3085.
- (34) Lee, H. J.; Goodrich, T. T.; Corn, R. M. *Analytical Chemistry* **2001**, *73*, 5525-5531.
- (35) Delamarche, E.; Bernard, A.; Schmid, H.; Michel, B.; Biebuyck, H. *Science* **1997**, *276*, 779-781.
- (36) Wabuyele, M. B.; Ford, S. M.; Stryjewski, W.; Barrow, J.; Soper, S. A. *Electrophoresis* **2001**, *22*, 3939-3948.
- (37) Marquette, C. A.; Blum, L. J. *Analytica Chimica Acta* **2004**, *506*, 127-132.
- (38) Liu, Y. J.; Rauch, C. B. *Analytical Biochemistry* **2003**, *317*, 76-84.
- (39) Makamba, H.; Kim, J. H.; Lim, K.; Park, N.; Hahn, J. H. *Electrophoresis* **2003**, *24*, 3607-3619.
- (40) Marquette, C. A.; Blum, L. J. *Analytica Chimica Acta* **2004**, *506*, 127-132.
- (41) Hermanson, G. T.; Editor *Bioconjugate Techniques*; Academic Press: San Diego, 1995.
- (42) Ross, J. *Nucleic Acid Hybridization: Essential Techniques*; John Wiley & Sons: New York, 1997.
- (43) Duffy, D. C.; McDonald, J. C.; Schueller, O. J. A.; Whitesides, G. M. *Analytical Chemistry* **1998**, *70*, 4974-4984.
- (44) Kaczmarek, H.; Kaminska, A.; Van Herk, A. *European Polymer Journal* **2000**, *36*, 767-777.
- (45) van der Wel, H.; Lub, J. *Surface and Interface Analysis* **1993**, *20*, 373-378.

CHAPTER 4

IMMOBILIZATION OF MOLECULAR BEACONS: A NEW STRATEGY USING UV-ACTIVATED PMMA SURFACES TO PROVIDE LARGE FLUORESCENCE SENSITIVITIES FOR REPORTING ON MOLECULAR ASSOCIATION EVENTS*

4.1 Introduction

4.1:1 Molecular Beacon Technology

Recent advances in genetic analyses using a variety of enabling tools have produced new biosensor technology platforms that can be used for the rapid screening and sensitive detection of unique molecular signatures, such as genes. Genetic analyses typically require highly sensitive and specific DNA/RNA detection techniques that can be accomplished through the use of DNA probes that not only provide molecular recognition of unique DNA structures, but also report on the molecular association through a fluorescence transduction event that have become very attractive assemblies in a variety of applications. Examples of such probes are molecular beacons (MBs), which were originally described by Tyagi and Kramer for the detection of specific nucleic acids in homogeneous solutions.¹ MBs are hairpin probes consisting of a loop and stem structure. The loop portion is the sequence recognition section of the MB while the stem, which is comprised of complementary sequences, intra-molecularly hybridizes in the absence of the loop complement. The stem sequences flank either side of the loop sequence. On one end of the arm, a fluorophore is attached, while the other end possesses a quencher. Upon hybridization of these two arm sequences, the closed hairpin structure forms placing in close proximity the fluorophore and quencher producing quenching of the fluorescence reporter either through contact mediation or energy transfer. When the recognition loop hybridizes to the complementary target sequence, the stem opens spatially removing the fluorophore from the quencher restoring the fluorescence (see Figure 4.1 below).

* Reprinted with permission from Analytical Biochemistry 2007, 363(1), 35-45

These probes have found numerous applications, such as the detection of pathogenic retroviruses,² discrimination of wild type and single point mutations,^{3,4} real time monitoring of DNA/RNA in solution/living specimens^{1,5} and single nucleotide polymorphism detection.⁶ One major advantage of MBs is the possibility of their use in real-time hybridization monitoring.

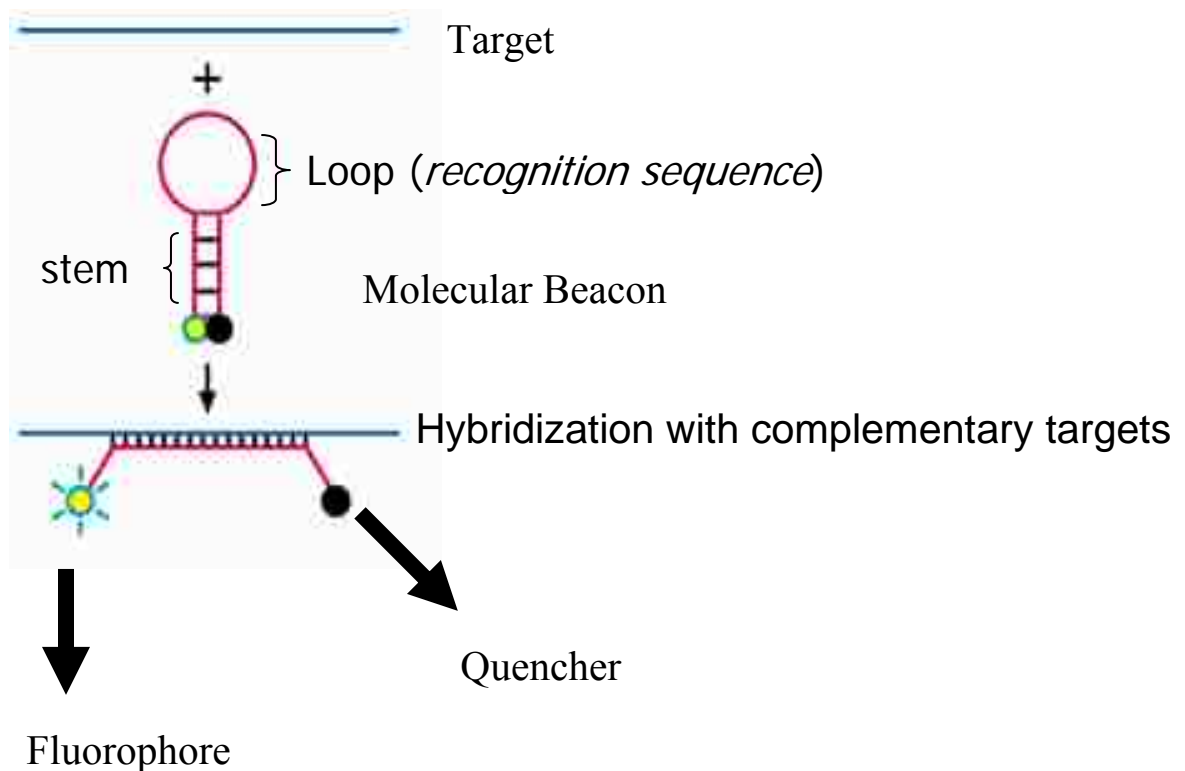


Figure 4.1: Molecular beacons. In the absence of a complementary target sequence, the molecular beacon remains closed and there is no appreciable fluorescence. When the molecular beacon unfolds in the presence of the complementary target sequence, the fluorophore is no longer quenched, and the molecular beacon fluoresces.

This offers a simple closed-tube format assay that reduces the chances of contamination, reducing the potential for false positives. Also, depending on the application, MBs can be designed to have structural variations making them very flexible. For example, peptide nucleic acid (PNA) oligomers can be used instead of DNA.⁷ PNAs are DNA mimics with pseudopeptide (polyamide) backbone instead of sugar-phosphates in DNA. The flexibility of the sugar-phosphate and polyamide backbones of DNA and PNA, respectively, in combination with a

strong hydrophobic interaction between the fluorophore and the quencher keeps these structures in a closed form in the absence of targets.

Another example depicting structural flexibility of MBs are catalytic MBs.⁸⁻¹² These are DNA constructs that combine the features of MBs and hammerhead-type deoxyribozymes with RNase activity which are located on two different modules as illustrated in Figure 4.2 below. A DNA construct is made that combines the features of a molecular beacon and a hammerhead-type deoxyribozyme with RNase activity; these are located on two different modules (see Figure 4.2 below).

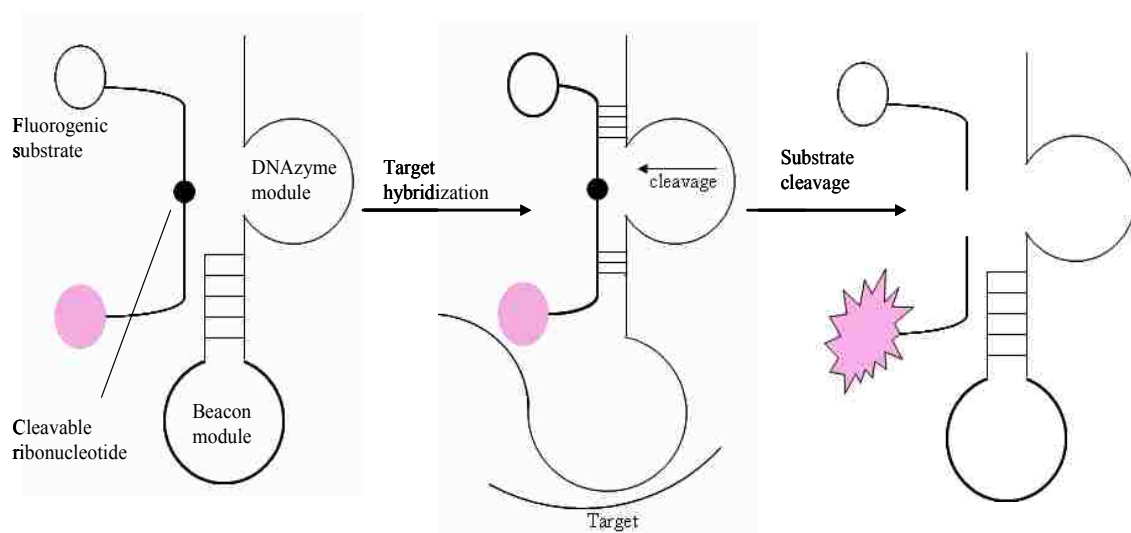
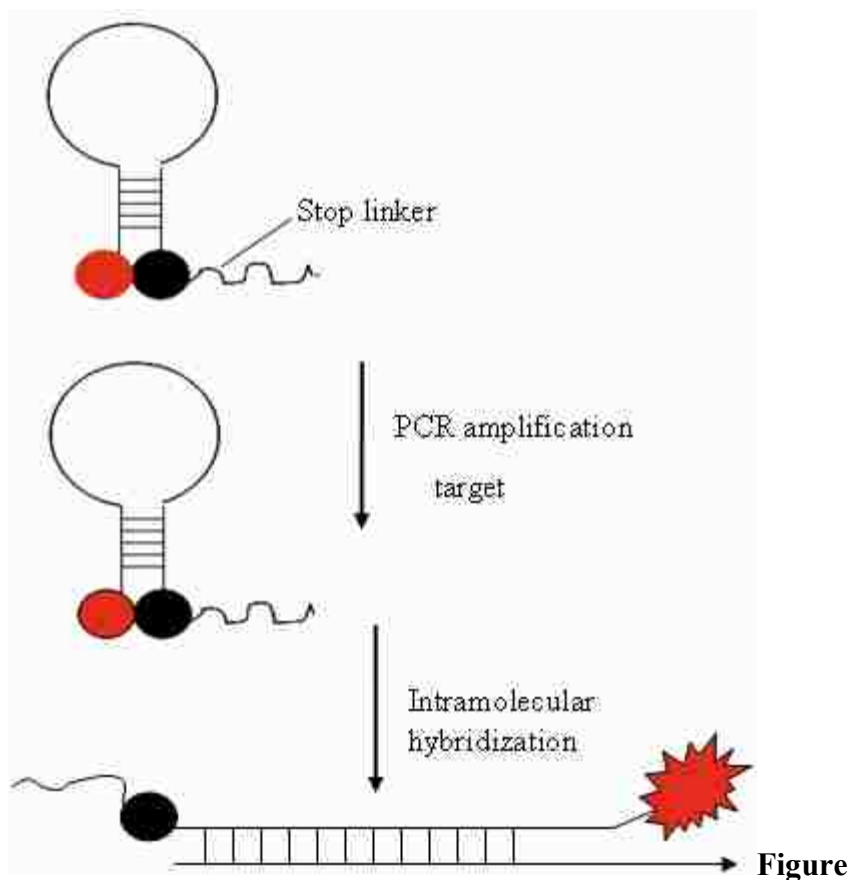


Figure 4.2: Catalytic molecular beacon. In the absence of targets, the MB hybridizes with the deoxyribozyme module. When the target is present, the MB changes its conformation and allows the substrate (a stemless fluorogenic oligonucleotide) to hybridize with the deoxyribozyme module. The deoxyribozyme cleaves the substrate, which results in increasing fluorescence.¹²

In the absence of a target, the beacon module hybridizes with the deoxyribozyme module. In the presence of a target, the beacon module changes its conformation and allows the substrate to hybridize with the deoxyribozyme module. The substrate is a stemless fluorogenic oligonucleotide. The deoxyribozyme cleaves the substrate at a cleavable ribonucleotide, which results in increasing fluorescence. The substrate dissociates on cleavage and the beacon module hybridizes with the deoxyribozyme module and the cycle is repeated.¹² Further developments of

the molecular beacon technology involve use of a scorpion probe simultaneously as a PCR primer and a molecular beacon (see Figure 4.3 below).



4.3: The scorpion-probe approach. A stem-loop shaped probe is incorporated into PCR primer, allowing unimolecular target detection, which ensures faster kinetics and higher stability of the complex than the bimolecular reaction.¹²

In this approach, the PCR primer is designed to have a 5'-extension that has all the attributes of a beacon; a loop region complementary to a target flanked by the self complementary stems and a fluorophore and a quencher at the 5'- and 3'-ends of the extension, respectively. The stem-loop extension is linked to the PCR primer via a linker, which stops DNA polymerase from replicating the stem-loop. During PCR, when the primer is extended and the target is synthesized, the stem-loop unfolds and the loop sequence hybridizes intramolecularly with its target, which increases fluorescence. Thus, the scorpion-primer approach uses a

unimolecular mechanism of probe-target hybridization, compared with the bimolecular recognition in the traditional molecular beacon assay. This ensures faster kinetics and greater stability of the probe-target complex.¹²

4.1.2 Hairpin versus Linear Oligonucleotide Probes

MBs have advantages over their linear nucleic acid probe counterparts most commonly found in microarray technology. One important advantage is their recognition specificity. The stem probe structure of a molecular beacon makes it better able to discriminate single base mismatches (compared to linear probes) because the hairpin makes mismatched hybrids thermally less stable than hybrids between the corresponding linear probes and their mismatched target. Bonnet et al. have studied the thermodynamic hybridization behavior of linear and stem-loop MB probes and found that the MBs demonstrate significantly higher specificity.^{13,14} By analyzing free energy phase diagrams of MBs in solution with matched and mismatched targets, the authors indicated that structurally constrained MBs can distinguish mismatches over a wider range of temperatures compared to unstructured (linear) probes.^{13,14} Riccelli and coworkers have also compared the hybridization of ssDNA targets to immobilized complementary hairpin versus linear capture probes.¹⁵ They used a micro titer-based assay system to measure the time-dependence and thermodynamic stability of target hybridization with hairpin and linear probes. Their results showed that target capture by hairpin probes is faster than with linear probes and that, once formed, hairpin complexes are thermodynamically more stable.

Another advantage of MBs is that unhybridized forms do not fluoresce, making it unnecessary to remove them from the hybridized probes offering the advantage of detection without separation. Additionally, the target molecules do not require labeling, thus the beacon is both the probe and the transducer of the molecular association event. Furthermore, unlike linear probes, quenching of molecular beacons has been shown to occur through a direct transfer of

energy from fluorophore to quencher. Consequently, a common quencher molecule can be used, increasing the number of possible fluorophores that can easily be used as reporters. This is an important advantage when designing Polymerase Chain Reactions (PCR) experiments in which several molecular beacons with different colored fluorophores are used to detect multiple targets in the same tube (multiplexing).

4.1.3 Molecular Beacons Used on Arrays

Although previous research involving MB probes has been performed in homogeneous phases, surface immobilization of MBs has not been reported extensively. Surface immobilization has the advantage of allowing spatially multiplexed detection with a probe that not only offers selective affinity for its complement, but also reports on the molecular association, obviating the need for labeling of the solution complement. The implementation of surface immobilized MBs or other molecular probes into an array format also enables the seamless integration of this technology to various sample processing steps by the direct coupling of the array to a microfluidic system, which offers high levels of automation and reduced sample and reagent consumption, lowering assay costs.¹⁶

MB probes have been immobilized onto solid surfaces but unfortunately, they display lower sensitivities, where the sensitivity here is defined as the ratio of fluorescence of the probe upon binding to its target with that of the probe in its closed (non-fluorescent) form, compared to their solution-based counterparts. The lower sensitivity is due in part to inefficient quenching of the surface-attached MBs; which is caused by increased non-specific surface interactions with the solid support that destabilizes the hairpin structure.^{17,18,19} As such, a significant effort has been exploited into exploring various solid supports and appropriate probe designs that provide better sensitivities for MBs. For example, MBs have been attached onto optical fiber core surfaces via biotin-avidin/streptavidin interactions,²⁰⁻²³ however, higher background noise from

both the closed form (quencher) of the MB and the cladding of the optical fibers was an issue in these reports.

Glass has been widely used as a solid support for the immobilization of MBs.^{17,20,24,25} Unfortunately, glass suffers from well-documented problems due primarily to interfacial effects; the static charging experienced by glass surfaces can partially open the closed hairpin structure resulting in high levels of fluorescence for the immobilized MB in its closed conformation. MBs have also been immobilized onto micro-wells/porous surfaces using agarose or polyacrylamide gel films, which provide a solution-like environment rather than the typical heterogeneous liquid-solid interface.^{26,27} However, the use of these gel films slows the hybridization process due to diffusion limited mass transport of the targets through the gel network.

Gold metallic surfaces have also been studied as viable substrates for the attachment of MB probes, where the gold serves the purpose of being a solid support and also a quencher of the fluorescence.^{11,28-30} Even though MBs can be tethered easily onto gold surfaces via self-assembly of alkane thiols, nitrogen-based moieties along the probe's DNA backbone can chemisorb to these same surfaces resulting in non-specific adsorption of the DNA to the gold surface. Non-specific interactions of the solution target with the gold surface must be minimized by employing blocking agents to prevent the nitrogen containing nucleotide bases from interacting directly with the gold surface.²⁹ Other artifacts that affect the sensitivity, specificity and hybridization kinetics of the MBs on gold include the non-uniform distribution of hairpin probes on the gold surface causing surface-induced aggregation.^{29,31,32} In another attempt to improve the sensitivity of surface immobilized MBs, Zuo et al. designed MBs that contained a linker arm spacer and a restriction site within its loop structure.³³ These authors reported improvements in the fluorescence sensitivity enhancement of 5.2-fold compared to glass and a MB not containing a restriction site. Their results also showed that the loop of the immobilized MB didn't open effectively upon hybridization with

cDNA targets. The reaction thermodynamics and kinetics of surface immobilized MBs differ from those in solution as a result of interfacial concentration gradients, species-interface interactions and steric hindrance. For example, surface electrostatics greatly affects the binding parameters of these surface immobilized probes because of the wide distribution of probe-surface distances among these probes due to entropic effects, which can contribute to variations in hybridization melting temperatures.³⁴⁻³⁶ For surface hybridization, nucleic acid targets can be repelled or attracted to the surface depending on the immobilization material as well. Electrostatic repulsion between single stranded nucleic acid targets and the surface immobilized probes (due to the high negative charge of nucleic acid oligomers) can result in coulomb blocking of hybridization events. Tethered probes with long linker molecules have electrostatic interactions that can dominate short-range Van der Waals forces. Also, steric hindrance, which increases with increasing surface probe densities, can alter the hybridization efficiencies of surface immobilized probes due to the presence of repulsive electrostatic interactions.³⁷

Solid-supports specifically tailored for the immobilization of MBs or any probe for that matter, must possess the following attributes; (a) the attachment chemistry must be chemically stable to a variety of conditions; (b) the linker should be long enough to eliminate undesired steric interferences from the underlying substrate; (c) the chemical attachment method should not produce non-specific binding to the surface and; (d) in the case of MB probes, the substrate should not interact with the closed form of the MB to lower the sensitivity of the probe (*i.e.*, induced open form of the MB probe). In this work, we report on an immobilization strategy for MB probes to enhance their sensitivity when configured in a microarray format. The approach adopted a two pronged strategy; (i) designing appropriate linker structures to minimize probe aggregation effects on the surface and; (ii) the use of a support that provided simple and stable attachment chemistries and minimized electrostatic effects. The MBs contained a C6 amino linker appended to their stems

to aid in surface immobilization and also contained discrete polyethylene glycol (dPEG) cross linkers. The dPEG cross linkers are both extremely water/organic soluble and hydrophilic. The commonly used alkyl linker/spacers have the characteristic of being hydrophobic and can suffer from increased aggregation and/or precipitation effects at the surface.³⁸ The dPEG linkers greatly decrease these artifacts.^{38,39}

We also used a UV photo-modification process as previously described⁴⁰⁻⁴² to activate a poly(methyl methacrylate), PMMA, surface onto which the MBs were attached via carbodiimide coupling chemistry. The same MBs were attached to glass surfaces using conventional siloxane-based chemistry and the sensitivity of the MBs on glass and PMMA rigorously compared. The performance of these surface immobilized MBs was also compared to their solution counterpart assays as well. As an example of the performance of this appropriately designed linker and support system for MB probes, the loop sequences were used for the analysis of cDNAs specific for *fruitless (fru)* and *Ods-site homeobox (OdsH)* genes extracted from *Drosophila melanogaster* fruitflies. The *fru* gene functions in the central nervous system, where it is necessary for sex determination and male courtship behavior while *OdsH* is involved in transcriptional regulation and plays a role in hybrid dysfunction in spermatogenesis.

4.2 Experimental Section

4.2.1 Design of the Molecular Beacon Probes

The process of molecular beacon design begins with the selection of the probe sequence, which will depend on the application. For example, whether it is for detection of PCR products, single-nucleotide allele discrimination assays e.t.c. The probe (loop) length sequence usually ranges between 15-30 nucleotide bases. After selecting the probe sequence, two complementary arm sequences are added on either side of the probe sequence. The length and the GC content of the stem sequence are designed in such a way that in the absence of the target, the molecular

beacons remain closed and non-fluorescent. This is achieved by using DNA folding programs such as the Zuker DNA folding program, which is available at www.bioinfo.rpi.edu/applications/mfold/dna/form_1.cgi. It is important that the conformation assumed by the free molecular beacons be the intended hairpin structure rather than other secondary structures that either does not place the fluorophore in the immediate vicinity of the quencher, or that forms longer stem than intended. The former will cause high background signals and the latter will make the molecular beacons sluggish in binding to their targets. The oligonucleotide sequences for both the probes and targets used in these assays are given in Table 4.1. We designed two different MBs, one for *fru* (MB1) and the other for *OdsH* (MB2) detection. The beacons were labeled at their 5' ends with a CY 5.5 fluorophore and at their 3' ends with BHQ-3 dark quencher. Also, the stem was functionalized with a C6 amino linker (see Figure 4.4 c) for attachment onto the solid supports. The MBs were synthesized by Gene Link Inc. (Hawthorne, NY) and used without further purification.

Table 4.1: Molecular beacon probes and target sequences.

MB1 and MB2 are molecular beacon sequences. Lower case denotes the stem sequences of the beacons while the upper case is the recognition loop sequence. T1 and T2 are target sequences complementary to MB1 and MB2, respectively. The underlined sequence is the section complementary to the MBs. T3 is non-complementary to both MB1 and MB2. All targets (T1, T2, and T3) are cDNAs extracted from *Drosophila melanogaster* for *fruitless (fru)*, *Ods-site homeobox (OdsH)* and *Actin 5C (Act5C)* genes, respectively. Actin 5 c is non-complementary both to MB1 and MB2 and it was used as a negative control in these studies.

| | Sequence 5' to 3' |
|-----|-------------------------------------------------------------------------------------------------------------------------------------------------------------------------------------------------------------------------------------------------------------------------------|
| MB1 | (CY5.5) - ccagcTGTACAAGGGCGAGGTCAACGTGGG gctgg-(BHQ-3) |
| MB2 | (CY5.5) -cgaccCAACAAGCTGATGAAGAAAGCCggtcg-(BHQ-3) |
| T1 | GCAGCGAACTCTG <u>ACCCACGTTGACCTCGCCCTTGTACATGAAGTCGAGCAGAGATCGC</u> ATCTCTGAGTATCTGACATCTTTCAAGTAGATGATGGGATA |
| T2 | CTTCTTCGCTGCCGTTTCGATGGCTTTCTTCATCAGCTTGTGCGCTGGGCTAGTTCT TTGGCGGAAAGTTCGCTAAGTGGAATGGGGTTACCACTGCAGCTCTGGGGATGGGA ACTATGAAAA |
| T3 | TGCACAATGGAGGGGCCGNACTCGTCNTACTCCTGCTTGGAGATCCACATCTGCTGGA AGGTGGACAGCGAAGCCAGGATGGAACCACCNATCCAGACAGAGTACTTGCCTCTGG TGGGGCAATGATCTTGATCTTCATGGTCNACGGGGCCAGGGCGGTGATCTCCTTCTGCA TACNGTCGGCGATGCCAGGGTACATGGTGGTGCCACCNACAGCACGGTGTGGCATA CANATCCTTACGGATATCCAAGC |

4. 2.2 Preparation of cDNA Target Samples

Three genes, *Odysseus H (OdsH)*, *fruitless (fru)* and a control gene *Actin5C (Act5C)*, were chosen for these investigative studies based on their potential influence on the spermatogenesis pathway, role in the sex-determination pathway, and ubiquitous presence in many cell processes. cDNA from these genes was obtained from *Drosophila simulans*. To obtain the sequence of these genes in *D. simulans*, the sequence of *D. melanogaster* (obtained from FlyBase, <http://www.flybase.org>) was BLASTed (<http://www.ncbi.nlm.nih.gov/BLAST/>) against the whole genome sequence of *D. simulans*. Primers were designed to bind to the *D. simulans* sequence, which flanked an intron and did not have any sequence similarity to other genomic DNA. This allowed for a successful amplification of only the sequence of interest and also provided a means of differentiating cDNA amplification from DNA amplification. The PCR primer sequences were as follows:

OdsH-F, CTCATAGTTCCCATCCCCAGAG;

OdsH-R, AGCTATGTAATCGGCCTTCAGAC;

fru-F, ATCCCATCATCTACTTGAAAGATGT;

fru-R, GAGCGGTAGTTCAGATTGTTGTTAT;

Act5C-F, GGATATCCGTAAGGATCTGTATGC;

Act5C-R, CCAAGACAAGCGATCCTTCTTA.

Drosophila simulans stocks were maintained at 20°C, 12-h light:dark cycle. Virgin males were collected, aged 4 days, and then frozen at -80°C between 1-2 hours after “lights on” on the fourth day. RNA was extracted from 35-40 fruit flies using the QIAGEN (Valencia, CA) RNeasy Mini Kit. Reverse transcription was performed using the reverse primer with MMLV Reverse Transcriptase and RNasin from Promega. PCR amplification was performed in a 25 µl volume with 1.5 mM MgCl₂, 0.2 mM dNTPs, 1 µM of each primer, 1 unit of *Taq* polymerase,

and 5 μ l of cDNA template. Samples were amplified through; 1 cycle at 95° for 5 min; 3 cycles at 94° for 1 min/56° for 30 s/72° for 30 s; 3 cycles 94° for 1 min/ 53° for 30 s/72° for 30 s; 30 cycles 94° for 1 min/ 50° for 30 s/72° for 30 s. The PCR products were then run on a 2% agarose gel with both a positive (DNA) control and a blank (no RNA) negative control and the appropriate-sized band was extracted and purified using the QIAGEN Gel Extraction Kit. The isolated product was then used as the template for 8 replicate rounds of PCR amplification using the same protocol as stated above, except 1 μ l of template was used. The 8 replicates were pooled and purified with the QIAGEN PCR Purification Kit. The final product was then sequenced to confirm that the correct product was obtained and the sequence was used to design the probe and target.

4. 2.3 Immobilization of Molecular Beacons onto Solid Substrates

PMMA polymer substrates (1 mm thickness) were obtained from Goodfellow (Berwyn, PA) while aldehyde functionalized glass substrates were purchased from Telechem International, Inc. (Sunnyvale, CA). 2-[N-morpholino]ethanesulfonic acid (MES), N-hydroxysuccinimide (NHS), 1-ethyl-3-(3-dimethylaminopropyl) carbodiimide hydrochloride (EDC), phosphate and TRIS buffer solutions were obtained from Sigma (Milwaukee, WI). Deionized water (17.9 M Ω) from an E-pure water purification system (Barnstead, Dubuque, IA) was used for the preparation of all buffers and rinsing reagents.

MBs were covalently attached onto both PMMA and glass substrates using the appropriate linkage chemistry. For PMMA, the substrates were photo-activated by exposure to broadband UV radiation, which was performed using a UV station equipped with a UV light (500 W DUV, model UXM-501 MA, Ushio America, Cypress, CA). The substrates were placed at a distance of 1 cm from the source for 20 min with radiation intensities applied from the source equal to 15 mW/cm². Following UV activation for approximately 30 min, the PMMA

substrates were thoroughly rinsed with 2% isopropyl alcohol (IPA), then with ddH₂O followed by drying under nitrogen gas. The PMMA slides were cross-linked with a dPEG spacer (amino dPEG₁₂TM acid) obtained from Quanta Biodesign Ltd, (Powell, OH) using carbodiimide coupling chemistry. The surfaces were incubated with 100 mM MES containing 10 mM EDC / 5 mM NHS for 30 min followed by 100 μ M of the dPEG for ~5 h at room temperature after which the slides were thoroughly rinsed with ddH₂O and dried with pressurized air. Next, the MBs were dissolved in 100 mM MES at pH 5.5 containing 10 mM EDC / 5 mM NHS to a final concentration of 100 nM and spotted onto the surface and incubated for 2 h at room temperature. For glass, the aldehyde functionalized slides were incubated with 100 μ M dPEG spacer in phosphate buffer at pH 8.3 for at least 5 h then rinsed thoroughly with ddH₂O and dried with pressurized air. MBs were then immobilized in a similar fashion as that outlined for PMMA.

4.2.4 Hybridization of MB Probes to Their Targets

For solution-based assays, three different solutions were evaluated; 100 nM MB without target molecules, 100 nM MB with a 10-fold excess of non-complementary targets, and 100 nM MB with a 10-fold excess of complementary target molecules (see Table 1 for target sequences). All assays were performed in a hybridization buffer containing 20 mM TRIS-HCl, 10 mM MgCl₂, and 10 mM KCl at pH 7.5. The hybridization reaction was allowed to proceed for 30 min at room temperature and then fluorescence spectra were obtained ($\lambda_{exc} = 675$ and $\lambda_{em} = 694$) using a Fluorolog-3 fluorimeter (Jobin Yvon Inc., Edison, NJ). Array-based hybridization was accomplished by incubating the slides containing the immobilized MB probes in a pre-hybridization buffer for 30 min at room temperature, which facilitated the annealing of the stem to the probes. Then, target solutions (10-fold molar excess) were placed onto the MB spots and allowed to hybridize at room temperature for 2 h followed by fluorescence imaging of the array surface. Both glass and PMMA slides were imaged using a home-built near-IR fluorescence

scanner, which was described in Chapter 1.

4.3 Results and Discussion

4.3.1 MB Design

The most important design parameters associated with MBs are their probe and stem lengths and sequence content because at a given temperature, they largely control the fraction of MBs in the three different conformational states; bound-to-target, stem-loop hairpin or random coil.⁴³ Generally, the loop sequence consists of 15-25 nucleotide bases, with the content based upon the target sequence and melting temperatures required. The stem typically has 4-6 nucleotide bases and is chosen to have no sequence homology to that of the target. It has been shown that longer stem lengths are accompanied by a lower target affinity and a decreased probe-target hybridization rate, while MBs with short stems have faster hybridization kinetics and improved target affinities but lower sensitivities compared to those with longer stems.⁴⁴ On the other hand, MBs with longer loop lengths have improved target affinities and increased kinetic rates, but also display reduced specificities for discrimination between fully matched and mismatched target/loop duplexes.⁴⁴ In this study, we designed MBs with stems containing 5 bases and loops having either 25 nucleotide bases (Figure 4.4 A) or 22 nucleotide bases (Figure 4.4 B). Both MBs possessed a CY 5.5 fluorophore at their 5' ends and BHQ-3 (black hole quencher) at their 3' ends.

There are two possible quenching mechanisms that can be envisioned when these probes are in their hairpin configuration; contact quenching or energy transfer. Contact quenching occurs when there is a collision between the fluorophore and quencher, creating a disruption of the energy levels of the excited fluorophore and causing the quencher to dissipate the energy it receives from the fluorophore as heat rather than emitted light. Resonance energy transfer (RET) requires a spectral overlap between the emission spectrum of the donor (fluorophore) and the

acceptor's (quencher) absorption spectra. We took the quenching mechanism into consideration when selecting the fluorophore and quencher that provided good spectral overlap to maximize RET. For surface immobilization, it was important to have a functional group to aid in the attachment of the MB to the solid support. We also designed our MBs to have a C6 amino linker functionality on the stem. It was also highly desirable to have enough space between the solid support and the probes to enable the probes to be readily accessible to target molecules and also to minimize potential interactions between the MB probes and the surface, which could destabilize the hairpin conformation lowering MB sensitivity.

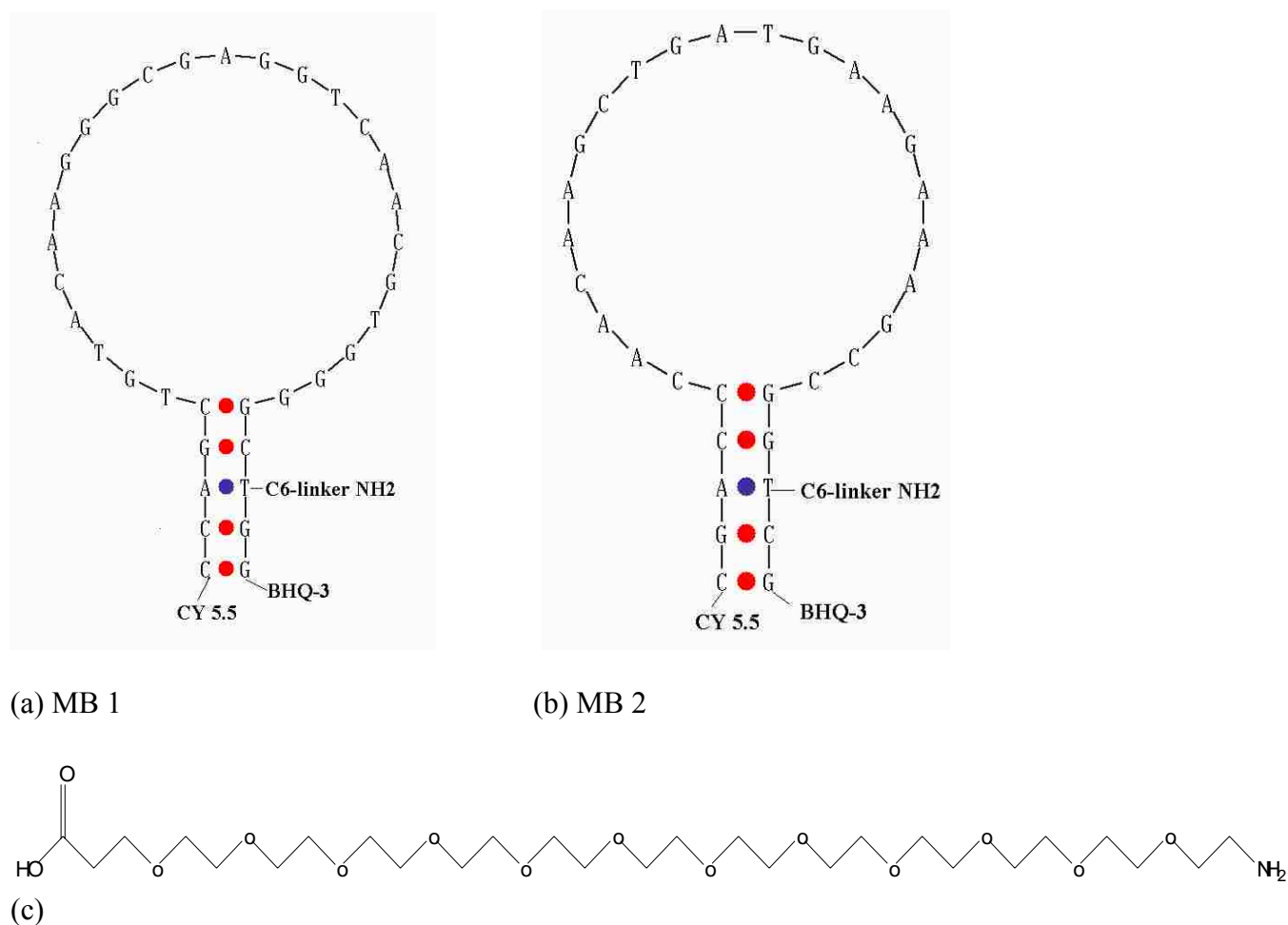


Figure 4.4: Molecular beacon probes for detection of fru gene MB1 (a) and ods-H gene MB 2 (b). Their stem structure has a C6 amino linker attached to aid in surface immobilization via a discrete polyethylene glycol (dPEG) cross linker (c).

We therefore used a dPEG spacer molecule (see Figure 4.4 c) to keep the probes spatially removed from the surface in order to minimize these artifacts and to avoid any possible steric effects hindering target accessibility to its respective probe.

4.3.2 Fluorescence of Hybridized MBs in Solution.

The results shown in Figure 4.5 indicate that the fluorescence sensitivity (ratio of fluorescence of the probe upon binding to its target with that of the probe in its closed (non-fluorescent) form) of these MBs when hybridized to their complementary cDNA targets in solution was 16 for MB1 and 14 for MB2. The MBs incubated without targets or those incubated with non-complementary targets had no or very minimal amounts of fluorescence recovered.

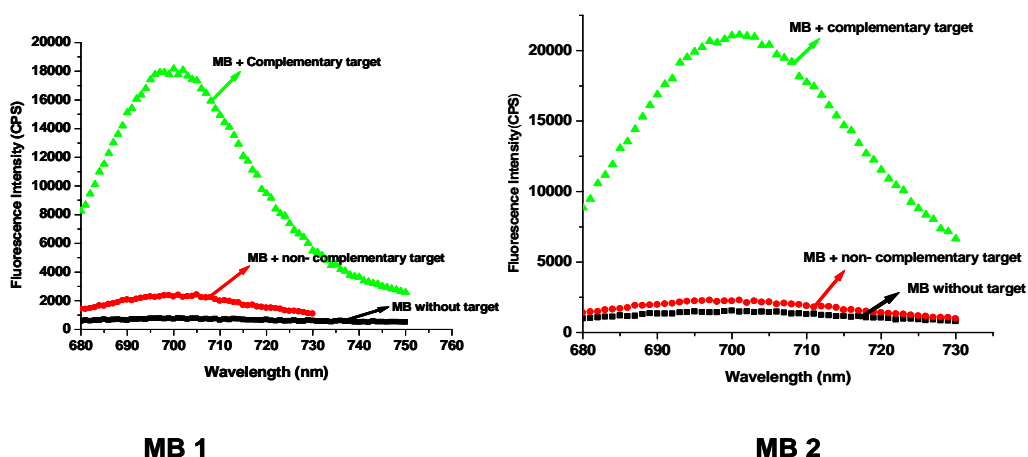


Figure 4.5: Solution based hybridization results for molecular beacons MB1 (A) and MB2 (B), respectively. Three solutions were used; 100 nM MB without target molecules, 100 nM MB with 10-fold excess of non-complementary targets and 100 nM MB with 10-fold complementary target molecules. The solutions were incubated for 30 min in a hybridization buffer (20 mM Tris-HCl, 10 mM MgCl₂, and 10 mM KCl at pH 7.5) and their fluorescence spectra was obtained using a fluorimeter ($\lambda_{exc} = 675$ nm and $\lambda_{em} = 694$ nm).

4.3.3 Immobilization of MBs onto PMMA and Glass Surfaces.

In order to capture complementary targets in an array format, MBs were immobilized onto PMMA and their sensitivities compared to MBs immobilized onto glass supports. For

PMMA, the immobilization was done by first activating the surface via exposure to UV irradiation, which introduced a scaffold of carboxylic acid functional groups onto its surface that were then used for coupling to a bifunctional polyethylene glycol linker through carbodiimide coupling chemistry. This linker molecule consisted of a terminal amine group, which was used to form an amide bond with the surface through the UV-generated carboxylic acids for PMMA or the aldehydes of glass. The PEG₁₂ cross-linkers also contained a carboxylic group to allow tethering of the MB, which contained an amino group. These linker molecules kept the immobilized MBs spatially removed from the solid surface, improving their hybridization efficiencies.^{45,46}

Recently, Tan et al. reported on the use of poly-T linker molecules to reduce MB associations with the glass surface to which they were attached. They found that when a long poly-T (>25 bases) was used, high negative charges could eventually repel the target DNA and reduce efficiency of duplex formation.²⁴ The use of the dPEG linkers minimizes this electrostatic artifact because the PEG linker carriers no charge at the pH values used for the work reported here. Another factor we considered when immobilizing the MBs onto the surfaces was the fact that high probe densities typically reduces the binding efficiency of the probes to targets. Vainrub and coworkers have discussed these effects by studying interface electrostatic interactions for chip array hybridizations. In their work, high probe densities lead to high negative charges resulting in strong repulsion between single stranded nucleic acid targets and their surface immobilized probes, giving rise to coulomb blockage of hybridization.³⁴⁻³⁶ Also, Peterson and coworkers have described how probe density was a controlling factor for efficient target capture as well as to produce favorable kinetics for target/probe hybridization.³⁷ They demonstrated that hybridization depends strongly on probe density in both the efficiency of duplex formation and the kinetics of target capture such that with low probe densities, essentially

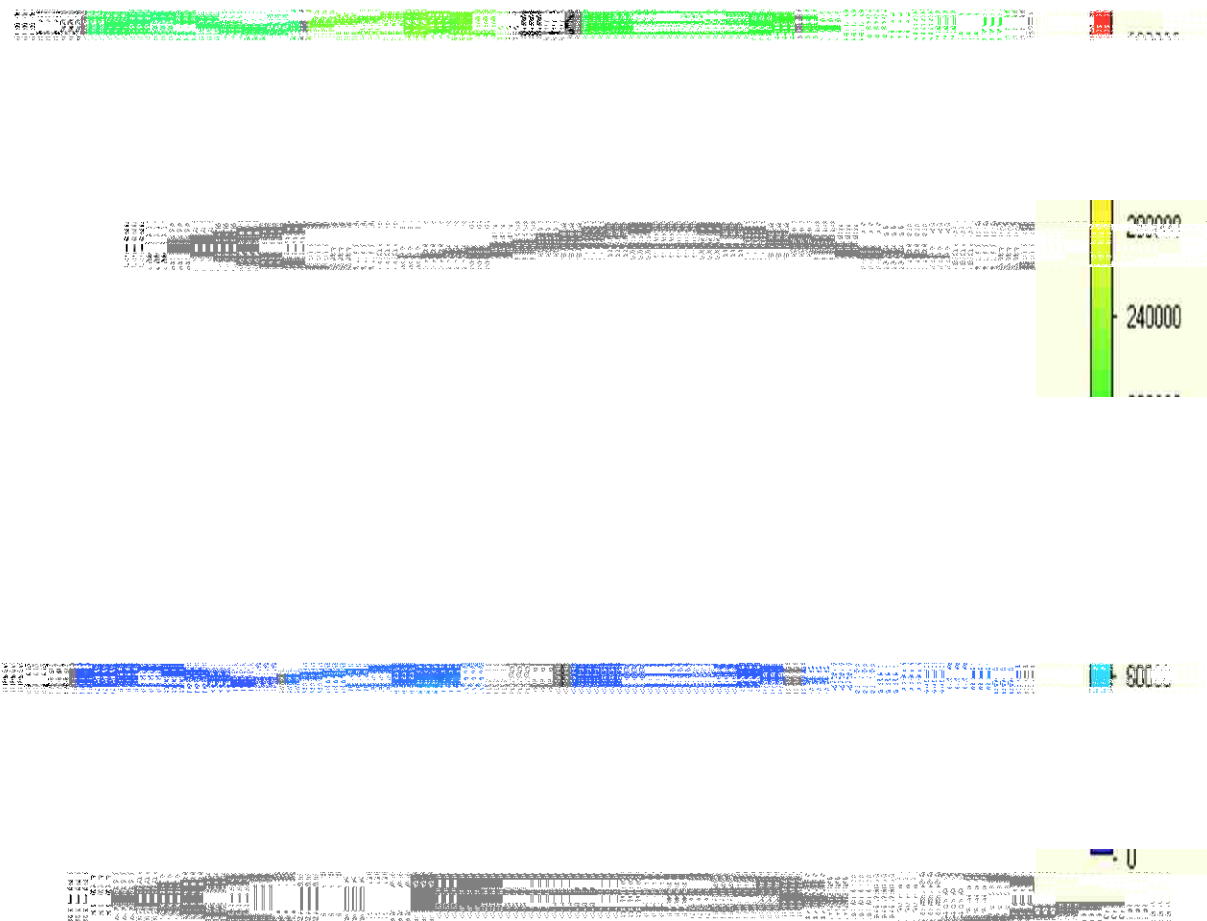


Figure 4:6: Comparison of fluorescence hybridization results for molecular beacons immobilized on glass (A) and poly(methyl methacrylate) (PMMA) (B) surfaces. Functionalized PMMA and glass substrates were used for coupling a bifunctional polyethylene glycol linker through carbodiimide coupling chemistry. These linker molecules were thereafter used for attachment of 100 nM MB probes. The probes were then used for capturing a 10-fold excess of complementary targets. Fluorescence images were obtained before hybridization (left) and after hybridization of the immobilized MB probes with their fully complementary targets (right) for both MB1 and MB2.

100% of the surface-immobilized probes were hybridized to their complementary targets with Langmuir-like binding kinetics, while hybridization efficiencies drop to ~10% in the case of high probe densities. In either case (i.e. low or high probe density), binding saturation at a particular

location of the array can lead to limited dynamic range for the expression profiling. To control the immobilization densities, we used low concentrations of probes (100 nM) and limited the immobilization times to less than 2 h. For our PMMA substrates and using carbodiimide attachment chemistry, probe densities were determined to be $\sim 2.4 \times 10^{12}$ molecules/cm². These probe densities are comparable to those shown to yield high hybridization efficiencies of 2×10^{12} molecules/cm².^{37,47} Following immobilization of the MBs onto the glass or PMMA surfaces, they were incubated in a pre-hybridization buffer containing divalent (Mg^{2+}) cations to facilitate stem annealing to further reduce the background fluorescence of the unhybridized probes. Figures 4.6 A and 4.6 B shows fluorescence images obtained after hybridization with complementary oligonucleotide targets using glass and PMMA supports, respectively. Two different MBs were used in these studies; MB1 and MB2 (see Table 4.1 for the sequences of these probes). Both images indicated recovery of the fluorescence upon binding with complementary targets. Interestingly, glass exhibited a much higher autofluorescence level at the excitation wavelengths used in these studies compared to PMMA. The autofluorescence arises from the substrate itself and is measured in areas on the surface where no covalently immobilized MB is found.

Figure 4.7 gives the fluorescence sensitivities of the surface immobilized MBs in comparison to the same probes used in solution. The fluorescence sensitivity found for the PMMA support was ~ 8 while for glass it was 4 for both MB probes, but both substrates resulted in reduced sensitivities compared to their solution counterparts. In solution, the MBs encounter higher fluorescence sensitivity because they can bind freely with their targets compared to their constrained surface immobilized counterparts. When MBs are in solution with their targets, they can exist in an open conformation (bound to targets) or closed conformation (free of targets). This two-state model is an equilibrium process with the closed state characterized by lower enthalpy than the open state due to base pairing and stacking. The opening rate depends on the

unzipping energy of the hairpin probes.^{13,14,48} In solution, these hairpin probes diffuse more freely and are unperturbed by surface interactions, hence the ease of interaction with target molecules. On the other hand, surface immobilized probes lack this freedom. In addition, MBs that are immobilized onto solid surfaces have different electrostatic properties at the surface/liquid interface affecting the local ionic strengths and making them differ from those in bulk solution as noted above.

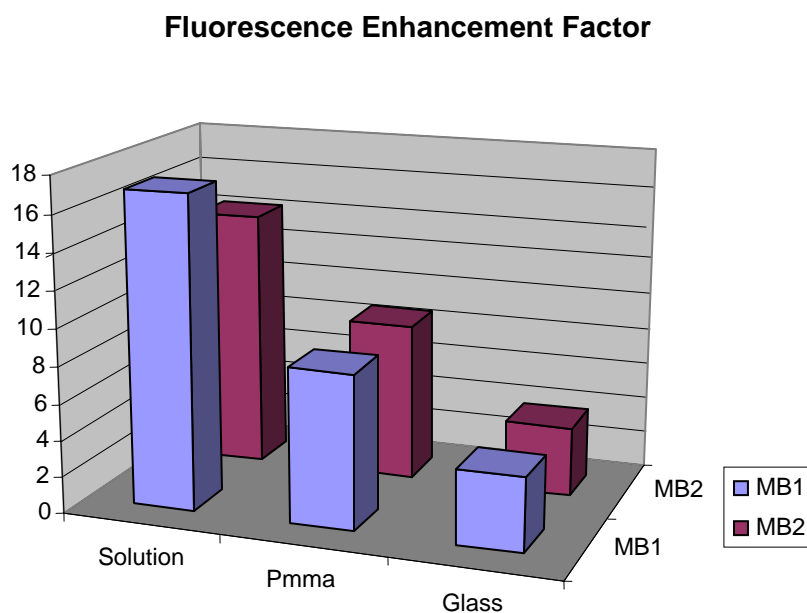


Figure 4.7: Fluorescence increment ratios for solution-based hybridization events and surface-immobilized beacons on glass and PMMA. The fluorescence increment was obtained by getting the ratios of; observed intensities of MB probe after hybridization with targets subtracted from the background with observed intensities of MB hairpin probes before hybridization with targets minus the background.

Surface effects can also destabilize the stem structures of the immobilized MB probes, reducing their quenching efficiency when they are in their closed configuration. For the optical set up used in these assays, glass exhibited autofluorescence backgrounds that were 240,000

counts per image pixel while PMMA exhibited a background of 40,000 counts per image pixel. When the autofluorescence background was subtracted from the intensities of the MBs probes without targets (closed configuration) or that of these MBs after incubation with non-complementary targets, the net signal was 40,000 for both surfaces. The lack of difference between these values indicates that both surfaces affect the closed configurations of the surface-immobilized MBs to the same degree, which is not too surprising given the fact that in both PMMA and glass, a monolayer of the dPEG-linker is formed over the underlying surfaces. However, upon binding of the MB probes to their full complementary targets, glass exhibited intensities of 160,000 counts per image pixel while PMMA showed a value of 340,000 counts per image pixel (both were background subtracted). The lower MB sensitivity on glass surface could arise due to static charging. On the other hand, PMMA exhibited better fluorescence sensitivity due to its electrostatic surface effects (thermodynamic equilibrium distribution), which affects the probe-target binding strength near the surface in a more favorable manner. It has been shown that strong attraction of a probe-target duplex to the surface promotes duplex formation, while surface repulsion of the probe-target duplex will shift the hybridization equilibrium toward melting of the duplexes.³⁵

4.3.4 Analytical Sensitivity of MBs Immobilized onto PMMA Substrates.

When carrying out MB hybridization assays, it is desirable for the loop sequence to only hybridize to the specific sequence of interest and also to work within useful target concentrations. We immobilized MB probes onto PMMA surfaces with the loop sequences corresponding to the *OdsH* gene (MB1) and *fru* gene (MB2) of the *Drosophila melanogaster*. The target samples were prepared by creating cDNA from messenger RNA (mRNA) through reverse transcription. Before being used in the hybridization assays, the cDNAs were denatured for 5 min at 95°C and then immediately cooled on ice. Figure 4.8 shows the fluorescence images

obtained after hybridization of MB probes immobilized onto PMMA surfaces without targets (A), upon hybridization with a 10-fold excess of complementary cDNAs (B) and after hybridization with a 10-fold excess of non-complementary cDNAs (C). *Actin 5C (Act5c)* gene is non-complementary to both MB1 and MB2 and therefore was used as a negative control in these studies (see Table 4.1). For both immobilized probes, those without targets (A) and with non-

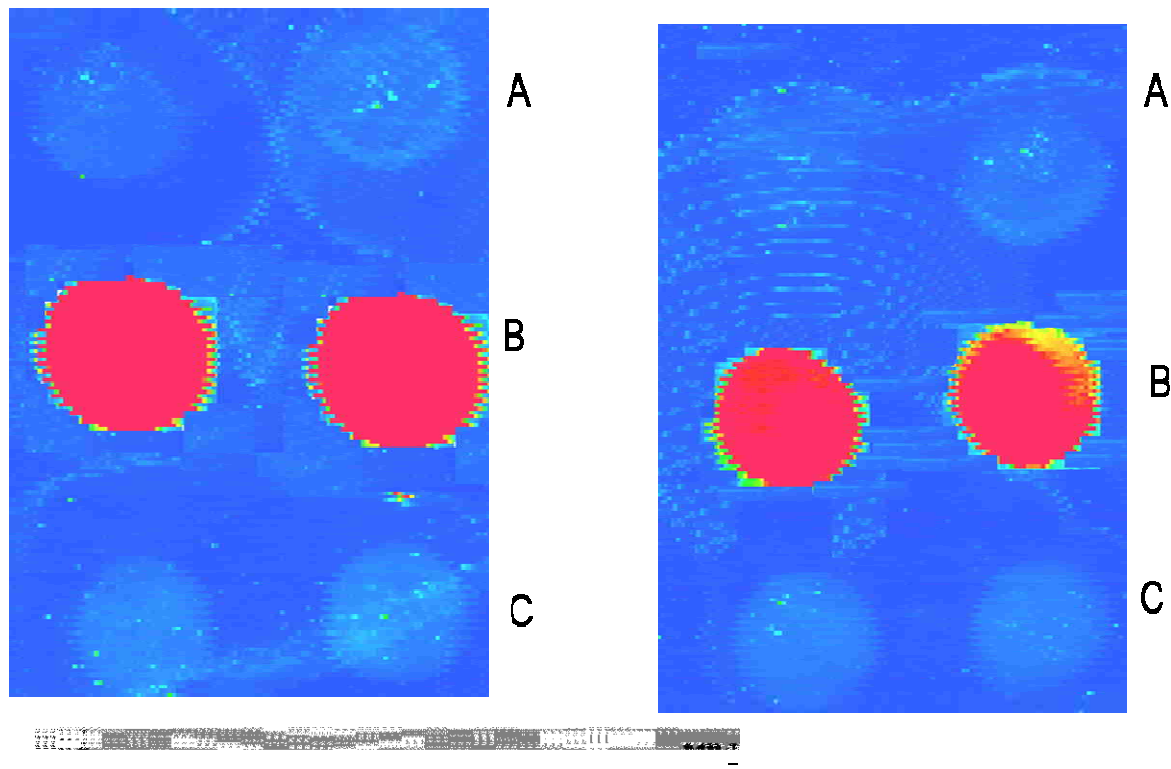


Figure 4:8: PMMA substrates were activated by being exposed to UV radiation for 20 min followed by immobilization of 100 nM MB probe solutions. These probes were used for hybridization with a 10-fold excess of perfect complementary targets and a 10-fold excess of non-complementary targets for 2 h at room temperature. Fluorescence images were obtained after hybridization of surface immobilized molecular beacons; (A) without targets, (B) with fully complementary targets and; (C) with non-complementary targets. The complementary targets T1 / T2 and non-complementary targets T3 (refer to Table 1) are cDNAs extracted from drosophila melanogaster fruit flies.

complementary targets (C) did not show any significant fluorescence, while those with perfect complementary targets (B) exhibited strong fluorescence. The MB probes did bind to their target sequences forming probe-target hybrids that were more stable than the stem hybrid. Only perfect

complementary hybrids were sufficiently stable to force the stem-hybrid to open, resulting in higher fluorescence.

The analytical sensitivity for reporting on the concentration of the solution complements using these immobilized MB probes was then determined using different concentrations of the targets and constructing calibration plots.

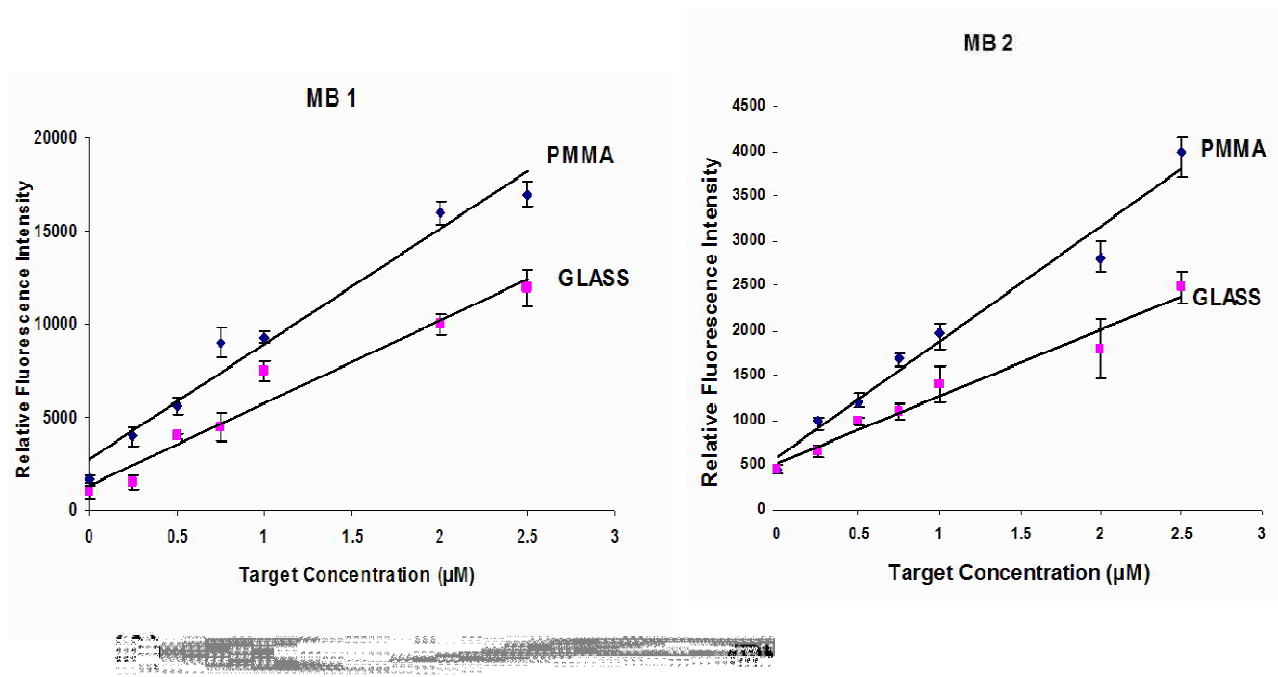


Figure 4.9: Calibration curves for the observed fluorescence intensities versus target concentrations for MB1 (A) and MB2 (B), respectively. A solution containing 100 nM of the MBs was immobilized onto PMMA slides and they were used for binding with their complementary target solutions varying from a range of 100 nM to 2.5 µM. The error bars represent the standard deviation of three measurements taken.

For each MB probe, the experiments were performed in triplicate on different PMMA slides using a solution cDNA ranging from 100 nM to 2.5 µM. Figure 4.9 shows the calibration plots for the observed fluorescence intensities versus target concentrations for MB1 (Figure 4.9 A) and MB2 (Figure 4.9 B). Low target concentrations required longer reaction times to reach steady-state while increased target concentrations promoted more intermolecular duplex formation. The plots were linear with a correlation coefficient of $R^2 = 0.96$ for MB 1 and $R^2 =$

0.97 MB 2. The presence and abundance of targets within a sample are usually indicated by the intensity of the hybridization signal at the corresponding probe sites. Alternatively, the abundance of the targets can be obtained by reverse transcription (RT)- PCR based assays, which are common methods for comparing mRNA levels in different sample populations. The mRNA levels are measured and normalized to reference genes, which allow each gene expression to be measured as a numerical value that enables direct comparison between experiments. The relative abundance of the genes used in this study has been determined and the normalized expression values obtained were *Fru* mRNA (9.12), *OdsH* mRNA (3.43) and *Actin 5 C* mRNA (11.24).⁴⁹ These results indicate that the *Fru* mRNA is highly abundant in *D. Simulans*, while the *OdsH* is near the threshold of detection of conventional arrays.

4.4 Conclusions

These studies were based on the concept that proper MB design and careful solid support choice with robust surface chemistries could lead to improved sensitivities for surface immobilized MBs. We chose a surface modification procedure described earlier in our lab⁴² to produce functional scaffolds consisting of carboxylic groups that allowed covalent attachment of amine functionalized MB probes onto PMMA surfaces through carbodiimide coupling. These processes involved only broadband UV exposure of the polymer surface followed by carbodiimide coupling of amine-containing MB probes to the surface (via an amide bond). Surface-bound probes require enough interstitial space to improve hybridization efficiency. Therefore, we employed dPEG cross-linker molecules to minimize any steric effects that might occur as well as minimizing surface aggregation effects. MBs immobilized onto PMMA showed higher fluorescence restoration compared to those immobilized onto glass surfaces. In this study, PMMA was found to be a better substrate compared to glass for the designed probes and wavelengths used for their interrogation. The ability to perform quantitative assays using these

types of MB probes and proper substrates will be a useful tool in gene expression analysis. In quantitative expression analysis, the abundance of genes, mRNAs or proteins may differ by a large factor. It is therefore highly desired that emerging technologies should successfully measure all the genes, mRNAs or proteins across a broad dynamic range. The surface-immobilized MB probes described here were limited by a narrow dynamic range hence the need to improve the analytical sensitivity of these probes. One possible way will be use of probes with perfect quencher/fluorophore pairs that have the capability of quenching effectively when targets are absent at the same time be able to exist in the open configuration when hybridized to targets even at low target concentrations. Secondly, the probes should possess fluorophores that are both bright and stable as well as showing a high propensity for fluorescence quenching when in the closed MB conformation. We therefore investigated the use phthalocyanine dyes as reporter molecules for the synthesis of molecular beacons and other FRET-based probes as will be detailed in Chapter 5.

4.5 References

- (1) Tyagi, S.; Kramer, F. R. *Nature Biotechnology* **1996**, *14*, 303-308.
- (2) Vet, J. A. M.; Majithia, A. R.; Marras, S. A. E.; Tyagi, S.; Dube, S.; Poesz, B. J.; Kramer, F. R. *Proceedings of the National Academy of Sciences of the United States of America* **1999**, *96*, 6394-6399.
- (3) Tyagi, S.; Bratu, D. P.; Kramer, F. R. *Nature biotechnology* **1998**, *16*, 49-53.
- (4) Kostrikis, L. G.; Tyagi, S.; Mhlanga, M. M.; Ho, D. D.; Kramer, F. R. *Science* **1998**, *279*, 1228-1229.
- (5) Tang, Z.; Wang, K.; Tan, W.; Li, J.; Liu, L.; Guo, Q.; Meng, X.; Ma, C.; Huang, S. *Nucleic Acids Research* **2003**, *31*, e148/141-e148/147.
- (6) Mhlanga, M. M.; Malmberg, L. *Methods (San Diego, CA, United States)* **2001**, *25*, 463-471.
- (7) Nielsen, P. E. *Current Opinion in Biotechnology* **2001**, *12*, 16-20.

- (8) Liu, J.; Lu, Y. *Methods in Molecular Biology (Totowa, NJ, United States)* **2006**, 335, 275-288.
- (9) Tian, Y.; Mao, C. *Talanta* **2005**, 67, 532-537.
- (10) Sando, S.; Narita, A.; Abe, K.; Aoyama, Y. *Journal of the American Chemical Society* **2005**, 127, 5300-5301.
- (11) Swearingen, C. B.; Wernette, D. P.; Cropek, D. M.; Lu, Y.; Sweedler, J. V.; Bohn, P. W. *Analytical Chemistry* **2005**, 77, 442-448.
- (12) Stojanovic, M. N.; De Prada, P.; Landry, D. W. *ChemBioChem* **2001**, 2, 411-415.
- (13) Bonnet, G.; Tyagi, S.; Libchaber, A.; Kramer, F. R. *Proceedings of the National Academy of Sciences of the United States of America* **1999**, 96, 6171-6176.
- (14) Bonnet, G.; Krichevsky, O.; Libchaber, A. *Proceedings of the National Academy of Sciences of the United States of America* **1998**, 95, 8602-8606.
- (15) Riccelli, P. V.; Merante, F.; Leung, K. T.; Bortolin, S.; Zastawny, R. L.; Janeczko, R.; Benight, A. S. *Nucleic Acids Research* **2001**, 29, 996-1004.
- (16) Situma, C.; Hashimoto, M.; Soper, S. A. *Biomolecular Engineering* **2006**, 23, 213-231.
- (17) Brown, L. J.; Brown, T.; Cummins, J.; Hamilton, A. *Chemical Communications (Cambridge)* **2000**, 621-622.
- (18) Du, H.; Strohsahl, C. M.; Camera, J.; Miller, B. L.; Krauss, T. D. *Journal of the American Chemical Society* **2005**, 127, 7932-7940.
- (19) Swearingen Carla, B.; Wernette Daryl, P.; Cropek Donald, M.; Lu, Y.; Sweedler Jonathan, V.; Bohn Paul, W. *Analytical chemistry* **2005**, 77, 442-448.
- (20) Fang, X.; Liu, X.; Schuster, S.; Tan, W. *Journal of the American Chemical Society* **1999**, 121, 2921-2922.
- (21) Liu, X.; Farmerie, W.; Schuster, S.; Tan, W. *Analytical Biochemistry* **2000**, 283, 56-63.
- (22) Steemers, F. J.; Ferguson, J. A.; Walt, D. R. *Nature Biotechnology* **2000**, 18, 91-94.
- (23) Epstein, J. R.; Leung, A. P. K.; Lee, K.-H.; Walt, D. R. *Biosensors & Bioelectronics* **2003**, 18, 541-546.
- (24) Yao, G.; Tan, W. *Analytical Biochemistry* **2004**, 331, 216-223.
- (25) Li, J.; Tan, W.; Wang, K.; Xiao, D.; Yang, X.; He, X.; Tang, Z. *Analytical Sciences* **2001**, 17, 1149-1153.

- (26) Culha, M.; Stokes, D. L.; Griffin, G. D.; Vo-Dinh, T. *Biosensors & Bioelectronics* **2004**, *19*, 1007-1012.
- (27) Wang, H.; Li, J.; Liu, H.; Liu, Q.; Mei, Q.; Wang, Y.; Zhu, J.; He, N.; Lu, Z. *Nucleic Acids Research* **2002**, *30*, e61/61-e61/69.
- (28) Du, H.; Disney, M. D.; Miller, B. L.; Krauss, T. D. *Journal of the American Chemical Society* **2003**, *125*, 4012-4013.
- (29) Du, H.; Strohsahl Christopher, M.; Camera, J.; Miller Benjamin, L.; Krauss Todd, D. *Journal of the American Chemical Society* **2005**, *127*, 7932-7940.
- (30) Fan, C.; Plaxco, K. W.; Heeger, A. J. *Proceedings of the National Academy of Sciences of the United States of America* **2003**, *100*, 9134-9137.
- (31) Sauthier, M. L.; Carroll, R. L.; Gorman, C. B.; Franzen, S. *Langmuir* **2002**, *18*, 1825-1830.
- (32) Jin, R.; Wu, G.; Li, Z.; Mirkin, C. A.; Schatz, G. C. *Journal of the American Chemical Society* **2003**, *125*, 1643-1654.
- (33) Zuo, X.; Yang, X.; Wang, K.; Tan, W.; Li, H.; Zhou, L.; Wen, J.; Zhang, H. *Analytica Chimica Acta* **2006**, *567*, 173-178.
- (34) Vainrub, A.; Pettitt, B. M. *Chemical Physics Letters* **2000**, *323*, 160-166.
- (35) Vainrub, A.; Pettitt, B. M. *Biopolymers* **2003**, *68*, 265-270.
- (36) Vainrub, A.; Pettitt, B. M. *Biopolymers* **2004**, *73*, 614-620.
- (37) Peterson, A. W.; Heaton, R. J.; Georgiadis, R. M. *Nucleic acids research* **2001**, *29*, 5163-5168.
- (38) Davis, P. D.; Crapps, E. C.; (Quanta Biodesign, Ltd., USA). Application: WO 2004, pp 108 pp.
- (39) Kidambi, S.; Chan, C.; Lee, I. *Journal of the American Chemical Society* **2004**, *126*, 4697-4703.
- (40) Wei, S.; Vaidya, B.; Patel, A. B.; Soper, S. A.; McCarley, R. L. *Journal of Physical Chemistry B* **2005**, *109*, 16988-16996.
- (41) McCarley, R. L.; Vaidya, B.; Wei, S.; Smith, A. F.; Patel, A. B.; Feng, J.; Murphy, M. C.; Soper, S. A. *Journal of the American Chemical Society* **2005**, *127*, 842-843.
- (42) Situma, C.; Wang, Y.; Hupert, M.; Barany, F.; McCarley, R. L.; Soper, S. A. *Analytical Biochemistry* **2005**, *340*, 123-135.

- (43) Tsourkas, A.; Behlke, M. A.; Bao, G. *Nucleic Acids Research* **2002**, *30*, 4208-4215.
- (44) Tsourkas, A.; Bao, G. *Briefings in Functional Genomics & Proteomics* **2003**, *1*, 372-384.
- (45) Lin, Z.; Strother, T.; Cai, W.; Cao, X.; Smith, L. M.; Hamers, R. J. *Langmuir* **2002**, *18*, 788-796.
- (46) Pena, S. R. N.; Raina, S.; Goodrich, G. P.; Fedoroff, N. V.; Keating, C. D. *Journal of the American Chemical Society* **2002**, *124*, 7314-7323.
- (47) Vainrub, A.; Pettitt, B. M. *Journal of the American Chemical Society* **2003**, *125*, 7798-7799.
- (48) Grunwell, J. R.; Glass, J. L.; Lacoste, T. D.; Deniz, A. A.; Chemla, D. S.; Schultz, P. G. *Journal of the American Chemical Society* **2001**, *123*, 4295-4303.
- (49) Moehring J. Amanda, T. J. C., Noor A.F.Mohamed *Molecular Biology Evolution* **2006**, *in press*.

CHAPTER 5

QUENCHING STUDIES OF PHTHALOCYANINE DYES FOR USE IN FLUORESCENCE RESONANCE ENERGY TRANSFER APPLICATIONS

5.1 Introduction

5.1.1 Phthalocyanines: Spectroscopic Properties and Applications

Phthalocyanines known systematically as tetrabenzo [5, 10, 15, 20] tetraaza porphyrins¹ are a class of macrocyclic planar aromatic compounds that exhibit many physical and chemical properties (see Figure 5.1 A). Most phthalocyanines are water and air stable, thermally stable, and nontoxic. Their synthetic literature is vast, and they are also relatively inexpensive and easy to prepare.^{1,2} These symmetrical macrocyclic compounds are composed of four iminoisindoline units with a central cavity of sufficient size to accommodate various metal ions (see Figure 5.1 B).²

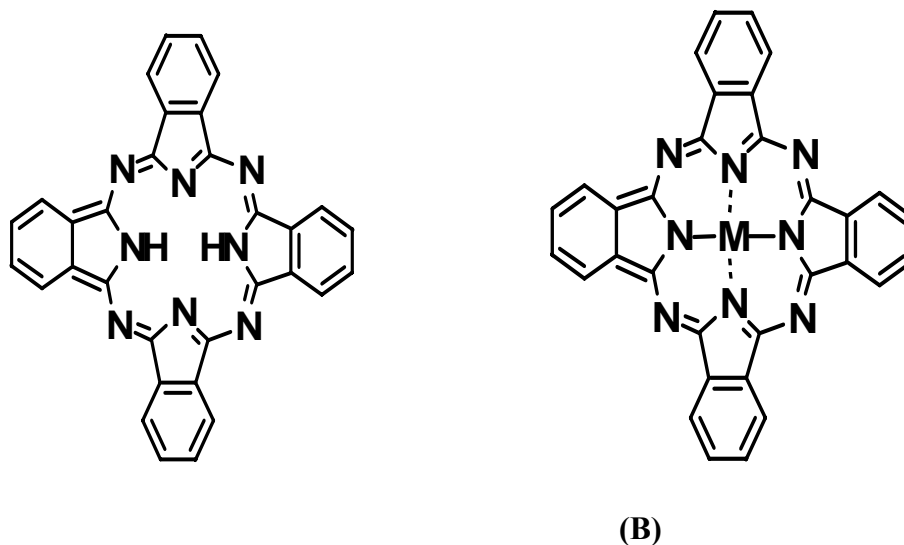


Figure: 5.1: Molecular structure of a normal phthalocyanine (A) and a typical main group metal phthalocyanine complex (B).

The phthalocyanine molecule is able to coordinate hydrogen and metal cations in its center by coordination bonds with four isoindole nitrogen atoms. Metallation of the phthalocyanine dianion with a metal that maintains the planarity of the molecule increases its

symmetry from D_{2h} for H_2Pc (non-metallated) phthalocyanines to D_{4h} for metallated phthalocyanines however, this symmetry drops to C_{4v} for metals that do not fit inside the ring.³

Phthalocyanines are important molecules due to their versatile industrial applications they afford. Examples of these applications are their use as blue or green pigments,^{4,5} absorbents in optical disks,⁶ charge generators for photocopies,⁷ photosensitizers in photodynamic therapy of cancer^{8,9} and optical communication (in non-linear optics).⁷ Figure 5.2 below gives a detailed description of the actual and potential uses of the phthalocyanines.

Most phthalocyanines dissolve in coordinating solvents, such as dimethylaniline (DMA), dimethylsulfoxide (DMSO) and dimethylformamide (DMF) but the solubility can vary depending on the coordinated central metal. For example, magnesium phthalocyanines, lithium phthalocyanines and ruthenium phthalocyanines are readily soluble in acetone, acetonitrile, and methylene chloride but other phthalocyanines do not dissolve in these solvents.^{10,11} The solubility properties of phthalocyanines can however, be maneuvered by substituting the benzo group periphery with strong electron-withdrawing or strong electron donating groups.^{10,11} Dimerization/polymerization of phthalocyanines is usually problematic in aqueous/alcohol-based solvents, which is attributed to: (a) direct linkages or bridges between two or more phthalocyanine rings that place the ring close enough in space so that intra-molecular association can occur; (b) covalent bonding involving the metal, frequently as μ -oxo links; (c) sandwich-type complexes in which two rings share one central metal and; (d) through weak association where peripheral substitution holds two rings adjacent in spaces.^{3,12} Phthalocyanines are known to be very stable against thermal and chemical decomposition and they possess very intense optical absorptions in the visible/UV region.¹³ The intense absorption of phthalocyanines are observed as a result of allowed non-degenerate transitions (free base spectrum), π - π^* transitions (D_{4h} spectrum of phthalocyanine macrocyclic ring) and bands due to metal-to-ligand or ligand-to-

metal charge transfer (*i.e.* charge transfer transitions between the central metal and the π ring).^{14,15}

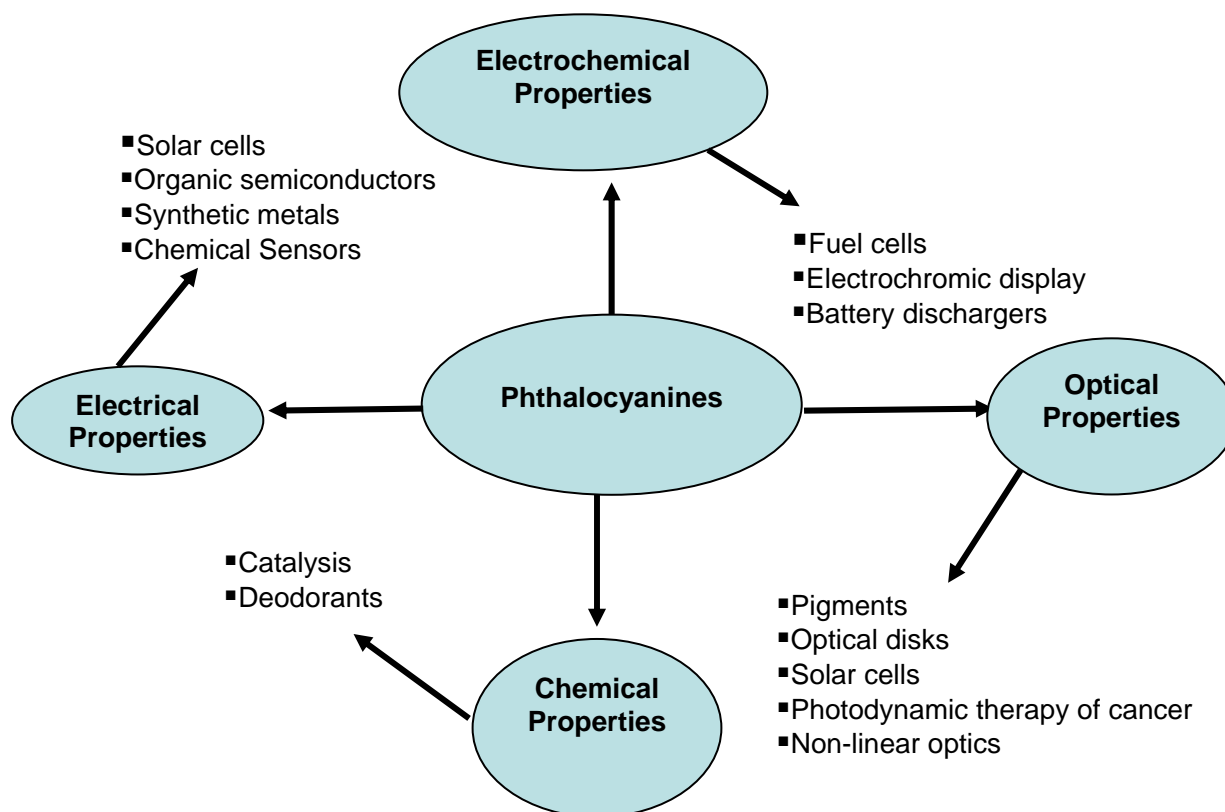


Figure 5.2: Actual and potential industrial applications of phthalocyanines.

The optical spectra of metal phthalocyanine complexes have been widely described by using the Gouterman's model.^{16,17} This model, which is based on a four-orbital linear combination of atomic orbitals, is a theoretical treatment that unites a 16-atom, 18- π electron system with a Hückel treatment that takes into account the structure of the phthalocyanine ring. The molecular orbital diagram (Figure 5.3) is derived from this model and it illustrates the one-electron transitions that give rise to absorption bands in the 200 nm - 1000 nm wavelength range. In this case, the orbital angular momentum (OAM) associated with pairs of orbitals in the inner perimeter 16 atom, 18- π - electron aromatic ring system follows from the assignment of the molecular orbitals of a cyclic polyene aromatic ring. In terms of the OAM that is associated with

the complex wave functions, the angular momentum (M_L) equals 0, ± 1 , $\pm 2 \dots \pm 7$, and 8 in an ascending energy sequence. The highest occupied molecular orbital (HOMO) has an M_L value of 4 while the lowest unoccupied molecular orbital (LUMO) has an M_L value of 5. With this scheme, there are four possible transitions between these two levels involving changes in orbital angular momentum (ΦM_L) of 1 for allowed transitions (B or α) bands and (ΦM_L) of 9 for forbidden transitions (Q or Soret bands). Magnetic Circular Dichroism (MCD) spectroscopy has confirmed the allowed and forbidden nature of the B and Q bands of the metal phthalocyanines complexes.^{19,20} MCD spectroscopy provides the ground and excited state degeneracy information, which is required to fully understand the electronic structure of high symmetry

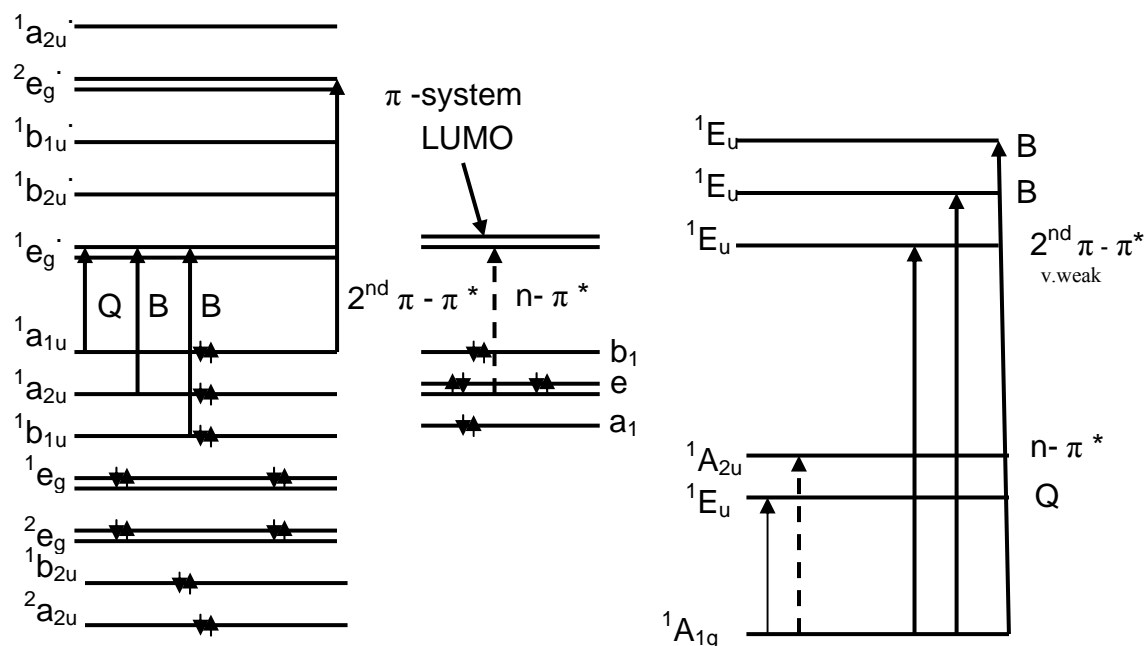


Figure 5.3: Molecular orbital (left) and state level (right) diagrams of metal phthalocyanine complexes showing the one-electron transitions that are predicted to give rise to absorption bands in the 280 nm to 1000 nm range. The orbital ordering on the left is based on Gouterman's model of the inner ring of phthalocyanines while the orbitals on the right are the four azanitrogen lone pair orbitals. The associated bands are referred to in the sequence as Q, second $\pi - \pi^*$, B1, B2, N and L in ascending energy.¹⁸

molecules. Gouterman proposed that the aza linkages and fused benzenes break the accidental degeneracy of the a_{1u} and a_{2u} orbitals (Figure 5.3) resulting in mixing between the excited states such that previously forbidden Q transitions gain significant intensity from the allowed B transitions.¹ This leads to an intense band with molar extinction coefficients of approximately 10^5 to be observed near 670 nm for metal Phthalocyanine complexes. The major $\pi - \pi^*$ bands within the UV-Vis optical spectra are currently referred to as Q, B1, B2, N and L in a sequence ordered by ascending energy on the basis of Gouterman's nomenclature.

The spectroscopy of phthalocyanine complexes, which have been structurally modified by substitution of peripheral protons and introduction of central metal ions instead of the two hydrogen atoms in the main molecular macrocycle, is continually being explored. These substitutions lead to spectral changes due to the electron withdrawing or donating effects of the substituents on the π system that lead to slight shifts in the wavelengths of the major band centers.²¹⁻²³ It is this useful property of wavelength tuning of metal phthalocyanines complexes by chemical modification of the molecular structure or rearrangement of the conformation of these molecules that motivated us to explore the possibility of their potential applications as Fluorescence Resonance Energy Transfer (FRET) pairs.

5.1.2 Fluorescence Quenching Mechanisms

Fluorescence quenching is any process that decreases the observed fluorescence intensity of a sample. This is usually considered to be a detrimental phenomenon in fluorescence spectroscopy however, it can be useful in biological analysis when it is carefully controlled. Examples of molecular interactions that result in fluorescence quenching are excited state reactions, molecular rearrangements, energy transfer, ground state complex formation and collisional quenching.²⁴ Quenching requires molecular contact between the fluorophore and the quencher. This contact can be due to diffusive encounters (dynamic/collisional) or to complex

formation (static quenching). Dynamic quenching involves the collision and subsequent formation of a transient complex between an excited-state fluorophore and a ground-state quencher.²⁴ Since the complex must be formed during the excited-state lifetime of the fluorophore, the quenching is diffusion controlled. This quenching mechanism results in a decrease both in the fluorescence intensity and fluorescence lifetime of a fluorophore, which can be described by the Stern-Volmer equation:

$$F_0 / F = \tau_0 / \tau = 1 + K_q \tau_0 [Q] = 1 + K_D [Q] \quad (1)$$

Where F_0 and τ_0 are the fluorescence intensity and fluorescence lifetime of the fluorophore in the absence of quencher, respectively, F and τ is the fluorescence intensity and the fluorescence lifetime of the fluorophore in the presence of quencher, respectively. The Stern-Volmer quenching constant is given by $K_q \tau_0$ with K_q representing the bimolecular quenching constant, which can reflect the efficiency of quenching or the accessibility of the fluorophores to the quencher. When the quenching is known to be dynamic, the Stern-Volmer constant is represented by K_D otherwise, this constant is described as K_{SV} and $[Q]$ is the quencher concentration.

Static quenching on the other hand involves formation of a complex between ground-state fluorophore and a ground-state quencher. In the case of dynamic quenching, there is an equivalent decrease in fluorescence intensity and lifetime. The decrease in lifetime occurs because quenching is an additional rate process that depopulates the excited state. Static quenching does not decrease the lifetime because only the fluorescent molecules are observed while the un-complexed fluorophores have the unquenched lifetimes τ_0 therefore for this quenching mechanism, $\tau_0 / \tau = 1$ while for dynamic quenching $\tau_0 / \tau = F_0 / F$. Because of this, equation (1) shown above for static quenching is represented as $F_0 / F = 1 + K_S [Q]$. In this case, the dependence of F_0 / F on $[Q]$ is also linear and identical to that of dynamic quenching except

that the quenching constant is now the association constant.²⁴ Both static and dynamic quenching requires molecular contact between the fluorophore and the quencher. Because of this, close range interactions are required for quenching; the extent of quenching is sensitive to molecular factors that affect the rate and probability of contact including steric shielding and charge-to-charge interactions.²⁵

Another quenching mechanism involves transfer of the excited state energy from initially excited fluorophore (donor) to the quencher (acceptor) also known as Resonance Energy Transfer (RET). RET occurs when the emission spectrum of the donor overlaps with the absorption spectrum of the acceptor. The theory of energy transfer is based on the concept of a fluorophore as an oscillating dipole, which can exchange energy with another dipole, which has a similar resonance frequency.²⁶ Figure 5.4 below illustrates the above mentioned quenching mechanisms in a modified Jablonski diagram. Factors that affect the rate of energy transfer are the extent of overlap of the emission spectrum of the donor with the absorption spectrum of the acceptor, the relative orientation of the donor and acceptor transition dipoles, and their distance. The energy received by the acceptor is less than that given by the donor with the remaining energy being consumed by radiationless transitions to the ground state. The rate of energy transfer (k_{ET}) from a specific donor to a specific acceptor is given by;

$$K_{ET} = 1/\tau_D (R_0/r)^6 \quad (2)$$

where τ_D is the lifetime of the unquenched donor in the absence of acceptor, r is the distance between donor and acceptor and R_0 is the Förster distance (distance at which the efficiency of energy transfer is 50%). At R_0 , one half of the donor molecules decay by energy transfer and the other half due to the usual radiative and non-radiative transitions. The necessary conditions for RET to occur are; (a) the donor and acceptor molecules have to be in close proximity (typically 10-100 Å), (b) the absorbance spectrum of the acceptor has to overlap the fluorescence emission

spectrum of the donor and (c) the donor and acceptor transition dipole orientations have to be approximately parallel, and must not be oriented perpendicularly to each other.^{24,27}

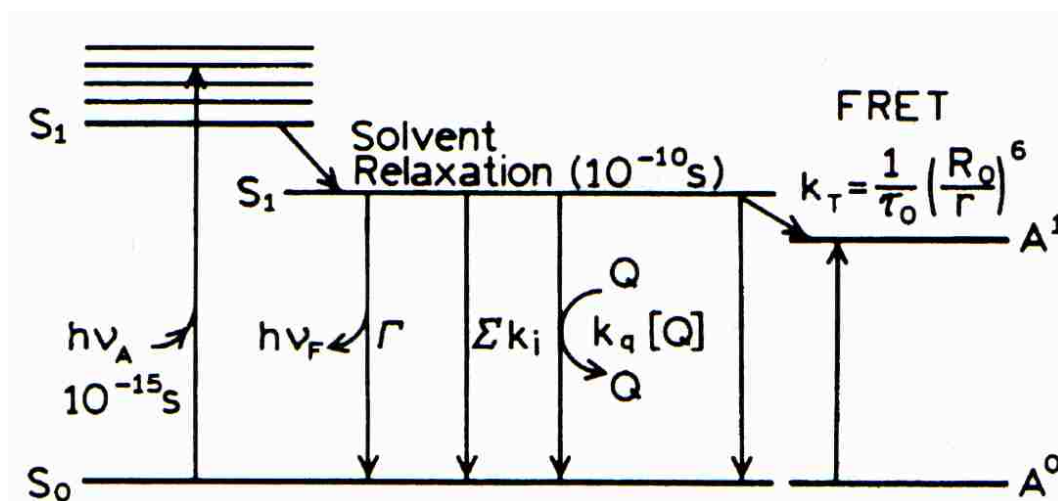


Figure 5.4: Modified Jablonski diagram for the processes of absorption ($h\nu_A$), fluorescence emission ($h\nu_F$), non-radiative pathways (Σk_i), dynamic quenching $k_q[Q]$ and FRET.²⁴

5.1.3 Research Focus

Since its introduction in the early 1950's by Förster,²⁸ FRET has been utilized as a powerful physical and biophysical technique for the analysis of fluorophores, which are in close contact. The most wide spread application of this phenomenon is its use as a “spectroscopic ruler”²⁹ because the rate of resonance energy transfer depends strongly on donor-acceptor distance, which is inversely proportional to r^6 as shown in equation (2) above. This technique has also been used to study the structure and conformation of proteins³⁰ or nucleic acids,³¹ understanding the spatial distribution and assembly of protein complexes,³² investigation of receptor/ligand interactions,³³ probing interactions of single molecules,³⁴ and the detection of hybridization events.³⁵ In Chapter 4, we demonstrated an example of how quenching (dynamic, static or FRET) can be used for the detection of hybridization events by using molecular beacon probes. Regardless of the application, it is important to have suitable donor-acceptor pairs, since

there are no universal quenchers or acceptors for any given fluorophore. Suitable fluorophore/quencher matches are usually desired in order to achieve high sensitivity, especially when using fluorescence quenching techniques for analysis. Examples of different donor–acceptor combinations that have been reported are Fluorescein–Rhodamine, cyanine dyes like Cy3–Cy5, 4-[[4-(dimethylamino)phenyl]azo]benzoic acid (DABCYL) – 5-[(2-aminoethyl)amino]-1-naphthalenesulfonic acid (EDANS), blue and green fluorescent proteins.³⁶ Despite there being a large number of reported fluorophore/quencher or acceptor/donor systems, the sensitivity or efficiency of energy transfer still remains an issue. This has led to a continued study and exploration of many compounds for these purposes. An example of how this sensitivity has been improved is by the use of lanthanide complexes, such as europium complexes and terbium complexes, which are known to have strong fluorescence and long excited state lifetimes up to the range of ms.³⁷ One major drawback of these systems however, is their relatively low stability, resulting in their dissociation at low concentrations. Phthalocyanines, on the other hand, are known to be thermally and chemically stable; they have high extinction coefficients and quantum yields and depending on the transition metal inserted in the macrocyclic ring, their photo-physical and spectral properties are tunable.

We were therefore motivated to study the quenching of the fluorescence emission among some metal phthalocyanine complexes, especially those whose absorption and emission spectra could overlap. Phthalocyanines are also known to aggregate (intermolecular or intramolecular) and this aggregation provides an efficient non-radiative energy relaxation pathway that shortens the excited state of the fluorescing phthalocyanine molecule. These quenching properties of phthalocyanines could be very useful where fluorescence measuring techniques are applied in any given analysis. In particular, 2,9,16,23-tetrakis(4-carboxyphenoxy) phthalocyanato zinc (II), referred to as carboxylated zinc phthalocyanine throughout this Chapter, was used as the

fluorophore (donor) while 2,9,16,23-tetrakis(4-carboxyphenoxy) phthalocyanato nickel (II) (carboxylated nickel phthalocyanine), 2,9,16,23-tetrakis(4-carboxyphenoxy) phthalocyanato copper (II), (carboxylated copper phthalocyanine); 2,9,16,23-tetrakis(4-carboxyphenoxy) phthalocyanato palladium (II), (carboxylated palladium phthalocyanine), were used as the quenchers (acceptors) due to the fact that these metal/phthalocyanines complexes show very little amounts of fluorescence. The quenching of carboxylated zinc phthalocyanine by the above mentioned phthalocyanine quencher derivatives was then compared with a commercial Black Hole Quencher (BHQ-3). BHQ-3 was chosen for comparative studies because it has no native fluorescence and its absorption spectrum is broad, ranging from 620 nm to 730 nm. Therefore, it would maximize spectra overlap when used with carboxylate zinc phthalocyanine, whose emission is at 690 nm. This overlap was desired to increase the efficiency of quenching.

5.2 Experimental

5.2.1 Materials and Methods

The dyes used as fluorophore/quencher sets were chosen based on the fact that the emission band of the fluorophore/donor (carboxylated zinc phthalocyanine) overlaps with the absorption bands of all of the quenchers (acceptors) studied; hence, energy transfer from the excited carboxylated zinc phthalocyanine may occur in the series of the quenchers selected. The molecular structures of these organic dyes are tabulated in Table 5.1 shown below.

Dimethyl sulfoxide (DMSO) solvent that was used for making all dilutions was obtained from Sigma Aldrich (St.Louis, MO) while the Black Hole Quencher (BHQ-3) was purchased from Trilink Biosearch INC. (San Diego, CA) in its succinimide ester derivative. A series of solutions with constant carboxylated zinc phthalocyanine concentrations (1 μM) and varying quencher concentrations (500 nM, 1000 nM, 1500 nM and 2000 nM) were prepared. The steady state fluorescence spectra were obtained ($\lambda_{\text{exc}} = 675 \text{ nm}$) using a Fluorolog-3 fluorimeter (Jobin

Yvon Inc., Edison, NJ). The fluorescence intensities were then observed at a single wavelength (690 nm) and the bimolecular rate constants for the fluorescence quenching was determined by using Stern-Volmer plots. Time-resolved fluorescence quenching measurements were performed using a Fluo Time (PicoQuant GmbH, Berlin, Germany) lifetime measurement spectrometer. Excitation pulses were obtained by a laser (Picoquant GmbH model PDL800, Berlin, Germany) with the laser being operated at a wavelength of 680 nm and a repetition rate of 40 MHz. The fluorescence photon counts were obtained using a time-correlated single photon counting detection system and the data was treated by using fluofit fluorescence decay data analysis software.

5.2.2 Calculations: Stern-Volmer Quenching Constants, Overlap Integrals and Förster Distances

Stern-Volmer plots

Stern-Volmer plots were prepared by calculating the fluorescence power at a single wavelength in the emission spectra. The ratio of the fluorescence intensity in the absence and presence of the quencher was then graphed as a function of the quencher concentrations. From the slope of the graph, the Stern-Volmer constants were determined by linear regression according to equation (1) shown above.

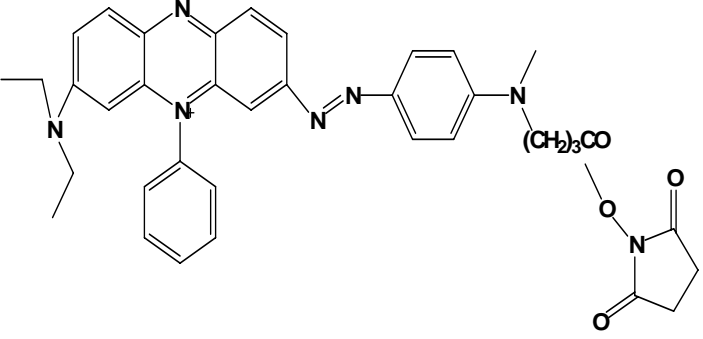
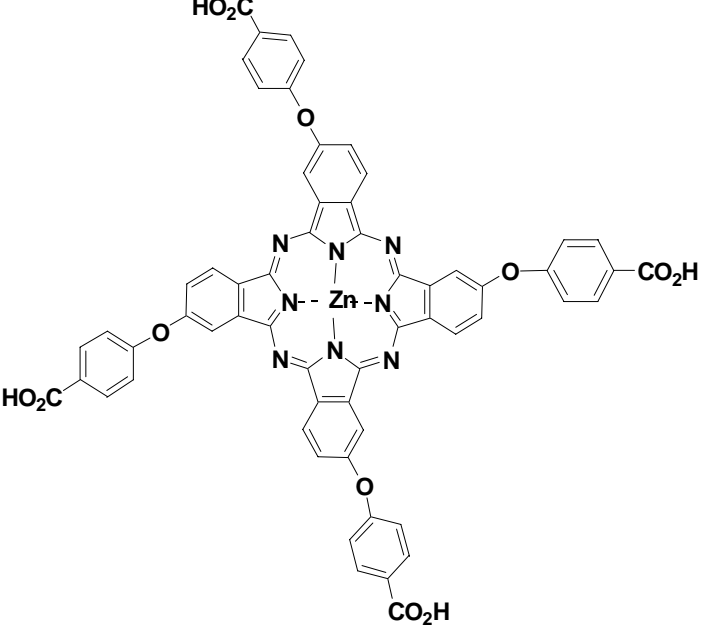
Overlap integrals

Since the rate of energy transfer depends upon the extent of spectral overlap of the emission spectrum of the donor with that of the absorption spectrum of the acceptor, these overlap integrals were evaluated for each donor/acceptor pair. The overlap integral $[J(\lambda)]$ was calculated from the corrected emission spectrum of donor with its area normalized to unity using the equation;

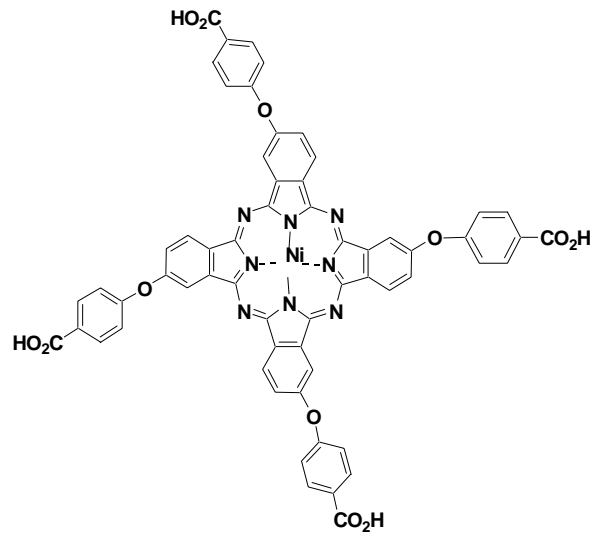
$$J(\lambda) = \int_0^{\infty} F_D(\lambda) \epsilon_A(\lambda) \lambda^4 d\lambda \quad (3)$$

where $J(\lambda)$ is the overlap integral; $F_D(\lambda)$ is the corrected fluorescence intensity of donor in the wavelength range of (λ) to $(\lambda) + \Delta(\lambda)$ with the total intensity (area under curve) normalized to unity; $\epsilon_A(\lambda)$ is the extinction coefficient of the acceptor (quenchers) at wavelength (λ) ; and (λ) is the wavelength of the light (excitation wavelength).

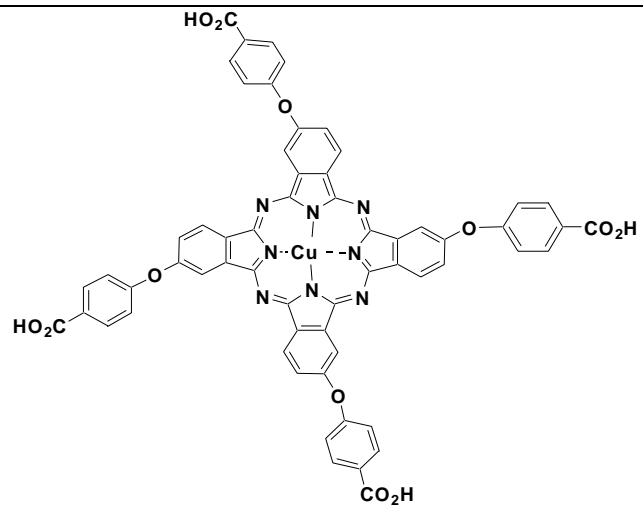
Table 5.1: Molecular structures of the organic dyes used in the quenching studies

| Fluorophore / Quencher name | Molecular Structure |
|----------------------------------------------------------------------|--------------------------------------------------------------------------------------|
| Black Hole Quencher (BHQ-3), carboxylic acid, succinimidyl ester. |  |
| 2,9,16,23-tetrakis(4-carboxyphenoxy)phthalocyanato zinc (II) |  |

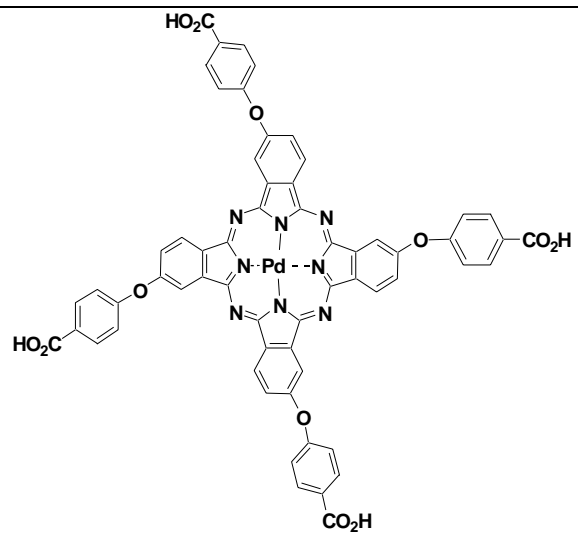
2,9,16,23-tetrakis(4-carboxyphenoxy)phthalocyanato nickel (II)



2,9,16,23-tetrakis(4-carboxyphenoxy)phthalocyanato copper (II)



2,9,16,23-tetrakis(4-carboxyphenoxy)phthalocyanato palladium (II)



Förster distance

The distance at which resonance energy transfer is 50% efficient is typically in the range of 10-100 Å. This distance was calculated from the spectral properties of the donor and acceptors using the equation;

$$R_0 = 0.211 [k^2 n^{-4} Q_D J(\lambda)]^{1/6} \quad (4)$$

where k^2 is a factor describing the relative orientation in space of the transition dipoles of the donor and acceptor, typically k^2 is assumed to be equal to 2/3, which is the value for donors and acceptors that randomize by rotational diffusion prior to energy transfer while n is the refractive index of the medium (assumed to be 1.4 for biomolecules in aqueous solution). Q_D is the quantum yield of the carboxylated zinc phthalocyanine donor while $J(\lambda)$ is the overlap integral of each fluorophore/quencher pair. The extinction coefficient and quantum yield of carboxylated zinc phthalocyanine is 27,900 $M^{-1}cm^{-1}$ and 0.66, respectively, while the extinction coefficients of the acceptor/quenchers used in this study are shown in Table 5.2 below.

Table 5.2: Molar extinction coefficients of the quenchers used in this study

| Acceptor dye | Molar extinction coefficients ($M^{-1}cm^{-1}$) |
|---------------------------------------|---------------------------------------------------|
| Black Hole Quencher (BHQ-3) | 42,700 @ 670 nm |
| Carboxylated Nickel Phthalocyanine | 25,000 @ 670 nm |
| Carboxylated Palladium Phthalocyanine | 16,000 @ 662 nm |
| Carboxylated Copper Phthalocyanine | 21,000 @ 655 nm |

5.3 Results and Discussions

Fluorescence quenching can occur via static, dynamic (contact) or RET modes. Quenching by the RET mechanism requires that the emission spectrum of the donor dye overlaps with the absorption spectrum of the acceptor dye while static or dynamic modes requires that the

fluorophore and quencher be very close to each other. One advantage of contact quenching over RET is the fact that all fluorophores can be quenched equally well even if the emission spectrum of the fluorophore does not overlap the absorption spectrum of the quencher greatly. In the RET mechanism, the acceptor and donor are brought close, within a range of 10-100 Å, resulting in the intensity of the acceptor increasing while that of the donor decreasing. When non-fluorescent acceptors are used, the intensity of fluorescence can be measured directly and not as an alteration in the shape of the emission spectrum. Recently, non-fluorescent acceptor dyes have been widely used both in RET and contact quenching modes.^{33,38-40} In this work, the quenching of carboxylated zinc phthalocyanine was studied using different quenchers (carboxylated nickel phthalocyanine, carboxylated copper phthalocyanine, carboxylated platinum phthalocyanine, carboxylated palladium phthalocyanine and Black Hole Quencher (BHQ-3)). The absorption spectrum of all these selected quenchers overlaps with the fluorescence emission of carboxylated zinc phthalocyanine and they are also non-fluorescent.

Dilute solutions of carboxylated zinc phthalocyanine in DMSO displayed strong fluorescence centered at 690 nm that originated from the excited singlet state when excited into the Q-band (675 nm). In the presence of a quencher, the fluorescence intensity of the carboxylated zinc phthalocyanine is reduced. Successive additions of quencher caused a steady decrease in the observed fluorescence intensities (see Figure 5.5 (a)). Quenching data was expressed as the ratio of unquenched to quenched fluorescence intensity using the Stern-Volmer equation (1), where F_0 and F are the fluorescence intensities in the absence and presence of the quencher, respectively. The Stern-Volmer quenching constants, which is the product of the bimolecular quenching rate constant (k_q) and the lifetime of the carboxylated zinc phthalocyanine (fluorophore) in the absence of the quencher (τ_0) were determined for each fluorophore/quencher pair.

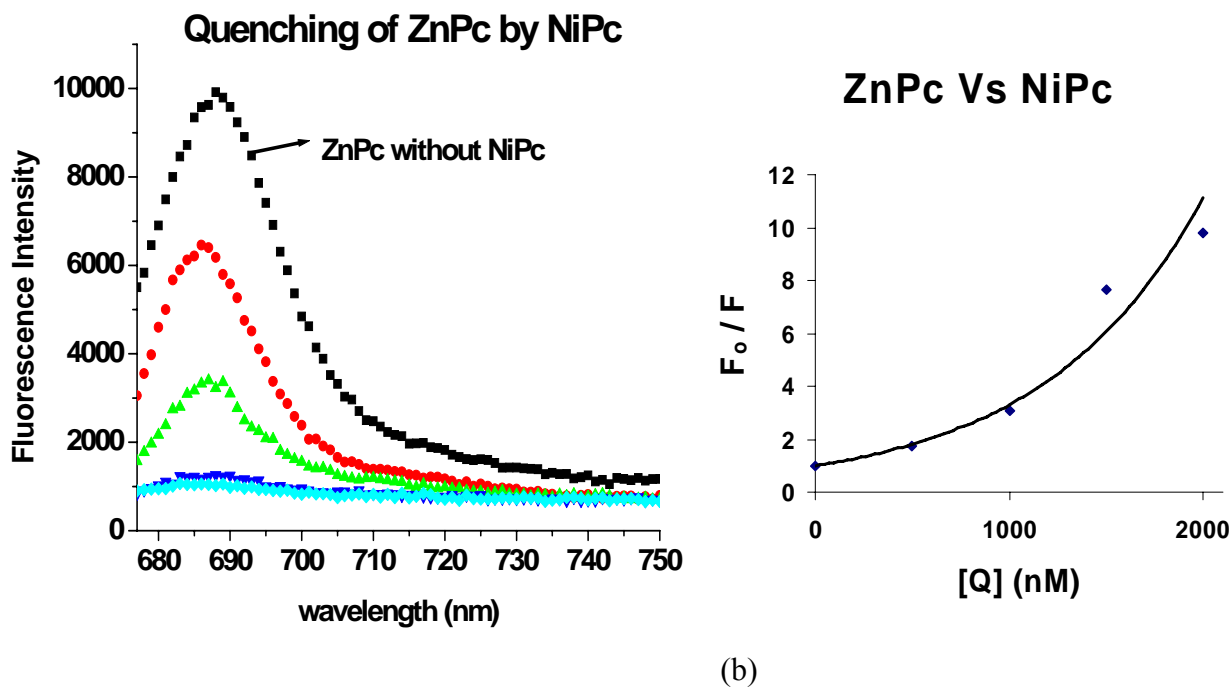


Figure 5.5: (a) Fluorescence spectra ($\lambda_{exc} = 675$ nm) of 1 μ M carboxylated zinc phthalocyanine and variable concentrations of carboxylated nickel phthalocyanine (500 nM, 1000 nM, 1500 nM and 2000 nM) in DMSO. (b) F_0/F versus carboxylated nickel phthalocyanine concentration relationship (Stern-Volmer plot) at 690 nm fluorescence emission maximum.

Figure 5.5 shown above gives the quenching of carboxylated zinc phthalocyanine by carboxylated nickel phthalocyanine. The Stern-Volmer plot for quenching of carboxylated zinc phthalocyanine by carboxylated nickel phthalocyanine appeared non-linear (Figure 5.5 (b)) on successive increases of quencher concentrations and this may be due to an interaction between the quencher and fluorophore in a stoichiometry other than 1:1.^{41,42} This is quite possible because increased quencher (carboxylated nickel phthalocyanine) concentrations could have increased its dimer/monomer ratio leading to the observed trend in the Stern-Volmer plot. Possibility of dimer/monomer derivatives in the solution was confirmed from the UV-vis spectrum, which appeared to be significantly broader as shown in Figure 5.6. Many dyes, including cyanines and fluorescein derivatives, form dimers and higher-order aggregates in different solvents. At high dye concentrations, hydrophobic and electrostatic effects promote aggregation effects. It is

possible that at increased quencher concentrations, there is intermolecular aggregation, which has been found to provide an efficient non-radiative energy relaxation pathway that leads to a short lived excited state of the fluorophore.⁴³ Another reason for the observed upward curvature in the Stern-Volmer plot could be due to a large extent of quenching of the carboxylated zinc phthalocyanine by the carboxylated nickel phthalocyanine or the possibility of both static and dynamic quenching. In static quenching, there is formation of a ground state complex that may alter the absorption spectrum of the fluorophore. As seen in Figure 5.6, the absorption spectrum of the carboxylated zinc phthalocyanine and carboxylated nickel phthalocyanine complex was substantially altered due to aggregation, hence, this aggregation enabled contact/static quenching to occur.

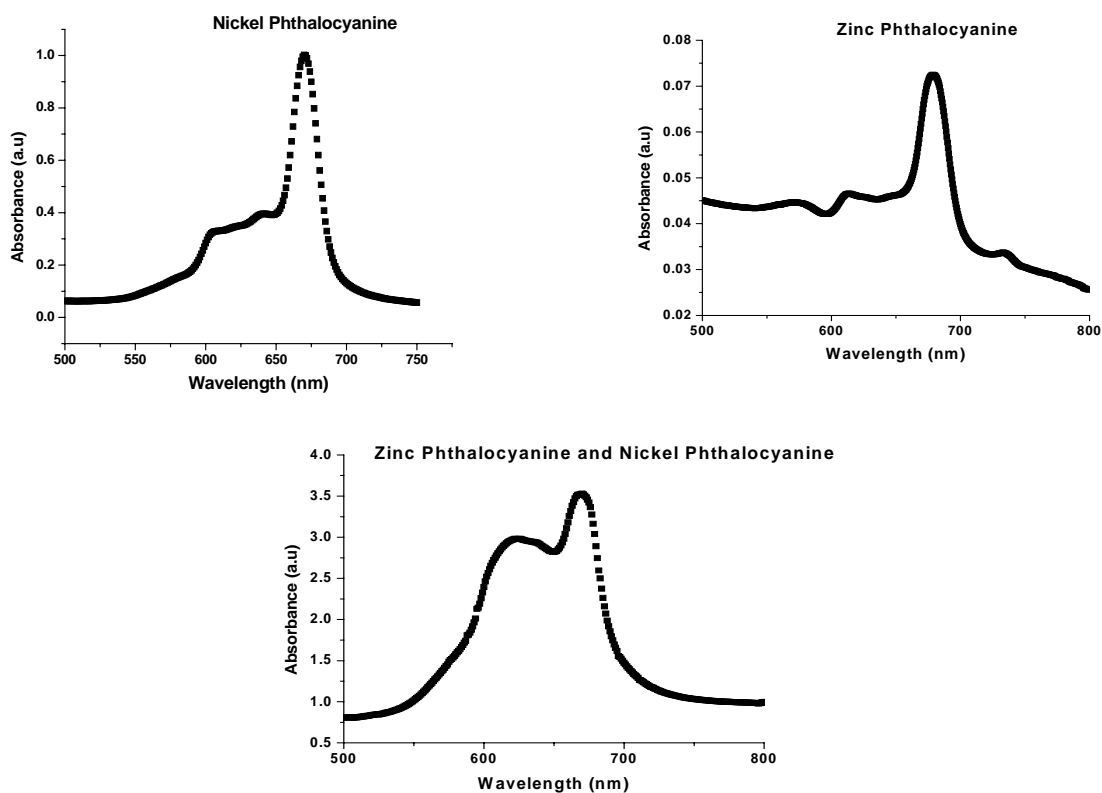


Figure 5.6: Absorption spectra of carboxylated nickel phthalocyanine, carboxylated zinc phthalocyanine and a mixture of both. The spectrum of carboxylated nickel phthalocyanine and carboxylated zinc phthalocyanine complex has a much broader band, which could be attributed to aggregation.

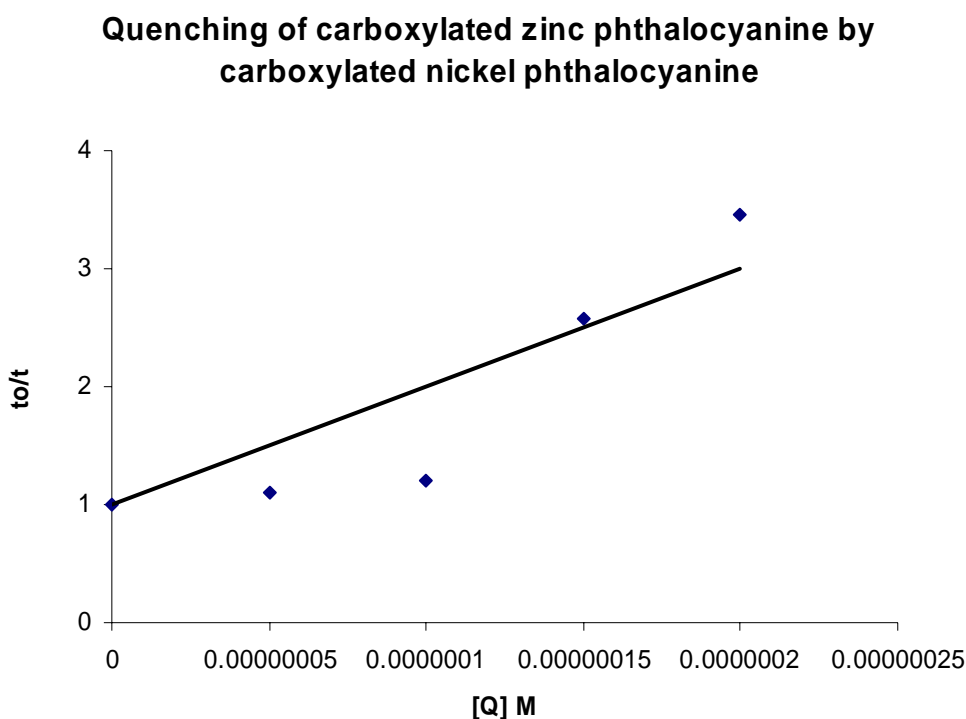
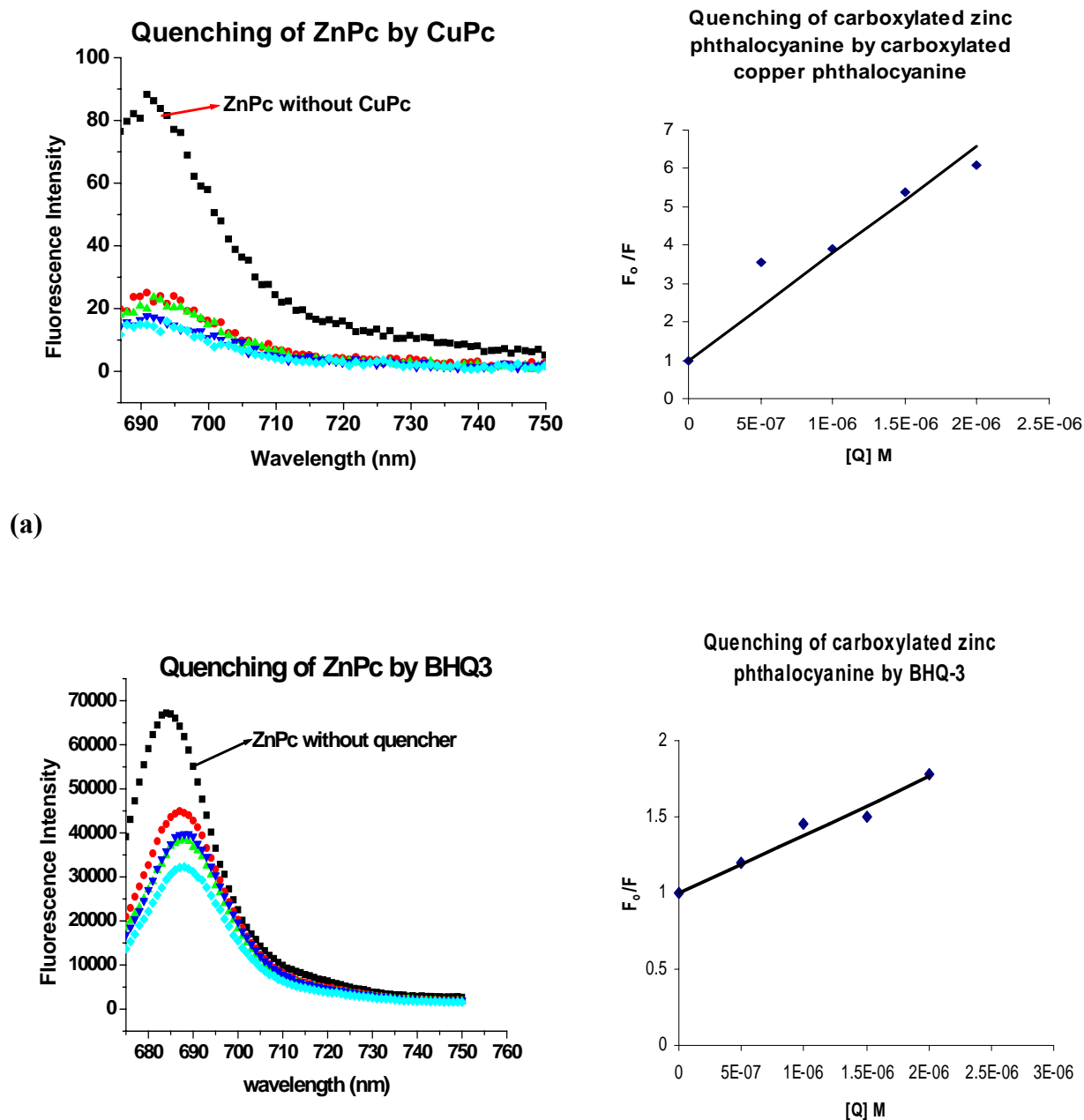


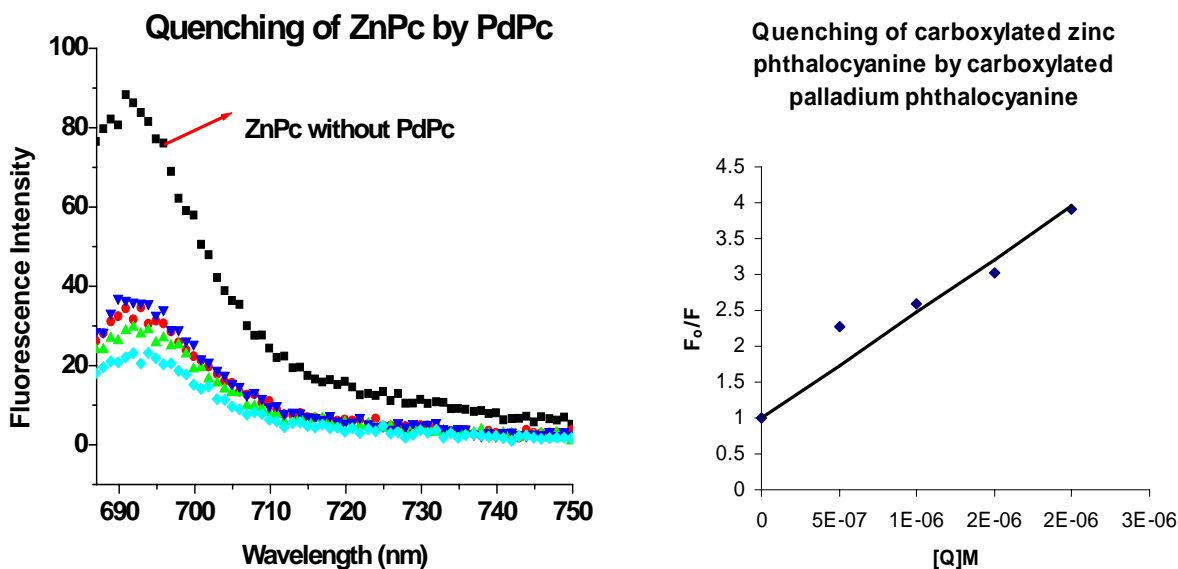
Figure 5.7: Stern–Volmer plots showing τ_0/τ versus carboxylated nickel phthalocyanine with quencher concentrations of 50 nM, 100 nM, 150 nM and 200 nM.

Because dynamic quenching is a non-radiative process that decreases the observed fluorescence lifetime, the attenuation of lifetime as a function of quencher concentration was also used to determine the quenching constants. Fluorescence lifetimes are important because they determine the time available for the fluorophore to interact with or diffuse to the quencher in its environment during the fluorophore's excited state. For lifetime studies, the quencher concentrations were reduced (50 nM, 100 nM, 150 nM and 200 nM) compared to steady state fluorescence measurements (500 nM, 1000 nM, 1500 nM and 2000 nM) to minimize aggregation-induced quenching. The ratio of the fluorescence lifetime in the absence of quencher to that in the presence of the quencher (τ_0/τ_f) was calculated as a function of the quencher concentration. A plot of τ_0/τ_f vs quencher concentration (Figure 5.7) resulted in a linear Stern-Volmer plot from

which the quenching constant was calculated. From these results, we concluded that the extensive quenching by nickel phthalocyanine is due to both static and dynamic quenching.



(b) **Figure 5.8:** Left: Fluorescence spectra ($\lambda_{exc} = 675 \text{ nm}$; $\lambda_{em} = 690 \text{ nm}$) for the quenching of carboxylated zinc phthalocyanine by (a) carboxylated copper phthalocyanine (b) BHQ-3 and (c) carboxylated palladium phthalocyanine in DMSO. **Right:** Stern-Volmer plots for quenching of carboxylated zinc phthalocyanine by (a) carboxylated copper phthalocyanine (b) BHQ-3 and (c) carboxylated palladium phthalocyanine in DMSO.



(c)

Figure 5.8 continued.

Quenching of carboxylated zinc phthalocyanine by the other metal phthalocyanines-based quenchers was performed as well and these quenching data are shown in Figure 5.8. There were successive decreases in the fluorescence intensities of the carboxylated zinc phthalocyanine with increasing quencher concentrations for all the quenchers studied. The Stern-Volmer plots were prepared by plotting the fluorescence intensity ($\lambda_{em} = 690$ nm) at various quencher concentrations. The Stern-Volmer plots were obtained by calculating the ratio of the fluorescence intensity in the absence and presence of the quenchers, which was eventually graphed as a function of the quencher concentrations and they were all found to be linear. From the slope of the graph, the Stern-Volmer constants could be obtained according to equation (1) by linear regression. For a RET quenching mechanism, energy transfer occurs without the appearance of a photon and results from a long range dipole-dipole interaction between the acceptor and the donor. The donor molecules typically emit at shorter wavelengths, which overlap with the absorption spectrum of the acceptor.²⁴ For non-fluorescent quenchers that were

used here, the quencher returns to the ground state without emission of light following energy transfer from the donor. Because RET occurs whenever there is spectral overlap between the emission spectrum of the fluorophore donor and the absorption spectrum of the quencher (acceptor), we determined the extent of spectral overlap by calculating the overlap integral of each fluorophore/quencher pair and observed its contribution to the quenching efficiency. This was achieved by using equation (3) that utilized the extinction coefficients of the quenchers (see Table 5.2) and the corrected fluorescence intensity of the carboxylated zinc phthalocyanine with its total intensity normalized to unity. The rate of energy transfer also depends on the Förster distance (R_0), which was obtained from the spectral properties of each donor/acceptor pair by using equation (4). Table 5.3 shown below gives a summary of the Stern-Volmer constants (K_{SV}), overlap integrals (J_λ) and the Förster distance (R_0) of the carboxylated zinc phthalocyanine and the various quenchers studied. From Table 5.3, BHQ-3 had higher R_0 values (distance at which resonance energy transfer is 50% efficient) followed by carboxylated copper phthalocyanine, carboxylated nickel phthalocyanine and then carboxylated palladium phthalocyanine. This trend is expected because acceptors with larger extinction coefficients result in larger R_0 values. The extinction coefficients of the acceptors used in this study are given in Table 5.2. The fluorophore/quencher pairs with greater overlap of the emission spectrum of the donor with that of the absorption spectrum of the acceptor ($J(\lambda)$ values) also exhibited higher R_0 values. Carboxylated nickel phthalocyanine had a higher quenching efficiency from the Stern-Volmer constant values (K_{SV}), then carboxylated copper phthalocyanine, carboxylated palladium phthalocyanine and lastly BHQ-3 even though the carboxylated zinc phthalocyanine / BHQ-3 pair had higher $J(\lambda)$ and R_0 values. From these results, it is observed that the spectral overlap is not a significant determinant of quenching efficiency in cases where the fluorophore and quencher come within close contact distance of each other. It is possible that the intermolecular

aggregation between the phthalocyanine fluorophore / quencher pairs brings them together (intermolecular aggregation) resulting in higher quenching efficiencies even with less spectral overlap as compared to the carboxylated zinc phthalocyanine / BHQ-3 pair. Tyagi and co-workers studied the efficiencies of energy transfer and contact mediated quenching for a large number of combinations of commonly used fluorophores and quenchers and they found that besides the photochemical characteristics, the tendency of the fluorophore and the quencher to bind to each other has a strong influence of the quenching efficiencies.⁴⁴

Table 5.3 Stern-Volmer constants (K_{SV}), overlap integrals (J_{λ}) and the Förster distance (R_0) of different fluorophore/quencher pairs used in these quenching studies.

| | Carboxylated Zinc Phthalocyanine vs BHQ-3 | Carboxylated Zinc Phthalocyanine vs Carboxylated Nickel Phthalocyanine | Carboxylated Zinc Phthalocyanine vs Carboxylated Copper Phthalocyanine | Carboxylated Zinc Phthalocyanine vs Carboxylated Palladium Phthalocyanine |
|---------------------------------------------------------------|--------------------------------------------------|-------------------------------------------------------------------------------|-------------------------------------------------------------------------------|----------------------------------------------------------------------------------|
| R_0 (Å) | 116.81 | 78.88 | 100.29 | 29.40 |
| J (λ) ($M^{-1}cm^{-1}$ (nm) ⁴) | 2.51×10^{17} | 2.38×10^{16} | 1.00×10^{17} | 4.15×10^{16} |
| K_{SV} (M^{-1}) | 3.8×10^5 | 1×10^7 | 3×10^6 | 1×10^6 |

We can therefore attribute the observed poor quenching efficiency of the carboxylated zinc phthalocyanine by BHQ-3 compared to the metal phthalocyanine acceptors due to less binding/attraction between the carboxylated zinc phthalocyanine/BHQ-3 pair. Of the metal phthalocyanines, high quenching was observed for carboxylated nickel phthalocyanine followed by carboxylated copper phthalocyanine, and then carboxylated palladium phthalocyanine. From the results obtained here, extensive quenching by nickel phthalocyanines could be due to both static and dynamic quenching as shown in the upward curvature of the Stern-Volmer plot. The

ability of the phthalocyanines to aggregate might have played a key role in the quenching trend observed.

5.4 Conclusions

Fluorescence quenching of carboxylated zinc phthalocyanine by carboxylated nickel phthalocyanine, carboxylated copper phthalocyanine, carboxylated palladium phthalocyanine and BHQ-3 was studied herein. Carboxylated nickel phthalocyanine exhibited higher quenching efficiency compared to the other metal phthalocyanines and the commercial quencher BHQ-3 even though BHQ-3 had higher J (λ) and R_0 values. The tendency of non-fluorescent metal-phthalocyanines to form ground-state aggregates might have contributed to the observed trend in the quenching efficiencies. From this study, the carboxylated zinc phthalocyanine fluorophore and the carboxylated nickel phthalocyanine quencher would be a perfect match for labeling oligonucleotides and other molecular probes, which utilize fluorescence quenching transduction techniques for sample analysis. Examples of such systems are molecular beacons, taqman probes, competitive hybridization assays.

5.5 References

- (1) Leznoff, C. C.; Lever, A. B. P.; Editors *Phthalocyanines: Properties and Applications*, 1989.
- (2) McKeown, N. B. *Porphyrin Handbook* **2003**, *15*, 61-124.
- (3) Leznoff, C. C.; Lam, H.; Nevin, W. A.; Kobayashi, N.; Janda, P.; Lever, A. B. P. *Angewandte Chemie* **1987**, *99*, 1065-1067.
- (4) Zhang, T.; Zhou, C. *Dyes and Pigments* **1997**, *35*, 123-130.
- (5) Hill, R. F. *Journal of the Oil and Colour Chemists' Association* **1965**, *48*, 603-612.
- (6) Gu, D.; Chen, Q.; Shu, J.; Tang, X.; Gan, F.; Shen, S.; Liu, K.; Xu, H. *Thin Solid Films* **1995**, *257*, 88-93.
- (7) Gregory, P. *Journal of Porphyrins and Phthalocyanines* **2000**, *4*, 432-437.
- (8) Lukyanets, E. A. *Journal of Porphyrins and Phthalocyanines* **1999**, *3*, 424-432.

- (9) Dini, D.; Hanack, M. *Journal of Porphyrins and Phthalocyanines* **2004**, *8*, 915-933.
- (10) Whalley, M. *Journal of the Chemical Society* **1961**, 866-869.
- (11) Ough, E.; Nyokong, T.; Creber, K. A. M.; Stillman, M. J. *Inorganic Chemistry* **1988**, *27*, 2724-2732.
- (12) Nevin, W. A.; Liu, W.; Greenberg, S.; Hempstead, M. R.; Marcuccio, S. M.; Melnik, M.; Leznoff, C. C.; Lever, A. B. P. *Inorganic Chemistry* **1987**, *26*, 891-899.
- (13) Orti, E.; Bredas, J. L.; Clarisse, C. *Journal of Chemical Physics* **1990**, *92*, 1228-1235.
- (14) Lever, A. B. P.; Pickens, S. R.; Minor, P. C.; Licoccia, S.; Ramaswamy, B. S.; Magnell, K. *Journal of the American Chemical Society* **1981**, *103*, 6800-6806.
- (15) Taube, R. *Pure and Applied Chemistry* **1974**, *38*, 427-438.
- (16) Gouterman, M.; Wagniere, G.; Snyder, L. C. *Journal of Molecular Spectroscopy* **1963**, *11*, 108-127.
- (17) Gouterman, M. *Porphyrins* **1978**, *3*, 1-165.
- (18) Mack, J.; Stillman, M. J. *Inorganic Chemistry* **2001**, *40*, 812-814.
- (19) Briat, B.; Schooley, D. A.; Records, R.; Bunnenberg, E.; Djerassi, C. *Journal of the American Chemical Society* **1967**, *89*, 7062-7071.
- (20) Briat, B.; Schooley, D. A.; Records, R.; Bunnenberg, E.; Djerassi, C. *Journal of the American Chemical Society* **1967**, *89*, 6170-6177.
- (21) Stillman, M. J. *Phthalocyanines* **1993**, *3*, 227, 229-296.
- (22) Leznoff, C. C.; Lever, A. B. P.; Editors *Properties and Applications*. [In: *Phthalocyanines, 1993; 2*], 1993.
- (23) Golovin, M. N.; Seymour, P.; Jayaraj, K.; Fu, Y. S.; Lever, A. B. P. *Inorganic Chemistry* **1990**, *29*, 1719-1727.
- (24) Lakowicz, J. R. *Principles of Fluorescence Spectroscopy*, 1983.
- (25) Goodpaster, J. V.; McGuffin, V. L. *Applied Spectroscopy* **1999**, *53*, 1000-1008.
- (26) Clegg, R. M. *Chemical Analysis (New York)* **1996**, *137*, 179-252.
- (27) Rolinski, O. J.; Birch, D. J. S. *Journal of Chemical Physics* **2000**, *112*, 8923-8933.
- (28) Foerster, T. *Mod. Quantum Chem., Lect. Istanbul Int. Summer Sch.* **1965**, 93-137.

- (29) Stryer, L.; Haugland, R. P. *Proceedings of the National Academy of Sciences of the United States of America* **1967**, *58*, 719-726.
- (30) Luo, Y.; Wu, J.-L.; Gergely, J.; Tao, T. *Biophysical Journal* **1998**, *74*, 3111-3119.
- (31) Furey, W. S.; Joyce, C. M.; Osborne, M. A.; Klenerman, D.; Peliska, J. A.; Balasubramanian, S. *Biochemistry* **1998**, *37*, 2979-2990.
- (32) Watson, B. S.; Hazlett, T. L.; Eccleston, J. F.; Davis, C.; Jameson, D. M.; Johnson, A. E. *Biochemistry* **1995**, *34*, 7904-7912.
- (33) Gagne, A.; Banks, P.; Hurt, S. D. *Journal of Receptors and Signal Transduction* **2002**, *22*, 333-343.
- (34) Ha, T.; Enderle, T.; Ogletree, D. F.; Chemla, D. S.; Selvin, P. R.; Weiss, S. *Proceedings of the National Academy of Sciences of the United States of America* **1996**, *93*, 6264-6268.
- (35) Tyagi, S.; Kramer, F. R. *Nature Biotechnology* **1996**, *14*, 303-308.
- (36) Heim, R.; Tsien, R. Y. *Current Biology* **1996**, *6*, 178-182.
- (37) Alpha, B.; Lehn, J. M.; Mathis, G. *Angewandte Chemie* **1987**, *99*, 259-261.
- (38) Knemeyer, J.-P.; Marme, N.; Sauer, M. *Analytical Chemistry* **2000**, *72*, 3717-3724.
- (39) Dubertret, B.; Calame, M.; Libchaber, A. J. *Nature Biotechnology* **2001**, *19*, 680-681.

CHAPTER 6

LABELING OF OLIGONUCLEOTIDE PROBES FOR FRET APPLICATIONS

6.1 Introduction

Nucleic acids are heteropolymers consisting of four different monomers A, C, T G as explained in Chapter one. Oligonucleotides are short segments of these nucleic acids ranging from 10 – 100 monomer building blocks. While proteins may contain fluorescent amino acids such as tryptophan, the intrinsic fluorescence emission of nucleic acid bases (A, C, G, T / U) is too weak to be useful for biological applications.¹ Because of this, oligonucleotide probes are usually labeled with fluorescent tags which enable them to be analyzed by using fluorescence based techniques. Labeling of oligonucleotide probes can be achieved by employing non-covalent / or covalent techniques as explained below.

6.1.1 Non-Covalent Labeling of Oligonucleotide Probes

Non- covalent labeling techniques involve use of intercalating dyes such as ethidium bromide. Intercalators are specified by non-covalent, reversible interactions with nucleic acids based on hydrophobic as well as electrostatic effects. They are typically planar, polyaromatic compounds with cationic residues. Hydrophobic residues enable stacking of the dyes with nucleobases while the ionic residues interact with the phosphate backbone of the DNA. When intercalating dyes are mixed with DNA, they lie in between base-pairs such that covalent binding between the fluorophore and nucleic acid is not required. These dyes do not interfere with the major and minor grooves of DNA however; they require that there be cavity of two hybridized DNA strands for optimal labeling efficiency to be obtained. Some examples of intercalating dyes are ethidium bromide, acridines, thiazole orange, and phenazines.²⁻⁴

6.1.2 Covalent Labeling of Oligonucleotide Probes

Covalent labeling of oligonucleotides can be achieved by using pre-synthetic or post-synthetic methods. In pre- synthetic labeling, fluorescent labels are chemically bound to the

nucleic acids building blocks of the oligonucleotide probe during its chemical synthesis which is commonly done by use of phosphoramidite chemistry. Solid phase phosphoramidite chemistry was introduced by Beacage and Carathers^{5,6} and it involves use of a solid phase like glass controlled pore (CPG) with that starts with a 5' end deprotection of the CPG-bound nucleoside (see Figure 6.1). The generated free hydroxyl group then reacts with the 3' phosphoramidite of the next nucleoside that has been activated with 1 H-tetrazole. The remaining hydroxyl groups are then capped to prevent elongation of missense strands and the resulting dinucleoside phosphate is oxidized to the corresponding phosphate with a mixture of iodine in water then the cycle is repeated. With this oligonucleotide synthesis, covalent introduction of fluorescent labels can be done at specific positions (3', 5' or internal) depending on the applications.

The fluorescent labels can be introduced at the sugar residue or base labeling as depicted in Figure 6.2. An example of modifications at the sugar residue has been described by Yamana and co-workers⁷ who uses several methods for introducing pyrenes via short linkers to a 3' or 5' terminal hydroxyl group of oligonucleotides. The incorporation of the dye to the 5' end was initiated by preparation of 5'-(1-pyrenylmethyl) thymidine followed by its conversion to the phosphorobisdiethylamidite derivative which was then subsequently used for oligonucleotide synthesis. Commercial 5' labeling also uses the sugar residue by using 4, 4-dimethoxytrityl group (DMTr) for protecting the 5' hydroxyl functional group. This protecting group can easily be used to label oligonucleotides at the 5' end during the last reaction cycle of the solid phase phosphoramidite synthesis which follows 3' -5' direction. Modifications at the base residues can also be used by utilizing the exocyclic amino functions in purine and pyrimidine bases for the attachment of fluorescent labels.

An example of this labeling is described by Sigmund et al. who prepared labeled phosphoramidites of 2'-deoxyadenosine, 2'-deoxyguanosine and 2'-deoxycytidine by coupling

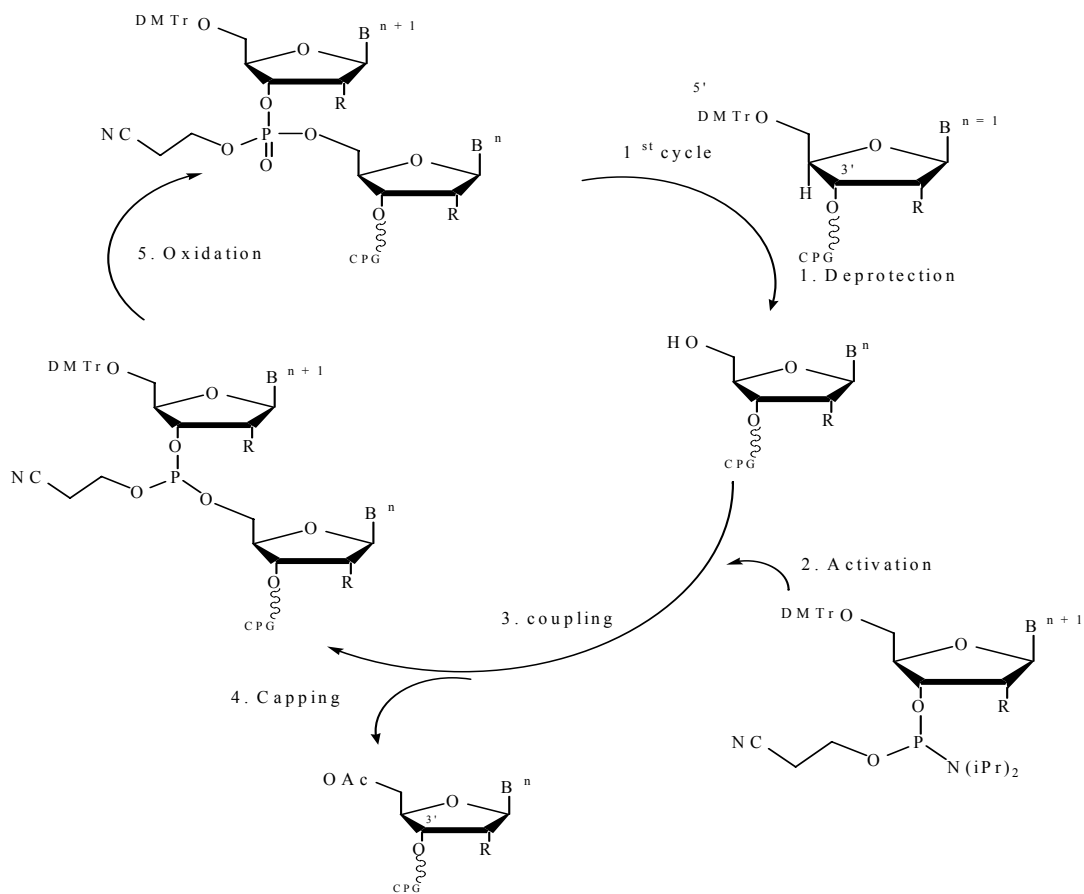


Figure 6.1: Oligonucleotide synthesis reaction cycle. DMTr = 4, 4'- dimethoxytriphenylmethyl, CPG = controlled pore glass, B = base, n is the number of nucleosides, R = DNA. Addition of one phosphoramidite to the growing cycle involves four chemical steps: Detritylation that leads to cleavage of the DMTr protecting group providing a free 5' hydroxyl group (1), activation and coupling (2, 3) steps involves condensation of two nucleotide units, the phosphite group of the phosphoramidite is not reactive towards hydroxyl groups but can be easily activated by weak 1 H tetrazole acid which converts the amidite into a tetrazolide. Capping (4) of any unreacted 5' hydroxyl groups then follows by using a mixture of acetic anhydride, 4-dimethylaminopyridine, and 2, 4, 6-collidine in acetonitrile. The phosphite triester is then oxidized (5) to the more stable phosphate triester by using a mixture of iodine, collidine, and water in acetonitrile before starting the next cycle.^{5,6}

the amino groups with fluorescein via a carbamoyl spacer.⁸ The authors showed that the various amino functions in common nucleosides can be activated by treatment with phenoxy carbonyl tetrazolide, which resulted in conversion of the free amino group to the corresponding urethane. These intermediates then easily reacted with 5'-amino fluorescein. Maier and co-workers also attached a fluorescein molecule and its quencher 2, 4-dinitroaniline to a single base (the

exocyclic amino function of a guanine residue) before converting this to 2'-deoxynucleoside analogue to its corresponding phosphoramidite.⁹

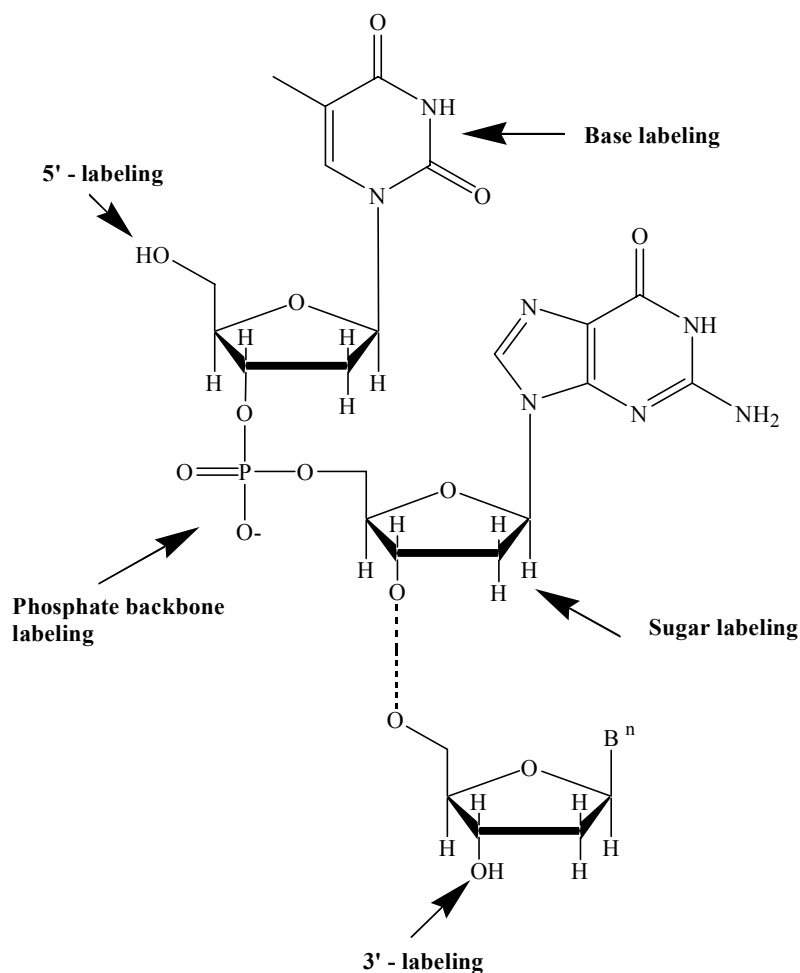


Figure 6.2: Schematic representation of an oligonucleotide strand with arrows indicating the possible 5' end, 3' end, base and sugar labeling sites. Bⁿ is number of bases.

The last example of pre-synthetic oligonucleotide labeling is by using fluorescent dyes in their amidite derivatives. The dye phosphoramidites can serve as 5' labeling reagents, they can also be used with a dimethoxytrityl protected hydroxyl group for internal labeling or they can be coupled to a solid support for 3' labeling.¹⁰⁻¹²

Post-synthetic labeling involves incorporation of a reactive group that aids in the dye attachment after the probe has been synthesized. Some commonly used reactive groups are amino groups, thiol groups, and carboxyl groups. This labeling can be done at the 5' end or 3'

end of the pre-synthesized oligonucleotides. An example of a primary amine serving as the reactive group for post-synthetic labeling is shown in Figure 6.3 B below.

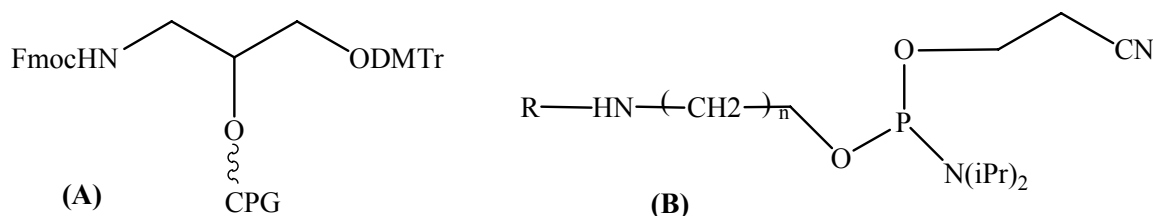


Figure 6.3: (A) Amino modified controlled pore glass (CPG) as a solid support which provides a reactive group for 3' post labeling. (B) Chemical structure of a 5' amino-modifier phosphoramidite, R = amino protecting group (4-monomethoxytriphenyl; trifluoroacetyl). Both are commercially available from Glen Research.¹³

It contains a monomethoxytrityl protecting group that is easily removed and a linker depending with the application of the fluorescent reporter groups. When a fluorescent dye is desired at the 3' terminus of the oligonucleotide, CPG (see Figure 6.3 A) is used as a solid support functionalized with a protected amine for post-synthetic dye coupling and a dimethoxytrityl protected hydroxyl group for standard nucleoside coupling can be used. The conditions for post synthetic labeling step have to be considered carefully because oligonucleotides can easily be hydrolyzed under acidic conditions or at elevated temperatures and they only dissolve in water and organic solvents like acetonitrile, DMSO or DMF. To offset the insolubility of most fluorescent dyes in water, new dyes with ionic residues are used mostly in their active ester form like succinimides or maleimides, as sulfonyl chlorides or thiol reactive iodo and bromo acetamides.¹⁴

6.1.3 Research Focus

In Chapter 4, the response elicited from surface immobilized molecular beacons was optimized by carefully designing these probes and use of a one step surface immobilization strategy detailed in Chapter 3. Besides surface chemistry and proper solid support selection,

stable fluorescence reporting molecules that have high quantum yields are highly desired hence the need for creation of more reporter systems for these applications. In Chapter 5, we attempt to find other reporter systems for FRET applications besides the commonly used commercial ones and it was found that carboxylated zinc phthalocyanine and carboxylated nickel phthalocyanine form a great pair. An example of biological probes that utilize fluorophore/quencher or FRET based measuring techniques is the molecular beacon technology that has been described in Chapter 4. Besides the molecular beacon technology, these fluorescence measuring techniques can also be used with taqman probes. Taqman probes just like molecular beacons, use fluorescence quenching/FRET to detect and quantitate the synthesized PCR product via a fluorophore coupled to the 5' end and a quencher attached to the 3' end of an oligonucleotide substrate. These probes are used with Taq polymerase in the 5' to 3' amplification of DNA. The Taq probe contains both a fluorophore and a quencher in close proximity to one another which inhibits fluorescence in the probe hybridized to the target sequence or in excess probes in solution. When the target strand is amplified during the TaqMan PCR reaction, the Taq polymerase, which is an exonuclease, will degrade the probe resulting in the separation of the fluorophore and the quencher. Thus the fluorescence of the sample will be proportional to the number of amplicons that have been created. In addition to the target specificity and stability of the probe-target duplex, brightness of the fluorophore being used is also a main factor that determines the sensitivity of a DNA probe. We take advantage of the high quantum yields of phthalocyanine dyes for these applications but in order for the phthalocyanine dyes to be useful in recognizing and reporting the signature of DNA sequences by these techniques; they need to be covalently attached to the biomolecules. The synthesis, spectroscopic properties and their conjugation to oligonucleotide primers have been successively achieved¹⁵⁻¹⁸ and we therefore detail here a summary of the experimental design and covalent dual labeling strategies of the

phthalocyanine dyes to oligonucleotide probes which will eventually be used in various FRET applications.

6.2 Synthesis of Molecular Beacon Probes with Carboxylated Zinc Phthalocyanine Reporter Groups and Carboxylated Nickel Phthalocyanine Acceptor Groups

6.2.1 Probe Design

The molecular beacon probe loop sequences were designed to be complementary to sections of EpCAM mRNA which are known to be over-expressed in breast cancer. The biological application of these oligonucleotide probes is that when the molecular beacons are microinjected in cells, they will detect the specific intracellular EpCAM mRNA molecules in the intact cells and also enable their levels of expression to be determined via fluorescence imaging technology. The stability of the stem (5 bases) - loop (15 bases) structure was determined by using the Zuker folding program (www.bioinfo.rpi.edu/applications/mfold/old/dna/form/cgi). The sequences for the designed probes are given below. The oligonucleotides have a functional amino group at the 3' end and another protected amino group at 5' end. The acid labile protecting group used was a methoxytrityl (MMT) group.

5'-(MMT protecting group)-C₆ amino CCCCT ATT AAA GTT TGA CCA AGGGG-(C₇ amino-) 3'

5'-(MMT protecting group)-C₆ amino GGGTG AAG TAA ATA GAA AGG CACCC-(C₇ amino-) 3'

The oligonucleotides have their spacer molecules (C6 linker) attached to the base analogues because it has been shown that labeling at the sugar and phosphate labeling sites result to significant duplex destabilization even at low degrees of dye conjugations.¹⁹⁻²¹

6.2.2 Labeling of Free 3' Amino Group with Carboxylated Zinc Phthalocyanine

Before labeling, the oligonucleotides were purified to remove any amine containing impurities by ethanol precipitation. The oligonucleotides were dissolved in 100 µl of water and extracted three times with an equal volume of chloroform. The oligonucleotides were then

precipitated by adding 10 μl of 3M NaCl and 250 μl of cold absolute ethanol it was then mixed thoroughly and placed at $-20\text{ }^{\circ}\text{C}$ for 30 minutes. This solution was then centrifuged at 12,000 g for 30 minutes then the supernatant was removed leaving a pellet which was dried and re-dissolved in water.

(A)

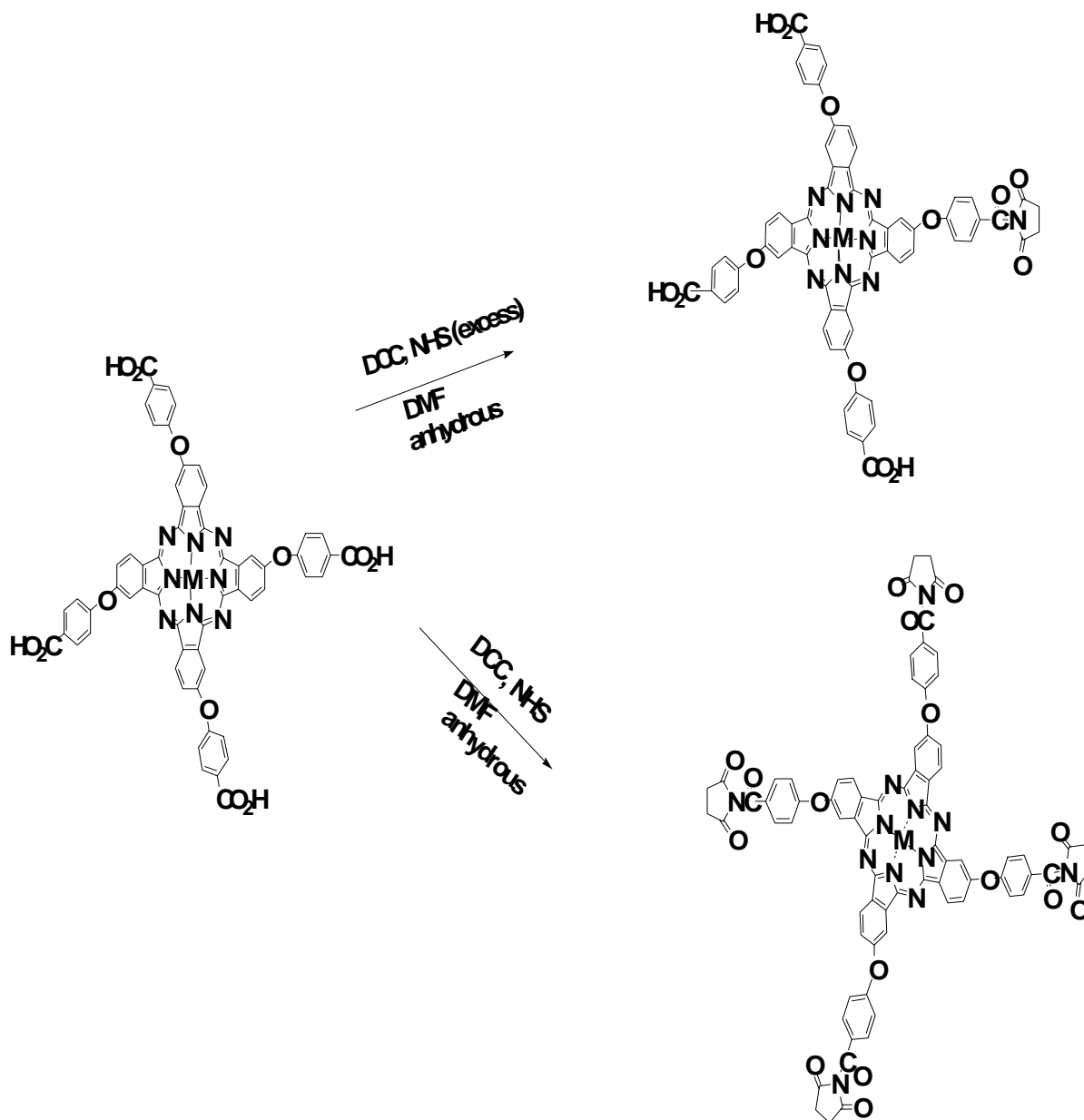


Figure 6.4: (A) Conversion of carboxylated dyes to their N-hydroxysuccinimidyl ester derivatives (B) Initial labeling of oligonucleotide using carboxylated nickel phthalocyanine.

(B)

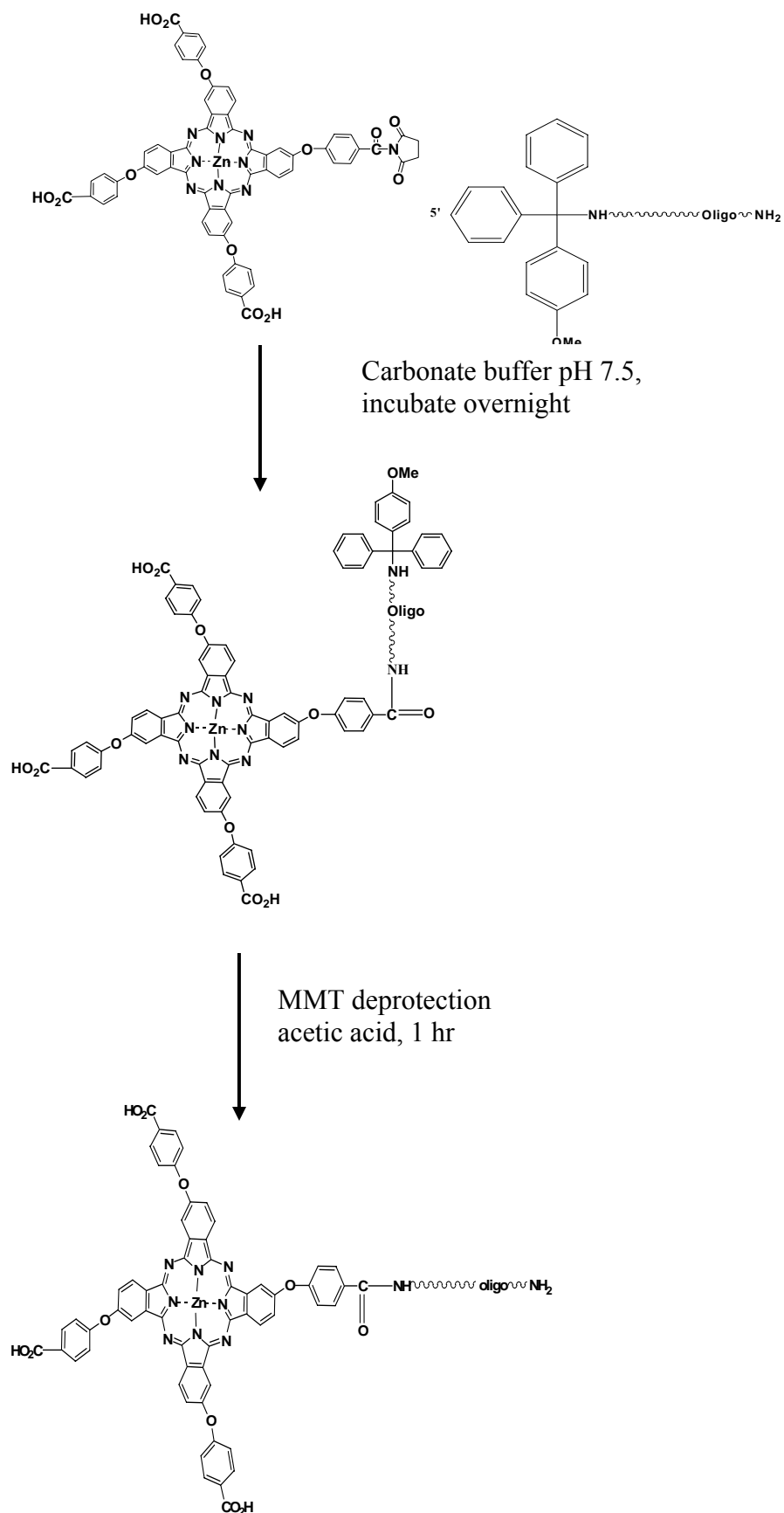


Figure 6.4 Continued.

After oligonucleotide purification, the fluorophores were covalently attached to the oligonucleotides via a C₇ amino linker by formation of an amide bond between the primary amino linker and the active N-hydroxysuccinimidyl ester derivative of the dye as shown in the Figure 6.4. Part A of Figure 6.4 shows the conversion of the carboxylated zinc phthalocyanine to its N-hydroxysuccinimidyl ester derivative while part B illustrates the conjugation process between the dye and a 3'- amine modified oligonucleotide. The dye and oligonucleotide were prepared in carbonate buffer pH 7.5 in a ratio of 10:1 (dye: oligonucleotide) and incubated at room temperature overnight while being protected from light. After this labeling process, the conjugate was purified by ethanol precipitation as described above. The DNA oligonucleotide/dye conjugate was then dried before being used in the deprotection step.

6.2.3 Deprotection of 5' MMT- Amino Group

After the first labeling of the oligonucleotide with the reporter dye (carboxylated zinc phthalocyanine) at the 3' terminal, deprotection of the MMT group attached at the 5' end was done to enable the second labeling of the quencher/acceptor dye. This was achieved by incubating the oligonucleotide/dye conjugate obtained above with an acetic acid/water mixture (80:20 v/v) for 1 h at room temperature. Upon completion of the deprotection step; the oligonucleotide/dye conjugate was purified again by ethanol precipitation then it was reconstituted with water. The preliminary data obtained by HPLC analysis (Figure 6.5) indicated that there was possibility of hydrolysis of the oligonucleotide during this step hence optimization of these procedure was necessary. Other deprotection procedures were therefore performed by; (a) treating the oligonucleotide/dye conjugate in 2% trifluoroacetic acid in chloroform for 5 minutes (b) using 3% trichloroacetic acid in dichloromethane for 5 minutes. In both cases, the reaction was quenched by using phosphate buffer followed by ethanol precipitation. The preliminary data shown below indicates that deprotection by using either trifluoroacetic acid or

trichloroacetic acid does not result in oligonucleotide hydrolysis as is the case of deprotecting the oligonucleotide/ dye conjugate in acetic acid for 1 hour therefore it was adopted for all preceding deprotection steps.

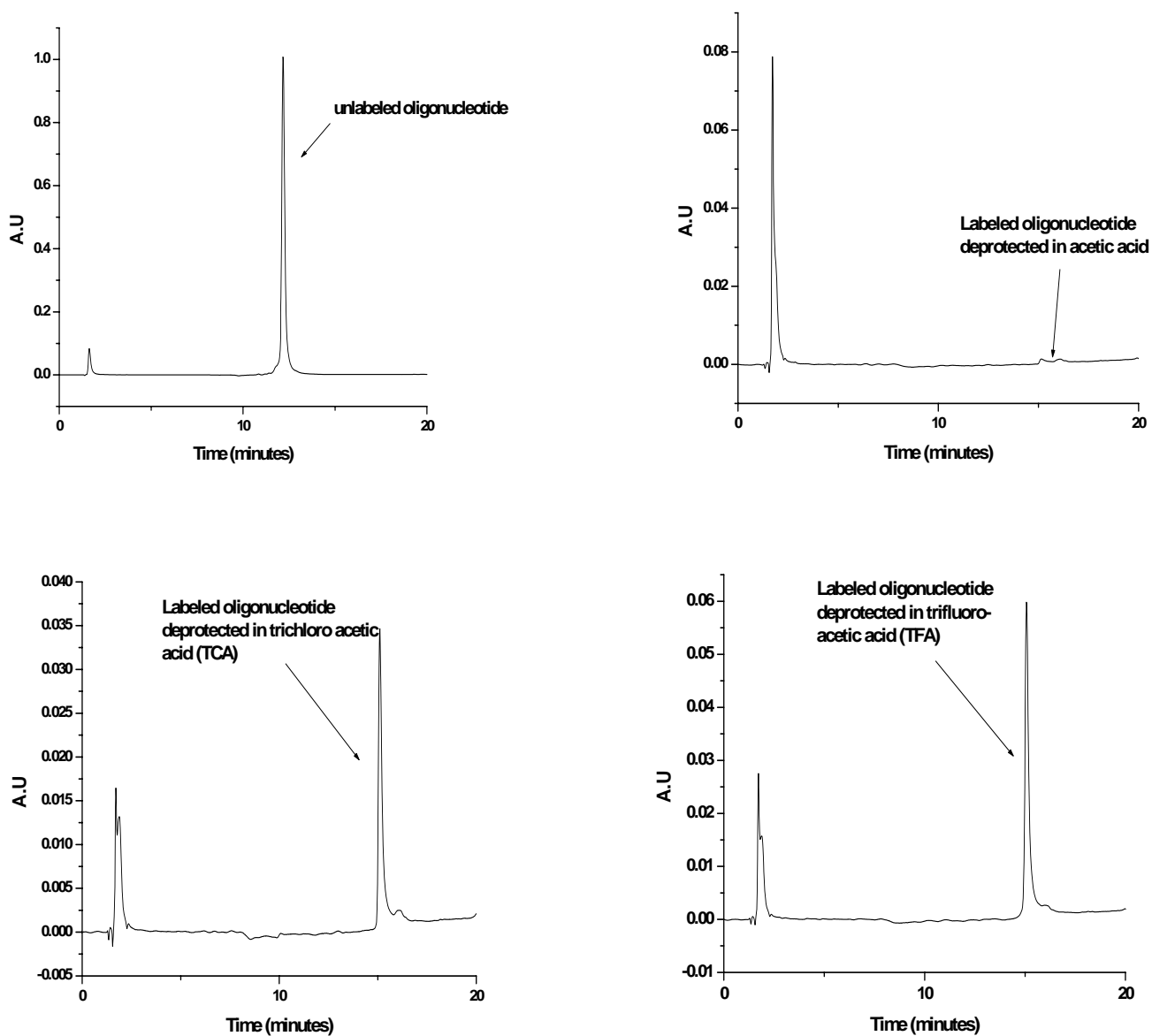


Figure 6.5: HPLC analysis of deprotected oligonucleotides. The oligonucleotides were chromatographed using a Zorbax SB-C18 column (Hewlett Packard, Wilmington, DE, USA) consisting of particle size 5 μm , 150 mm length and 4.6 mm diameter as the stationary phase. The mobile phase consisted of methanol and triethylammonium acetate (TEAA) buffer. The elution was done using the following gradient conditions: 5 min 95% methanol, 15min 50 % TEAA followed by 5 min 50 % TEAA. The HPLC system was operated at 1 ml / min with the diode array detector set at 260 nm and an injection volume of 10 μl .

6.2.4 Labeling of Free 5' Amino Group with Carboxylated Nickel Phthalocyanine

Just like the 3' labeling, the 5' labeling of the N-hydroxysuccinimidyl ester derivative of the carboxylated nickel phthalocyanine with the oligonucleotide was done under similar conditions as the 3' labeling.

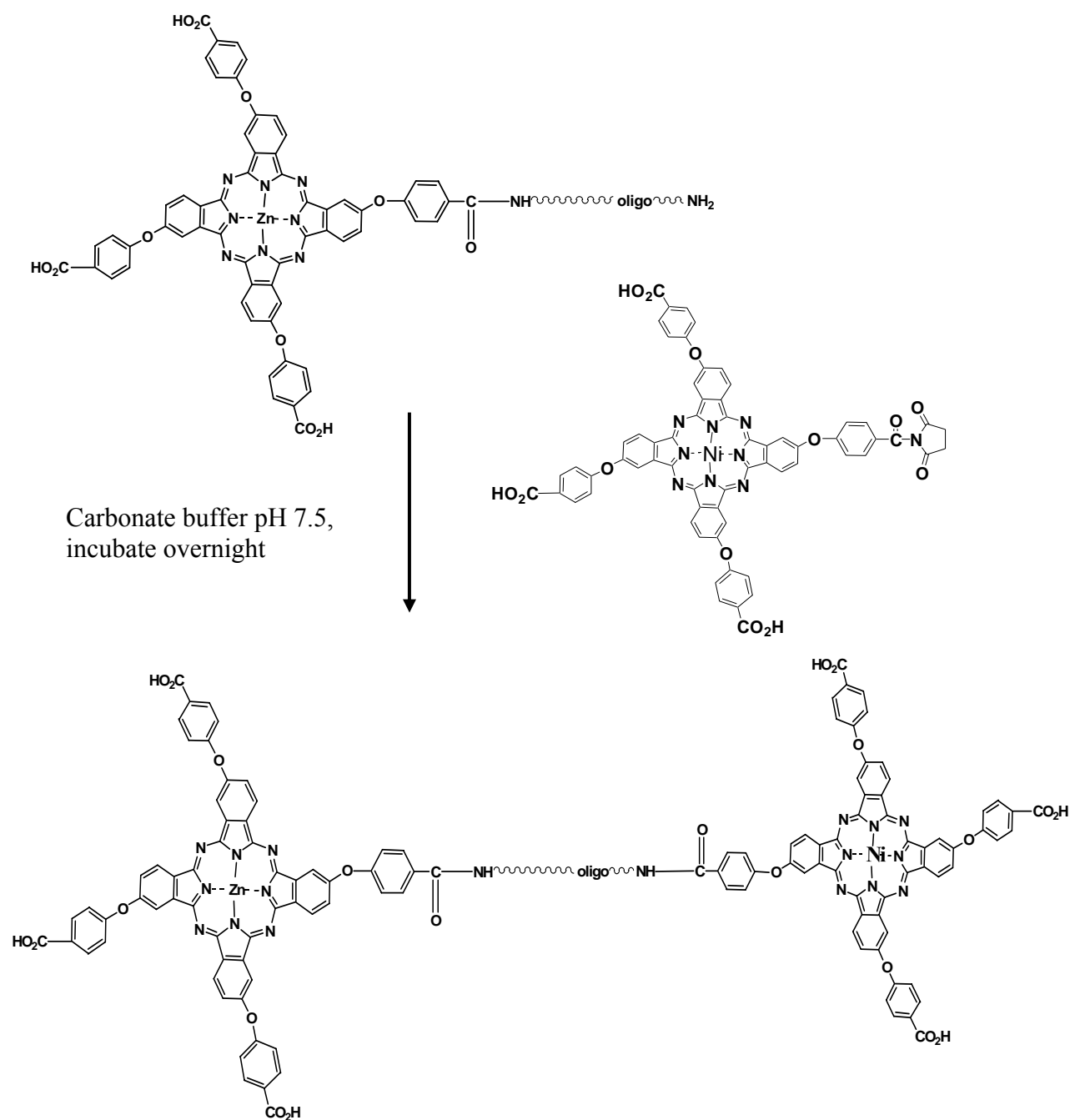


Figure 6.6: Second labeling of oligonucleotide using carboxylated nickel phthalocyanine.

In summary, the dye and oligonucleotide were prepared in carbonate buffer pH 7.5 in a ratio of 10:1 (dye: oligonucleotide) and incubated at room temperature overnight while being protected from light. After this labeling process, the conjugate was purified by ethanol precipitation as described earlier. Figure 6.6 above illustrates the reaction steps of the second conjugation process. Preliminary data of this second conjugation revealed that labeling with carboxylated nickel phthalocyanine was more problematic as compared to the initial labeling using carboxylated zinc phthalocyanine especially because of the large extent of aggregation exhibited by the nickel complex. Current studies of the optimization of this second labeling step are underway after which the activity (solution based assays) of these dual labeled probes will be compared to a commercial probe consisting of the same probe labeled with a CY 5.5 fluorophore and a BHQ-3 quencher.

6.3 References

- (1) Jameson, D. M.; Eccleston, J. F. *Methods in Enzymology* **1997**, *278*, 363-390.
- (2) Zamaratski, E.; Chattopadhyaya, J. *Tetrahedron* **1998**, *54*, 8183-8206.
- (3) LePecq, J. B.; Paoletti, C. *Journal of molecular biology* **1967**, *27*, 87-106.
- (4) Benson, S. C.; Mathies, R. A.; Glazer, A. N. *Nucleic Acids Research* **1993**, *21*, 5720-5726.
- (5) Beaucage, S. L.; Iyer, R. P. *Tetrahedron* **1993**, *49*, 6123-6194.
- (6) Beaucage, S. L.; Iyer, R. P. *Tetrahedron* **1992**, *48*, 2223-2311.
- (7) Yamana, K.; Nunota, K.; Nakano, H.; Sangen, O. *Tetrahedron Letters* **1994**, *35*, 2555-2558.
- (8) Sigmund, H.; Maier, T.; Pfeleiderer, W. *Nucleosides & Nucleotides* **1997**, *16*, 685-696.
- (9) Maier, T.; Pfeleiderer, W. *Nucleosides & Nucleotides* **1995**, *14*, 961-965.
- (10) Korshun, V. A.; Pestov, N. B.; Birikh, K. R.; Berlin, Y. A. *Bioconjugate Chemistry* **1992**, *3*, 559-562.

- (11) Schubert, F.; Ahlert, K.; Cech, D.; Rosenthal, A. *Nucleic Acids Research* **1990**, *18*, 3427.
- (12) Lewis, F. D.; Zhang, Y.; Letsinger, R. L. *Journal of the American Chemical Society* **1997**, *119*, 5451-5452.
- (13) *Glen Research, User Guide to DNA modifications* **1996**.
- (14) Waggoner, A. *Methods in Enzymology* **1995**, *246*, 362-373.
- (15) Hammer, R. P.; Owens, C. V.; Hwang, S.-H.; Sayes, C. M.; Soper, S. A. *Bioconjugate Chemistry* **2002**, *13*, 1244-1252.
- (16) Irina v.Nesterova, V. T. V., Serhii Pakhomov, robert P. Hammer, and steven A.Soper *Manuscript in preparation* **2006**.
- (17) Flanagan, J. H., Jr.; Owens, C. V.; Romero, S. E.; Waddell, E.; Kahn, S. H.; Hammer, R. P.; Soper, S. A. *Analytical chemistry* **1998**, *70*, 2676-2684.
- (18) Flanagan, J. H., Jr.; Khan, S. H.; Menchen, S.; Soper, S. A.; Hammer, R. P. *Bioconjugate chemistry* **1997**, *8*, 751-756.
- (19) Aurup, H.; Tuschl, T.; Benseler, F.; Ludwig, J.; Eckstein, F. *Nucleic Acids Research* **1994**, *22*, 20-24.
- (20) Ozaki, H.; McLaughlin, L. W. *Nucleic Acids Research* **1992**, *20*, 5205-5214.
- (21) Ozaki, H.; McLaughlin, L. W. *Nucleic acids symposium series* **1992**, 67-68.

CHAPTER 7

CONCLUSIONS AND FUTURE WORK

7.1 Conclusions

The focus of this work involved development of polymer surface modification chemistries, probe attachment protocols and fluorescence-based techniques for biomolecular recognition and reporting. A background of DNA microarray technologies and its applications was discussed in Chapter 1. Also presented in this Chapter are the commonly used solid support materials for fabrication of DNA microarrays and the probe attachment chemistries associated with them. Lastly, several detection modes of microarrays were discussed with fluorescence spectroscopy being the common commercially adopted technique for microarray detection.

Chapter 2 reviewed the current research that involves coupling microarrays to microfluidics with emphasis on DNA arrays, protein arrays and cell-based arrays with concluding remarks on potential improvements required for future developments that will allow the benefits of microfluidics/microarray devices to be fully utilized for applications in diagnostics and the understanding of biological function for discovery-based projects.

In Chapter 3, a one step surface photo-activation of PMMA substrates that introduced functional carboxyl groups was given. This allowed covalent attachment of DNA probes via carbodiimide coupling chemistries to be achieved. Microfluidic devices fabricated in PDMS substrates were then used together with these probe attachment chemistries for multiple detection of 4 different low abundant *KRAS* 2 mutations that are known to be of diagnostic value for colorectal cancers via coupling of Ligase Detection Reaction (LDR) and universal zipcode microarrays. Incorporation of microfluidics into the array construction enabled parallel processing of different DNA targets to be achieved without the need for spotting and use of these microchannels also enabled homogeneous and sufficient amounts of target DNA or probe molecules to be distributed across the entire array and therefore uniform hybridization signals

without non-specific interaction between poly-anionic DNA and the PMMA surfaces was observed.

In Chapter 4, a description on the use of FRET / fluorescence quenching-based assays that couple molecular beacon technology and microarray technologies was illustrated. This was done by immobilizing molecular beacon probes onto solid surfaces by using the probe attachment protocols described in Chapter 3 for PMMA substrates and well known siloxane based chemistries for the immobilization of these probes onto glass substrates. Improvement of the performance of these molecular beacon probes used for arrays was achieved by careful molecular beacon design (consideration of the stem/loop sequences and length, selection of good fluorescence reporter molecules) and the use of stable surface modification/probe attachment chemistries. An example of the performance was used for the analysis of mRNAs specific for *fruitless (fru)* and *Ods-site Homeobox (OdsH)* genes that were extracted from *Drosophila melanogaster* fruitflies.

In Chapter 5, we studied the fluorescence and quenching properties of phthalocyanine dyes which are known to be thermally and chemically stable; they possess high extinction coefficients and quantum yields and depending on the transition metal ions inserted in their macrocyclic ring, their photo-physical/spectral properties are tunable. It was found that zinc phthalocyanine and nickel phthalocyanine complexes form a suitable donor/acceptor pair when fluorescence quenching is desired for analysis. This acceptor/donor pair was therefore used in Chapter 6 for dual labeling of molecular beacon probes. Upon completion of these labeling procedures, it will be interesting to see how the phthalocyanine pair compares to commercially available organic fluorophores and quenchers.

7.2 Current and Future work

7.2.1 Molecular Beacons for Real-Time Analysis of EpCAM mRNAs Expressed in MCF-7 Cells

Advances in fluorescence microscopy techniques and probe technology have provided possibilities to study the distribution of RNA in living cells. One such technique is Fluorescence in Situ Hybridization (FISH) which is a highly efficient method of localizing DNA/RNA in living cells. Essential steps in these protocols are the fixation of the biological sample, the subsequent permeabilization of the specimen to improve the probe penetration, the hybridization of a probe to an RNA target sequence, and finally a proper washing and detection procedure.^{1,2} This method however; requires fixation procedures as described in FISH protocols that are not compatible with imaging DNA/RNA molecules in living cells.^{3,4} The second technique involves microinjection of radio/fluorescence labeled RNA/DNA into living cells^{5,6} but the main problem associated with this is the fact that modification of RNA/DNA of interest and denaturation of their linking proteins are inevitable in the synthesis and extraction procedures making it difficult to ensure that the observed patterns truly reflect the behaviors of the RNA/DNA in living cells. Fluorescently labeled linear oligonucleotides that are complementary to target RNAs have also been used but they are not preferred because there is difficulty in separating the hybridization signals from the fluorescence of free probes. Molecular beacon probes have provided the capability of detecting specific target molecules without the need of labeling the targets and separating unbound probes with superior specificity/selectivity. Even though molecular beacon probes are known to be very selective, it is worth noting that their sensitivities is still dependant on the brightness of reporter/acceptor dye molecules properties hence the need to use systems that can report these molecular association events with very high effectiveness. In this work, molecular beacons containing phthalocyanine reporter dyes as detailed in Chapter 5 will be used for real-time detection of mRNAs in living cells.

Current ongoing work is based on finalizing the optimization of high efficiency dual labeling protocols of molecular beacons that will be used for analysis of EpCAM (epithelial cell adhesion molecules) mRNAs. EpCAM is a cell surface molecule that is known to be highly expressed in colon, breast and other carcinomas.⁷⁻⁹ Because EpCAM is involved in cell-to cell adhesion, it has been the target of antibody therapy in several clinical trials and its importance as a novel target for breast cancer gene therapy has drawn considerable interest in assessing its value. For example, Walid and co-workers performed a real-time reverse transcription –PCR to quantify the level of EpCAM mRNA expression in normal breast tissue and primary/metastasis breast cancers and they found that EpCAM is over expressed in both primary and metastasis breast cancers.¹⁰ In this case study, we take the approach of using molecular beacon probes to determine the expression of EpCAM mRNA in MCF-7 breast cancer cells. This approach gives us the advantage of determining the expression levels of the mRNAs present in the MCF-7 cells directly without having to perform a reverse transcription-PCR for quantitation.

The molecular beacons have been designed such that their loop sequences are complementary to the EpCAM mRNA sequence (see Chapter 6). The synthesized molecular beacons will be microinjected into MCF-7 cells then the binding events of the beacons and EpCAM can be read out by fluorescence imaging. With these assays, it is expected that the fluorescence intensities observed should correlate with the expression levels of the EpCAM. Negative control assays will also be done by; (i) fluorescence imaging of cells without molecular beacons to rule out any autofluorescence that might arise from the cell compartments; (ii) fluorescence imaging of molecular beacons in a cell dish containing no cells which should result to no or very minimal fluorescence because these probes will be in their “off” configuration; (iii) use of molecular beacons for cells that are known not to express EpCAM, an example of such cells are Jurkat cells which will be non-complementary to the loop sequence of the designed

molecular beacons. These assays will enable us to study the performance of using phthalocyanine dyes for molecular beacon synthesis in comparison to existing organic dyes and it is also desired that these techniques will be another contribution towards using EpCAM as a target for breast cancer gene therapy via real-time detection.

7.2.2 Reverse-Molecular Beacons for Detection of Low Abundant DNA point Mutation and Pathogenic Analysis via Single Molecule Detection

The second application involves design of oligonucleotide probes that function in a reverse-molecular beacon style.¹¹ Here, the probes are designed such that labeling is done at the end of two separate individual primers. The two different fluorophores are attached to the ends of the stem of separate primers such that RET occur when the stem-loop structure is formed as illustrated in Figure 7.1 shown below.

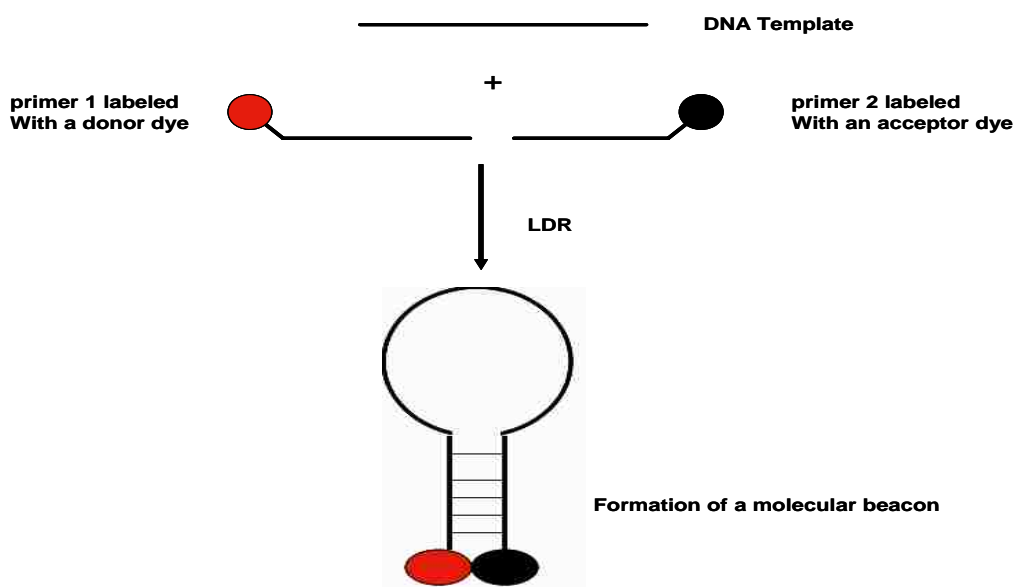


Figure 7.1: Illustration of the use of reverse molecular beacon technology for analysis.

When primers are separated in solution, they exhibit fluorescence but upon binding to the template e.g. during an LDR reaction, the donor fluorescence intensity is diminished or disappears while the acceptor fluorescence intensity is enhanced for fluorescent acceptors. In this

case the acceptor dye will be tin phthalocyanine and the donor will be zinc phthalocyanine whose absorption spectrum and emission spectrum have been shown to overlap hence allowing RET to occur.¹² The design of the loop and stem sequences will be such that when the probes are coupled with LDR assays; they can be used for the detection of low abundant DNA mutations in colorectal cancers (*KRAS 2* genes) and also for pathogenic detection of bacteria (*Escherichia coli*, *Staphylococcus aureus* and *Staphylococcus epidermidis*) via single molecule detection techniques.

7.3 References

- (1) Dirks, R. W. *Histochemistry and Cell Biology* **1996**, *106*, 151-166.
- (2) Macville, M. V. E.; Van Dorp, A. G. M.; Dirks, R. W.; Fransen, J. A. M.; Raap, A. K. *Histochemistry and Cell Biology* **1996**, *105*, 139-145.
- (3) Dirks, R. W.; Molenaar, C.; Tanke, H. J. *Histochemistry and Cell Biology* **2001**, *115*, 3-11.
- (4) Levsky, J. M.; Singer, R. H. *Journal of Cell Science* **2003**, *116*, 2833-2838.
- (5) Mirzayans, R.; Aubin, R. A.; Paterson, M. C. *Mutation Research* **1992**, *281*, 115-122.
- (6) Korzh, V. P.; Burakova, T. A.; Neifakh, A. A.; Mazin, A. L. *Biopolimery i Kletka (1985-2000)* **1985**, *1*, 14-20.
- (7) Balzar, M.; Winter, M. J.; De Boer, C. J.; Litvinov, S. V. *Journal of Molecular Medicine (Berlin)* **1999**, *77*, 699-712.
- (8) de Boer, C. J.; van Krieken, J. H.; Janssen-van Rhijn, C. M.; Litvinov, S. V. *J Journal of pathology* **1999**, *188*, 201-206.
- (9) Spizzo, G.; Gastl, G.; Wolf, D.; Gunsilius, E.; Steurer, M.; Fong, D.; Amberger, A.; Margreiter, R.; Obrist, P. *British Journal of Cancer* **2003**, *88*, 574-578.
- (10) Osta, W. A.; Chen, Y.; Mikhitarian, K.; Mitas, M.; Salem, M.; Hannun, Y. A.; Cole, D. J.; Gillanders, W. E. *Cancer Research* **2004**, *64*, 5818-5824.
- (11) Wabuyele, M. B.; Farquar, H.; Stryjewski, W.; Hammer, R. P.; Soper, S. A.; Cheng, Y.-W.; Barany, F. *Journal of the American Chemical Society* **2003**, *125*, 6937-6945.
- (12) Irina v.Nesterova, V. T. V., Serhii Pakhomov, Robert P. Hammer, and Steven A.Soper *Manuscript in preparation* **2006**.

APPENDIX: LETTER OF PERMISSION

ANALYTICAL BIOCHEMISTRY (2005),37(1),103-113

We hereby grant you permission to reprint the aforementioned material at no charge in your thesis subject to the following conditions:

1. If any part of the material to be used (for example, figures) has appeared in our publication with credit or acknowledgement to another source, permission must also be sought from that source. If such permission is not obtained then that material may not be included in your publication/copies.
2. Suitable acknowledgment to the source must be made, either as a footnote or in a reference list at the end of your publication, as follows:

"Reprinted from Publication title, Vol number, Author(s), Title of article, Pages No., Copyright (Year), with permission from Elsevier".
3. Your thesis may be submitted to your institution in either print or electronic form.
4. Reproduction of this material is confined to the purpose for which permission is hereby given.
5. This permission is granted for non-exclusive world English rights only. For other languages please reapply separately for each one required. Permission excludes use in an electronic form. Should you have a specific electronic project in mind please reapply for permission.
6. This includes permission for UMI to supply single copies, on demand, of the complete thesis. Should your thesis be published commercially, please reapply for permission.

Yours sincerely

Steph Smith
Rights Assistant

Elsevier Ltd
The Boulevard
Langford Lane
Kidlington
Oxford OX5 1GB

-----Original Message-----

From: csituml@lsu.edu [mailto:csituml@lsu.edu]
Sent: 21 March 2007 20:17
To: Rights and Permissions (ELS)
Subject: Obtain Permission

This Email was sent from the Elsevier Corporate Web Site and is related to Obtain Permission form:

Product: Customer Support
Component: Obtain Permission
Web server: <http://www.elsevier.com>
IP address: 10.10.24.149
Client: Mozilla/5.0 (Windows; U; Windows NT 5.1; en-US;
rv:1.8.0.10) Gecko/20070216 Firefox/1.5.0.10
Invoked from:
http://www.elsevier.com/wps/find/obtainpermissionform.cws_home?isSubmitted=yes&navigateXmlFileName=/store/prod_webcache_act/framework_support/obtainpermission.xml

Request From:
Graduate Student catherine situma
Louisiana State university
232 Choppin Hall Box DD2
70803
Baton Rouge
United States

Contact Details:
Telephone: 2255787709
Fax: 2255783458
Email Address: csituml@lsu.edu

To use the following material:

ISSN/ISBN:
Title: Analytical Biochemistry
Author(s): Catherine Situma, Yun Wang, Steven A. Soper
Volume: 1
Issue: 340
Year: 2005
Pages: 123 - 135
Article title: Fabrication of DNA microarrays onto PMMA

How much of the requested material is to be used:
the entire article

Are you the author: Yes
Author at institute: Yes

How/where will the requested material be used: [how_used]

Details:

In a thesis or dissertation

Additional Info:

- end -

For further info regarding this automatic email, please contact:
WEB APPLICATIONS TEAM (esweb.admin@elsevier.co.uk)

BIOMOLECULAR ENGINEERING (2006),23(5),213-231

We hereby grant you permission to reprint the aforementioned material at no charge in your thesis subject to the following conditions:

1. If any part of the material to be used (for example, figures) has appeared in our publication with credit or acknowledgement to another source, permission must also be sought from that source. If such permission is not obtained then that material may not be included in your publication/copies.
2. Suitable acknowledgment to the source must be made, either as a footnote or in a reference list at the end of your publication, as follows:

"Reprinted from Publication title, Vol number, Author(s), Title of article, Pages No., Copyright (Year), with permission from Elsevier".
3. Your thesis may be submitted to your institution in either print or electronic form.
4. Reproduction of this material is confined to the purpose for which permission is hereby given.
5. This permission is granted for non-exclusive world English rights only. For other languages please reapply separately for each one required. Permission excludes use in an electronic form. Should you have a specific electronic project in mind please reapply for permission.
6. This includes permission for UMI to supply single copies, on demand, of the complete thesis. Should your thesis be published commercially, please reapply for permission.

Yours sincerely

Steph Smith
Rights Assistant

Elsevier Ltd
The Boulevard
Langford Lane
Kidlington
Oxford OX5 1GB

-----Original Message-----

From: csituml@lsu.edu [mailto:csituml@lsu.edu]
Sent: 21 March 2007 20:37
To: Rights and Permissions (ELS)
Subject: Obtain Permission

This Email was sent from the Elsevier Corporate Web Site and is related to Obtain Permission form:

Product: Customer Support
Component: Obtain Permission
Web server: <http://www.elsevier.com>
IP address: 10.10.24.149
Client: Mozilla/5.0 (Windows; U; Windows NT 5.1; en-US; rv:1.8.0.11) Gecko/20070312 Firefox/1.5.0.11
Invoked from:
http://www.elsevier.com/wps/find/obtainpermissionform.cws_home?isSubmitted=yes&navigateXmlFileName=/store/prod_webcache_act/framework_support/obtainpermission.xml

Request From:
Graduate Student catherine situma
Louisiana State University
232 Choppin Hall Box DD2
70803
Baton Rouge
United States

Contact Details:
Telephone: 2255787709
Fax: 2255783458
Email Address: csituml@lsu.edu

To use the following material:

ISSN/ISBN:
Title: Biomolecular Engineering
Author(s): Catherine Situma, Hashimoto masahiko, steven soper
Volume: 23
Issue: 5
Year: 2006
Pages: 213 - 231
Article title: Merging microfluidics with microarrays

How much of the requested material is to be used:
entire article

Are you the author: Yes
Author at institute: Yes

How/where will the requested material be used: In a thesis or
dissertation

Details:

Additional Info:

- end -

For further info regarding this automatic email, please contact:
WEB APPLICATIONS TEAM (esweb.admin@elsevier.co.uk)

ANALYTICAL BIOCHEMISTRY (2007),363 (1),35-45

We hereby grant you permission to reprint the aforementioned material at no charge in your thesis subject to the following conditions:

1. If any part of the material to be used (for example, figures) has appeared in our publication with credit or acknowledgement to another source, permission must also be sought from that source. If such permission is not obtained then that material may not be included in your publication/copies.
2. Suitable acknowledgment to the source must be made, either as a footnote or in a reference list at the end of your publication, as follows:

"Reprinted from Publication title, Vol number, Author(s), Title of article, Pages No., Copyright (Year), with permission from Elsevier".
3. Your thesis may be submitted to your institution in either print or electronic form.
4. Reproduction of this material is confined to the purpose for which permission is hereby given.
5. This permission is granted for non-exclusive world English rights only. For other languages please reapply separately for each one required. Permission excludes use in an electronic form. Should you have a specific electronic project in mind please reapply for permission.
6. This includes permission for UMI to supply single copies, on demand, of the complete thesis. Should your thesis be published commercially, please reapply for permission.

Yours sincerely

Steph Smith
Rights Assistant

Elsevier Ltd
The Boulevard
Langford Lane
Kidlington
Oxford OX5 1GB

-----Original Message-----

From: csituml@lsu.edu [mailto:csituml@lsu.edu]
Sent: 21 March 2007 20:25
To: Rights and Permissions (ELS)
Subject: Obtain Permission

This Email was sent from the Elsevier Corporate Web Site and is related to Obtain Permission form:

Product: Customer Support
Component: Obtain Permission
Web server: <http://www.elsevier.com>

IP address: 10.10.24.148
Client: Mozilla/5.0 (Windows; U; Windows NT 5.1; en-US;
rv:1.8.0.10) Gecko/20070216 Firefox/1.5.0.10
Invoked from:
http://www.elsevier.com/wps/find/obtainpermissionform.cws_home?isSubmitted=yes&navigateXmlFileName=/store/prod_webcache_act/framework_support/obtainpermission.xml

Request From:
Graduate Student catherine situma
Louisiana State University
232 Choppin Hall Box DD2
70803
Baton Rouge
United States

Contact Details:
Telephone: 2255787709
Fax: 2255783458
Email Address: csituml@lsu.edu

To use the following material:

ISSN/ISBN:
Title: Analytical Biochemistry
Author(s): catherine situma, moehring amanda J, soper steven
Volume: 1
Issue: 363
Year: 2007
Pages: 35 - 45
Article title: Immobilized molecular beacons:

How much of the requested material is to be used:
entire material

Are you the author: Yes
Author at institute: Yes

How/where will the requested material be used: [how_used]

Details: In a thesis or dissertation

Additional Info:

- end -

For further info regarding this automatic email, please contact:
WEB APPLICATIONS TEAM (esweb.admin@elsevier.co.uk)

VITA

Catherine Nabifwo Situma was born to Mr. Richard Situma Zadock and Mrs. Juliet Mutonyi Situma on November 22nd, 1977 in Bungoma, Kenya. She has two brothers and three sisters. She obtained her high school diploma from 1991-1994 at Shikoti Girls High school in Kakamega, Kenya. Upon graduation, she enrolled at Jomo Kenyatta University of Agriculture and Technology (JKUAT), Kenya, in January 1996 and graduated with a Bachelor of Science degree in chemistry in 2000. In the summer of 2001, she began graduate school at Louisiana State University in the department of chemistry, Baton Rouge. Catherine N. Situma is currently a candidate for the degree of Doctor of Philosophy in analytical chemistry, which will be awarded at the May 2007 Commencement.